

THE UNIVERSITY OF ASTON IN BIRMINGHAM

EVALUATION AND MODELLING
OF
A WATER-TO-WATER HEAT PUMP SYSTEM

by

Mohd Yusof Hj Othman
B.Sc(Hons), M.Sc.

Department of Physics

January, 1984.

The University of Aston in Birmingham
EVALUATION AND MODELLING OF A WATER-TO-WATER
HEAT PUMP SYSTEM

Thesis for the Degree of PH.D

by Mohd Yusof Hj Othman

S U M M A R Y

In the present work, a water-to-water heat pump system has been assembled, with sensors mounted at appropriate places around the system to measure such quantities as temperature, pressure and flow rate.

The necessary electronic instrumentation for each transducer was developed, and the transducer-instrument combinations tested, calibrated and interfaced to a microcomputer.

The performance of the heat pump for water heating in an ordinary domestic hot water tank was analysed in three different modes;

1. With thermal stratification; condenser water flow rate controlled by water regulator.
2. With thermal stratification; water regulator bypassed, i.e. flow uncontrolled.
3. Without stratification; deliberate water mixing, water regulator in circuit.

The analysis shows that the best C.O.P. is given by mode 1. This shows that, for water heating purposes, a suitable hot water tank design is required to match the heat pump system.

Analysis of heat being extracted from a storage tank was also carried out by recycling the water through the evaporator. The performance of the system during heat extraction as a function of reducing evaporating temperature was observed. The analysis enables one to predict the performance of the system during heat extraction from a heat store. It shows that the C.O.P. of the heat pump system is higher the hotter the water, and the higher the flow rate passing through the evaporator.

The performance of each component of the heat pump system was also analysed in a quantitative manner. In order to analyse and calculate the heating load for the system, empirical mathematical relations based on experimental data were developed.

A computer model for the system was developed based on these empirical equations. The model includes details of the heat source and sink system. The effects on performance of various evaporator water flow rates and various condensing pressures could be observed.

Key word: Heat pump - Refrigerant cycle - Heating load-
Performance - simulation.

LIST OF CONTENTS

	Page
Acknowledgements	vii
List of Tables	viii
List of Figures	xii
Nomenclature	xix

CHAPTER 1

INTRODUCTION

Introduction	1
--------------	---

CHAPTER 2

THEORY OF THE HEAT PUMP AND ITS PRINCIPLE OF OPERATION

2.1 Introduction	5
2.2 The Principle of Operation of The Heat Pump - The Reversed Carnot Cycle.	6
2.2.1 Coefficient of Performance of The Reversed Carnot Cycle.	10
2.2.1 Using Vapour As a Refrigerant	11
2.3 The Vapour Compression Cycle	14
2.3.1 Coefficient of Performance of The Ideal Vapour-compression Cycle.	18
2.4 The Practical Heat Pump Cycle	19
2.4.1 Coefficient of Performance of The Practical Heat Pump Cycle	23

2.5	Choice of Refrigerant	24
2.5.1	Thermodynamic Properties of Refrigerant - Graphical Representation	27
2.6	Work Transfer in a Reversible Reciprocating Compressor.	30
2.6.1	Working Analysis of The Ideal Compressor	33
2.6.2	Efficiencies of a Reciprocating Compressor	40

CHAPTER 3

HEAT PUMP COMPONENTS AND ASSEMBLY

3.1	Introduction	43
3.2	Piping and Joints	45
3.3	Compressor	48
3.4	Thermostatic Expansion Valve	50
3.5	Heat Exchanger	55
3.5.1	Condenser	56
3.5.2	Evaporator	60
3.6	Water Regulator	61
3.7	Filter Drier	63
3.8	Leak Testing, Moisture Removal and Refrigerant Loading Process	66
3.9	Water Pump	67

CHAPTER 4

TRANSDUCERS AND SENSORS FOR THE ASSEMBLED HEAT PUMP

4.1	Introduction	69
4.2	The Thermocouple	70
4.2.1	The Temperature Calibration	73
4.3	The Pressure Transducer	76
4.4	The Watt Meter	79
4.4.1	The Watt Meter Calibration	86
4.5	The Water Flow Meter	89
4.5.1	The Water Flow Calibration	93

CHAPTER 5

DATA ACQUISITION SYSTEM

5.1	Introduction	96
5.2	The Computer	96
5.3	Analogue-digital Converter	99
5.3.1	Analogue-digital Converter PCI1001	99
5.3.2	Analogue-digital Converter PCI1002	103
5.4	The Frequency-voltage Converter	105
5.4.1	Input Signal Conditioning	108
5.5	The Computer Program	111
5.6	Flow Diagram Description	114

CHAPTER 6

PERFORMANCE ANALYSIS DURING WATER HEATING

6.1	Introduction	120
6.2	Single Pass: Water Circulated Through The Condenser	127
6.2.1	Mode 1: Water Passing Through Condenser Controlled by The Water Regulator	128
6.2.2	Mode 2: Constant Flow Through The Condenser - Bypassing The Water Regulator	131
6.3	Mode 3: Water Passing Through The Condenser with Tap 1 and Tap 2 Open	133
6.4	The Water Temperature Profile in The Tank During Water Heating	145
6.5	Discussion and Conclusions	151

CHAPTER 7

PERFORMANCE ANALYSIS

OF THE WATER-TO-WATER HEAT PUMP SYSTEM AND ITS MODELLING

7.1	Introduction	156
7.2	The Compressor	160
7.3	The Effect of Water-jacketing The Compressor Cylinder	166

7.4	The Compressor Efficiencies	170
7.4.1	Volumetric Efficiency (η_{vol})	170
7.4.2	Isothermal Efficiency (η_{iso})	172
7.4.3	Isentropic Efficiency (η_{isen})	175
7.4.4	Mechanical Efficiency (η_m)	177
7.5	Refrigerant Mass Flow Rate (\dot{m}_F)	179
7.6	The Evaporator	185
7.7	The Condenser	189
7.8	Heat Pump Modelling	194
7.8.1	System Simulation and Heat Pump Modelling	194
7.8.2	Description of Modelling Flow Diagram	195
7.8.3	The Limitation of The Modelling	202
7.9	Performance Trends of The Heat Pump	205
7.10	General Conclusions	219

APPENDICES

Appendix I	: Operating Subroutines for PCI1001 and PCI1002	224
Appendix II	: The Computer Program for Sampling Experimental Data.	226
Appendix III:	The Mathematical Equations of The Thermodynamic state of The Refrigerant R12 used in The Computer Model Based on The Data Given by ASHRAE [43]	231

Appendix IV: The Computer Program for The Water- to-water Heat Pump Model.	239
-------------------------------------------------------------------------------	-----

REFERENCES AND FURTHER READING	246
--------------------------------	-----

ACKNOWLEDGEMENTS

I would like to express my deep gratitude to Mr. C.G. Pearce for his continued help and guidance throughout the project, together with Professor W.E.J. Neal, Mr. M.S. Wrenn and Dr. P.N.Cooper for their advice and discussions.

I would also like to thank Mr. H. Arrowsmith, Mr. T.J. Kennedy, Mr. R. Bassi and other technicians in Department of Physics for their help in assembling the equipment and their interest in all my activities during my stay at the University.

I would like to thank very much the National University of Malaysia and the Government of Malaysia for financial support during my stay in United Kingdom and giving me the opportunity to carry out the project.

And, finally, I would like to express my gratitude to my wife, Hasnah, my daughter Siti Khadijah and my sons Mohd Helmi and Mohd Taufiq and to all my family for their help, moral support, patience and understanding throughout the whole project.

LIST OF TABLES

Table No:		Page
2.1	Information on some of the refrigerants.	26
2.2	Thermodynamic properties of refrigerants R11 and R12 at evaporating temperature of 0°C and condensing temperature of 50°C.	29
3.1	Compressor specifications.	550
3.2	The capacity of the thermostatic expansion valve.	55
3.3	Water pump specifications.	68
4.1	The least squares curve fitting for copper-constantan thermocouple.	75
4.2	The specification of the pressure transducers.	78
4.3	The specification of the reflective opto switch.	83
4.4	Calibration value of Watt meter as a function of input voltage to the analogue-digital converter.	89
4.5	Calibration value of the water flow rate as a function of output voltage for condenser (a) and evaporator (b).	94
5.1	Specifications for frequency-voltage converter for water flow meters and Watt meter.	109

6.1	Listing of data file showing time dependence of some of recorded variables.	125
6.2(a)	Parameters of initial condition for mode 1 experiment.	135
6.2(b)	Parameters of initial condition for mode 2 experiment.	135
6.2(c)	Parameters of initial condition for mode 3 experiment.	135
6.3(a)	Numerical values for cycles A,B and C shown in figure 6.8(a).	144
6.3(b)	Numerical values for cycles A,B and C shown in figure 6.8(b).	144
6.3(c)	Numerical values for cycles A,B and C shown in figure 6.8(c).	144
6.4	Experimental performance data showing various output water temperatures at different water flow rates passing through the evaporator. Entry water temperature to evaporator and condenser is 15°C.	155
7.1	Numerical values of constants A,B and C calculated for equations 7.3,7.4 and 7.5.	165
7.2	Numerical values of constants for equation 7.8.	170
7.3	The compressor efficiencies of the water-to-water heat pump system at three different discharge pressures. The efficiencies decrease as the pressure ratio P_1/P_4 increases.	174

7.4	Comparison of refrigerant mass flow calculated by using energy absorbed by the evaporator Q_e (MF) and the work done by the compressor W_R (MG) with mechanical efficiency of 0.85, 0.90 and 0.95.	178
7.5	Numerical values of constants for equation 7.19.	189
7.6	Numerical values of the constants for equations 7.21 and 7.22.	194
7.7	Numerical values of constants for equation 7.26	199
7.8	Illustrative result from the computer model with guessed value of $T_e = 0^\circ\text{C}$.	203
7.9	A comparison of the experimental and simulation results for various water flow rates (\dot{m}_e) and output water temperatures of condenser ($T_{W_{CO}}$) at entering condenser water temperature of 15°C	206
7.10(a)	Computer simulation for various operating conditions at 20ml/s water flow rate through the evaporator.	207
7.10(b)	Computer simulation for various operating conditions at 30ml/s water flow rate through the evaporator.	208
7.10(c)	Computer simulation for various operating conditions at 40ml/s water flow rate through the evaporator.	209

- 7.11 Computer simulation showing the minimum water flow rate through the evaporator (\dot{m}_e) at low input water temperatures. Water input temperature to condenser is 15°C. 211
- 7.11 Computer simulation showing the maximum water flow rate through the evaporator (\dot{m}_e) at various input water temperatures. Water input temperature to condenser is 15°C. 214

LIST OF FIGURES

Figure No:		Page
2.1	Thermodynamic model of (a) Heat engine and (b) Heat pump.	7
2.2.	Temperature-entropy diagram for a reversed Carnot cycle heat pump.	9
2.3	(a) Heat pump cycle when a gas is the refrigerant. (b) Reversed Carnot cycle when a refrigerant is used.	13
2.4.	The ideal vapour-compression cycle.	14
2.5.	Schematic diagram of a vapour-compression cycle.	16
2.6.	Pressure-enthalpy diagram for ideal vapour-compression cycle.	17
2.7.	The practical heat pump cycle.	20
2.8.	P-V and P-v diagrams for ideal compressor.	34
3.1.	The water-to-water heat pump components.	44
3.2.	Position of thermocouples in, (a) Water line. (b) Refrigerant line.	47
3.3	Compressor Danfoss SC10H performance as given by manufacturer.	49
3.4.	(a) Schematic diagram of thermostatic expansion valve. (b) Operation of control system by the expansion valve.	52
3.5.	Heat exchanger. (a) Condenser. (b) Evaporator.	57

3.6.	Construction of the condenser showing the sight glass, accumulator, remote bulb of the expansion valve, compressor and pressure transducer.	58
3.7.	(a) Schematic diagram of water regulator. (b) Operation control by the water regulator.	62
3.8.	Filter drier.	65
3.9.	Link-up system of leak testing, moisture removal and refrigerant loading process.	65
4.1.	The position of sensors and transducers in the heat pump system.	71
4.2.	Thermocouple junction with gain x100 connected to PCI1001.	74
4.3.	The copper-constantan thermocouple calibration.	75
4.6.	The electrical details of the reflective opto switch.	81
4.7.	The reflective opto switch in operation, detecting the scale divisions passing per second.	81
4.8.	The electronic circuit of the reflective opto switch.	84
4.9.	The block diagram of the power measurement for the compressor.	84
4.10.	The block diagram for Watt meter calibration.	84
4.11.	Watt meter calibration.	86
4.12.	Block diagram for the water flow rate measurement.	92

4.13	Water flow rate calibration; (a) Condenser and (b) Evaporator.	94
5.1	The data acquisition system for the water-to-water heat pump system.	97
5.2	The experimental set-up for the water- to-water heat pump system.	98
5.3	Analogue-digital converter PCI1001 with connections to pressure transducers, water flow meter and Watt meter.	1022
5.4	The schematic diagram for the frequency-voltage converter.	107
5.5	Input voltage limiting.	108.
5.6	The circuit for the water flow meter.	110
5.7	The circuit for the Watt meter.	110
5.8	Position of sensors in the heat pump system.	112
5.9	Position of sensors in refrigerant and water lines.	112
5.10	The flow diagram of the sampling program.	117
6.1	The experimental set-up of the heat pump in producing hot water.	121
6.2(a)	The temperature variation at the inlet and outlet of the condenser for mode 1 experiment.	136
6.2(b)	The temperature variation at the inlet and outlet of the condenser for mode 2 experiment.	136
6.2(c)	The temperature variation at the inlet and outlet of the condenser for mode 3 experiment.	136

6.3(a)	Temperatures T_2 and TW_i corresponding to figure 6.2(a). Enlarged scale.	137
6.3(b)	Temperatures T_2 and TW_i corresponding to figure 6.2(b). Enlarged scale.	137
6.3(c)	Temperature T_2 and TW_i corresponding to figure 6.2(c).	137
6.4(a)	The variation of water flow rate through the evaporator and condenser for mode 1 experiment.	138
6.4(b)	The variation of water flow rate through the evaporator and condenser for mode 2 experiment.	138
6.4(c)	The variation of water flow rate through the evaporator and condenser for mode 3 experiment.	138
6.5(a)	Pressure variation across the expansion valve and compressor for mode 1 experiment.	139
6.5(b)	Pressure variation across the expansion valve and compressor for mode 2 experiment.	139
6.5(c)	Pressure variation across the expansion valve and compressor for mode 3 experiment.	139
6.6(a)	Variation of electrical power consumption to the compressor for mode 1 experiment.	140
6.6(b)	Variation of electrical power consumption to the compressor for mode 2 experiment.	140

6.6(c)	Variation of electrical power consumption to the compressor for mode 3 experiment.	140
6.7(a)	Variation of energies Q_c, Q_e and W_c for mode 1 experiment.	141
6.7(b)	Variation of energies Q_c, Q_e and W_c for mode 2 experiment.	141
6.7(c)	Variation of energies Q_c, Q_e and W_c for mode 3 experiment.	141
6.8(a)	Variation of C.O.P. for mode 1 experiment.	142
6.8(b)	Variation of C.O.P. for mode 2 experiment.	142
6.8(c)	Variation of C.O.P. for mode 3 experiment.	142
6.9(a)	The refrigerant cycle of the mode 1 experiment.	143
6.9(b)	The refrigerant cycle of the mode 2 experiment.	143
6.9(c)	The refrigerant cycle of the mode 3 experiment.	143
6.10(a)	Temperature profile for water heating in the water tank - water controlled by water regulator.	146
6.10(b)	Temperature profile for water heating in the tank - water regulator not in the circuit, flow rate kept constant.	146
6.11	Water flow rate in the condenser and evaporator for figure 6.10 (a) (.) and figure 6.10 (b) (+).	147

6.12	Temperature profile of the water in the tank during water heating - electric element heater of 1.2kiloWatt.	147
6.13	Schematic diagram for water heating using an electric element.	150
7.1	Experimental set-up for heat extraction using the heat pump system.	162
7.2	Refrigerating capacity and the power requirement of the compressor.	165
7.3	Energy pick-up during compressor cooling.	168
7.4	The variation of polytropic index against the pressure ratio across the compressor.	168
7.5	Indicator diagram for an ideal isothermal compression cycle and ideal polytropic compression cycle.	173
7.6	Refrigerant mass flow rate at three different discharge pressures.	184
7.7	Pressure losses in the evaporator for different discharge pressures.	184
7.8	Relation between the temperature of refrigerant after the expansion valve (T_3) and evaporating temperature (T_e).	188
7.9	Relation between temperature of the suction superheated gas (T_4) and the temperature after the expansion valve (T_3).	188
7.10	The relation between temperature difference across the evaporator ($T_{W_{ei}} - T_{W_{eo}}$), and temperature of the refrigerant after the expansion valve (T_3) at three different water flow rates.	190

7.11	The pressure losses across the condenser at three discharge pressures.	190
7.12	The effect of the discharge pressure on the water flow rate through the condenser.	193.
7.13	The minimum allowable water flow rate to avoid freezing in the evaporator. Output water temperature of the evaporator ($T_{w_{e0}}$) set at 1.0°C .	212
7.14	The maximum permissible water flow rate to limit the temperature after the expansion valve (T_3) to 10.0°C .	215

NOMENCLATURE.

A.C.	alternating current.
c_p	specific heat of gas at constant pressure.
c_v	specific heat of gas at constant volume.
c_w	specific heat of water.
C.O.P	coefficient of performance of a heat pump.
C.O.P.(WP)	coefficient of performance of a heat pump including power for water pump.
D.C.	direct current.
H	enthalpy.
H_1	enthalpy of discharge gas.
H_C	vapour-gas enthalpy at condensing pressure.
H_L	liquid-vapour enthalpy at condensing pressure.
H_2	enthalpy of subcooled liquid.
H_3	enthalpy after the expansion valve.
H_E	vapour-gas enthalpy at evaporating pressure.
H_4	enthalpy at superheat gas.
H_I	enthalpy at the end of isentropic compression.
\dot{m}_c	water mass flow rate through the condenser.
\dot{m}_e	water mass flow rate through the evaporator.
\dot{m}_F	refrigerant mass flow rate in the refrigerant cycle.
Δm_c	mass of refrigerant gas in clearance volume.

n	polytropic index.
P_1	discharge pressure.
P_2	outlet pressure of the condenser.
P_3	pressure after the expansion valve.
P_4	suction pressure.
P_C	condensing pressure.
P_E	evaporating pressure.
Q	quantity of heat.
Q_c	energy delivered by the condenser.
Q_e	energy absorbed by the evaporator.
Q_y	energy pick-up during compressor cooling.
R	gas constant.
S_s	entropy of suction superheated gas.
T_1	refrigerant discharge temperature.
T_2	refrigerant temperature at the evaporator inlet.
T_3	refrigerant temperature at the evaporator inlet.
T_4	refrigerant temperature at the evaporator outlet (compressor inlet).
T_F	refrigerant temperature between filter drier and expansion valve.
T_c	refrigerant condensing temperature.
T_e	refrigerant evaporating temperature.
$T_{W_{ei}}$	input water temperature to the evaporator.
$T_{W_{eo}}$	output water temperature from the evaporator.

TW_i	input water temperature to the condenser.
TW_o	temperature of water after the compressor.
TW_{ci}	temperature of water coming from water supply or water tank.
TW_{co}	output water temperature from the condenser.
TK	temperature of water in the water tank at various levels.
V	quantity of volume.
v	specific volume of a gas.
V_c	clearance volume.
V_s	swept volume.
W	quantity of work done.
W_c	electrical power to the compressor.
W_p	polytropic work.
W_R	work done on the superheated gas.
W_{iso}	isothermal work.
η_{iso}	isothermal efficiency.
η_{isen}	isentropic efficiency.
η_m	mechanical efficiency.
η_{vol}	volumetric efficiency.

CHAPTER 1.

INTRODUCTION.

Lord Kelvin [1,2] in 1850s gave the name 'heat multiplier' to a device which absorbed heat at a low temperature and rejected it at a higher temperature. The modern term for such a device is 'heat pump'. This device permits an environment to be heated to a higher temperature than the ambient temperature, by using less fuel in the device than if such fuel was burned directly in a furnace. He proposed a scheme for heating houses by absorbing energy from the earth [1].

Very little attention was given to the heat pump ideas in the United Kingdom, since in the 1950s the high capital cost of the devices and the poor reliability prevented them competing effectively with existing heat generators using fossil fuels[3]. It seems

that since the Middle East crisis in 1973, when the price of fossil fuel rose sharply, heat pump costs can now be considered to be more acceptable. Together with the emphasis on using energy more effectively the circumstances for the use of heat pumps may now be more economically favourable.

The first heat pump in Britain was built by J.G.N. Haldane in 1930 [1,4], followed by J.A. Sumner in 1946 [2]. The former unit provides heat for hot water and space heating for domestic purposes, using outside air as the heat source. The latter was a much larger commercial unit using soil and underground water supplies as the heat sources.

Several projects have been carried out recently using solar assisted heat pumps to optimise the performance of the system, for example Neal et al [5] have reported their work for a domestic space and water heating system using a solar assisted heat pump, Mac Arthur et al [6] reported on a solar assisted heat pump system with a conventional back-up unit and Morgan [7] describes a series solar heat pump using freon R11 as the working fluid designed specifically for use in a tropical climate.

A basic modern compression closed cycle heat pump comprises two heat exchangers, a compressor and an

expansion valve, refrigerant is taken around a closed loop. The environment of the evaporator and the condenser define the type of heat pump.

In this study, a water-to-water heat pump system suitable for domestic use has been investigated. This type of heat pump absorbs heat from cold water and delivers it as hot water. In order to study the performance of the system, a heat pump was assembled in such a way that the required parameters (temperature, pressure and flow rate) could be easily measured.

The objectives of the study were to;

1. Analyse the performance of the assembled heat pump. In order to do the analysis, the performance of each component making up the heat pump has to be investigated.
2. Analyse the performance of the system during water heating in a domestic hot water tank.
3. Develop suitable instrumentation to interface with a micro computer.
4. Develop a computer model based on experimental data. Then, the performance of the system within its working range

could be predicted by using the model,
which would then be used in other design.

In order to achieve these objectives, the
following steps were carried out;

1. Assembling of the heat pump system.
2. Attachment of the sensors to the system
at appropriate points, e.g. thermocouples,
pressure transducers, Watt meter and water
flow meters.
3. Construction of the electronic systems
leading to a microcomputer where the
information from the sensors could be
recorded and displayed during sampling.
4. Variation of the input parameters to the
system, e.g. temperature of the water to
be heated, and of the energy source; water
flow rate; and hot water output temperature,
so that the response of the system to a
change in input parameters could be studied.

The development of this study towards these
objectives permits the identification of situations
where a domestic water-to-water heat pump system could
be operated with optimum performance.

CHAPTER 2.

THEORY OF THE HEAT PUMP AND ITS PRINCIPLE OF OPERATION.

2.1 Introduction.

The thermodynamic analysis of the heat pump is similar to the analysis of the refrigerator. In fact they are the same machine which absorbs heat at a low temperature and rejects it at a higher one [9,10] . The distinguishing factor that makes them differ is only the application. In refrigeration attention is given to the absorption of heat and the cooling of a chilled space. If attention is given to the heat rejected at the other end of the machine and to heating applications, then it is called a heat pump. Because of this, the involvement of thermodynamic parameters like temperature, pressure, specific volume, enthalpy

and entropy in both refrigerators and heat pumps are the same.

Like other equipment, heat pumps are limited in operation. These limitations are not only imposed by mechanical and engineering problems but also by the environment in which they operate, e.g. how much the condenser water temperature needs to be increased. These limitations can be better appreciated if the principle of operation and the thermodynamic properties are well understood.

Since the theory of the heat pump is based upon thermodynamics, the subject matter presented in this chapter consists principally of the thermodynamic cycle involved, with particular emphasis upon those elements which have direct application to heat pumps.

2.2 The Principle of Operation of The Heat Pump - The Reversed Carnot Cycle.

The principle of operation of a heat pump can be shown schematically on the same diagram as the heat engine as shown in figure 2.1. In the heat engine, heat is supplied at a high temperature T_c , mechanical work is performed and the residual heat is rejected at a low temperature T_e [4]. By referring to

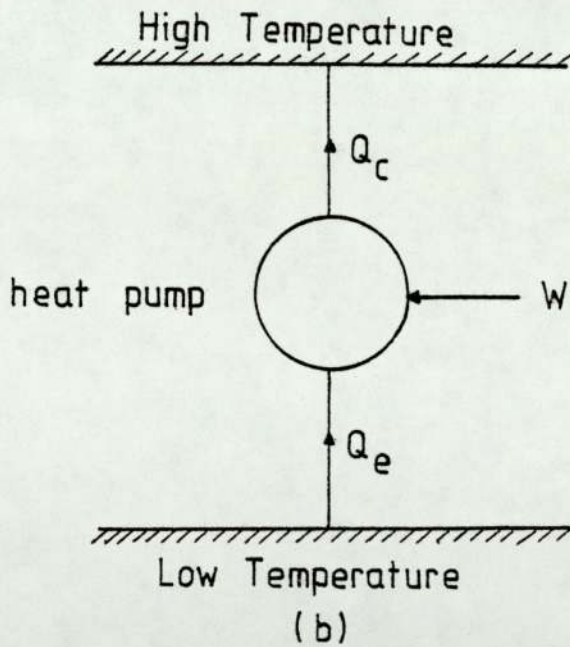
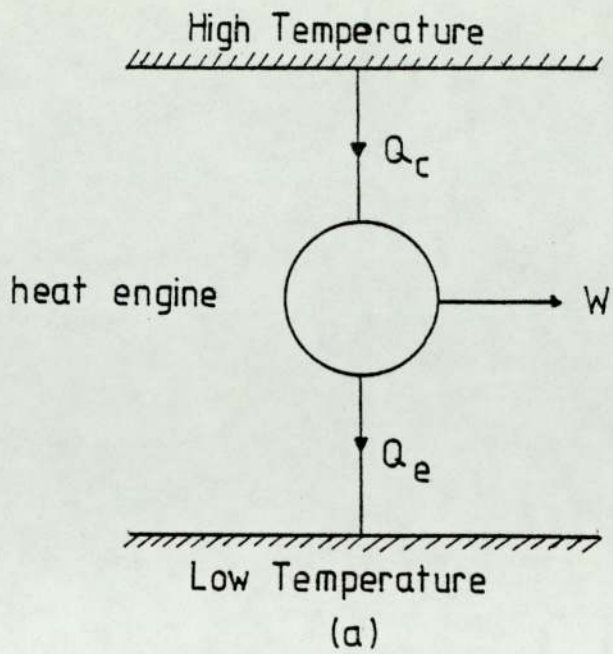


Figure 2.1: Thermodynamic model of,
a. Heat engine.
b. Heat pump.

figure 2.1, the equation of energy balance can be written as,

$$Q_c = Q_e + W \quad 2.1$$

where Q_c is the quantity of heat given to the heat engine, Q_e is the heat rejected and W is the work performed by the engine.

By contrast, in the case of the heat pump, the heat is supplied at a low temperature; mechanical work is done to effect its transfer to the high temperature. The heat, that is the sum of heat supplied and mechanical work done, is rejected to the high temperature sink. Thus, equation 2.1 is still valid with the origin of Q_c and Q_e different from those in the heat engine.

The cycle involved in this ideal operation is called the Carnot cycle for the heat engine and reversed Carnot cycle for the heat pump [10]. This cycle operating as a heat engine or as a heat pump is familiar from the study of thermodynamics [11].

The Carnot heat pump cycle can be illustrated by using a temperature-entropy diagram as shown in figure 2.2. The sequence of operation on the working fluid can be explained as follows;

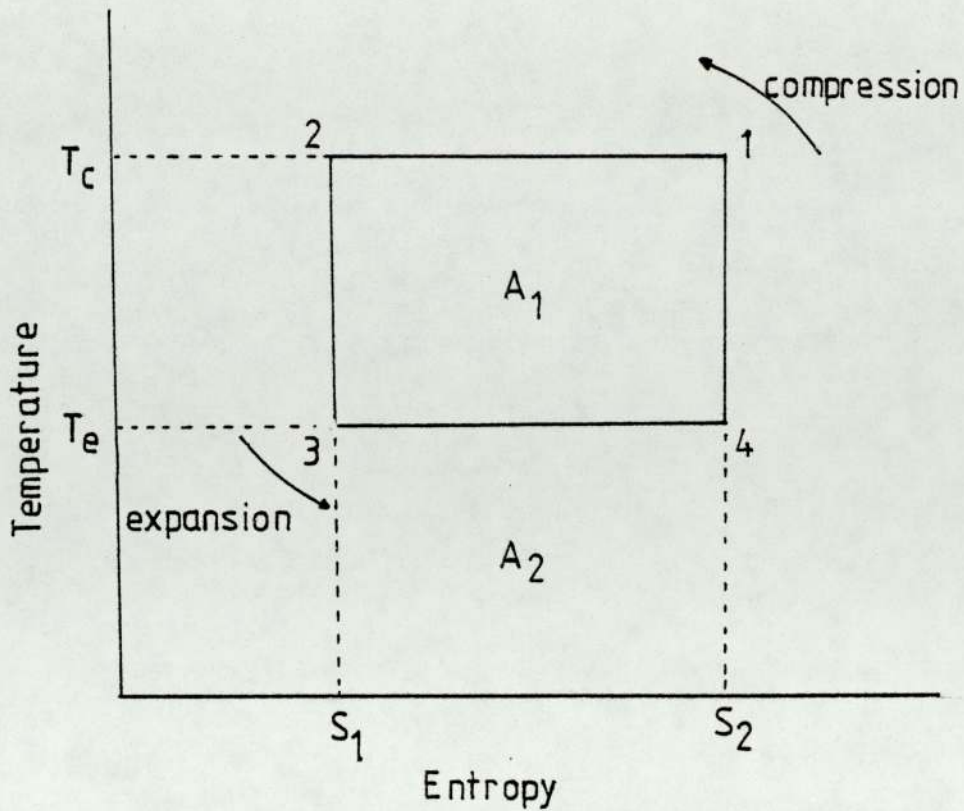


Figure 2.2: Temperature-entropy diagram for a reversed Carnot cycle heat pump.

- 4 - 1: The refrigerant is compressed adiabatically to high temperature T_c .
- 1 - 2: Heat Q_c is rejected isothermally at high temperature T_c .
- 2 - 3: The refrigerant is allowed to expand isenthalpically to low temperature T_e .
- 3 - 4: A quantity of heat Q_e is absorbed isothermally at low temperature T_e .

All the processes in the Carnot cycle are thermodynamically reversible since ideal operation is considered to take place. As a result, processes 4-1 and 2-3 are isentropic. Since the Carnot cycle consists of reversible processes, its efficiency is higher than could be achieved in an actual cycle. This means that the Carnot cycle can be used as a standard of comparison as well as a convenient guide to the maximum effectiveness which could be achieved by a machine operating between the evaporating and condensing temperatures.

2.2.1 Coefficient of Performance of The Reversed Carnot Cycle.

The efficiency of the heat pump cycle is called the coefficient of performance [8,9].

Its symbol is C.O.P. It is defined as;

$$\text{C.O.P.} = \frac{\text{The amount of heat delivered by heat pump}}{\text{The net work done by the system}} \quad 2.2$$

The performance of a Carnot heat pump cycle can be calculated based on the temperature-entropy diagram as in figure 2.2. The heat given out in a reversible process is;

$$Q_c = \int TdS$$

which is equivalent to the area $A_1 + A_2$. The net work

done by the system is represented by the area A_1 .

Therefore the C.O.P. of the Carnot heat pump cycle is;

$$\begin{aligned}(\text{C.O.P.})_C &= \frac{A_1 + A_2}{A_1} \\ &= \frac{T_c (S_2 - S_1)}{(T_c - T_e)(S_2 - S_1)} \\ &= \frac{T_c}{T_c - T_e} \qquad 2.3\end{aligned}$$

From this equation, the C.O.P. of a Carnot heat pump cycle is entirely a function of the temperature limits and it represents the highest performance that can theoretically be achieved.

The Carnot heat pump cycle is thermodynamically reversible, which carries with it certain limitations and restrictions. For example, the isothermal expansion and compression must be exactly that, and this is not possible to achieve in practice.

2.2.2 Using Vapour as a Refrigerant.

Stoecker and Jones [12] have shown that if a gas, such as air, is used as the refrigerant in the reversed Carnot cycle, the cycle would appear as in

figure 2.3(a) rather than figure 2.2 which has been mentioned earlier. The isentropic compression and expansion processes are 4-1 and 2-3 respectively. Processes 1-2 and 3-4 are constant-pressure cooling and heating processes respectively.

This cycle which uses vapour as a refrigerant, differs from the Carnot cycle operating between the same two temperatures by addition of areas x and y . At point 4 the temperature must be lower than the water passing through the evaporator so that as the gas receives heat in the constant-pressure process it rises to a temperature no higher than that of the water. For similar reasons T_c must be above the temperature of the water passing through the condenser [12]. The effect of area x is to increase the work required, which decrease the C.O.P. The effect of area y is to increase the work required and to reduce the amount of refrigeration capacity. Both these effects of area x and y reduce the C.O.P.

Figure 2.3(b) shows the reversed Carnot cycle when wet compression is operated. Process 1-2, a condensing process, occurs in the condenser and process 3-4, an evaporating process, occurs in the evaporator.

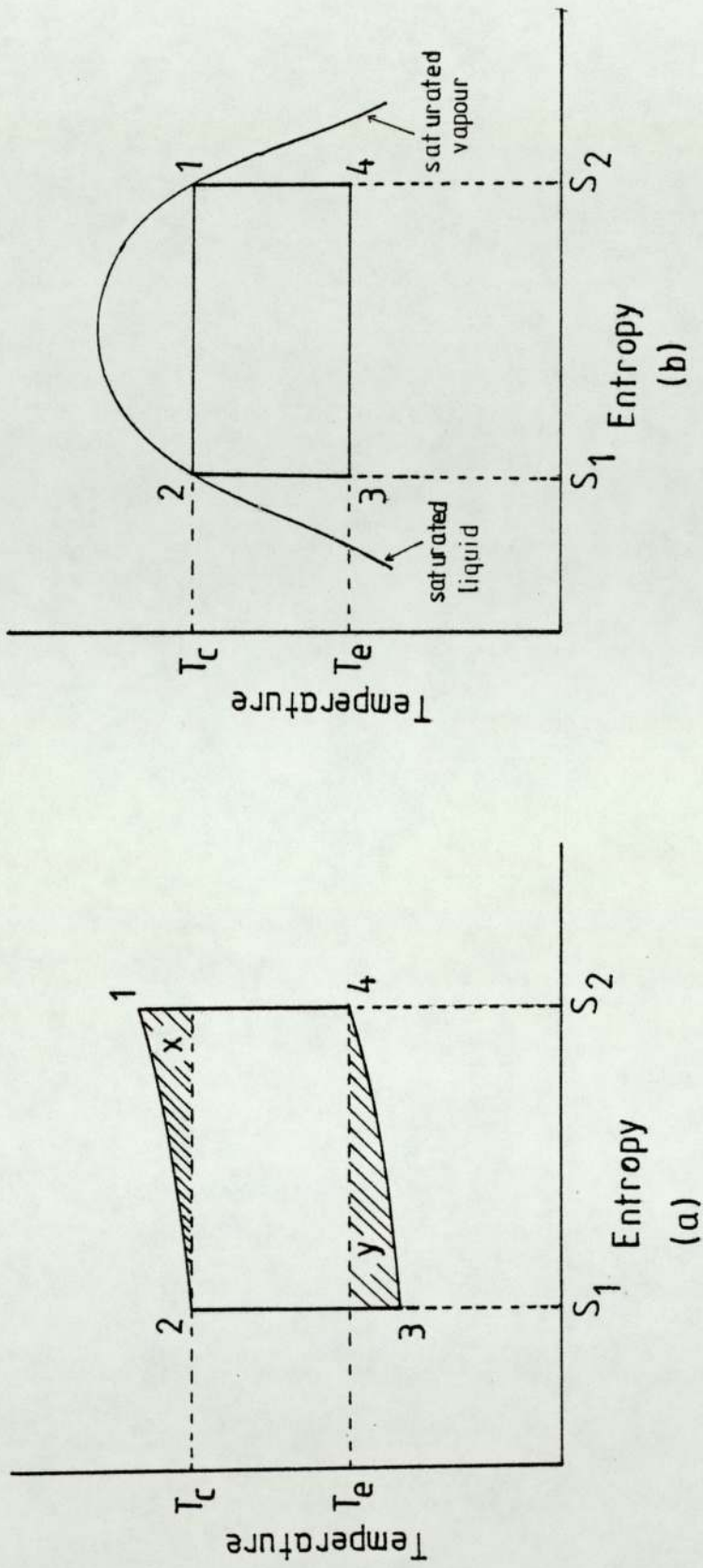


Figure 2.3: (a) Heat pump cycle when a gas is the refrigerant.
 (b) Reversed Carnot cycle when a refrigerant is used.

2.3 The Vapour Compression Cycle.

As has been mentioned earlier the reversed Carnot cycle is a theoretical cycle that cannot be operated practically. The compression process 4-1 in figure 2.3(b), for example, occurs in the liquid-vapour region. This process cannot be used in practice since the liquid refrigerant may be trapped in the head of the cylinder by the rising piston, which can damage the cylinder head in the compressor itself, when a reciprocating compressor is used [4,12]. Another possible danger of wet compression is that the droplets of liquid refrigerant may wash the lubricating oil from the walls of the cylinder, resulting in accelerating wear. Because of this dry compression is preferable, where the refrigerant enters the compressor in the form of saturated vapour as in figure 2.4.

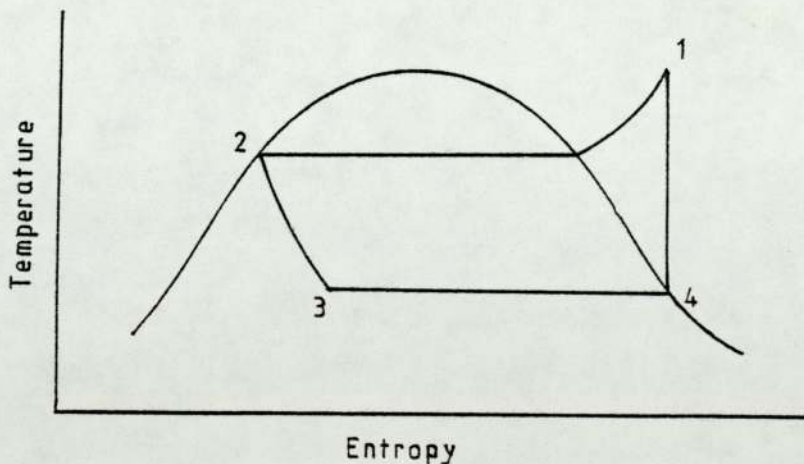


Figure 2.4: The ideal vapour-compression cycle.

Since the compression starts at the saturated vapour line, the refrigerant leaves the compressor in superheated form 1, with a temperature higher than in the reversed Carnot cycle.

Another revision of the Carnot cycle is the expansion process 2-3. In this process the pressure is reduced with no transfer of heat, that is an isenthalpic process. The isenthalpic throttling process is irreversible and during this process the entropy increases. So the throttling process takes place from 2-3 as in figure 2.4.

The cycle that operates as in figure 2.4 is called the ideal vapour-compression cycle. During this process the refrigerant is continuously changing its physical properties.

Figure 2.5 shows the schematic diagram of a vapour-compression circuit. By referring to figure 2.4 and 2.5, the operation of the ideal vapour-compression cycle can be explained as followed;

4 - 1: Dry saturated vapour refrigerant is reversibly compressed adiabatically to a high pressure and high temperature superheated vapour. The compression occurs at constant entropy.

1 - 2: The superheated vapour enters the

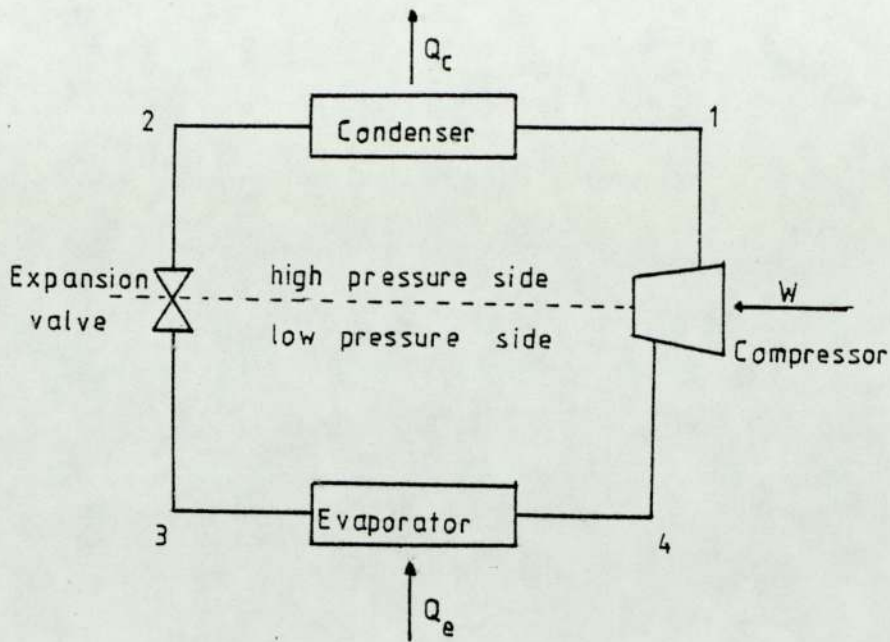


Figure 2.5: Schematic diagram of a vapour-compression circuit.

condenser at constant high pressure, causing desuperheating and condensation of the refrigerant. The refrigerant gives out heat at high temperature.

2 - 3: The refrigerant is expanded irreversibly at constant enthalpy from high saturated liquid pressure to low evaporating pressure.

3 - 4: At low pressure and temperature, the refrigerant absorbs heat causing evaporation to saturated vapour.

To this end, it is universal practice [4] to show the ideal vapour-compression cycle on a

pressure-enthalpy (p-h) diagram as in figure 2.6. Since the p-h diagram is also the usual graphic means of presenting refrigerant properties [13,14] , it is easier to show the ideal vapour-compression cycle by using a p-h diagram.

The transformation from a temperature-entropy diagram to a p-h diagram can well be understood by referring to figure 2.4 and 2.6. The operation steps 4-1-2-3-4 in both cycles can be explained on temperature-entropy (figure 2.4) and p-h (figure 2.6) diagrams respectively.

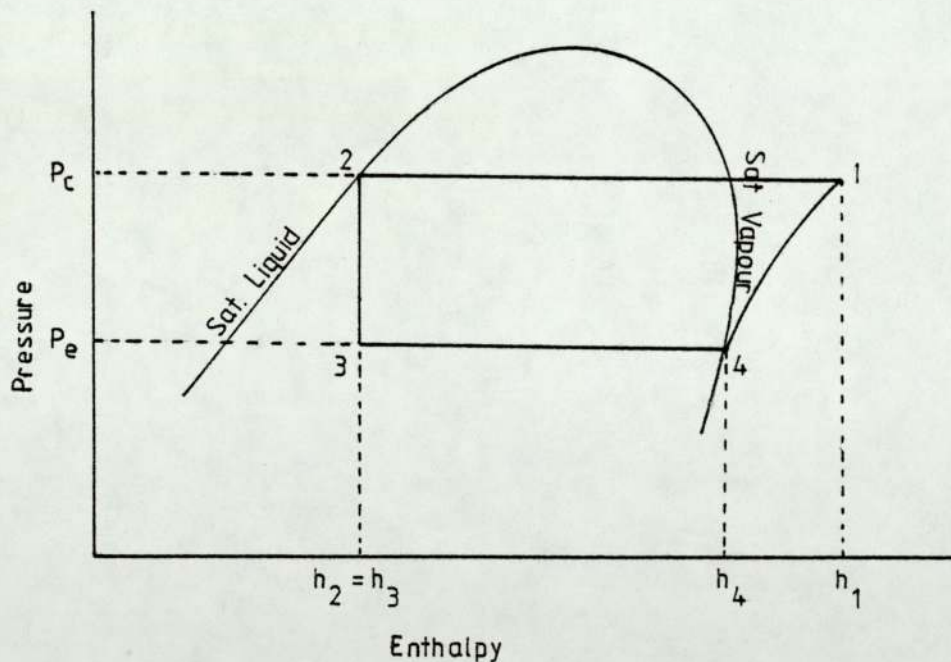


Figure 2.6: Pressure-enthalpy diagram for ideal vapour-compression cycle.

2.3.1 Coefficient of Performance of The Ideal Vapour-compression Cycle.

By referring to the ideal vapour-compression cycle in figure 2.6, the significant quantities of the cycle can be determined. During process 3-4, the heat transfer is Q_e into the system from the heat source at the evaporator. In the process 1-2, a quantity Q_c of heat is rejected at the condenser. The work of compression W_c is done during process 4-1 isentropically. The expansion process is the isenthalpic process where there is no heat loss or gain.

Both evaporating and condensing processes occur at constant pressures (low and high pressure respectively). The p-h diagram as in figure 2.6 shows clearly the irreversible nature of the isenthalpic throttling process 2-3 and the effect of the temperature difference through desuperheating. This implies that the ideal reversed Carnot cycle no longer occurs.

If h_1, h_2 and h_4 represent the enthalpies of the refrigerant at points 1, 2 and 4 (enthalpies at points 2 and 3 are the same), then energies involved in kilojoules per kilogram in the ideal vapour-compression cycle are;

$$4 - 1: \text{Work of compression } W_c = h_1 - h_4$$

1 - 2: Heat of condensation $Q_c = h_1 - h_2$

2 - 3: Isenthalpic expansion

3 - 4: Heat of evaporation $Q_e = h_4 - h_2$

Therefore, the C.O.P. of the ideal vapour-compression cycle as defined in equation 2.2 can be written as;

$$\begin{aligned} \text{C.O.P.} &= \frac{Q_c}{W_c} \\ &= \frac{h_1 - h_2}{h_1 - h_4} \end{aligned} \qquad 2.4$$

2.4 The Practical Heat Pump Cycle.

The working cycle described in the previous section is an ideal cycle, although it takes into account practical limitations in the need for dry vapour compression.

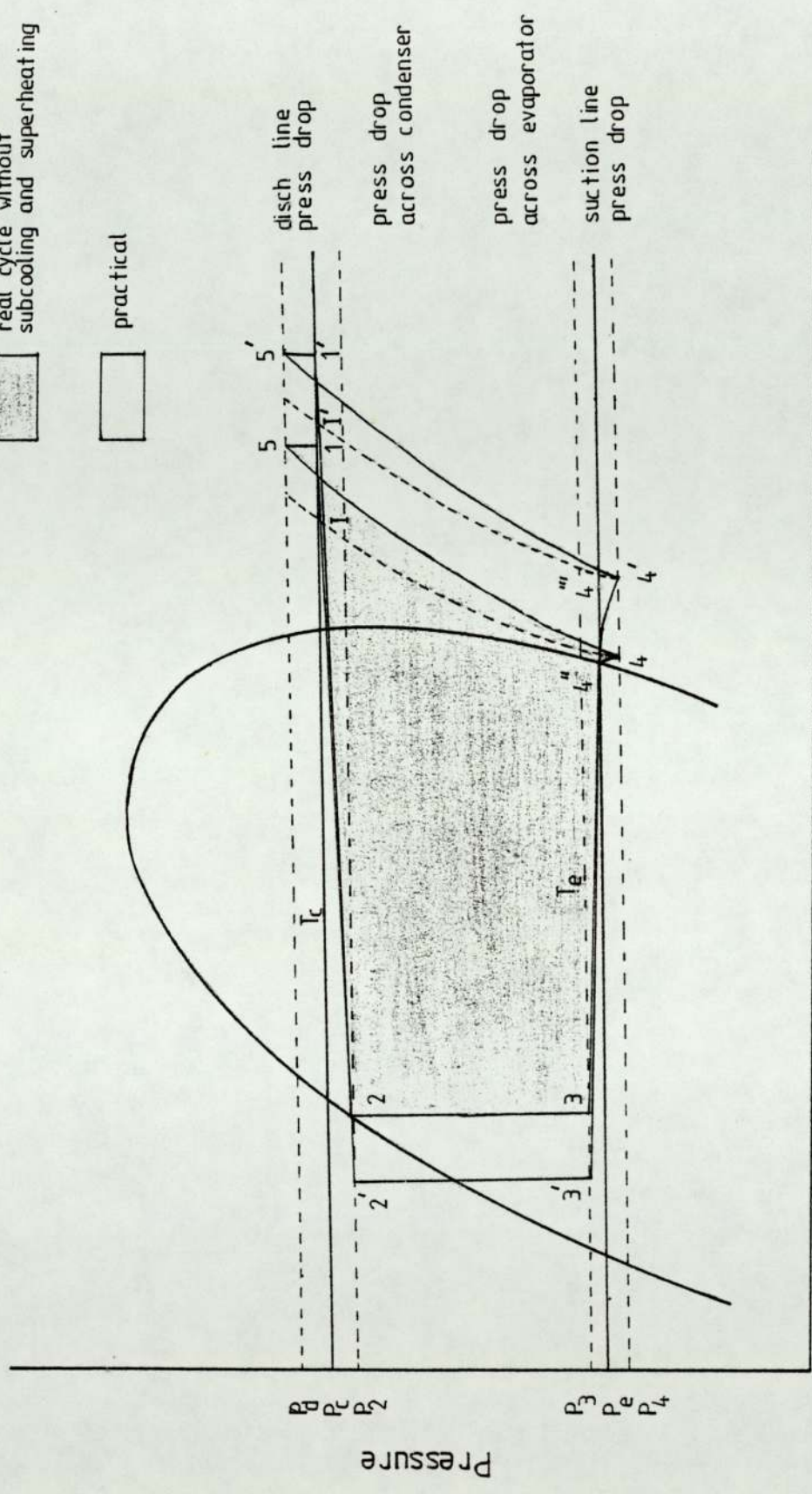
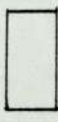
In practice, as well as the finite temperature difference effect already mentioned, most authors [4, 12,15] include the pressure losses in the pipe work, valves, condenser and evaporator.

One component which apparently dominates the design of the heat pump cycle is the compressor. The small reciprocating compressors appropriate to heat pump applications have a very poor tolerance for

real cycle without subcooling and superheating



practical



Enthalpy

Figure 2.7: The practical heat pump cycle.

liquid refrigerant. This is because the liquid, being incompressible, can cause extensive damage to valves and connecting rods if it is allowed to enter the cylinder of the compressor [8,15]. For this reason, the vapour should be slightly superheated in the evaporator. This is achieved by using a thermostatic expansion valve which controls the flow of refrigerant so that it superheats slightly before entering the compressor. This is shown in figure 2.7 where the refrigerant enters the compressor at state 4' instead of 4".

As a result of the drop in pressure in the evaporator, the vapour leaves the evaporator at a lower pressure and saturation temperature and with a greater specific volume than if no drop in pressure occurred. These effects are shown in figure 2.7 as 4 instead of 4" in the ideal cycle and 4' instead of 4"' in practical cycle. Line 4"-4' represents the drop in pressure experienced by the suction vapour in flowing through the suction line from the evaporator to the compressor inlet as well as the drop in pressure due to vapour flowing through the suction valves and passage of the compressor into the cylinder.

The first effect leads to the second major change to the working cycle, which is to lower the compressor efficiency. Because of heat transfer between

the refrigerant and the compressor and because of the irreversibility in the flow through the compressor, the compressor will increase the enthalpy by a greater amount than the ideal, which results in an increased discharge temperature. In figure 2.7 this effect is shown as 1 instead of I in ideal cycle and 1' instead of I' in practical cycle.

Lines 1-5 and 1'-5' represent the drops in pressure required to force the discharge valves open against the spring-loading and to force the vapour out through the discharge valves and passages of the compressor into the discharge line for the ideal cycle and practical cycle respectively.

Apart from compressor, there are practical inefficiencies in other components of the working cycle. A reasonably high refrigerant velocity should be maintained to avoid oil collecting in the evaporator and condenser; but as a consequence there will be pressure losses in the condenser and associated pipework. The effect is apparent both in the evaporator and the condenser as shown in figure 2.7.

Another final deviation from the ideal vapour-compression cycle is the subcooling. In the ideal cycle, the expansion starts from point 2 on the liquid saturation line. Any pressure loss, however, in the pipe between the condenser and expansion valve may

cause the formation of some vapour, which will impair the valve's performance. Therefore it is necessary to subcool the refrigerant to point 2' for example. This subcooling will also reduce the proportion of vapour entering the evaporator, and will increase the performance of the heat pump, as more heat can be released for the same power supply to compressor.

2.4.1 Coefficient of Performance of The Practical Heat Pump Cycle.

If h_1' , h_2' and h_4' represent the enthalpies of the refrigerant at state points 1', 2' and 4' (enthalpies at point 2' and 3' are the same) in the practical cycle shown in figure 2.7, then the energies involved in kilojoules per kilogram of refrigerant are;

4' - 1': Actual work of compression

$$W'_c = h_1' - h_4'$$

1' - 2': Actual heat of condensation

$$Q'_c = h_1' - h_2'$$

2' - 3': Isenthalpic expansion

3' - 4': Actual heat of evaporation

$$Q'_e = h_4' - h_2'$$

Therefore, from the practical cycle;

$$\text{C.O.P.} = \frac{h_1' - h_2'}{h_1' - h_4'} \quad 2.5$$

The performance indicated by the practical cycle is lower than the ideal Carnot cycle and ideal vapour-compression cycle due to the various considerations mentioned earlier. The pressure loss in the condenser reduces the condensing pressure (and T_c) and so reduces the heat output. Similarly the pressure loss in the evaporator lowers the suction pressure (and T_e), increasing the work of compression, and reducing Q_e . These effects will lower the C.O.P. of the practical cycle, even though the enthalpies h_1, h_2 and h_4 remain unaltered.

The amount of increase in enthalpy due to irreversibility of the compressor is often expressed by isentropic efficiency [4,16,17] . The isentropic efficiency is defined as;

$$\begin{aligned} \eta_{isen} &= \frac{\text{change of enthalpy on isentropic comp.}}{\text{change of enthalpy added by comp.}} \\ &= \frac{h_{1'} - h_{4'}}{h_1 - h_{4'}} \end{aligned} \quad 2.6$$

where $h_{1'}$ is the enthalpy at the end of isentropic compression. Therefore,

$$\eta_{isen} = \frac{W'}{W'_c} \quad 2.7$$

where W'_c is the actual work done by the compressor and W' is the isentropic work.

2.5. Choice of Refrigerant.

The refrigerant is the working fluid of the

heat pump. Heat is collected and released by changes of the refrigerant, and is moved by its circulation. The right choice of refrigerant is essential for optimum performance.

As mentioned earlier, the properties of the chosen refrigerant can be observed from the p-h diagram. Firstly, since the refrigerant changes its state during operation, its critical point (that point above which a separate liquid phase cannot exist) should be above the highest possible condensing temperature. It is also useful, to have the minimum saturation pressure in the cycle above atmospheric pressure, to ensure that any system leakage will be outward rather than inward to avoid moisture and air entering the system.

Secondly, the compression ratio between vapour pressure at the evaporator and condenser should be as small as possible to minimise the work of compression, and the condenser pressure should be reasonably low so that light weight equipment and piping can be used on the high pressure side.

Thirdly, the refrigerant should have the highest possible latent heat of evaporation and smallest possible specific volume at the compressor inlet. This means that the refrigerant can collect more heat during evaporation. The smaller the specific volume, the less the compressor work and size.

Other factors which are also important are its

R	Chemical name	Formula	Mol weight kg/k mol	Normal boiling point (°C)	Critical temperature (°C)	Freezing point (°C)
11	Trichloromono-fluoromethane	C Cl ₃ F	137.4	23.8	198.0	-111.0
12	Dichlorodifluoromethane	C Cl ₂ F ₂	120.9	-29.7	111.5	-157.8
13	Monochlorotri-fluoromethane	C Cl F ₃	104.5	-81.4	28.3	-181.1
14	Carbontetrafluoride	C F ₄	88.0	-128.0	-45.5	-183.9
21	Dichloromono-fluoromethane	CH Cl ₂ F	102.9	8.9	178.5	-135.0
22	Monochlorodifluoromethane	CH Cl F ₂	86.5	-40.7	96.0	-160.0
30	Methylene chloride	CH ₂ Cl ₂	84.9	40.6	235.0	-97.0
40	Methyl chloride	CH ₃ Cl	50.5	-23.8	143.1	-97.5
113	Trichlorotri-fluoroethane	C ₂ Cl ₃ F ₃	187.4	47.6	214.1	-35.0
114	Dichlorotetra-fluoroethane	C ₂ Cl ₂ F ₄	170.9	3.6	145.7	-93.9
115	Monochloropenta-fluoroethane	C ₂ Cl F ₅	154.5	-38.7	80.0	-106.0
116	Hexafluoroethane	C ₂ F ₆	138.0	-78.2		

Table 2.1: Information on some of the refrigerants.

chemical stability, toxicity, availability and cost. A discussion on these aspects is given by Dossat [15].

The most common refrigerants are the fluorinated hydrocarbons, but numerous other substances also function well as refrigerants, including many inorganic compounds and hydrocarbons. The groups of halogen compounds is divided into two, the first based on methane such as refrigerants R11, R12, R13, R14, R20, R21 and R22, and the second based on ethane such as refrigerants R110, R111, R112, R113 and R114. Table 2.1 gives information on some of these refrigerants [13,14]. From this table it can be seen that refrigerants R113 and R114 have high normal boiling points and relatively high critical temperature. R12 and R22 have intermediate normal boiling point and high critical temperatures and R13 and R14 have low normal boiling point and low critical temperature.

2.5.1. Thermodynamic Properties of Refrigerants - Graphical Representation.

No one refrigerant satisfies all the requirements for all heat pump systems. R11, R12 and R22 are commonly used in domestic type systems [6,7,18]. As an example

to show that the right choice of refrigerant is important to optimise the performance of the heat pump, consider refrigerants R11 and R12.

The thermodynamic properties of refrigerants R11 and R12 are presented in table 2.2. The values in the table are based on the ideal vapour-compression cycle [14] with an evaporating temperature of 0°C and condensing temperature of 50°C .

From an analysis of the properties of refrigerants R11 and R12 in table 2.2, it can be seen that some materials might be preferable to others. For, example, in an ideal vapour-compression cycle (Mc Mullan and Morgan [18] and Heap [9] call it an ideal reversed Rankine cycle), the heat pump operating between 0°C and 50°C with R12 as refrigerant, the work of compression is 24.42kJ/kg and the C.O.P. is 5.2; but, if R11 is used, the corresponding values are 31.06kJ/kg and 5.68 respectively. The discharge temperature of R12 is 56.7°C and R11 is 60°C . This makes it appear that R11 is the preferred refrigerant.

Further inspection of table 2.2, however, shows the difficulties. Firstly, the compression ratio is higher with R11, and the evaporator pressure is

	Refrigerant R11	Refrigerant R12
Evaporating temperature ($^{\circ}\text{C}$)	0	0
Condensing temperature ($^{\circ}\text{C}$)	50	50
Evaporating pressure (kPa)	40.19	308.69
Condensing pressure (kPa)	234.71	1219.64
Pressure ratio	5.84	3.95
Suction specific volume (m^3kg^{-1})	0.40309	0.05538
Discharge specific volume (m^3kg^{-1})	0.08066	0.01483
Discharge temperature ($^{\circ}\text{C}$)	60.0	56.7
Refrigerant effect (kJ kg^{-1})	145.38	102.59
Energy given out (kJ kg^{-1})	176.44	127.01
Compression power (kJ kg^{-1})	31.06	24.42
Coeff. of Performance	5.68	5.20

Table 2.2 : Thermodynamic properties of refrigerants R11 and R12 at evaporating temperature of 0°C and condensing temperature of 50°C .

lower than atmospheric pressure which is 101.325kPa. More importantly, however, the specific volume of R12 is only $0.05538\text{m}^3/\text{kg}$ compared to R11 which occupies $0.40309\text{m}^3/\text{kg}$. This is a serious difference since in any practical system the compressor displacement is fixed and is determined by the cylinder size and the piston speed. This means that for R11 as refrigerant, a compressor with a bigger cylinder volume or a faster piston speed would be required than would be the case for R12.

This analysis, based on the ideal vapour-compression cycle and the physical properties of the actual refrigerant used is very helpful as it gives a measure of the best possible performance with that particular refrigerant. However, this analysis takes no account of the performance of the system components themselves, of the irreversibilities introduced through friction, the non-adiabatic behaviour of the compressor or the finite temperature difference effects at the heat exchanger.

2.6 Work Transfer in a Reversible Reciprocating Compressor.

The function of the compressor in a heat pump system is to pump refrigerant around the circuit

and to produce the required increase in the pressure of the refrigerant vapour.

Thermodynamically, the process of compression on dry superheated refrigerant gas can be considered as a polytropic compression process [16]. In a real process, the state during compression can be described approximately by a relation of the form,

$$Pv^n = \text{constant} \quad 2.14$$

where n is a constant called index of compression or polytropic index [11,16,17] and P and v are average values of pressure and specific volume for the system.

For the reversible polytropic process, single values of P and v can truly define the state of a system, and work done per unit mass during a change from state 4 to 1 may then be calculated as follows. For the initial, final and any intermediate state,

$$P_4 v_4^n = P_1 v_1^n = Pv^n$$

Therefore, the work done per cycle on the gas,

$$\begin{aligned} W_R &= \int_4^1 P dv = P_4 v_4^n \int_{[4]}^{[1]} \frac{dv}{v^n} \\ &= P_4 v_4^n \frac{(v_1^{1-n} - v_4^{1-n})}{1-n} \end{aligned}$$

$$\therefore W_R = \frac{P_1 v_1 - P_4 v_4}{1-n} \quad 2.15$$

Therefore, the energy equation for a reversible polytropic process may be written as,

$$Q = \frac{(P_1 v_1 - P_4 v_4)}{1 - n} = (u_1 - u_4)$$

$$\therefore Q = (u_1 - u_4) + \frac{(P_1 v_1 - P_4 v_4)}{1 - n} \quad 2.16$$

where $u=h-Pv$ is the internal energy. When the fluid is a perfect gas, these expressions can be written as,

$$W_R = \frac{R}{1-n} (T_1 - T_4) \quad 2.17$$

$$Q = c_v (T_1 - T_4) + \frac{R}{1-n} (T_1 - T_4)$$

where c_v is the specific heat of the gas and R is its gas constant. Therefore,

$$Q = (c_v + \frac{R}{1-n}) (T_1 - T_4) \quad 2.18$$

Since $P_4 v_4^n = P_1 v_1^n$ and $Pv=RT$

Therefore,

$$\frac{T_1}{T_4} = \left(\frac{P_1}{P_4} \right)^{(n-1)/n} \quad 2.19$$

and
$$\frac{T_1}{T_4} = \left(\frac{v_1}{v_4} \right)^{1-n} \quad 2.20$$

If in the compression from state 4 to 1,

the values of T and P or T and v are known, the polytropic index n can then be calculated directly from the above equation.

Since the compression is reversible, the work done W_R in equation 2.15 can be considered as isentropic. If the work done per cycle in a real process is W_c , then from equation 2.7,

$$\eta_{isen} = \text{Isentropic efficiency} = \frac{W_R}{W_c} \quad 2.21$$

2.6.1 Working Analysis of The Ideal Compressor.

Consider a reciprocating compressor in operation with valves permitting the refrigerant to flow into and out of the cylinder. The volume displaced by the piston's stroke is called the swept volume (V_s). There is always minimum volume, the clearance volume (V_c), when the piston is at the end of the stroke. This is necessary to accommodate the valves and avoid contact of piston and cylinder head.

Figure 2.8(a) shows how the pressure in the cylinder varies during one revolution of the machine cycle. The change in state of the refrigerant as it

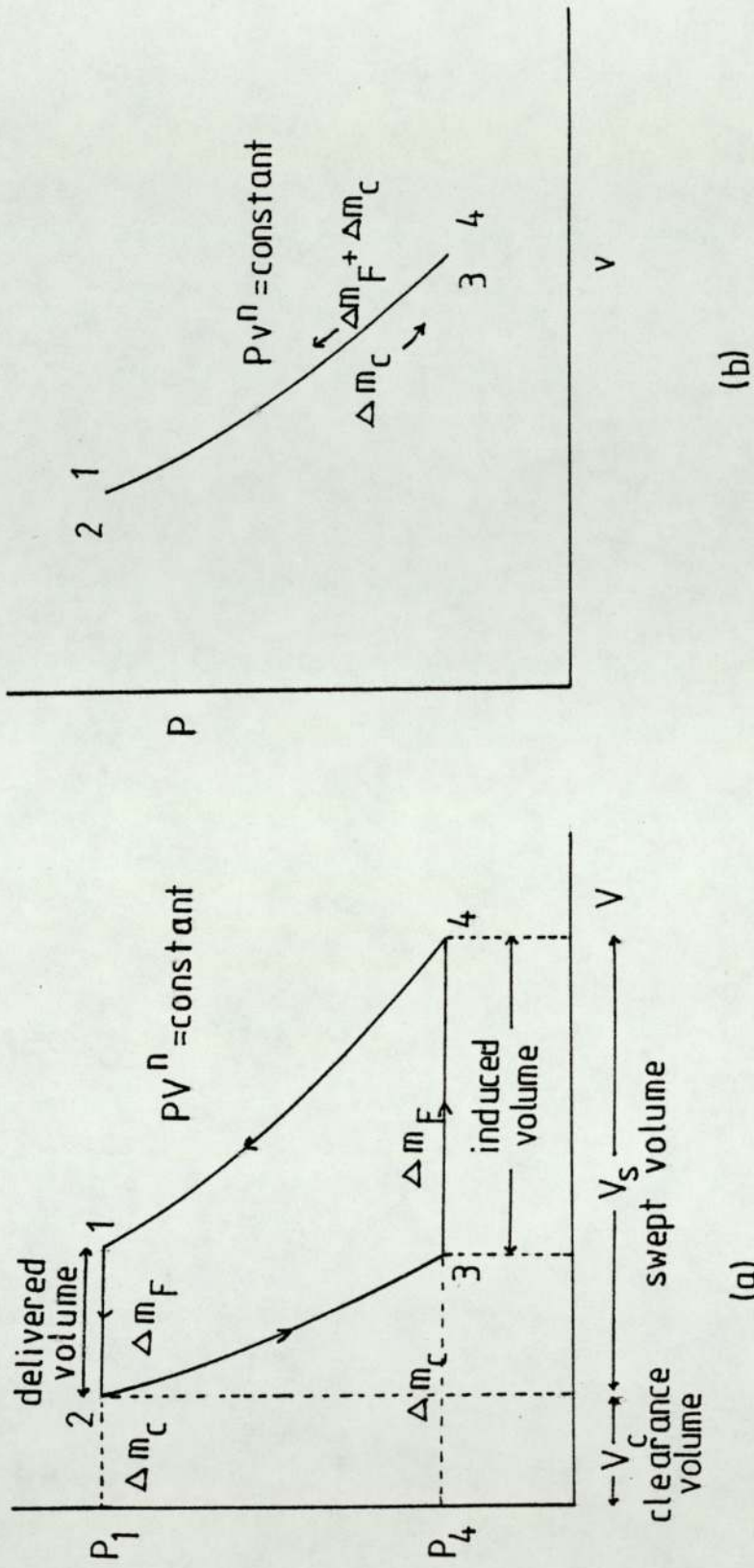


Figure 2.8: P-V and P-v diagrams for ideal compressor.

passes through the machine is shown in figure 2.8(b).

In the real compressor all processes are irreversible. The compression process and the expansion of the clearance volume gas are both considered to obey the same polytropic law, $Pv^n = \text{constant}$, and induction and delivery are at constant pressure [16,19]. The following analysis can be made,

3 - 4: The inlet valve is opened, and the mass of refrigerant Δm_F in state 3,4 enters the cylinder without change of state. It mixes reversibly with a mass Δm_C already present in the clearance volume in the same state.

4 - 1: Both valves are closed and the refrigerant gas ($\Delta m_C + \Delta m_F$) is compressed according to a law $Pv^n = \text{constant}$ to state 1,2.

1 - 2: The exhaust valve is opened and a mass Δm_F is delivered from cylinder without further change of state.

2 - 3: Both valves are closed and a mass Δm_C is expanded to original state 3,4.

The net work done per machine cycle is the

algebraic sum of the work transfers in the four processes. Referring to figure 2.8,

$$dW = \int_3^4 PdV + \int_4^1 PdV + \int_1^2 PdV + \int_2^3 PdV = \oint PdV$$

$dW =$ the area of the P-V diagram.

Since the compression and expansion are polytropic, equation 2.15 can be used. Therefore,

$$dW = P_4(V_4 - V_3) + \frac{(P_1 V_1 - P_4 V_4)}{1-n} +$$

$$P_1(V_2 - V_1) + \frac{(P_3 V_3 - P_2 V_2)}{1-n}$$

but $P_2 = P_1$ and $P_3 = P_4$, then,

$$dW = \frac{n}{1-n} \left[P_4(V_3 - V_4) + P_1(V_1 - V_2) \right] \quad 2.22$$

The work done per cycle can also be expressed in terms of the refrigerant properties at inlet and outlet by noting that there is no change of state in process 1-2 nor 3-4. Thus specific volume $v_3 = v_4$ and $v_1 = v_2$

$$V_4 = (\Delta m_F + \Delta m_c) v_4$$

$$V_1 = (\Delta m_F + \Delta m_c) v_1$$

$$V_2 = \Delta m_c v_1$$

$$V_3 = \Delta m_c v_4$$
2.23

substitute in equation 2.22;

$$\oint dW = \Delta m_F \frac{n}{1-n} (P_1 v_1 - P_4 v_4) \quad 2.24$$

The rate of work done is obtained by multiplying the net work done during the machine cycle by the number of cycles N per unit time. If the mass flow per unit time ($N\Delta m_F$) is denoted by m_F , the rate of work done is,

$$\begin{aligned} W_R &= m_F \frac{n}{1-n} (P_1 v_1 - P_4 v_4) \quad 2.25 \\ &= m_F \frac{n}{1-n} P_4 v_4 \left(\frac{P_1 v_1}{P_4 v_4} - 1 \right) \end{aligned}$$

$$\text{and } v_1/v_4 = (P_4/P_1)^{1/n}$$

Therefore,

$$W_R = m_F P_4 v_4 \frac{n}{1-n} \left[(P_1/P_4)^{(n-1)/n} - 1 \right] \quad 2.26$$

The exact path of the compression process, i.e. the value of the polytropic index n , depends upon the heat flow through the cylinder walls. Ideally, the heat is only transferred during the process 4-1 and 2-3, because processes 1-2 and 3-4 are merely mass transfers to and from the cylinder without change of state. Therefore, the heat transferred during the expansion of Δm_c along 2-3 is equal and opposite to the heat transferred during its compression from 4-1.

The net heat transfer per cycle is therefore that associated with the compression of Δm_F along 4-1. Since the system is closed during this process, the appropriate energy equation is;

$$\begin{aligned} \oint dQ &= \Delta m_F (u_1 - u_4) + \Delta m_F \int_4^1 P dv \\ &= \Delta m_F (u_1 - u_4) + \Delta m_F \frac{1}{1-n} (P_1 v_1 - P_4 v_4) \end{aligned}$$

Since $u = h - Pv$

$$\oint dQ = \Delta m_F (h_1 - h_4) + \Delta m_F \frac{n}{1-n} (P_1 v_1 - P_4 v_4)$$

Therefore the rate of heat transfer per unit time is;

$$Q = m_F (h_1 - h_4) + m_F \frac{n}{1-n} (P_1 v_1 - P_4 v_4) \quad 2.27$$

From the above analysis of the reversible reciprocating machine, two important points should be considered.

- a. equation 2.25 shows that, for a compressor to compress a refrigerant from state 4 to state 1, the amount of negative work decreases as polytropic index n decreases.
- b. Equation 2.24 shows that the clearance volume has no effect on the work done per unit mass flow. The mass Δm_c is compressed and

expanded along the same state path and no net work is done on or by it. However, the clearance volume, does affect the capacity of the machine, i.e. the mass Δm_c of refrigerant which a cylinder of given size can handle per machine cycle. The greater the clearance volume per unit swept volume, the smaller the amount of refrigerant that can be handled by the machine.

When refrigerant is considered to be a perfect gas, the equations 2.25, 2.26 and 2.27 can be written as,

$$W_R = m_F \frac{n}{1-n} R(T_1 - T_4) \quad 2.28$$

$$W_R = m_F \frac{n}{1-n} RT_4 \left[(P_1/P_4)^{(n-1)/n} - 1 \right] \quad 2.29$$

and

$$Q = m_F c_p (T_1 - T_4) + m_F \frac{n}{1-n} R(T_1 - T_4) \quad 2.30$$

where R is a gas constant.

Since $R = c_v(\gamma - 1)$ and $c_p = \gamma c_v$

then equation 2.30 becomes.

$$Q = m_F \frac{\gamma - n}{1 - n} c_v (T_1 - T_4) \quad 2.31$$

2.6.2 Efficiencies of a Reciprocating Compressor.

It was pointed out (equation 2.25) that work done on the refrigerant gas decreases as the value of n decreases. For this reason the compressor cylinder is cooled. The compression work is minimum when $n=1$, that is for isothermal compression. This leads to quoting the performance of a compressor in terms of an isothermal efficiency, which is defined by [17,19] ,

$$\eta_{iso} = \frac{\text{isothermal work}}{\text{actual indicated work}} \quad 2.32$$

The reversible isothermal work is obtained by repeating the derivation of equation 2.25 for the special case where $n=1$. This will lead to, for perfect gas

$$\begin{aligned} W_{iso} &= -m_F P_4 v_4 \ln(P_1/P_4) \\ &= -m_F RT_4 \ln(P_1/P_4) \end{aligned} \quad 2.33$$

Therefore for the ideal reversible compressor considered above, the isothermal efficiency is,

$$\eta_{iso} = \frac{\ln(P_1/P_4)}{\frac{n}{1-n} \left[(P_1/P_4)^{(n-1)/n} - 1 \right]} \quad 2.34$$

One other important point noted before is the clearance volume, which limits the mass flow rate

which can be passed by a compressor of given cylinder volume and speed. This leads to another quantity to assess the performance of a compressor, the volumetric efficiency, which is defined as the ratio of the actual volume induced per cycle to the swept volume,

$$\eta_{vol} = \frac{(\text{volume induced})_{P,T}}{\text{swept volume}} \quad 2.35$$

From diagram in figure 2.8(a)

$$\begin{aligned} \eta_{vol} &= \frac{V_4 - V_3}{V_s} = \frac{V_s - (V_3 - V_2)}{V_s} \\ &= 1 - \frac{V_2}{V_s} \left(\frac{V_3}{V_2} - 1 \right) \end{aligned}$$

$$\therefore \eta_{vol} = 1 - \frac{V_2}{V_s} \left[(P_1/P_4)^{1/n} - 1 \right] \quad 2.36$$

Therefore for a given clearance ratio (V_2/V_s), the volumetric efficiency decreases as pressure ratio increases.

In an actual compressor, due to the effect of bearing friction, windage, etc., the actual power required to drive the compressor will be greater than the polytropic power. This is taken into account

by use of a mechanical efficiency for the compressor, defined as [17],

$$\eta_m = \frac{\text{polytropic power}}{\text{power input to compressor}} \quad 2.37$$

The overall isothermal efficiency of a compressor is defined as [17],

$$\begin{aligned} \eta_o &= \frac{\text{isothermal power}}{\text{power input to compressor}} \\ &= \frac{\text{isothermal power}}{\text{polytropic power}} \times \frac{\text{polytropic power}}{\text{power input to comp.}} \end{aligned}$$

then,

$$\eta_o = \eta_{iso} \times \eta_m \quad 2.38$$

Taking account the isentropic efficiency of the compressor due to non-adiabatic compression, therefore, if the real work done on the refrigerant is W_R and the electrical power consumed by the compressor is W_c , then;

$$\begin{aligned} W_R &= \eta_{isen} \times \eta_o \times W_c \\ &= \eta_{isen} \times \eta_{iso} \times \eta_m \times W_c \end{aligned} \quad 2.39$$

CHAPTER 3.

HEAT PUMP COMPONENTS AND ASSEMBLY.

3.1 Introduction.

Figure 3.1 shows the components of the water-to-water heat pump system. The standard components such as compressor, thermostatic expansion valve, filter drier, sight glass, water regulator and pressure gauges were supplied by Danfoss. Some of the components, e.g. thermostatic expansion valve, filter drier and sight glass are also suitable for use in a refrigeration system. All components are suitable for freon R12 as the refrigerant.

The evaporator, condenser and accumulator were designed and made in the laboratory with the help of technicians. Apart from assembling

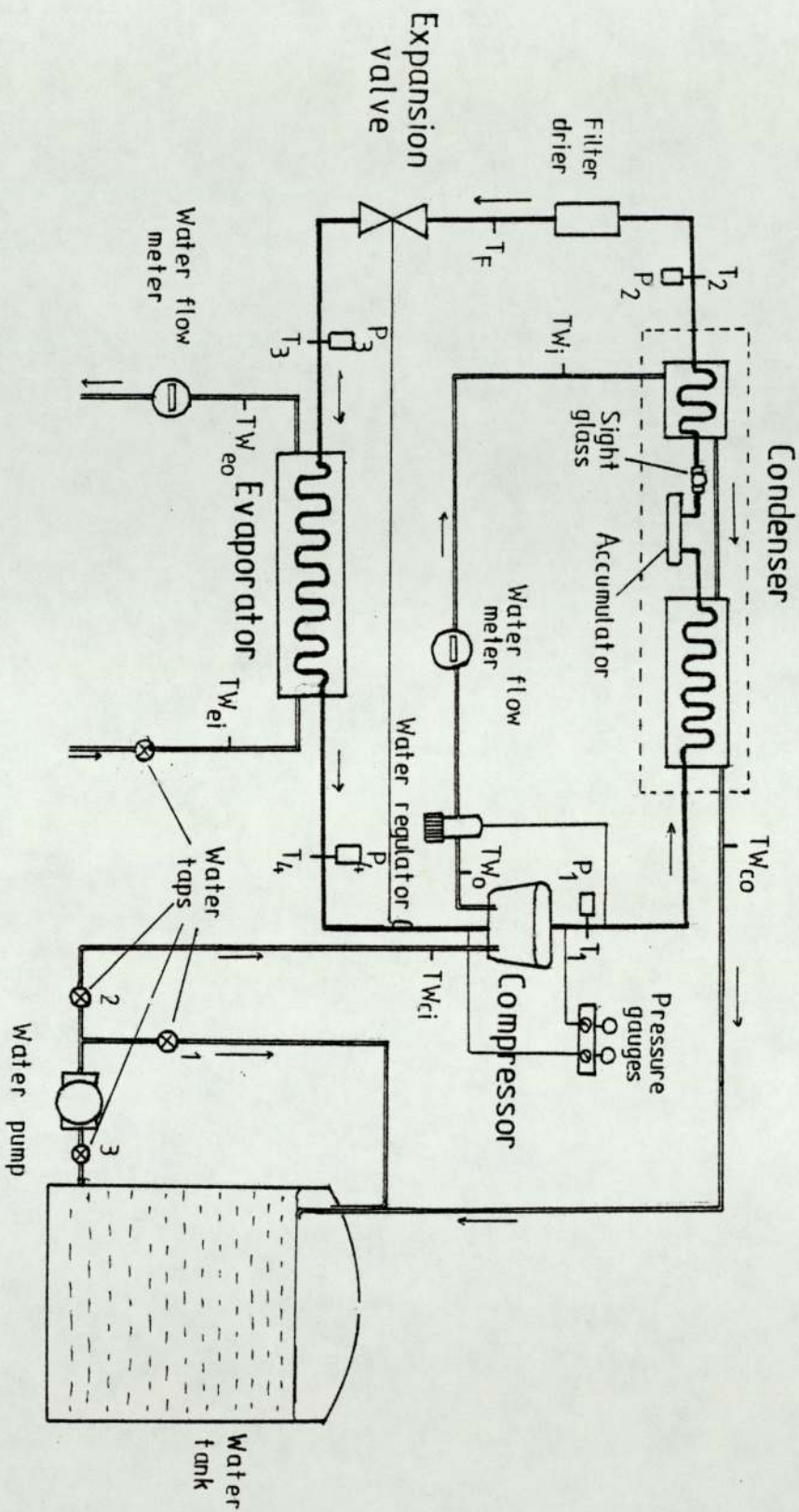


Figure 3.1: The water-to-water heat pump components.

components, consideration was also given to introducing sensors and transducers such as thermocouples, pressure transducers and water flow meters into places where the cycle of the system can be studied.

3.2 Piping and Joints.

To join the various components of the refrigerant circuit to each other and to contain the refrigerant itself, piping is required. It must be tight enough in order to contain the refrigerant at high pressure and also to keep out contaminants such as moisture.

Copper tubing was used around the refrigerant circuit. 5/16 inches copper tubes were used in connecting compressor to condenser, thermostatic expansion valve to evaporator and evaporator to compressor. In other parts $\frac{1}{4}$ inches copper tubes were used. This was done to suit the size of the standard components supplied by manufacturers. All joints in the copper tubing were done by brazing, fitting or flare. Since most of the components are standard and replacable, fitting and flare are more suitable.

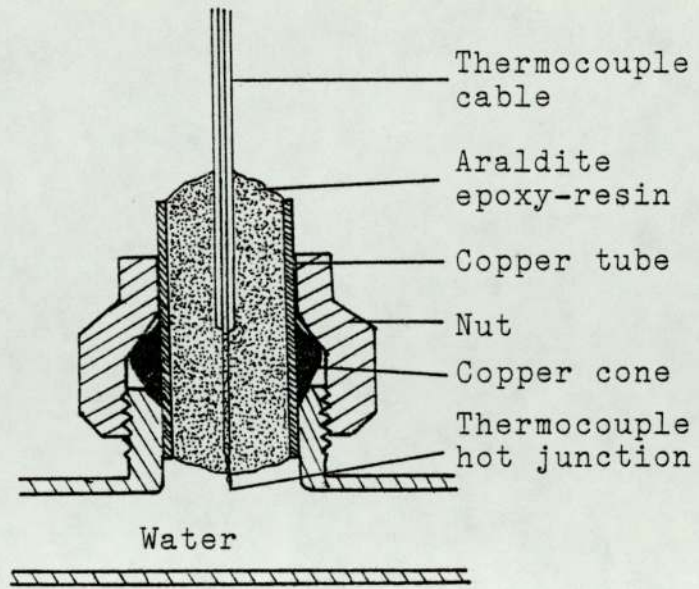
To connect evaporator and condenser to the water supply, plastic pipe was used. The bold line in figure 3.1 represents the refrigerant circuit and the dual line represents the water circuit. The diagram in this figure

was not drawn to scale. The heat exchanger, accumulator and sight glass comprise one unit, the condenser.

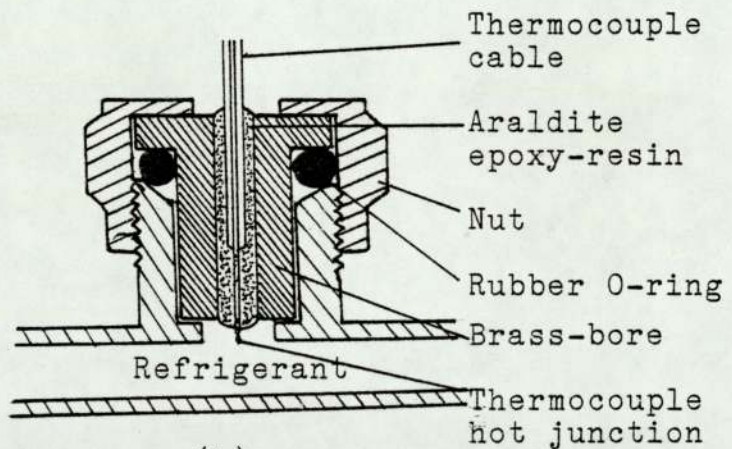
Thermocouples and pressure transducers were connected to the system by using cross and tee fittings. Cross fittings were introduced where temperature and pressure measurements were needed at the same point, such as after and before the compressor and after and before the thermostatic expansion valve. Tee fittings were introduced in water lines and before the filter drier in the refrigerant circuit, where thermocouples only were attached. All together there were eleven thermocouples and four pressure transducers in the refrigerant circuit and water lines. Five of the thermocouples were used to measure temperature around the refrigerant circuit and the other six were used to measure the temperature of the water going into and out of the system as shown in figure 3.1.

To measure the temperature profile in the water tank, eight thermocouples were placed vertically in the water tank at the centre with 10cm distance between them (not shown in figure 3.1).

Figure 3.2 shows how a thermocouple was introduced to measure the temperature of water in the water line (3.2(a)) and refrigerant in the refrigerant circuit (3.2(b)). To ensure that the connections to



(a)



(b)

Figure 3.2: Position of thermocouples in,
 (a) Water line.
 (b) Refrigerant line.

the refrigerant circuit were leak-tight a special brass-bored connector was used in every fitting in which the thermocouple cable was inserted. Araldite epoxy-resin was used to stick the thermocouple cable to the brass body and to ensure it was leak-tight. It also acted as an insulator.

3.3 Compressor.

The compressor used in the system was supplied by Danfoss [20], type SC10H. It is designed for smaller heat pump systems. It has an oil cooling coil in the oil sump, a feature of special significance in heat pump systems where water is used as the heat carrying medium on the hot side. In this water-to-water heat pump system, it is cooled by water used for carrying heat from the condenser as illustrated in figure 3.1.

The compressor is not recommended to do work at a condensing temperature higher than 60°C [20], this is in the interest of its working life and energy consumption.

The specifications of the compressor given by the manufacturer are as in table 3.1 and its performance as in figure 3.3. At 0°C evaporating temperature and 45°C condensing temperature, the heat output is

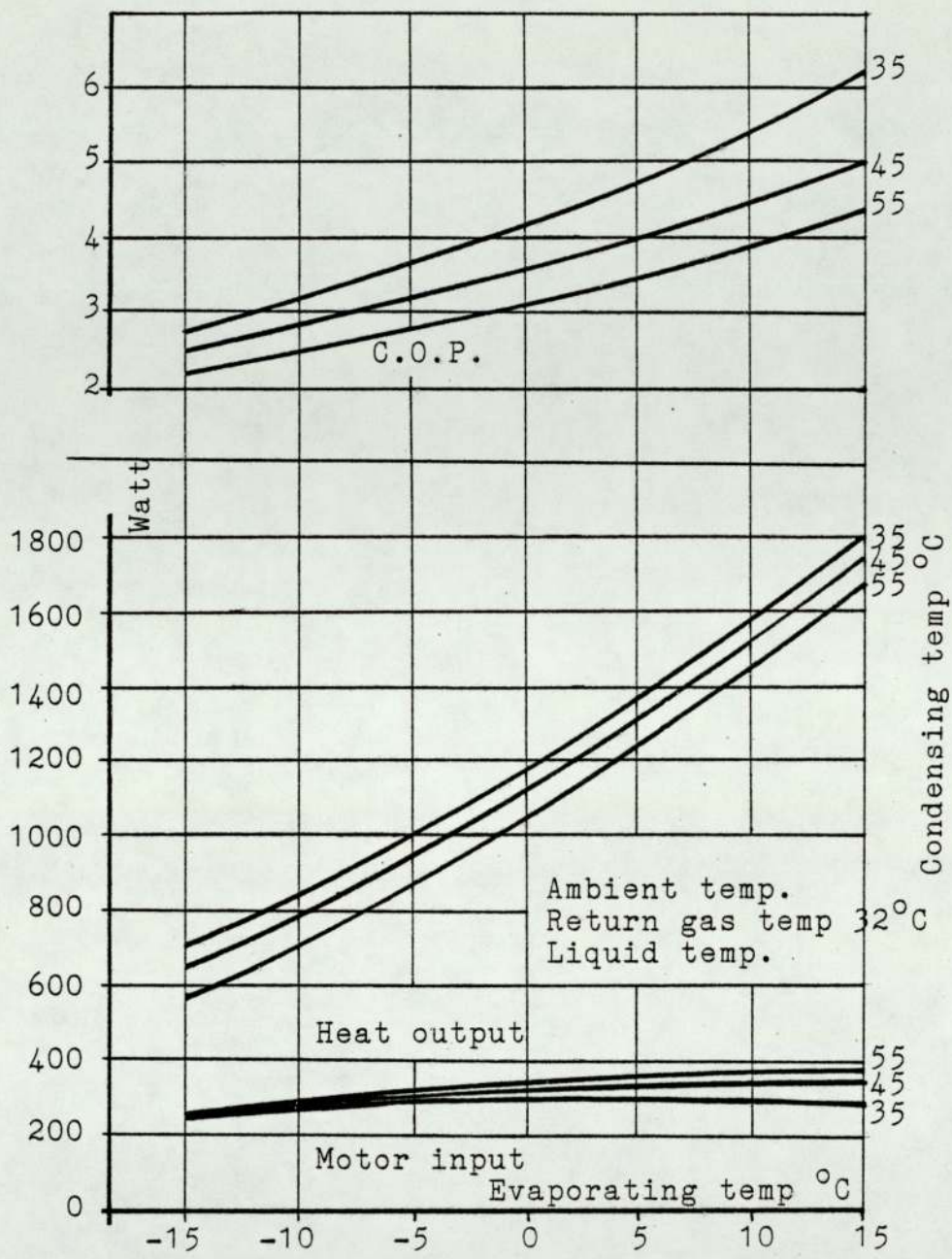


Figure 3.3: Compressor Danfoss SC10H performance as given by manufacturer.

1120 Watts, power consumed by compressor is 280 Watts and the C.O.P. is 3.89.

Type	SC10H
Refrigerant	R12
Compressor cooling	Oil or fan cooling (in this system, water is used)
Voltage range	198V-255V; 50Hz
Displacement	10.3 cm ³ /rev
Motor type	Induction motor with starting capacitor
Motor size	250 Watts
Starting current	10A
Oil charge	650 cm ³
Weight without equipment	12.1 kg
Code no	104L2515.

Table 3.1: Compressor specifications.

3.4 Thermostatic Expansion Valve.

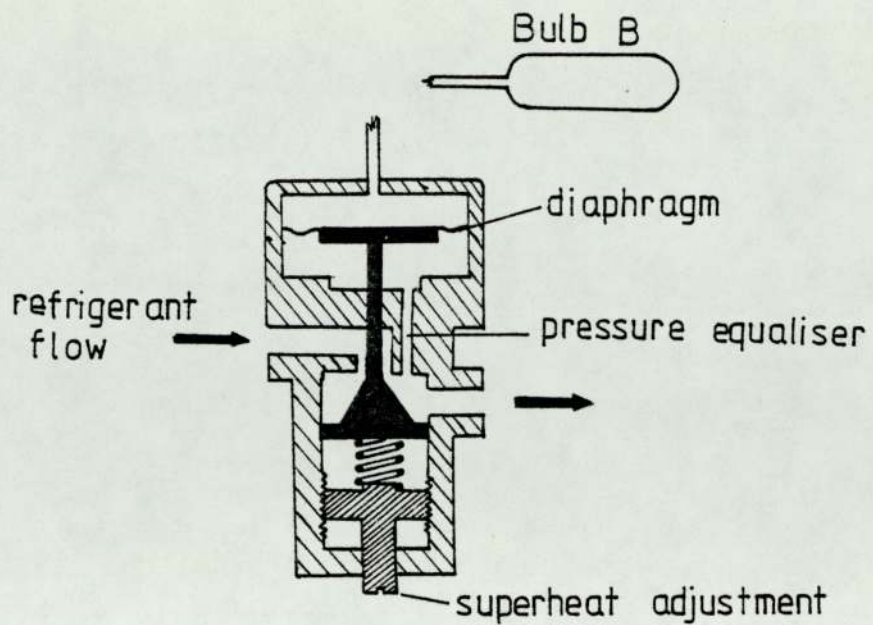
The thermostatic expansion valve is a

pressure-reducing device. It separates the high and low pressure sides of a vapour compression cycle. Its schematic diagram is shown in figure 3.4(a).

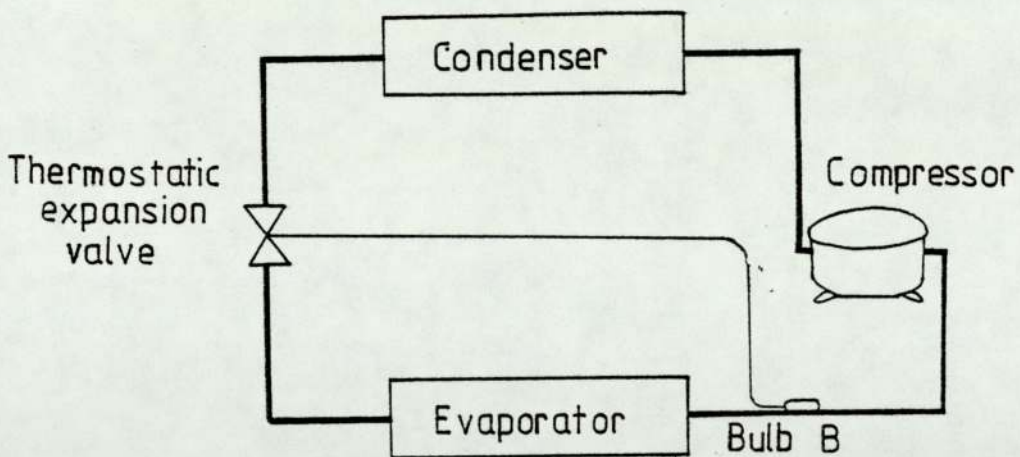
The valve consists of three main parts;

- a. An orifice, sited at low pressure side, immediately before the evaporator, which may be partially or fully closed by a spring-loaded needle or plunger.
- b. A diaphragm connected to the plunger.
- c. A sensing bulb connected via a capillary tube to the other side of the diaphragm.

Figure 3.4(b) shows the operation of the control system by the thermostatic expansion valve. The bulb B is attached to the suction pipe of the compressor with good thermal contact. If too much liquid refrigerant is admitted to the evaporator, so that it cannot all be evaporated, then liquid will appear in the suction pipe, and bulb B will be at the boiling temperature of the refrigerant in the system. As a consequence, the vapour pressure in bulb B will be the same as the refrigerant pressure in suction pipe and there will be no net force on the diaphragm due to the vapour pressure balance. However, the adjusting spring is set to add to the pressure on the refrigerant side of the diaphragm, and so the diaphragm moves up, closing the plunger



(a)



(b)

Figure 3.4: (a) Schematic diagram of thermostatic expansion valve.
 (b) Operation of control system by the expansion valve.

valve and reducing the supply of refrigerant. At this reduced refrigerant supply, the evaporator is more capable of fully evaporating its intake, and the process continues until a stage is reached where the evaporator fully evaporates the refrigerant before it reaches the end of the evaporator pipe. At this moment, the latter part of the evaporator pipe transfers sensible heat from the heat source to the refrigerant, superheating it so that it emerges from the evaporator at the bulb B with a temperature greater than the saturation temperature appropriate to the evaporator pressure. As a consequence, the bulb B is at higher temperature and the refrigerant charge inside it has a higher equilibrium pressures, which is transmitted to the upper side of the diaphragm in the expansion valve. If the pressure in the bulb B is greater than the combined effects of the refrigerant system pressure and the adjusting spring, the diaphragm will move downward, opening the plunger valve and allowing more refrigerant through.

In this process, the thermostatic expansion valve controls the refrigerant flow from evaporator to compressor such that it fully evaporates and indeed is slightly superheated. Thus the valve is acting to optimise the utilisation of the evaporator. The small degree of superheating is important to ensure that only vapourised refrigerant and not liquid is being admitted to the

compressor. Generally, the higher the superheat setting, the lower the evaporator capacity, since more heat is needed to create superheat to operate the valve [8] .

In the above system of thermostatic expansion valve, the valve uses internal equalisation, but in some cases external equalisation is used [21] where the pressure exerted on the underside of the diaphragm is the pressure at the suction pipe to compressor transmitted through the external equaliser. In the case where pressure drop through the evaporator coil is low, the use of an internal equaliser is best. Elonka and Minich [21] suggested that if pressure drop through an evaporator coil exceeds 34.47 kPa (5psi) on full load conditions, an external equaliser should be used to ensure full capacity of the coil.

In the water-to-water heat pump system assembled in the laboratory, the valve was supplied by Danfoss. The valve was factory set for 6°C superheat at a bulb temperature of 0°C. It is suggested by the manufacturer [22] that the best bulb position is on a horizontal suction line, rigidly clamped to its upper side by the supplied clip. The maximum permissible test pressure is 2687.0 kPa (375 psig). Table 3.2 shows the capacity of the valve operating at various pressure drops Δp across it [23] at given evaporating temperature.

Evaporating temp. (0°C)	Capacity in kW				
	at the pressure drop Δp across the valve				
	10^2 kPa				
	2	4	6	8	10
+10	1.0	1.2	1.3	1.5	1.6
0	1.0	1.1	1.3	1.5	1.6
-10	0.9	1.0	1.1	1.3	1.4
-20		0.8	0.9	1.0	1.1
-30		0.6	0.7	0.8	0.9
-40		0.4	0.5	0.6	0.6

Table3.2: The capacity of the thermostatic expansion valve.

3.5 Heat Exchanger.

In heat pump systems heat exchangers are needed both to collect heat into the refrigerant circuit at the evaporator and reject it at the condenser with some extra amount from the compressor. The right choice of heat exchangers, such as their sizing, is essential to the optimum performance of the system.

For this water-to-water heat pump system,

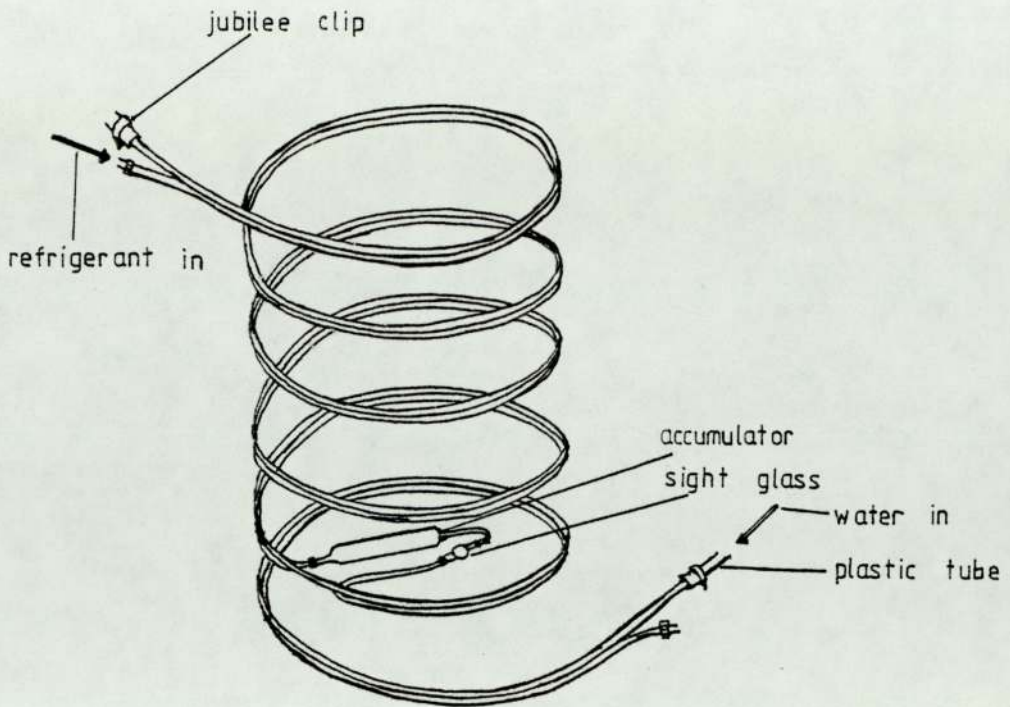
simple heat exchangers were designed. They were designed such that the system can extract heat from water and reject it to water. Consideration was also given to the design such that the refrigerant cycle and its variations could be explored.

3.5.1 Condenser.

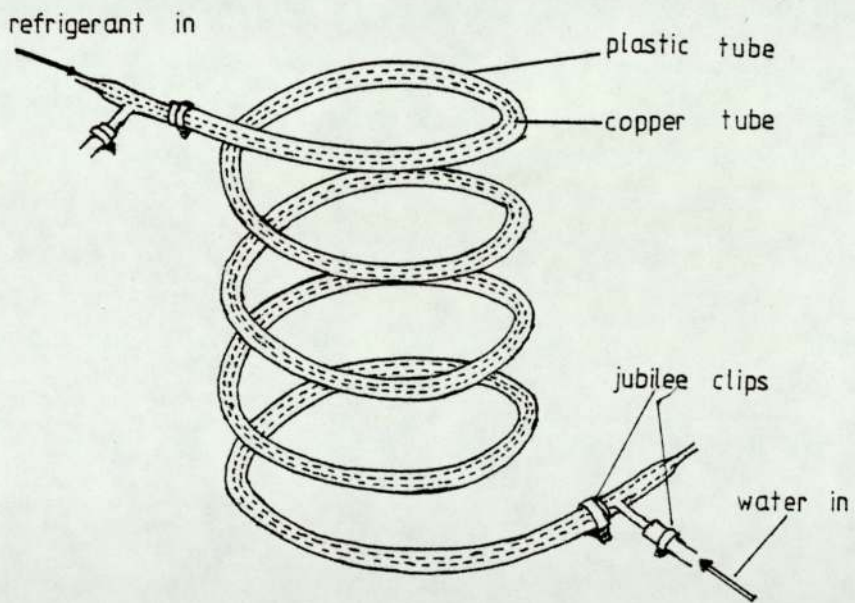
Figure 3.5(a) shows the design of the condenser used in this system. It consists of two copper pipes with different diameters ($1/4$ inches and $5/16$ inches). The $1/4$ inches pipe is for refrigerant flow and the $5/16$ inches pipe is for water to collect heat in counter direction.

The refrigerant pipe is divided into two parts. The first 12 meters was soldered to the water pipe, then to an accumulator and sight glass, then the next 3 meters was soldered again to water pipe. So The total length of the condenser is 15 meters.

In operation, the refrigerant gives out heat to water through heat exchange in the first part of the condenser. It then condenses and becomes liquid at high pressure and temperature. An accumulator is needed to hold this liquid. This provision for an accumulator is an essential feature of any heat pump system as the



(a) Condenser



(b) Evaporator

Figure 3.5: Heat exchanger.
 (a) Condenser.
 (b) Evaporator.

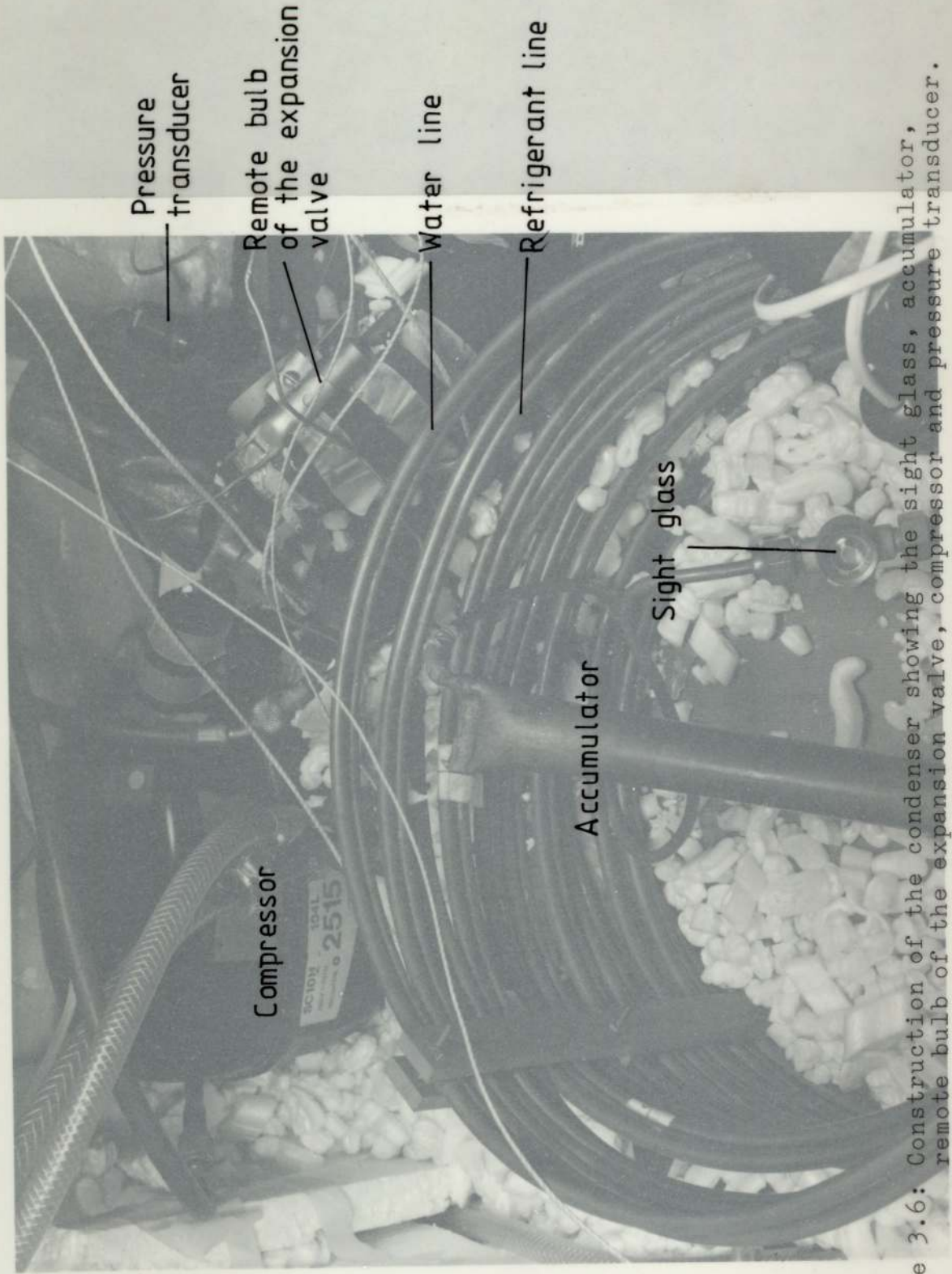
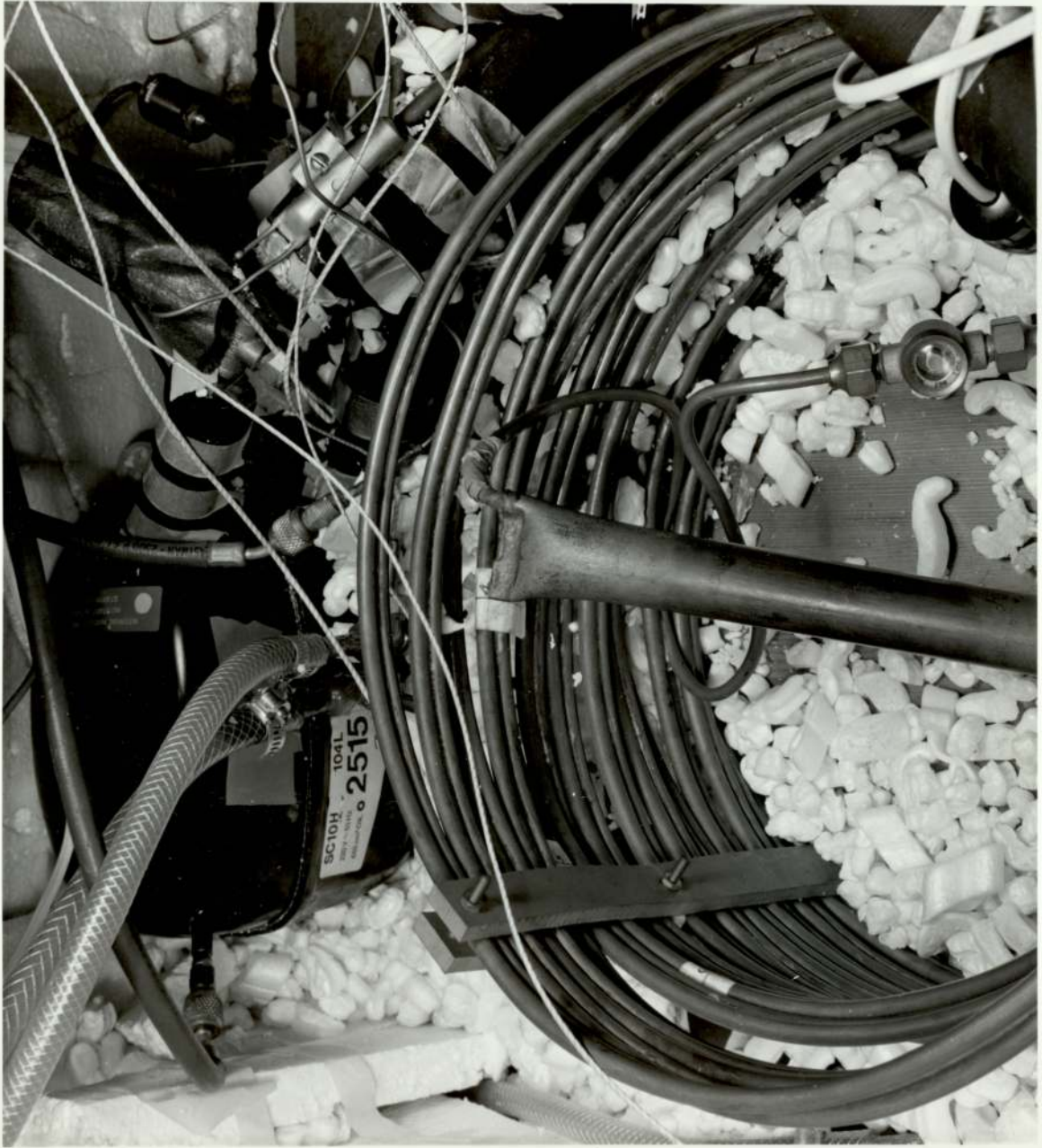


Figure 3.6: Construction of the condenser showing the sight glass, accumulator, remote bulb of the expansion valve, compressor and pressure transducer.



behaviour of the system varies according to the operating condition, with mass flow rate changing, so that storage space must be provided to stabilise the supply of liquid refrigerant to the evaporator.

Since the liquid refrigerant is still at high temperature in its subcooled state after the accumulator, part of its heat can still be given out to water in the second part of the condenser.

In the system assembled, accumulator and condenser form one unit. The accumulator was made of 1 inch diameter copper tube with 10 inches length.

To observe the refrigerant flows in subcooled region, a sight glass was fitted immediately after the accumulator. This unit consist of a brass body into which a glass window has been fitted. When the system is fully charged, refrigerant is hardly seen and the glass is said to be clear. The sight glass has an indicator at the centre of it, it becomes yellow when fully charged and green when dry [24] . Shortage of refrigerant is indicated by a stream of bubbles and when a system is very low on refrigerant, the liquid is seen to froth rapidly.

The sight glass unit in this system was supplied by Danfoss, type SGI. It was designed for freon R12,R22,R502 and R40 as refrigerant.

The whole system of the condenser, forms a spiral as in figure 3.5(a), insulated by using polystyrene beads. So in operation, the condenser cannot be seen since it was put in a box. To see the refrigerant in the system a light bulb was used.

3.5.2 Evaporator.

figure 3.5(b) shows a schematic diagram of the design of evaporator used in the system. It is a counter flow heat exchanger consisting of two pipes so arranged that one pipe is inside the other. The inner pipe is made of copper with 1/2 inches diameter and the outer is plastic pipe with 1inch diameter. The refrigerant flows in one direction through the inner pipe while the water flows in the opposite direction through the annular space between the inner and outer pipes. Both ends of the plastic pipe were clamped to tee junctions made of copper by using jubilee clips as shown in figure 3.5(b). The end which is connected to the compressor was connected to the water supply heat source.

The whole length of the evaporator is lagged by lagging insulation and the total length is 6 meters. It was put under the condenser box in a spiral manner as in figure 3.6.

3.6 Water Regulator.

In a water-cooled condenser as in this water-to-water heat pump system, a constant gas pressure can be maintained by using a water regulator. The main purpose of the water regulator is to regulate the water flow through the condenser in response to variations of refrigerant pressure. This is achieved as shown in schematic diagram in figure 3.7(a).

Like the thermostatic expansion valve, the orifice of the regulator valve is restricted by a valve plate. The valve is attached to a spring which can be controlled by using the handle, and the other side of the valve is attached to a thrust pad. The thrust pad is exposed to the discharge pressure which is conducted through a capillary tube via a flare fitting as shown in figure 3.7(b).

When the system is not in operation, the spring will shut the valve. When in operation, the discharge pressure will thrust the thrust pad and the balance force will open the valve. Handwheel adjustment enables the required pressure to be maintained. As the discharge pressure is always fluctuating in response to the motion of the piston in the compressor, the water flow through the valve, as well as through the condenser, is always fluctuating.

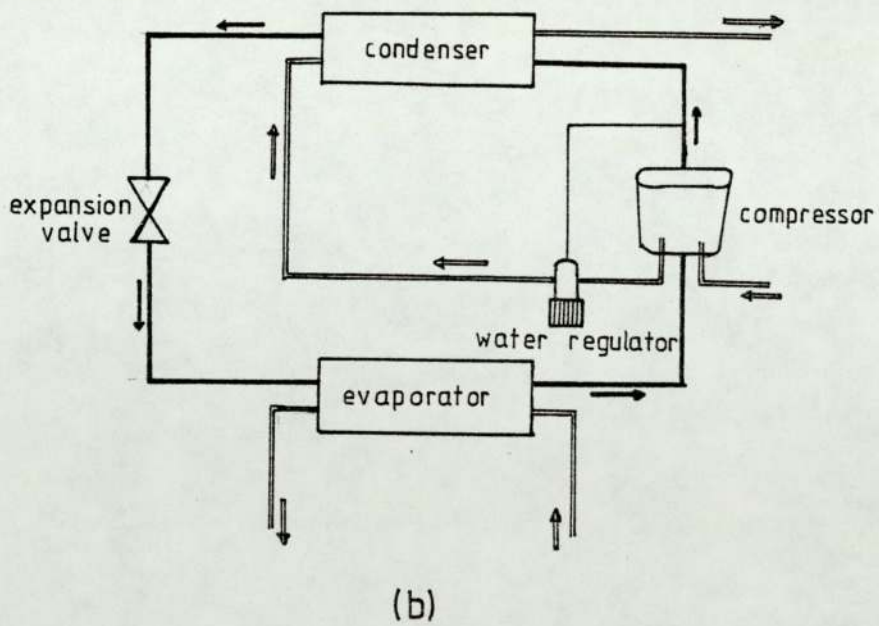
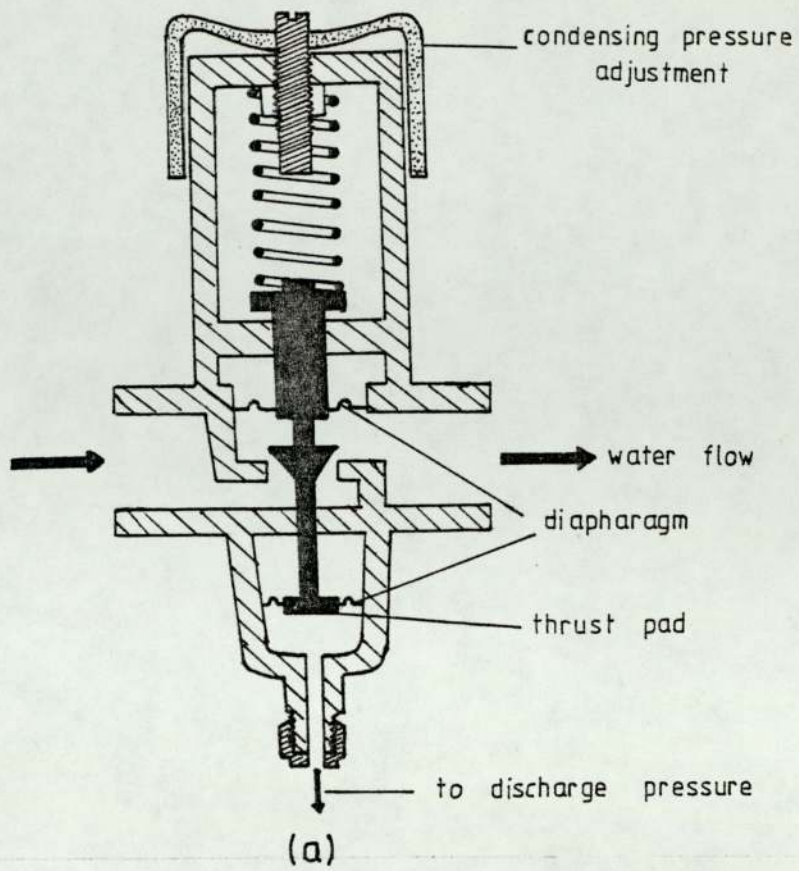


Figure 3.7 : (a) Schematic diagram of water regulator.
 (b) Operation control by the water regulator.

The water regulator used in the system was supplied by Danfoss. The maximum permissible test pressure for refrigerant 2687 kPa (375 psig) and the maximum water pressure is 1080.4 kPa (142 psig). The valve can be set to start opening at 446.1 kPa (50 psig) minimum discharge pressure [24] .

3.7 Filter Drier.

The filter drier, its schematic diagram is shown in figure 3.8, is inserted in the refrigerant cycle to absorb and hold moisture which has inadvertently entered the system.

Moisture is undesirable for two reasons. Firstly, it will eventually form as a bead of ice in the expansion valve and obstruct refrigerant flow; secondly, it will encourage the formation of acids which speed up corrosion.

The existence of moisture in the refrigerant cycle might come directly from factory but more generally it is introduced via open ended piping during installation, despite the precautions taken to prevent it.

A drier consists of a metal container holding a chemical, known as a desiccant, through which the

refrigerant must pass. The essential properties and requirement of a desiccant are [25] ;

- a. To have the capacity to reduce the moisture content in a refrigerant to a low level.
- b. To retain the moisture.
- c. To act rapidly so that moisture will be absorbed in one passage through the desiccant.
- d. To withstand the presence of refrigerant oil and temperature of discharge.
- e. To remain stable during use and not break up or lose its efficiency.
- f. To be proof against chemical reaction when containing water.

Two desiccants which meet these requirements and are widely used are silica gel and molecular sieves [25] . Generally, both chemicals are in the form of granules or beads but some driers are made with a solid core as in this system.

In the water-to-water heat pump system, the filter drier was supplied by Danfoss.

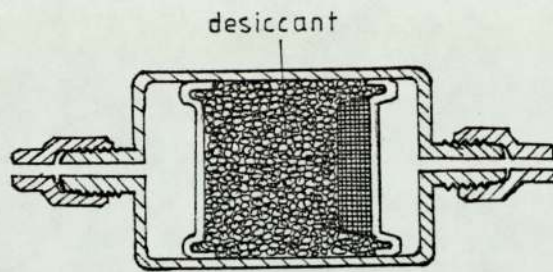


Figure 3.8: Filter drier.

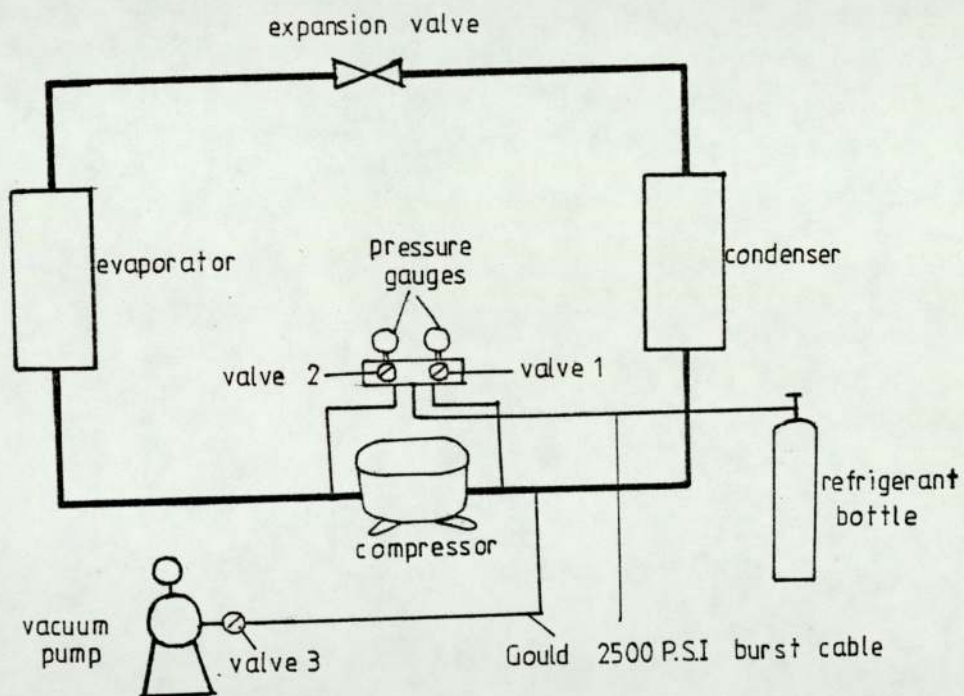


Figure 3.9: Link-up system of leak testing, moisture removal and refrigerant loading process.

3.8 Leak Testing, Moisture Removal and Refrigerant Loading Process.

Figure 3.9 shows a link up of vacuum pump, refrigerant and the heat pump system during leak testing, moisture removal and refrigerant loading process. Low vacuum pump system was used in the process to prevent the oil extraction from the compressor.

High vacuum cable Gould 2500 psi burst, supplied by Danfoss, was used in connecting the vacuum pump to the system via an ordinary valve similar to the valve used in vehicle tyres. When the cable was connected to the refrigerant line, it automatically opened the valve. With both valves 1 and 2 on the gauge closed, the valve 3 on the vacuum pump opened while the pumping process was carried out.

The pumping process ran until the pressure gauge read 0 psia. Then the valve 3 closed and both valves 1 and 2 were opened, allowing refrigerant R12 from the bottle to enter the system. The refrigerant was allowed to enter the system as much as possible. At this moment, the reading on the pressure gauge would read 411.6 kPa to 446.1 kPa (45 psig to 50 psig). Then both valves 1 and 2 were closed and both high vacuum cables connecting the system to vacuum pump and

refrigerant bottle were removed.

In the above process, the removal of moisture from the system and refrigerant loading were carried out simultaneously. The leak testing was carried out by introducing liquid soap on all joints when the pressure inside the system was higher than atmospheric pressure, that is when the refrigerant line was loaded with refrigerant. Any leak spotted would appear as a stream of bubbles. Since all joints were either flare or fitting, the leak was overcome by tighten the nut. To ensure that the system was leak-tight, every joint was glued from outside by using Araldite epoxy-resin.

3.9 Water Pump.

Apart from components which were directly involved in the refrigerant cycle, another component which can be considered important is the water pump. This water pump is needed to circulate the water through the condenser. It was also important to ensure that the water flow through the heat exchanger was constant. The water pump used in this system was supplied by Seal Motor Construction Co. Ltd., model Comet 130-45. The pump can be set at three difference speeds as shown in table 3.3 [26], with maximum working pressure 1034.3 kPa (150 psi) and maximum water temperature 110°C.



<u>Speed setting</u>	<u>r.p.m.</u>	<u>Input (Watts)</u>
I	2000	50
II	2300	60
III	2450	78

Table 3.3: Water pump specifications.

CHAPTER 4.

TRANSDUCERS AND SENSORS FOR THE ASSEMBLED HEAT PUMP.

4.1 Introduction.

A transducer is a device that converts or transduces one physical variable into another. Transducers provide convenient signals for measuring a process, recording these measurements when needed and providing a signal that can be used to control. It is not possible to control without measuring and so the fundamental basis of automation is the transducer [27] .

In principle, a transducer is a simple device. However, in practice it has limitations in operation due to the limited ability of the device itself. Each transducer has a different purpose.

In the water-to-water heat pump system the transducers which have been used to give information can be categorised into four types.

- a. Thermocouple - temperature measurements.
- b. Pressure transducer - pressure measurements.
- c. Watt meter - power measurement for compressor.
- d. Water flow meter - the rate of water flow measurements.

Figure 4.1 shows the position of transducers which have been attached to the water-to-water heat pump system.

In this chapter, the discussion on how the above measurements were carried out together with their calibration will be elaborated. The part in which measurements were recorded will be discussed in the following chapter, together with the data acquisition system used in the calibrations.

4.2 The Thermocouple.

Copper-constantan thermocouples were used to determine the temperature around the system. All together there were twenty thermocouple junctions attached to the system as shown in figure 4.1 (with eight junctions in the water tank attached to

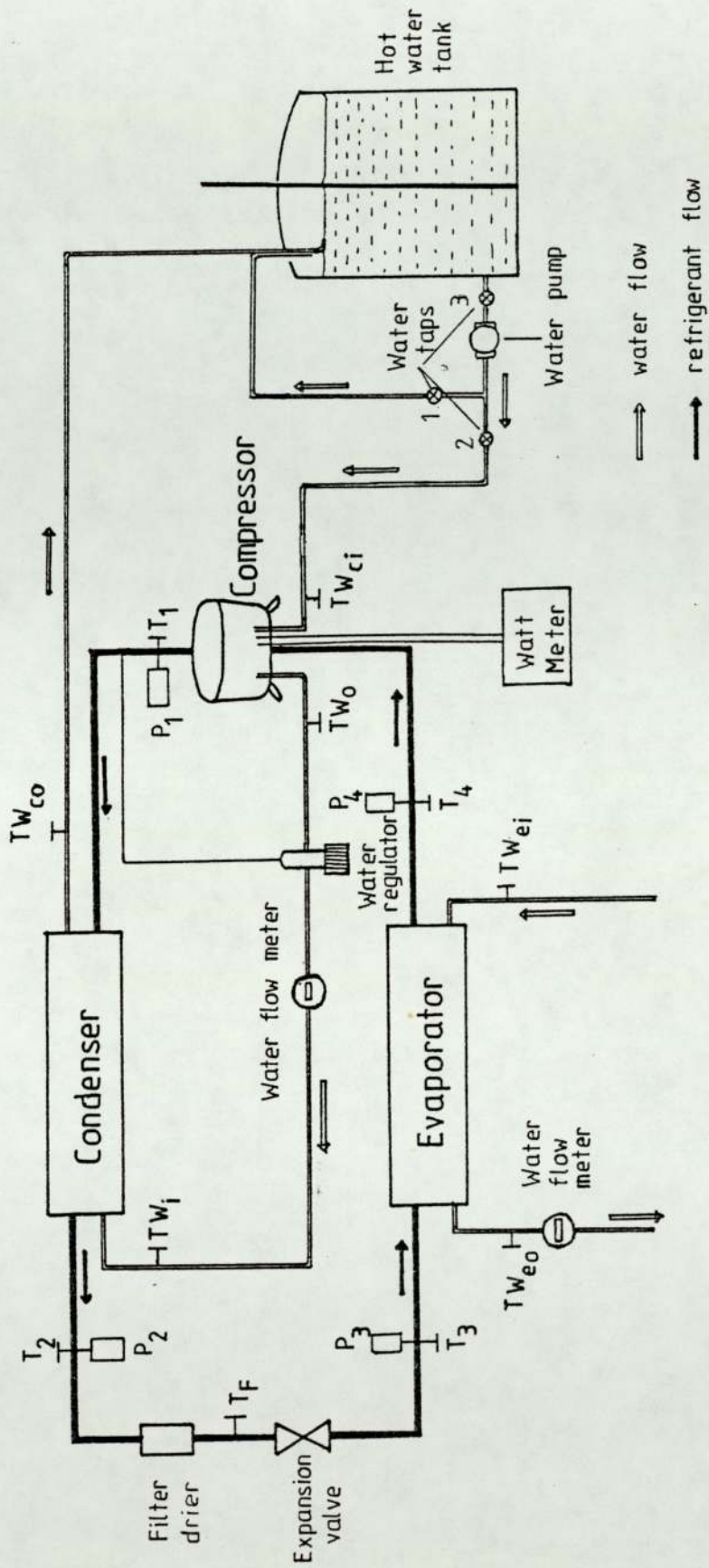


Figure 4.1: The position of the sensors and transducers in the heat pump system.

the plastic rod). Five of them were inserted in the refrigerant circuit; three in the high pressure side T_1, T_F and T_2 and two in the low pressure side T_3 and T_4 . T_1, T_2, T_3 and T_4 were attached to the refrigerant circuit by using cross fittings in which pressure transducers P_1, P_2, P_3 and P_4 were attached at the opposite arm. T_F was attached to the system by using a tee fitting between the filter drier and the thermostatic expansion valve.

Six other thermocouples were inserted in the water lines to measure the temperature of water before and after the evaporator TW_{ei} and TW_{eo} , before and after the condenser TW_i and TW_o and before and after the compressor TW_{ci} and TW_o . The twelfth thermocouple was placed outside the copper tube at the outlet of the water tank. The remaining eight thermocouples spaced 10cm. apart, were submerged vertically in the water at the centre of the tank supported by a plastic rod. These last eight thermocouples were used to measure the temperature of the water at various water levels in the tank.


The method by which the thermocouples were inserted into the refrigerant circuit and the water

lines has been discussed in chapter 2.

4.2.1 The Temperature Calibration.

The whole process of getting information from the transducers and sensors was carried out by using a mini computer, Commodore CBM model 4016 and recording it by using Commodore dual drive floppy disc model 4040. This was done through the analogue-digital converters. Two types of analogue-digital converters were used, namely PCI1001 and PCI1002. The operation of the analogue-digital converters will be discussed in the next chapter.

The first twelve thermocouples in the refrigerant circuit and the water lines, as seen in diagram 4.1, were connected directly to the analogue-digital converter PCI1002. The temperature calibration of the thermocouples were given by the manufacturer as in operating and maintenance manual for PCI series [28] .

The operating subroutine for the analogue-digital converter PCI1002 is shown in Appendix I. The thermocouples were internally connected to the platinum resistance  on the 'cold junction block' inside the device, and it was factory

set to give approximate error of $\pm 0.3^{\circ}\text{C}$ for the range of operation between -200°C to 0°C and $\pm 0.2^{\circ}\text{C}$ for the range of operation between 0°C to 400°C .

The eight thermocouples in the water tank were connected to the analogue-digital converter PCI1001. It is important to note that a thermocouple inevitably has two junctions, one is the hot junction and the other is cold junction. Since the e.m.f. produced by copper-constantan thermocouple is so small, 4.277mV for 100°C [29] and the input to the analogue-digital converter PCI1001 is 1.0V maximum, amplification is necessary. Figure 4.2 shows the circuit for the thermocouple considered. The cold junction is marked as X, where the constantan joins up again with the circuit. For an absolute measurement of temperature as in this process, the cold junction X was held at 0°C that is in melting ice [30].

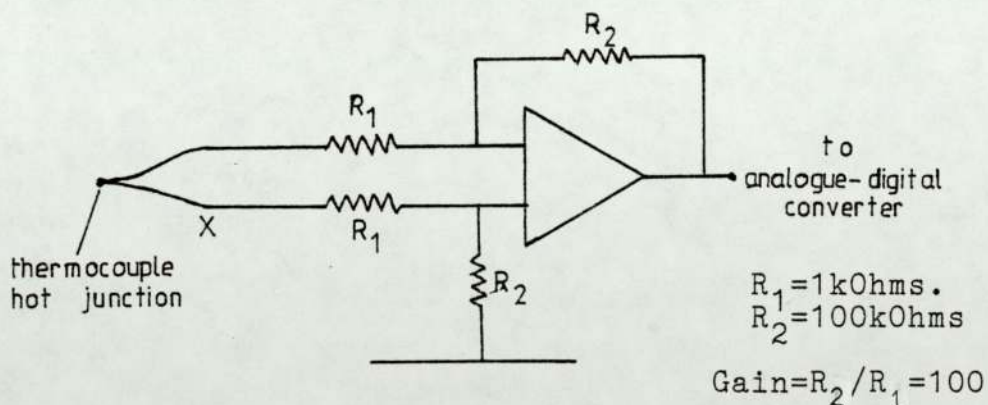


Figure 4.2: Thermocouple junction with gain x100 connected to PCI1001.

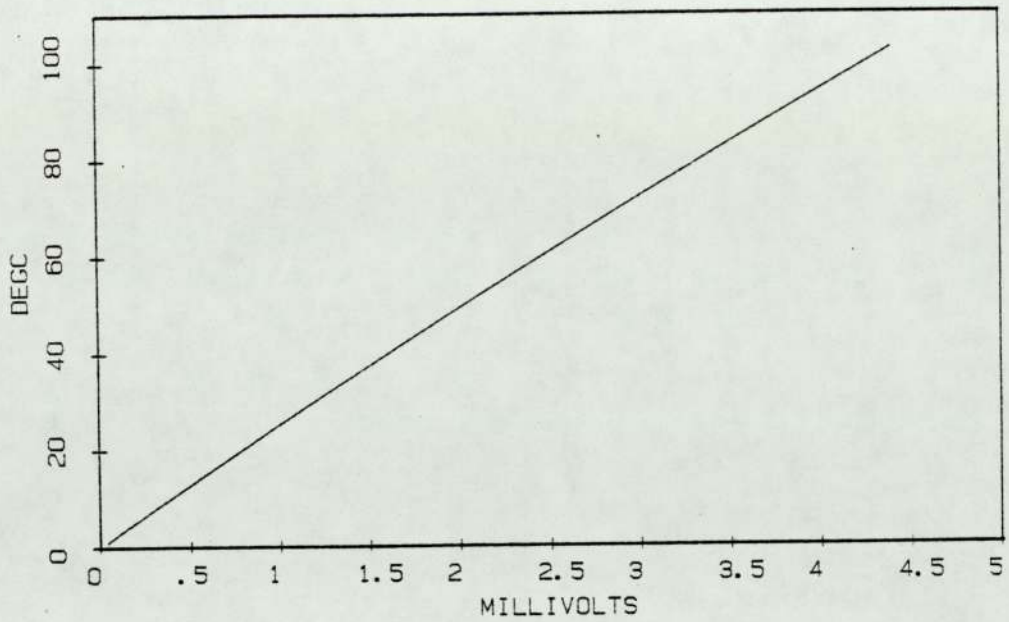


Figure 4.3: The copper-constantan thermocouple calibration.

EQUATION FOR CURVE FIT

$$T = -.0142500922 + 25.9026014 * V - .709851071 * V^2 + .0282697044 * V^3$$

V (MV)	T (DEGC)	T (FIT)
0.0	0.0	-0.01
0.195	5.0	5.01
0.391	10.0	10.01
0.589	15.0	15.00
0.789	20.0	19.99
0.992	25.0	25.01
1.196	30.0	30.00
1.403	35.0	35.01
1.611	40.0	39.99
1.822	45.0	44.99
2.035	50.0	50.00
2.250	55.0	54.99
2.467	60.0	59.99
2.687	65.0	65.01
2.908	70.0	70.00
3.131	75.0	75.00
3.357	80.0	80.01
3.584	85.0	85.00
3.813	90.0	90.00
4.044	95.0	95.00
4.277	100.0	100.00

SUM OF SQUARE ERROR=1.03067347E-03

TABLE 4.1: THE LEAST SQUARES CURVE FITTING FOR COPPER-CONSTANTAN THERMOCOUPLE.

The calibration value for the thermocouple was given by The Omega Temperature Measurement Handbook [29] in numerical form. Figure 4.3 shows the calibration of the thermocouple in graphical form.

In order to use the calibration given in the computer program for sampling, this calibration was converted to a polynomial equation by using least squares curve fitting [31]. Table 4.1 shows the calibration data and the fit for a copper-constantan thermocouple with cold junction at 0°C. The polynomial form of the calibration is;

$$T = a_1 + a_2 V + a_3 V^2 + a_4 V^3 \quad 4.1$$

where T is the temperature in degrees Centigrade and V is the e.m.f. in millivolt. The values of constants a are;

$$a_1 = -0.0142500922$$

$$a_2 = 25.9026014$$

$$a_3 = -0.709851071$$

$$a_4 = 0.0282697044$$

4.3 The Pressure Transducer.

In order to get accurate pressure measurements in the refrigerant circuit, a suitable pressure

transducer must be used. In this water-to-water heat pump system, the measurement of the pressures in the refrigerant circuit were carried out automatically by digital computer as in the temperature measurement discussed in the previous section.

Cerni [32] has discussed several types of transducer in digital process control, such as strain-gauge transducers, unbonded strain-gauge, bonded strain gauge transducers and semiconductor strain gauge transducers. The latter type is more suitable for heavy use, especially with self-contained electronics eventhough at that time (1964) they exhibited poor longterm temperature stability and excessive non-linearity. This latter type of transducer was used in measuring the pressures in the refrigerant circuit.

The pressure transducers were supply by Maywood Instrument Limited type P102, greatly improved compared to that discussed by Cerni [32] .

The construction of the pressure transducer P102 consists of an integrally machined, precipitation hardened stainless steel body and pressure sensing diaphragm. They were connected directly to the refrigerant circuit by using 1/4 inches cross fittings,

Press Transducers	P ₁	P ₂	P ₃	P ₄
Range (PSIG)	0-200	0-200	0-200	0-200
Test temperature	18°C	18°C	20°C	20°C
Excitation (Volts DC)	10	10	10	10
Full range output mV (FRO)	200.64	201.00	200.76	202.09
Non-linearity %(FRO)	±0.05	+0.03	+0.06	+0.05
Hysterisis and Repeatability %(FRO)	0.05	0.05	0.05	0.10
Input resistance (Ohms)	1433	1367	1316	1419
Output resistance (Ohms)	449	447	443	468
Compensated Temp. range (°C).	-18to65	-18to65	-18to65	-18to65
Thermal zero shift %(FRO)/°C	+0.02	+0.02	+0.01	+0.01
Thermal sensitivity shift (%(FRO)/°C)	+0.01	+0.01	+0.02	+0.01

Table 4.2: The specification of the pressure transducers.

two in the low pressure side before and after the evaporator and the other two in the higher pressure side before and after the condenser as shown in figure 4.1.

Every pressure transducer supplied was accompanied by its own calibration certificate and specifications as described in table 4.2.

Since the maximum output of each pressure transducer is 200mV and PCI1001 was used as the analogue-digital converter which has maximum input 1.0V, the gain used in amplification was 5. This was done by replacing both resistors R_1 in figure 4.2 with 20kOhms. So, all together four amplifiers in four channels of the analogue-digital converter PCI1001 were modified to give gain 5 to suit the four pressure transducers used in the heat pump system.

4.4 The Watt Meter.

The function of the Watt meter used in the system is to measure electrical power used by the compressor. A domestic Watt meter was supplied by The Midland Electricity Board and was modified so that the power could be measured and recorded by the computer automatically.

The Watt meter operation is based on the rotation of a scaled shining disc to measure power supplied to a load. The rate of the rotation of the disc is used to measure the power. In normal application the rate of rotation of the disc can be read directly on the pointers or counter located in front of the meter. To measure a load in a short time, the rate of rotation of the disc can be measured and the calibration value of the rate of rotation against power is usually written in front of every Watt meter supplied.

In this heat pump system, the normal measurement of the power was not carried out. Instead, a reflective opto switch [33] was mounted to measure the rate at which the scale on the disc passes between the light source and sensor.

The electrical details of the reflective opto switch is shown in figure 4.6. It comprises a GaAs infra-red emitting diode with a silicon photo Darlington transistor in a moulded rugged package as shown in figure 4.7. The sensor responds to the emitted radiation from the infra-red source only when a reflective object, is within

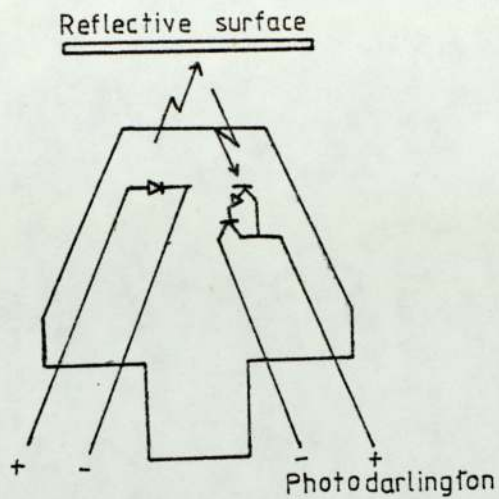


Figure 4.6: The electrical details of the reflective opto switch.

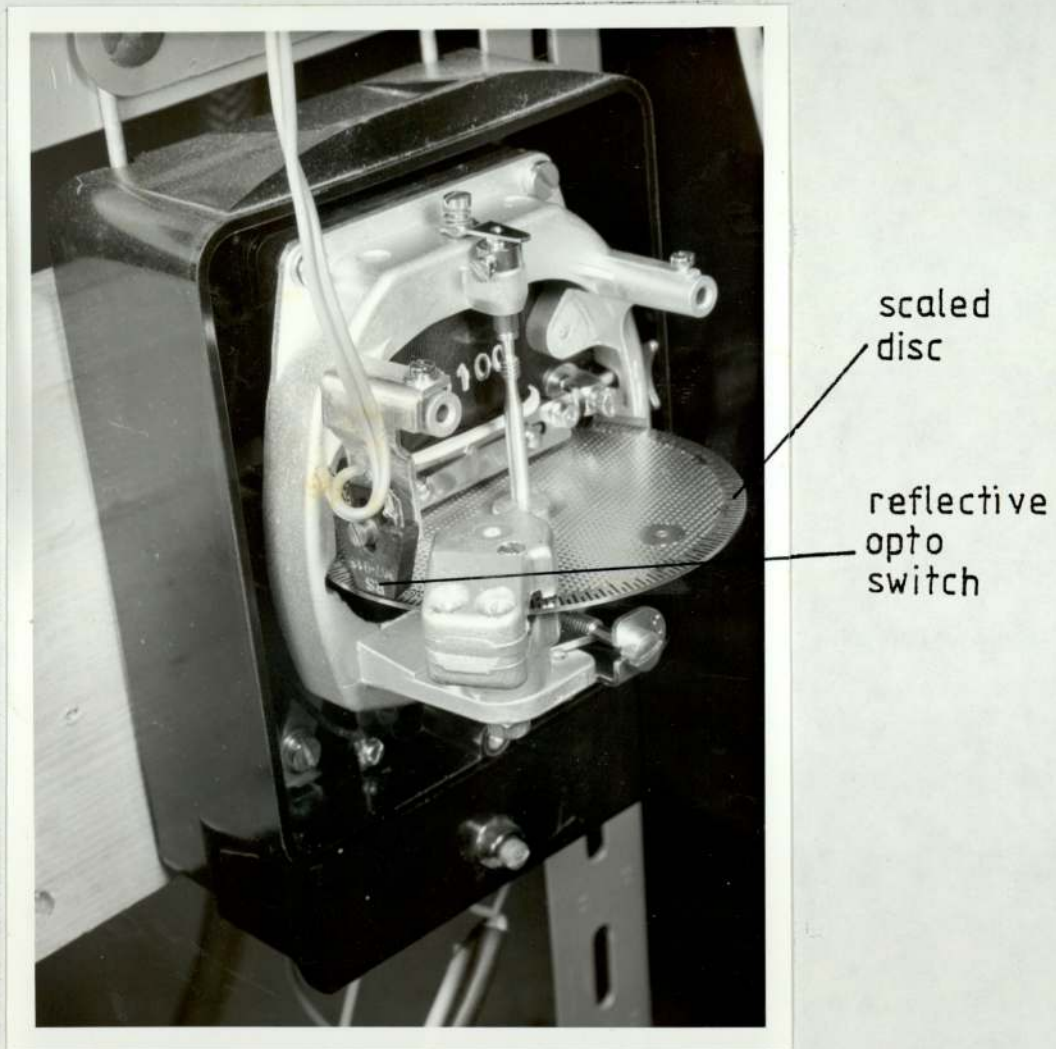


Figure 4.7: The reflective opto switch in operation, detecting the scale divisions passing per second.

the field of view of the source. When a scale marking on the Watt meter disc passes, light is not reflected, so the sensor will not respond, but when the reflecting part of the disc passes, it reflects the radiation. By using this process, the sensor responds to the reflective and non-reflective part of the disc alternately, and the rate of pulse production will be dependent on the power consumed.

The specification of the switch is given by the manufacturer [33] and shown here as in table 4.3.

The electronic circuit of the switch is shown in figure 4.8. The pulses produced by the sensor are amplified to $20V_{p-p}$, then reduced to $2V_{p-p}$ by using a potential divider to suit the frequency-to-voltage converter. Finally, the D.C. voltage produced is transmitted to the analogue-digital converter PCI1001 which then conveys the information to the computer for measurement and recording purpose.

Figure 4.9 shows in block diagram form how the power was measured and recorded. The process of measuring the power can be summarised as follows;

1. The domestic Watt meter rotates the scaled reflecting disc which measures the power consumed by the compressor.

Absolute maximum rating at 25°C.

Operating temperature range	0°C to 70°C
Storage temperature range	-20°C to 80°C
Lead soldering temperature (5sec)	260°C

Output diode.

Forward D.C. current	40mA.
Reversed D.C. voltage	2V.
Power dissipation	50mW.

Output sensor.

Collector-emitter voltage	15V.
Emitter-collector voltage	5V.
Power dissipation	50mW.

Electrical characteristics at 25°C.

Input diode.

Forward voltage V_F	= 1.8V.
Forward current I_F	= 40mA.
Reversed voltage V_R	= 2V.
Reversed current I_R	= 100uA.
Radiant power P_o	= 1.5mW.
Forward current I_F	= 20mA.

Output sensor.

Collector-emitter breakdown voltage BV_{ceo}	= 15V.
Collector-emitter current I_{ce}	= 100uA.
Emitter-collector breakdown voltage BV_{eco}	= 5V.
Emitter-collector current I_{ec}	= 100uA.

Table 4.3: The specification of the reflective opto swith.

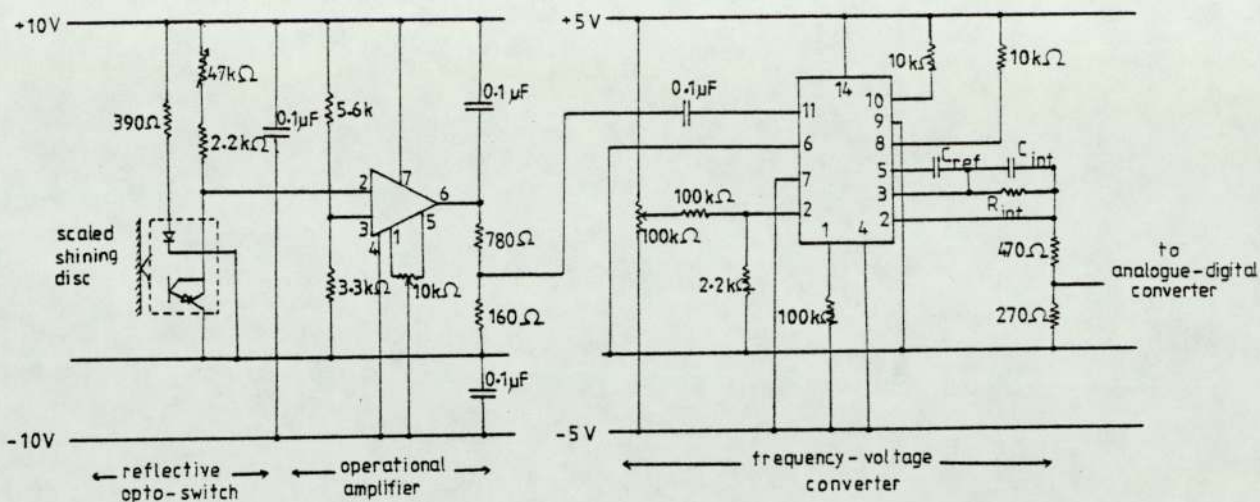


Figure 4.8: The electronic circuit of the reflective opto switch.

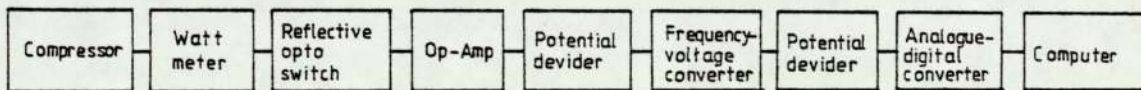


Figure 4.9: The block diagram of the power measurement for the compressor.

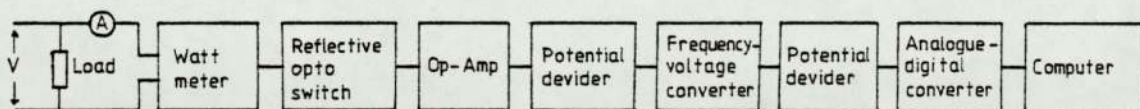


Figure 4.10: The block diagram for Watt meter calibration.

2. The reflective opto switch detects the rate of rotation of the disc by detecting the scale passes and pulses are produced.
3. The pulses produced are then amplified to give suitable sensitivity.
4. The pulses are then reduced to $2V_{p-p}$ maximum to suit the requirement for the frequency-voltage converter by using a potential divider.
5. The frequency-voltage converter converts the pulses produced to D.C. voltage. The maximum voltage output is 4V [34] .
6. The D.C. voltage output from frequency-voltage converter was then reduced to 1.0V by using another potential divider. This was done to suit the input to analogue-digital converter, since the maximum permissible input voltage was 1.0V.
7. The D.C. voltage produced is then fed to the analogue-digital converter which then conveys the message to the computer for measurement, sampling and recording.

So one channel of the analogue-digital converter PCI1001 was modified as for the pressure transducer, but this time with gain of unity. This was done by replacing the resistance R_1 , as in figure 4.2 to 100kOhms. The linearity of the measurement depends entirely on the rate of rotation of the disc and the linearity in converting the pulses to D.C. voltage in frequency-voltage converter.

4.4.1 The Watt Meter Calibration.

Since the parameter used to measure the power consumed is the output D.C. voltage from frequency-voltage converter, calibration of the Watt meter needs to be carried out.

Figure 4.10 shows the block diagram for the calibration. Three types of light bulbs were used as the load. They were two 100 Watts bulbs and one 150 Watts bulb. The voltage across the load was measured by using Solartron digital multimeter 7045 and the A.C. current was measured by using Gould Alpha IV digital multimeter. These values of A.C. current and voltage were used to measure the power consumed by the load. The output D.C. voltage from Watt meter was recorded by the computer. The sampling

for the calibration was done as the average of ten in each reading for 100 readings.

Table 4.4 shows the calibration values for the Watt meter mentioned above, and figure 4.11 is the form of the calibration values. It was found that the value of the output D.C. voltage was proportional to the power consumed by the load. In other words, the rotation of the disc and the frequency-voltage converter were linearly dependent on the power consumed by the load.

Based on the calibration values in table 4.4 and graph in figure 4.11, the calibration value for power consumed can be expressed in mathematical form by using least squares fit method [31]. The relation can be expressed as,

$$W_c = 12.6188195 + 495.329762V \quad 4.2$$

where W_c is the power consumed by the compressor in the heat pump system and V is the D.C. voltage output from frequency-voltage converter. The fitting value for this relation is shown as in table 4.4.

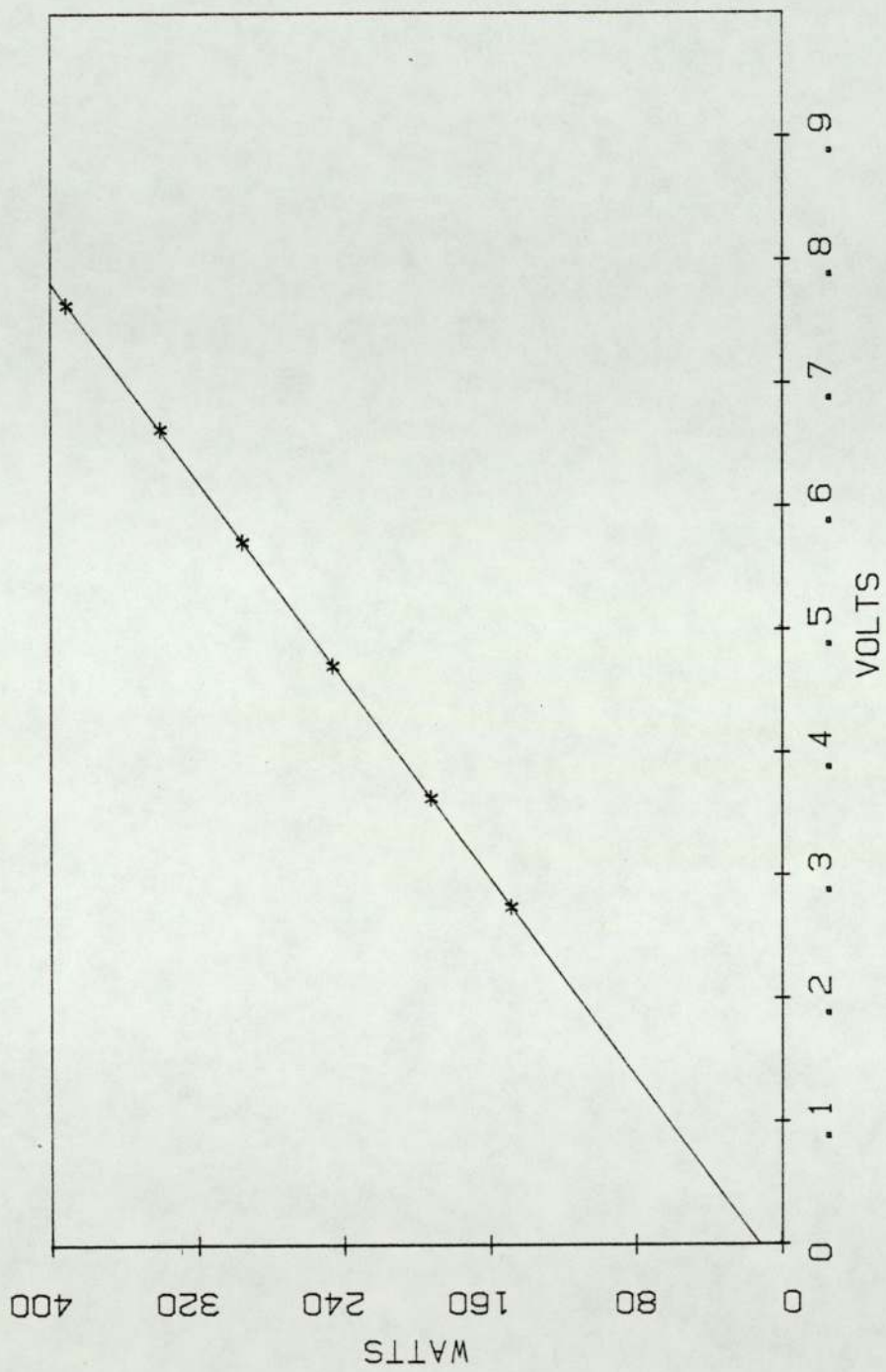


Figure 4.11: Watt meter calibration.

EQUATION FOR LEAST SQUARE FIT

=====

$$W = 12.6184134 + 495.329967 * V$$

=====

V(V)	W(WATT)	W(FIT)
0.27463	148.61	148.65
0.36347	192.63	192.66
0.47120	246.34	246.02
0.57156	295.74	295.73
0.66355	340.63	341.29
0.76445	391.67	391.27

=====

SUM OF SQUARE ERROR= 0.712138769

TABLE 4.4: CALIBRATION OF THE WATT METER AS A FUNCTION OF INPUT VOLTAGE TO THE ANALOGUE-DIGITAL CONVERTER.

4.5 The Water Flow Meter.

In order to measure energy absorbed by the evaporator and released by the condenser, the water flow rates passing through the evaporator and condenser must be measured. As in the previous cases, the measurement of this parameter was carried out automatically by the computer. Both water flow meters were supplied by Litre Meter Company Limited [35].

The water flow meter supplied consists of three main parts.

1. The body to which the water pipes are attached.

2. The electronics housing which makes the other side of the body.
3. The rotor assembly which consists of a stainless steel ring carrying sapphire cup bearings, which in their turn carry the rotor mounted on a stainless steel shaft with tungsten ball pivot.

In operation, when the water flows through the unit, the speed of the rotor is proportional to the flows as claimed by the manufacturer [35] . The shaft position remains vertical to maintain calibration, particularly at the low flows. The tips of the rotor contain ferrite rods and these are sensed inductively through the wall of the electronic housing.

The electronic circuits require between 10V to 20V D.C. at about 15mA producing a pulse for each passage of the rotor tips past the sensor. These pulses are of constant area and if applied to a moving coil meter, will give an indication proportional to the pulse rate or if the pulses are counted, they will give a reading proportional to the total flow. The latter method was adopted in

the sampling. The circuit is internally stabilised and is suitable for the temperature range non-condensing -10°C to $+70^{\circ}\text{C}$.

The devices were fixed to the water-to-water heat pump system as shown in figure 4.1. In fixing the meter in the water lines, consideration was given to eliminating bubbles in the water flow through it, since small bubbles in the water can attach themselves to the rotor, particularly at low flows, which will give a reduced reading. This was done by fixing the devices in the coolest part of the water flows since the water may release dissolved air as bubbles in the warmer part. In the condenser, the water flow meter was fixed in the line after entering the compressor cooling coil; and in the evaporator at the outlet as shown in figure 4.1.

The pulses produced by the meter, as a result of water flow through it, were converted to a D.C. voltage as in the power measurement for the compressor discussed in the previous section. Figure 4.12 shows the sampling process of water flow measurement which can be summarised as follows;

1. The water flow meter produces pulses as a result of water flow through it.

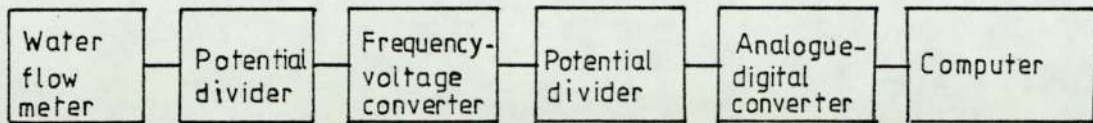


Figure 4.12: Block diagram for the water flow rate measurement.

2. The magnitude of the pulses was reduced to $1.0V_{p-p}$ by using the potential divider to satisfy the input to frequency-voltage converter.
3. The reduced pulses were then fed to the frequency-voltage converter. The maximum voltage produced which is proportional to the pulses is $4.0V$.
4. The D.C. voltage produced was reduced to maximum $1.0V$ by using the second potential divider to satisfy the input to analogue-digital converter PCI1001.
5. The analogue-digital PCI1001 converter conveys the message to the computer.

6. The sampling and recording were carried out by the computer.

As in the power measurement, the operational amplifiers of the two channels in the analogue-digital converter PCI1001 were modified to give gain unity by changing both resistors R_1 in figure 4.2 to 100kOhms.

4.5.1 The Water Flow Calibration.

Each flow meter supplied was accompanied by its calibration certificate based on water flow rate against pulses produced. Since in the sampling process D.C. voltage output was measured, the recalibration on both meters needed to be carried out. The voltage was measured by using the computer against the volume of water flow per second.

The voltage was measured as averages of ten readings for a hundred samples. The volume of the water was measured by using scaled cylinder, and the time by using a stopwatch. Table 4.5(a) and 4.5(b) show the calibration values for the water flows through the condenser and evaporator respectively. Figure 4.13 shows the calibration curves for water flow through the condenser (a) and evaporator (b).

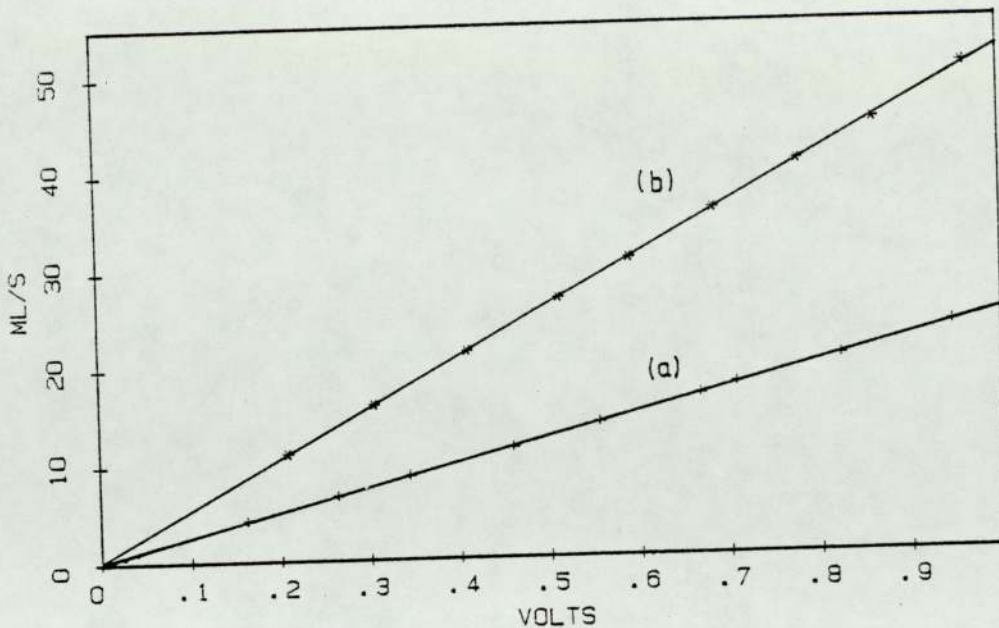


Figure 4.13: Water flow rate calibrations; (a) condenser and (b) evaporator.

TABLE 4.5(A)

O/P (V)	MC (ML/S)	MC (FIT)
0.1628	4.24	4.20
0.2635	6.71	6.68
0.3441	8.67	8.66
0.4596	11.38	11.50
0.5556	13.83	13.86
0.6675	16.59	16.61
0.7081	17.72	17.61
0.8233	20.37	20.44
0.9468	23.52	23.48

TABLE 4.5(B)

O/P (V)	ME (ML/S)	ME (FIT)
0.2086	11.08	11.04
0.3054	16.06	16.04
0.4096	21.43	21.44
0.5126	26.73	26.76
0.5910	30.77	30.82
0.6850	35.74	35.69
0.7788	40.56	40.54
0.8631	44.65	44.90
0.9623	50.24	50.03

LEAST SQUARE FIT EQUATION FOR CONDENSER:
 $MC = 0.200838053 + 24.5824341 * V$
 SUM OF SQUARE ERROR = 0.038315991

LEAST SQUARE FIT EQUATION FOR EVAPORATOR:
 $ME = 0.241682565 + 51.7421106 * V$
 SUM OF SQUARE ERROR = 0.116889251

Table 4.5: Calibration of the water flow rate as a function of output voltage to the analogue-digital converter for (a) Condenser and (b) Evaporator.

It can be seen in figure 4.13 that the voltage output is proportional to the water flow rate. As in power measurement for the compressor, the calibration value can be represented in mathematical form by using the least squares fit method [31] . The value computed for the condenser is;

$$\dot{m}_c = 0.200838053 + 24.5824341V \quad 4.3$$

and for the evaporator is;

$$\dot{m}_e = 0.24168258 + 51.7421106 V \quad 4.4$$

where \dot{m}_c is the water flow rate through condenser (ml/s), \dot{m}_e is the water flow rate through evaporator and V is the input voltage to the analogue-digital converter.

The mathematical relations in equations 4.3 and 4.4 were used in the computer program for the sampling process.

CHAPTER 5.

DATA ACQUISITION SYSTEM.

5.1 Introduction.

In order to get information from the water-to-water heat pump system, a system must be designed to link the system to a digital processor namely a mini computer, which would control the experiment, perform optimization, and do all the necessary calculations.

Figure 5.1 shows the data acquisition system designed to get information from the water-to-water heat pump system.

5.2 The Computer.

For sampling procedure the CBM computer Model 4016 supplied with dual drive floppy disk

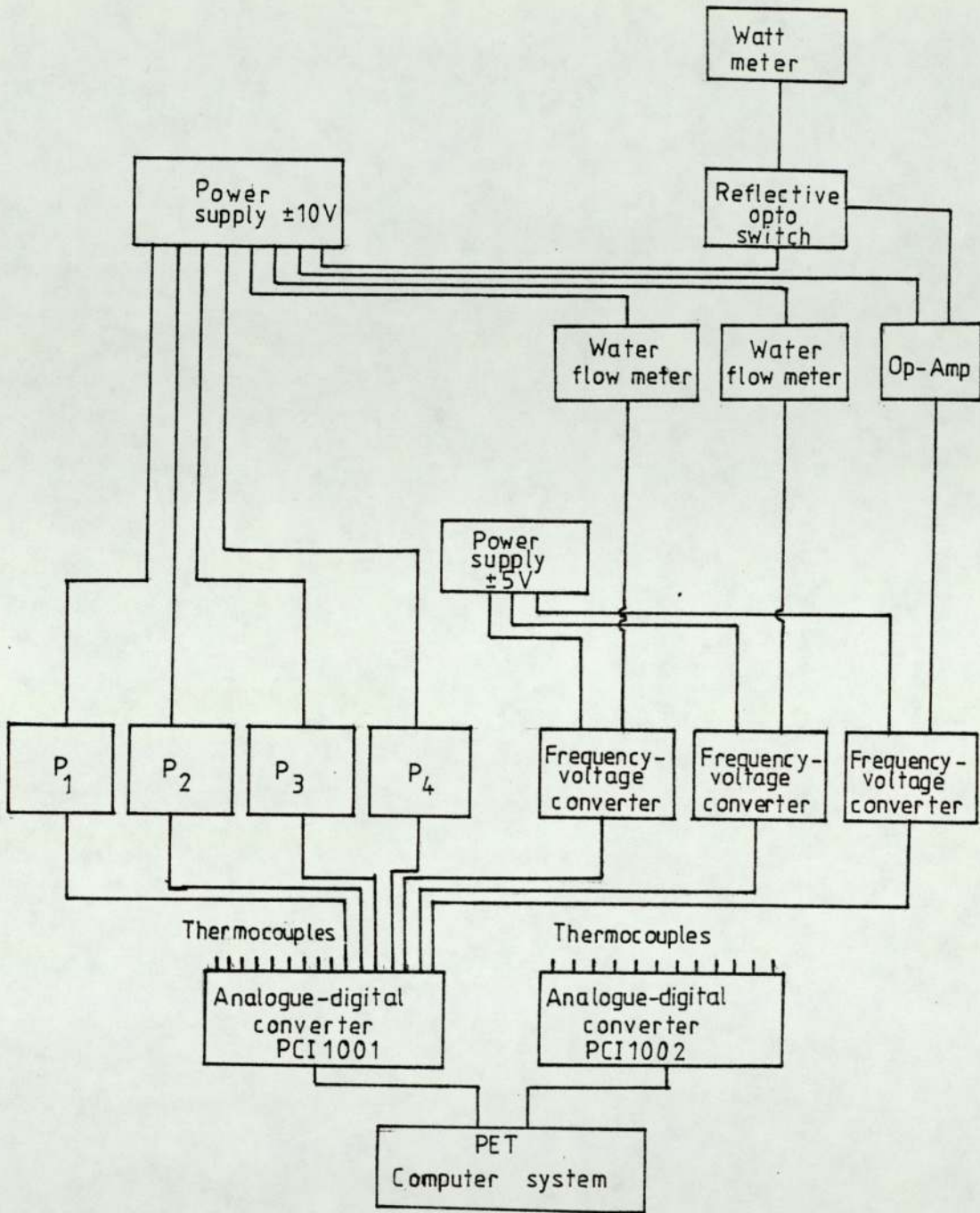
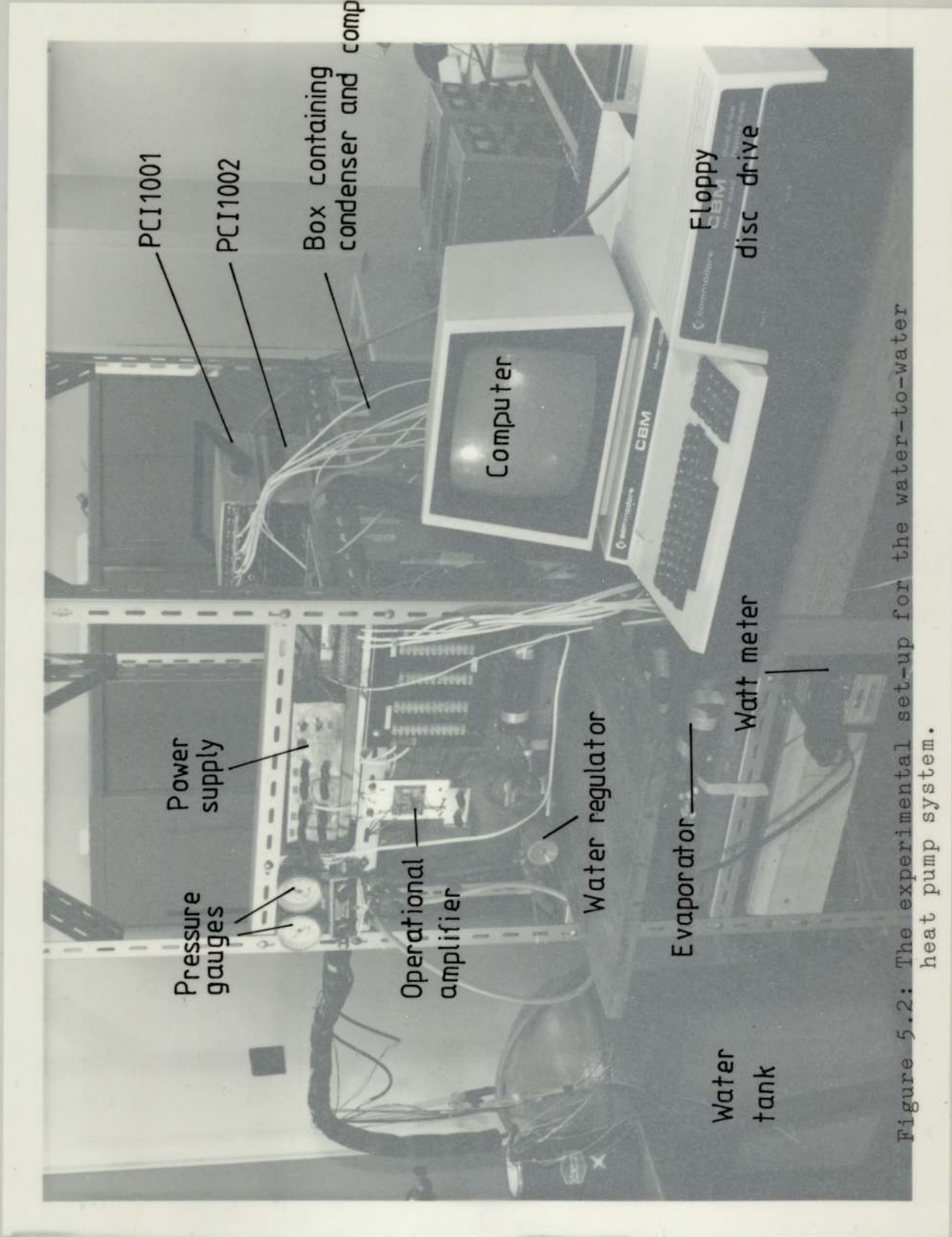


Figure 5.1: The data acquisition system for the water-to-water heat pump system.



PCI1001

PCI1002

Box containing
condenser and compressor

Computer

Floppy
disc drive

Power
supply

Pressure
gauges

Operational
amplifier

Water regulator

Evaporator

Watt meter

Water
tank

Figure 5.2: The experimental set-up for the water-to-water heat pump system.



model 4040 to record all the data were used. For analysis, the CBM Computer Model 4032, the printer Epson FX-80 and the plotter Hewlett-Packard 7470A were used.

5.3 Analogue-digital Converter.

The computer can only get information in digital form. In order to convert all analogue signals from the sensors to digital form as required by the computer, analogue-digital converters were used. As mentioned earlier in the previous chapter, two types of analogue-digital converters namely PCI1001 and PCI1002 were used.

5.3.1 Analogue-digital Converter PCI1001.

As shown in figure 5.1, the PCI1001 was used to convert the analogue signals from the water flow meters, Watt meter, the pressure transducers and copper-constantan thermocouple hot junctions submerged in the hot water tank.

The ~~operating~~ subroutine of the unit is given by the manufacturer as in appendix I [28]. The subroutine was used in the computer program for the sampling process.

In operation, for full scale voltage input to the unit, the output reading should read 4000 ± 1 digits. It should be noticed that the unit has been calibrated by the manufacturer at 4000 bits F.S.D. (full scale display). The overrange occurs at 4097 bits and underange occurs at -4097 bits. With all inputs short circuited the outputs should read 0 ± 1 digits.

Analogue-digital recovery time can cause cross talk between channels if one is in the overrange condition. Channels which are not being used may be left open circuit, when the output will read approximately zero. But in the sampling process only 15 channels were used. The first channel was left open circuit reserved for refrigerant mass flow meter. The second two channels were used for water flow measurements, the fourth for the Watt meter, the next four channels for the pressure transducers and the remaining eight channels for thermocouples to measure temperature profile in the hot water tank.

As mentioned in the previous chapter, each channel on the unit has it own operational-amplifier mounted inside the top cover of the unit with gain 100. All operational-amplifiers fixed with 0.1% accuracy resistors.

For full scale display output, the input

voltage to the analogue-digital converter is 1.0V D.C. Then the input to each channel cannot exceed more than 10.0 mV D.C. Modifications on the operational-amplifier have to be made to suit the analogue signals from the transducers and sensors as mentioned in the previous chapter. The modifications have been made as follows;

- a. The gain for first four channels has been changed to unity. These channels were reserved for refrigerant flow meter, for water flow meter in condenser and evaporator and for Watt meter respectively.
- b. Next four channels were modified to give gain 5 to suit the pressure transducers since their maximum output is 200mV D.C. corresponding to 1480.4kPa (200psig) pressure.
- c. The remaining eight were left as supplied by the manufacturer with 10mV maximum input. These channels are suitable for the thermocouple hot junctions and can be used to measured temperature up to 210°C with 0°C reference junction.

Figure 5.3 shows how the analogue-digital

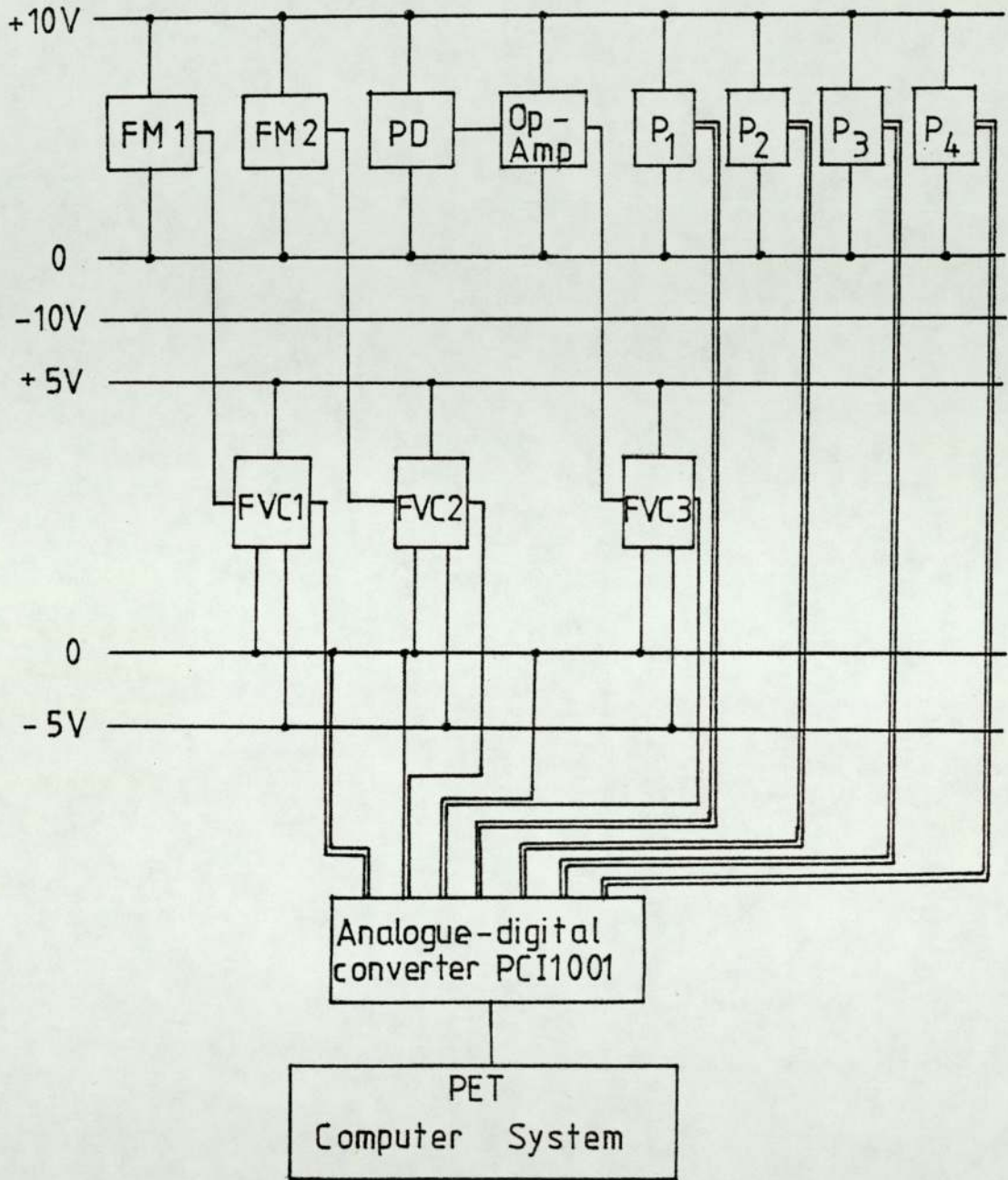


Figure 5.3 : Analogue-digital converter PCI1001 with connecting to pressure transducers water flow meters and Watt meter.

converter PCI1001 was connected from pressure transducers and sensors to the computer in the sampling process (not including the thermocouples). The symbols in the diagram are as follows;

FM1 =Water flow meter for condenser.
FM2 =Water flow meter for evaporator.
PD =Potential difference.
Op-Am =Operational amplifier.
P₁ =Pressure transducer.
P₂ =Pressure transducer.
P₃ =Pressure transducer.
P₄ =Pressure transducer.
FVC1 =Frequency-voltage converter.
FVC2 =Frequency-voltage converter.
FVC3 =Frequency-voltage converter.

5.3.2 Analogue-digital Converter PCI1002.

The operating subroutine for the unit is shown in Appendix I [28]. In operation, the inputs will be scanned displaying the output in bits for channels 1 and 2 and temperature in °C for channels 4 to 15.

The operation of each channel is as follow;
Channel 0: Internally connected to a proportion of

the power supply voltage. Used to identify the range the unit has been set to. Values are nominally approximately 400 bits for 100mV range, approximately 1333 bits for 30mV range and approximately 4000 bits for 10mV range.

Channel 1: These are directly connected to the and 2 multiplexer and are high level single ended input connections. Ranges are $\pm 1V$ (10mV range), $\pm 3V$ (30mV range) and $\pm 10V$ (100mV range). These two channels were not used during sampling.

Channel 3: Is internally connected to the platinum resistance thermometer on the cold junction block (via conditioning circuitary). By addressing this channel the cold junction temperature scaling will give;

0-100°C = 0-4000 bits for 10mV range.

0-100°C = 0-1333 bits for 30mV range.

0-100°C = 0-400 bits for 100mV range.

Channels : These channels are connected via thermo-4 to 15 couple material plugs and sockets and cable to the cold junction block. They are then fed to individual differential

amplifiers (gain=100) and then to the multiplexer.

In the system assembled, the copper-constantan thermocouple which is not linear, has been used. The PCI1002 produces data which is linear with microvolts rather than linear with temperature. Linearisation is simply carried out in software, by a fourth order polynomial expansion.

$$T = A_0 + A_1V + A_2V^2 + A_3V^3 + A_4V^4$$

where,

T is the temperature in °C.

U is the voltage in mV.

$$A_0 = 0$$

$$A_1 = 2.5661297 \times 10^{-2}$$

$$A_2 = -6.1954869 \times 10^{-7}$$

$$A_3 = 2.2181644 \times 10^{-11}$$

$$A_4 = -3.5500900 \times 10^{-16}$$

with approximate error = $\pm 0.2^\circ\text{C}$.

These values can be seen in the subroutine in the Appendix I.

5.4 The Frequency-voltage Converter.

The schematic diagram for the frequency-

voltage converter used in the system is shown in figure 5.4. The device virtually accepts any input frequency and provides a linearly proportional voltage output [36]. The linearity of the device in the water flow measurements and the Watt meter have been discussed in the previous chapter together with their calibrations.

The mode of operation of the device is given by the manufacturer as follow,

Input

- Frequency : 10Hz to 100kHz..
- Voltage : min -0.4,+0.4V
max -2.0,+5.0V
- Waveform : Sine, triangular,square
or pulse.
- Duty cycle : 0.5 μ s min. negative pulse
width.
5.0 μ s min positive pulse
width.
- Impedance : 10Meg Ohms.

Output

- V_{out} range :0 to 4.0V
- $V_{out} = f_{IN}(V_{ref} \cdot C_{ref} \cdot R_{int})$

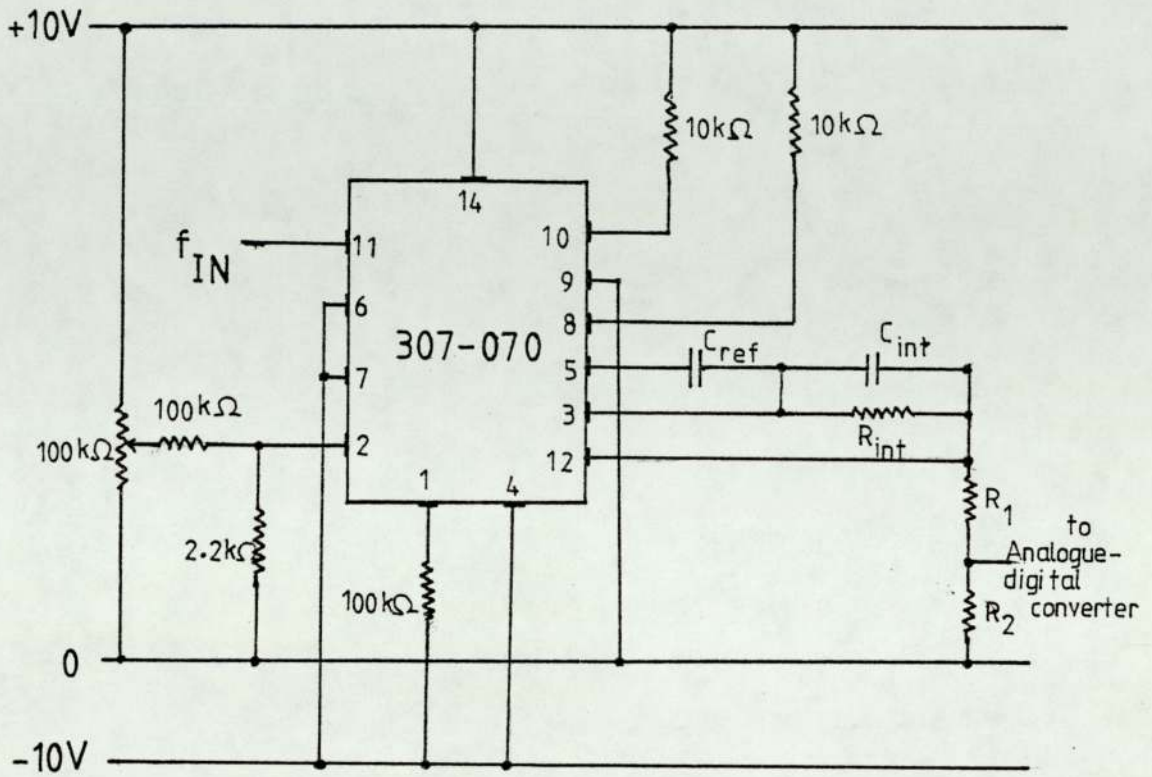


Figure 5.4: The schematic diagram for the frequency-voltage converter.

$$\text{Response time} = R_{\text{int}} \times C_{\text{int}}$$

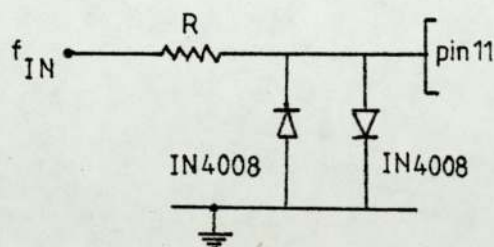
Ripple = inversely proportional to f_{IN}
and C_{int} .

Overall accuracy = Better than 0.1% full scale.

where V_{out} is the output voltage, f_{IN} is the input frequency and V_{ref} , C_{ref} and R_{int} are the voltage, capacitance and resistance as shown in figure 5.4.

5.4.1 Input Signal Conditioning.

1. For 100kHz max. input frequency, R_{int} should be decreased to 100kOhms.
2. The input signal must cross zero in order to trip the comparator. In order to overcome hysteresis the amplitude must be greater than $\pm 200\text{mV}$. If the input voltage exceeds 2.5V then the output will go to its maximum voltage for the duration of this over voltage. This input voltage can be overcome by incorporating a pair of back to back diodes and a series resistor as in figure 5.5.



$$R = (V_{\text{in(pk-pk)}} - 0.7) 10\text{kOhms}$$

Figure 5.5: Input voltage limiting.

Figure 5.6 shows the circuit for water flow meter and figure 5.7 shows the circuit for the Watt meter. Specifications used in those circuits are shown in table 5.1. The first part of the device used to measure the power to the compressor is the sensor which detects the shining surface of the rotating disc in the Watt meter. The second part is the operational amplifier 741S which amplifies the pulses produced. Then the pulses were converted to D.C. voltage by using frequency-voltage converter.

	Water flow meter		Watt meter
	condenser	evaporator	
C_{ref}	0.1 μ F	0.1 μ F	0.1 μ F
C_{int}	10 μ F	10 μ F	10 μ F
R_{int}	375k	250k	670k
R_1	370	560	470
R_2	180	220	270
$f_{IN\ max}$	23.5 Hz	56.0Hz	8.0Hz
Response time	3.75s	2.5s	6.7s

Table 5.1: Specifications for frequency-voltage converter for water flow meters and Watt meter.

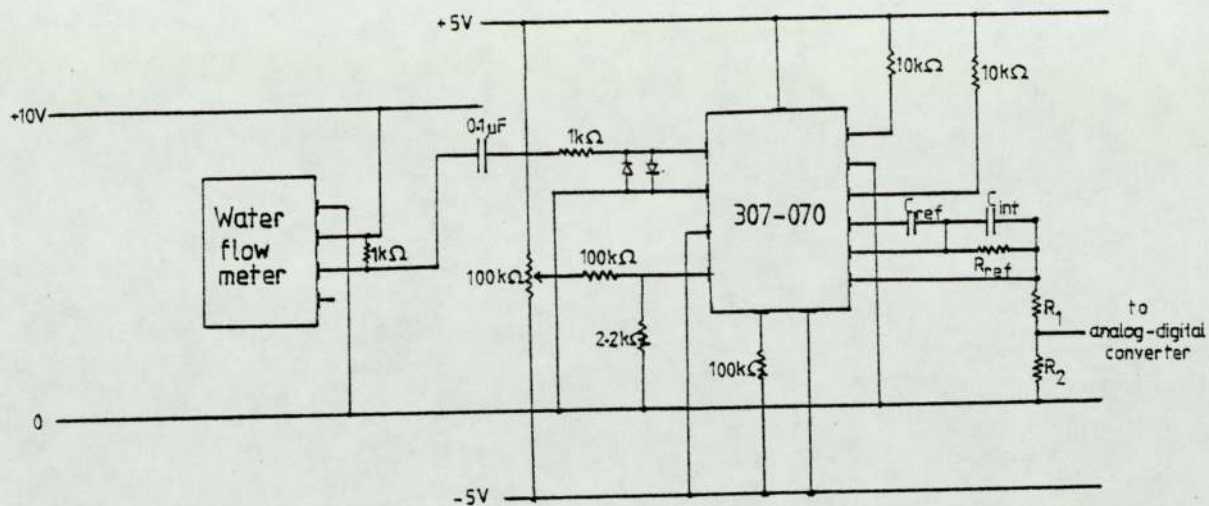


Figure 5.6 : The circuit for the water flow meter.

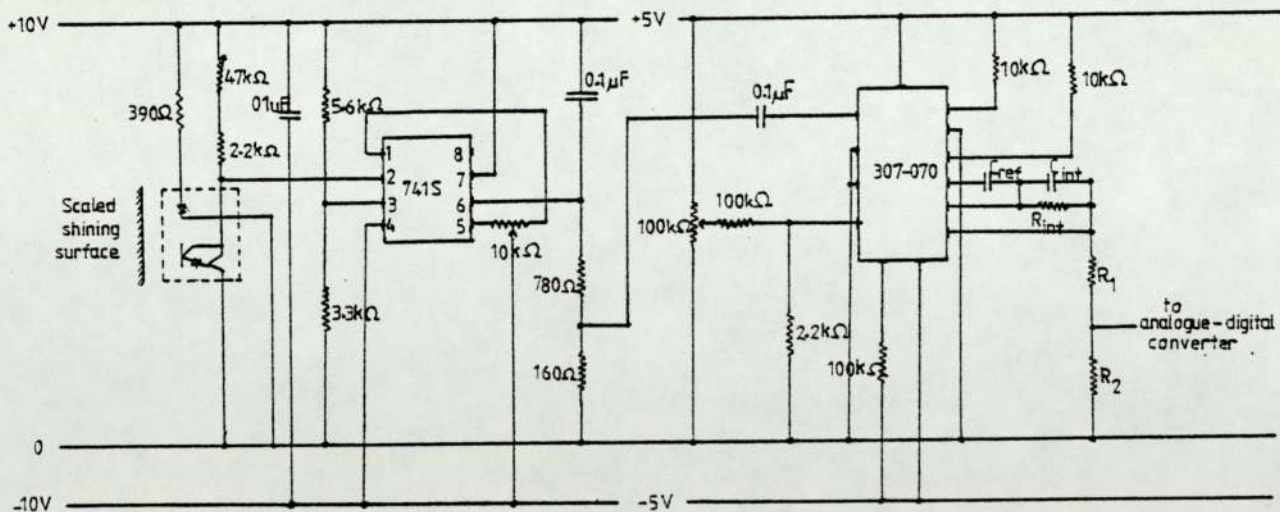


Figure 5.7: The circuit for the Watt meter.

The potential dividers have been fixed in those three output of the frequency-voltage converters for the reason that the input to analogue-digital converter cannot exceed 1.0V as mentioned earlier. In the Watt meter, potential divider has been fixed in the circuit after the operational amplifier to fulfill the second condition mentioned above.

The f_{IN} max. for Watt meter is lower than suggested by the manufacturer, but analysis shows that the overall Watt meter error still small, less than 2% as mentioned in the previous chapter.

5.5 The Computer Program.

Figure 5.8 shows the sensors and transducers which had been attached to the system corresponds to the pressure-enthalpy diagram in figure 5.9 . The thermocouples which were submerged in the water tank supported by a plastic rod at the centre of the tank are not shown in the diagram.

A BASIC program suitable for the PET Commodore computer was written in order to do the sampling. The temperature measurements in the system as shown in figure 5.8 and figure 5.9 were carried out through PCI1002 and the pressure and water flow measurements

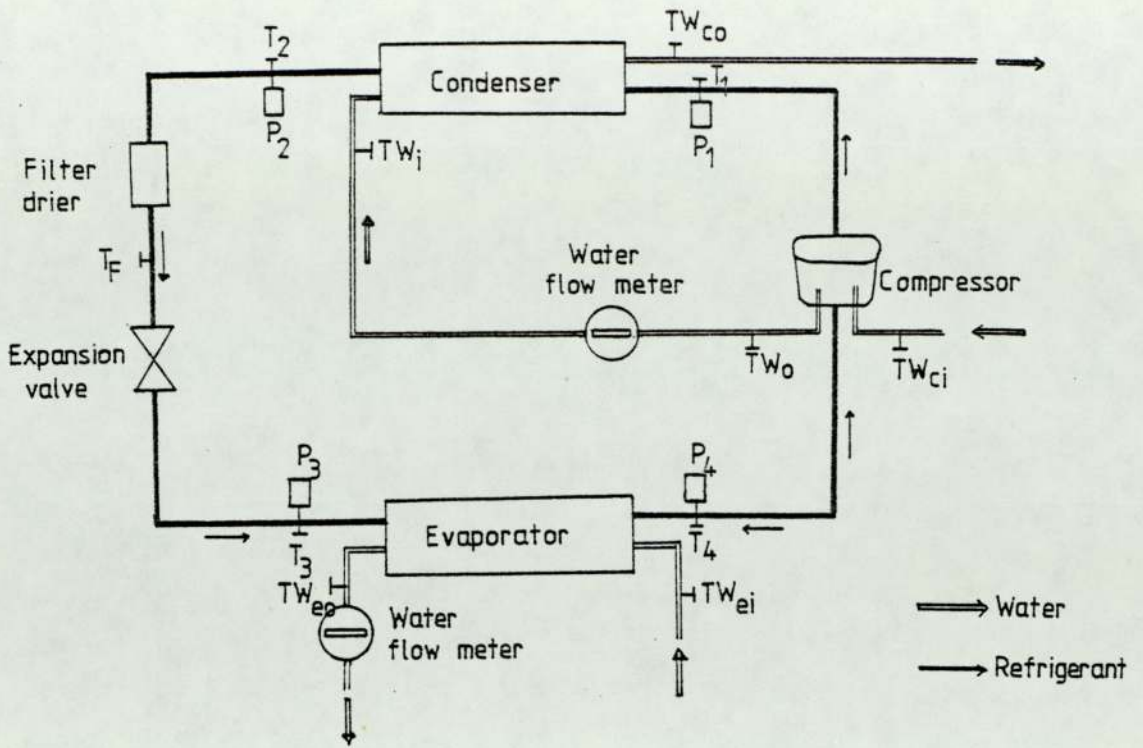


Figure 5.8 : Position of sensors in the heat pump system.

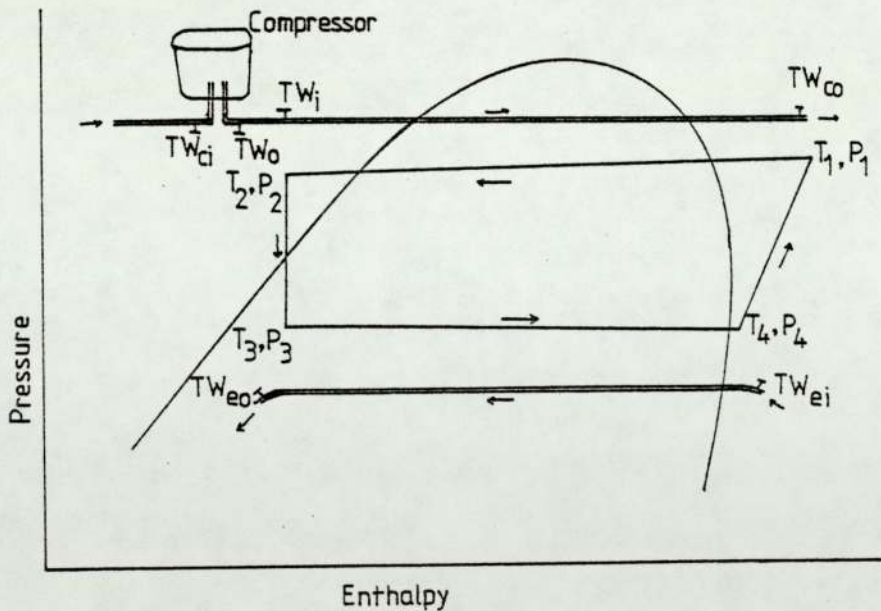


Figure 5.9: Position of sensors in Refrigerant and water lines.

were carried out through PCI1001. During the sampling process, all the calibration values as discussed in chapter 4 were used.

The energy absorbed by the evaporator (Q_e), given out by the condenser (Q_c), and picked-up during compressor cooling (Q_y), were calculated by using the relations;

$$Q_e = \dot{m}_e C_w (TW_{ei} - TW_{eo}) \quad 5.1$$

$$Q_c = \dot{m}_c C_w (TW_{co} - TW_i) \quad 5.2$$

$$Q_y = \dot{m}_c C_w (TW_o - TW_{ci}) \quad 5.3$$

where,

\dot{m}_e is the water flow rate through the evaporator.

\dot{m}_c is the water flow rate through the condenser.

C_w is the specific heat of water.

$TW_{ei}, TW_{eo}, TW_i, TW_o, TW_{ci}$ and TW_{co} are the temperature of water as in figure 5.9.

The total energy produced by the system is,

$$E_t = Q_c + Q_y \quad 5.4$$

Therefore the coefficient of performance is,

$$\begin{aligned} \text{COP} &= \frac{E_t}{W_c} \\ &= \frac{Q_c + Q_y}{W_c} \end{aligned} \quad 5.5$$

where W_c is the work done by the compressor.

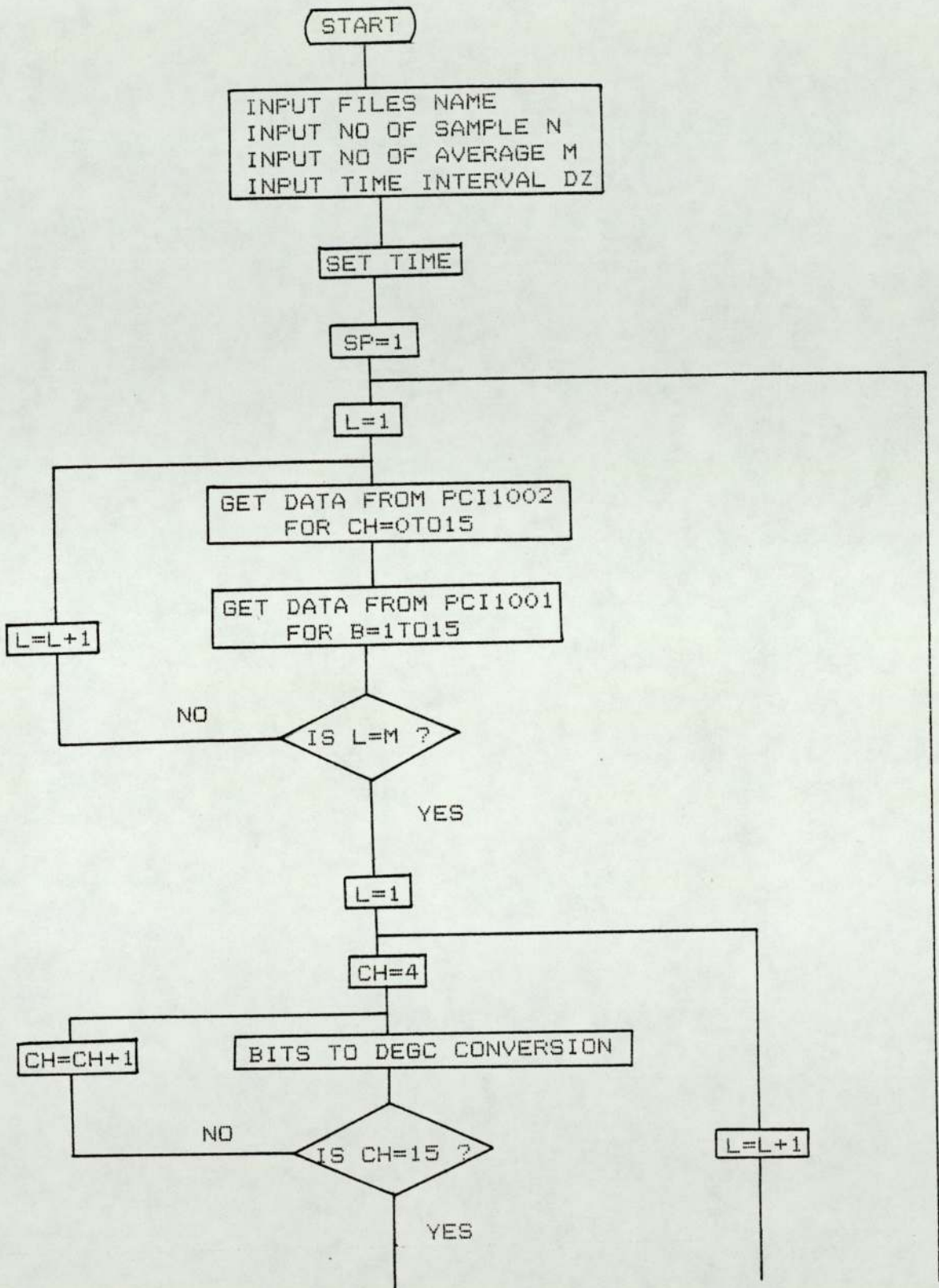
5.5.1 Flow Diagram Description.

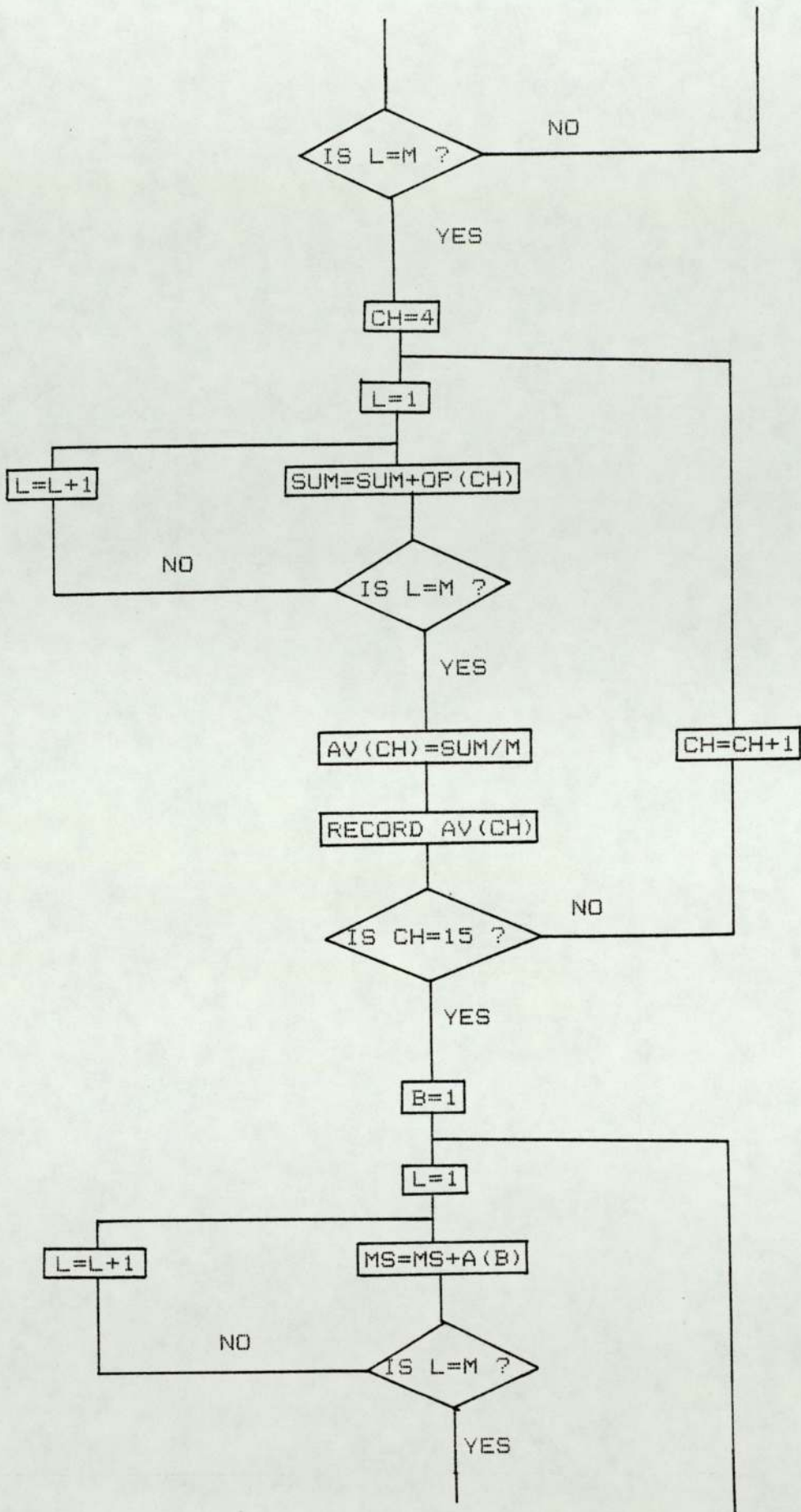
Figure 5.10 shows the flow diagram of the sampling program. The actual program is shown in Appendix II.

The program starts with naming the data file. Then proceeds with requesting the number of samples (N), the number of reading to be averaged (M) for each sample and the interval time required between each sampling ΔZ .

The program then proceeds with setting the clock in the computer to zero. Then the sampling is carried out by getting information from each channel on PCI1002 and PCI1001 for M times in sequence. The scanning process on each channel on each input to the corresponding channel is shown by a flashing light mounted on top of each channel. As soon as the scanning process has been completed M times, the time is recorded.

The next step is to measure the average values of each channel which had been scanned. For PCI1002 the bits recorded are converted to degrees Celsius, and for PCI1001 to D.C. voltage by using the subroutines





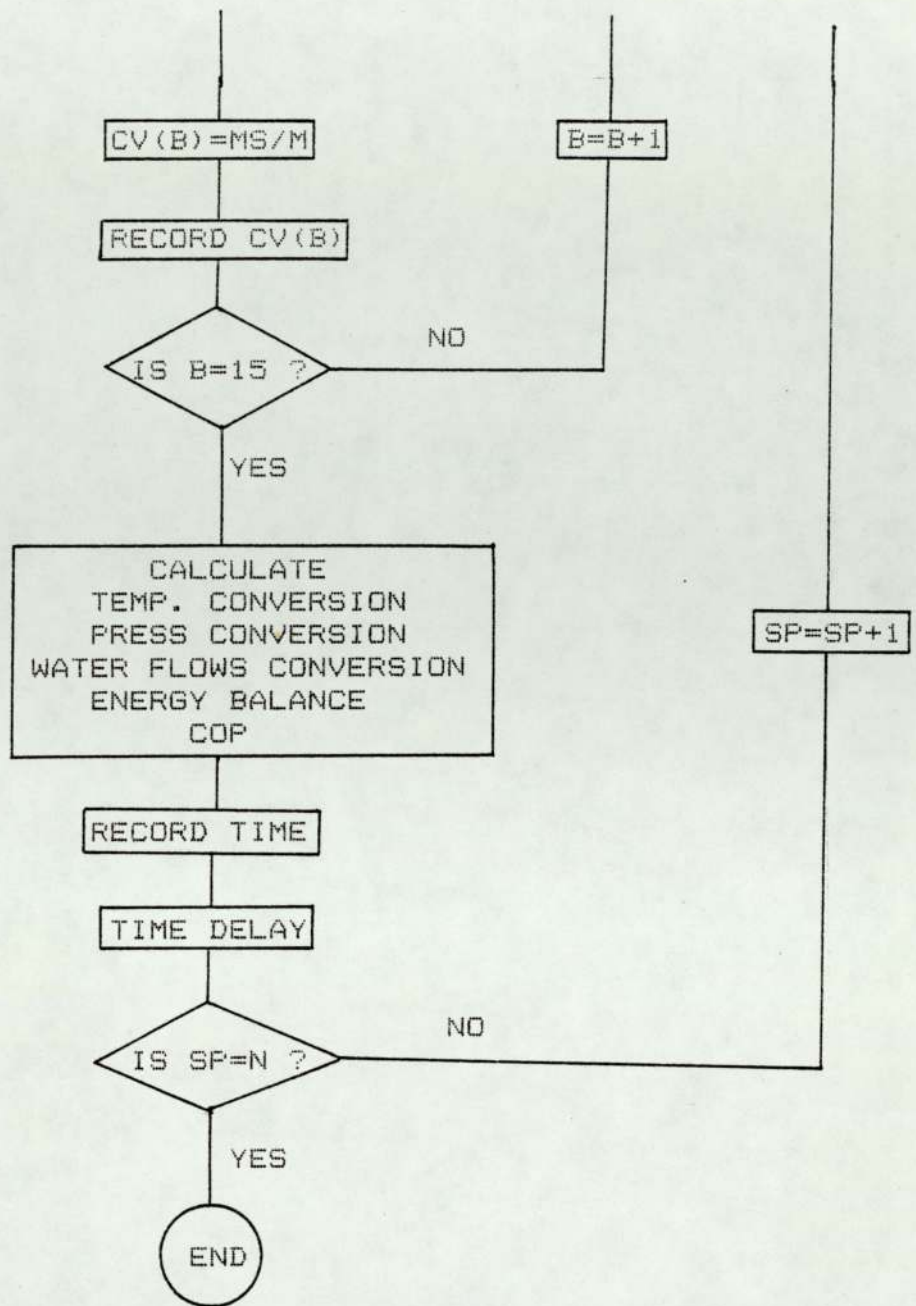


Figure 5.10: The flow diagram of the sampling program.

given by manufacturer as shown in Appendix I . The voltage is chosen as the recorded value since it is the fundamental value used for calibrations. For further analysis the voltage recorded can be converted to the calibration values as discussed in previous chapter. These values are then recorded in the floppy disc in sequence from channel 4 to 15 for PCI1002 and from channel 1 to 15 for PCI1001.

The next step is to convert the voltages recorded to temperature in degrees Celsius for the tank temperature profile, pressures around the refrigerant circuit, water flow rate, energy balance and coefficient of performance. These values are then displayed on the computer screen.

The time taken is also recorded in the floppy disc soon after the averaged values of each channel are recorded.

The whole process is then repeated for N samples.

The time taken by the computer to calculate and do the average is about 80 seconds. So the minimum interval time is 80 seconds. This time could be made more longer by setting delayed time DZ.

If the values for N, M and DZ are chosen to be 150, 10 and 10 seconds respectively, then the whole process of data acquisition will be finished in about 225 minutes. During this long time the variations of the heat pump system would be recorded.

CHAPTER 6.

PERFORMANCE ANALYSIS DURING WATER HEATING.

6.1 Introduction.

Figure 6.1 shows the experimental arrangement of the heat pump in producing domestic hot water.

Three different modes of heating the water in the tank were used;

Mode 1. Water flow regulator in circuit.

Tap 1 closed. Tap 2 open.

Thermal stratification present in storage tank.

Mode 2. Water flow regulator out of circuit.

Tap 1 closed. Tap 2 open.

Thermal stratification present in storage tank.

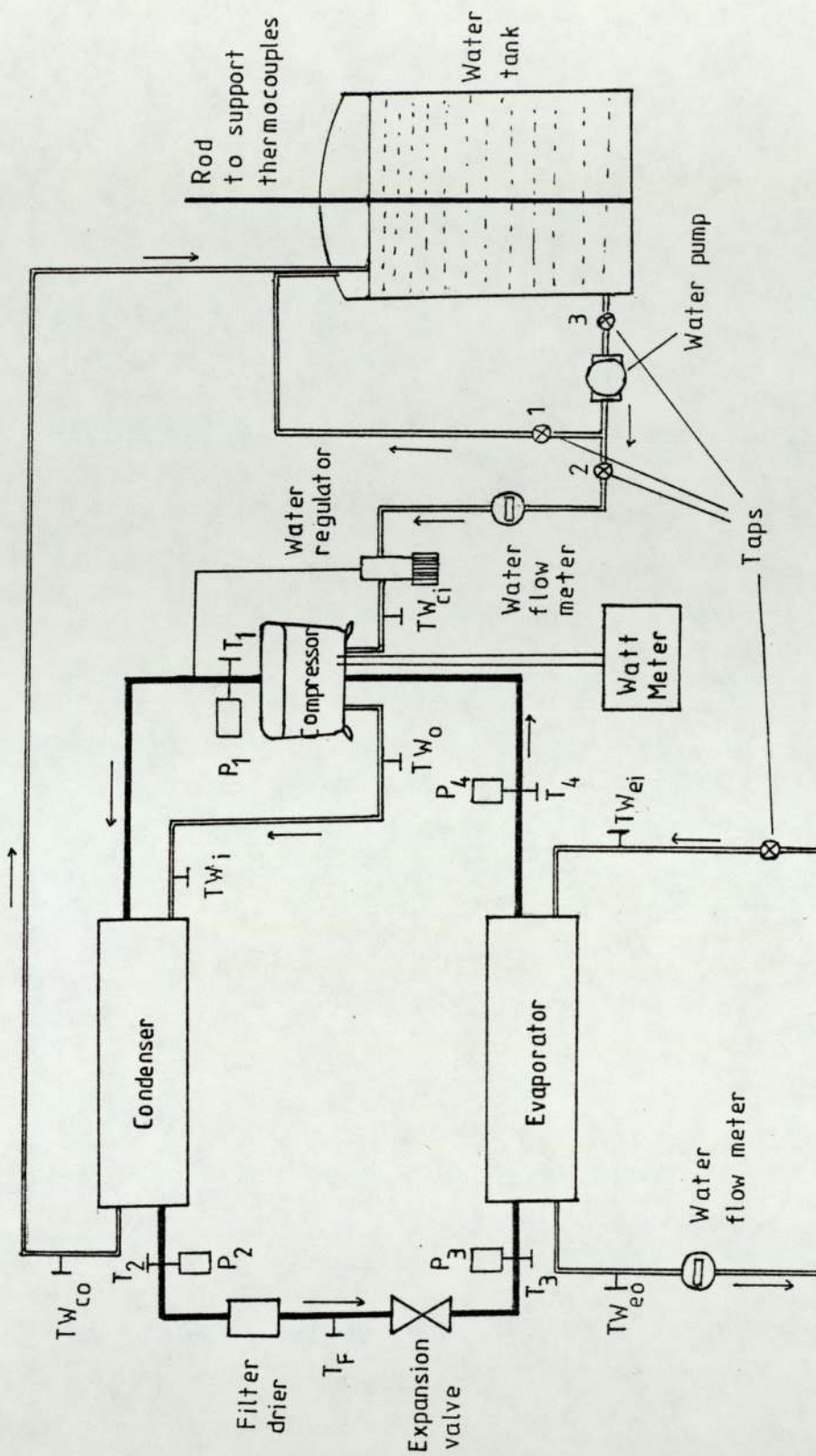


Figure 6.1: The experimental set-up of the heat pump in producing hot water.

Mode 3. Water flow regulator in circuit.

Tap 1 open. Tap 2 open.

No thermal stratification in storage tank.

The domestic hot water tank used was an indirect copper cylinder having standard internal heating coil. The height of the cylinder was 900mm and the diameter was 450mm with capacity 120 litres. The tank was insulated by using the manufacturer's coating of a commercial insulator.

The temperature profile of the water in the tank during water heating was measured by eight copper-constantan thermocouples situated along the vertical axis of the cylinder supported by a plastic rod. The junctions were placed at intervals of 10cm vertically with the first junction located at the bottom of the tank.

The data were recorded by the computer automatically, 150 samples being taken at roughly 100 seconds intervals. The system automatically switched off if the discharge pressure exceeded 1379.0kPa (200 psia) - the maximum pressure (and the maximum safe temperature) at which the pressure transducer can operate [28]. The computer program for the data acquisition system is shown in appendix II. During

the sampling process, the following parameters were recorded by the computer on the floppy disc for further analysis,

1. The temperature of all thermocouples - 5 in the refrigerant circuit, 6 in the water lines and 8 in the water tank.
2. The pressure at 4 points around the refrigerant circuit as in figure 6.1.
3. The water flow rate for the evaporator and condenser.
4. The electrical power for the compressor.
5. The time taken during each sampling.

The temperatures, recorded via analogue-digital converter PCI1002, were recorded in degree Celsius. All parameters recorded via analogue-digital converter PCI1001 were recorded as D.C. voltages. All parameters together with,

1. The amount of energy absorbed by the evaporator Q_e .
2. The energy delivered by the condenser Q_c .
3. The energy picked-up during the compressor cooling.

4. The energy balance.

5. The coefficient of performance.

were displayed on the computer screen during the sampling process. Table 6.1 shows a typical listing of the data file for some of the recorded variables.

Each sample reading was recorded as the average of ten successive readings to minimise small fluctuations due to noise coming from the signal in the sensor. The data were subject to some bias due to the fact that the sensor used to detect the water flow rate detects the variation of water flow, the temperature responds slightly later owing to the water taking time to reach the sensor.

Separate programs were used for final analysis of the data. The most direct analysis calculated the value of temperature, pressure, determining the electrical power to the compressor, energy released by condenser and absorbed by evaporator.

The electrical power for the water pump was not recorded by the computer since it could be set at constant speed with an electrical power consumption of 60 Watts.

FILE NAME:11:CON-RC1.S.R

TIME (MIN)	T1 (C)	T2 (C)	T3 (C)	T4 (C)	TW _{el} (C)	TW _{eo} (C)	TW _i (C)	TW _o (C)	TW _{el} (C)	TW _o (C)	P1 (MPA)	P2 (MPA)	P3 (MPA)	P4 (MPA)	WC (WATT)	ME (ML/S)	MC (ML/S)
68.38	72.2	19.5	.6	6.9	11.3	5.9	18.8	45.9	16.4	18.8	1.034	.9003	.3053	.2848	345.19	30.95	9.02
71.1	72.2	19.5	.5	6.8	11.3	5.9	18.9	45.8	16.5	18.9	1.035	.9017	.3040	.2836	342.91	30.87	9.26
73.82	72.3	19.7	.6	7.1	11.3	5.9	19	46	16.6	19	1.033	.8968	.3067	.2861	351.78	30.88	8.69
76.53	72.3	19.8	.6	7	11.3	5.9	19.1	45.9	16.7	19.1	1.035	.9011	.3055	.2850	345.11	30.75	8.89
79.27	72.4	19.9	.6	7	11.4	6	19.3	45.9	16.9	19.2	1.034	.9001	.3044	.2839	347.53	30.65	8.9
81.98	72.4	20	.6	6.5	11.4	6	19.4	45.8	17.1	19.4	1.036	.9036	.3033	.2829	345.88	30.62	9.25
84.7	72.4	20.1	.6	7.1	11.5	6	19.6	45.8	17.3	19.6	1.034	.9003	.3049	.2844	347.79	30.7	8.94
87.42	72.4	20.3	.7	7.2	11.6	6.1	19.7	45.8	17.5	19.8	1.033	.8980	.3068	.2862	347.15	30.64	8.78
90.13	72.5	20.4	.7	7.3	11.6	6.2	19.9	45.7	17.8	20	1.035	.8995	.3078	.2873	349.32	30.66	9.06
92.87	72.5	20.6	.7	7.2	11.8	6.2	20.2	45.7	18.1	20.3	1.034	.9005	.3072	.2867	346.24	30.64	9.14
95.58	72.4	20.8	1	7.1	11.8	6.3	20.4	45.5	18.5	20.6	1.038	.9026	.3099	.2895	347.31	30.64	9.74
98.3	72.4	21.1	1.1	7.8	11.9	6.4	20.8	45.6	19	21	1.034	.8962	.3115	.2907	345.09	30.63	9.45
101.02	72.4	21.5	1	7.8	12	6.4	21.2	45.5	19.4	21.4	1.035	.8986	.3112	.2905	343.33	30.74	9.57
103.73	72.4	21.8	1	7.7	12	6.5	21.6	45.3	19.9	21.8	1.035	.8990	.3109	.2903	343.00	30.63	9.9
106.45	72.3	22.2	1.2	7.8	12.1	6.5	22.1	45.3	20.5	22.4	1.037	.9007	.3128	.2922	343.00	30.54	10.2
109.17	72.4	22.7	1.3	8	12.1	6.5	22.6	45.1	21.2	23	1.037	.8998	.3145	.2939	345.06	30.61	10.46
111.97	72.5	23.2	1.1	7.8	12.1	6.5	23.2	44.9	21.9	23.6	1.033	.8989	.3100	.2894	343.36	30.59	10.53
114.6	72.6	23.7	1.3	8.1	12.2	6.6	23.8	44.9	22.7	24.3	1.035	.8986	.3140	.2932	345.66	30.63	10.57
117.32	72.7	24.3	1.4	8.1	12.1	6.6	24.5	44.4	23.5	25	1.031	.8943	.3149	.2942	343.00	30.58	11.49
120.03	72.8	25	1.5	8.2	12.2	6.6	25.3	44.4	24.4	25.8	1.038	.9013	.3159	.2951	343.63	30.64	12.23
122.73	72.9	25.7	1.4	8.2	12.1	6.6	26.1	44.2	25.4	26.7	1.037	.9023	.3144	.2936	341.66	30.63	12.77
125.45	73.1	26.5	1.6	8.1	12.1	6.6	27.1	44	26.5	27.6	1.040	.9064	.3157	.2950	346.17	30.6	13.94
128.17	73.2	27.4	1.4	8.1	12.1	6.6	28	43.8	27.7	28.7	1.037	.9054	.3137	.2930	341.47	30.63	15.3
130.88	73.4	28.3	1.7	8.6	12.2	6.7	29.1	44	28.9	29.8	1.042	.9079	.3189	.2981	344.09	30.58	16.04
133.6	73.6	29.3	1.7	8.5	12.1	6.7	30.3	43.6	30.2	31	1.040	.9094	.3173	.2966	342.33	30.58	18.1
136.32	73.8	30.5	1.9	8.7	12.1	6.8	31.6	43.4	31.7	32.3	1.046	.9173	.3201	.2994	344.01	30.6	20.9
139.05	74.2	31.8	1.9	8.7	12.1	6.8	33.1	43.4	33.3	33.8	1.056	.9307	.3205	.2999	343.53	30.65	22.98
141.77	74.9	33.2	2.2	8.9	12.1	6.9	34.7	44.2	34.9	35.3	1.082	.9600	.3226	.3020	348.11	30.72	24.22
144.47	75.9	34.6	2.2	8.9	12.1	6.9	36.1	45.5	36.4	36.8	1.116	.9978	.3234	.3027	350.14	30.64	24.38
147.17	77	35.8	2.4	9.2	12	6.9	37.4	46.7	37.8	38.1	1.145	1.028	.3261	.3055	350.63	30.73	24.46
149.87	78.1	36.9	2.5	9.2	12	7	38.5	47.8	38.9	39.2	1.172	1.059	.3275	.3068	359.23	30.68	24.43
152.58	79.1	37.8	2.6	9.3	11.9	7	39.4	48.7	39.8	40.1	1.196	1.084	.3285	.3078	358.86	30.67	24.29
155.28	80.1	38.5	2.5	9.3	11.9	7	40.1	49.4	40.5	40.8	1.213	1.104	.3277	.3072	360.89	30.68	24.25
157.98	81	39.2	2.6	9.4	11.7	6.9	40.7	50	41.1	41.5	1.231	1.123	.3283	.3076	361.88	30.62	24.12
160.68	81.8	39.7	2.5	9.3	11.6	6.9	41.2	50.5	41.6	41.9	1.243	1.137	.3274	.3068	362.50	30.73	24.12
163.38	82.5	40	2.5	9.1	11.5	6.9	41.6	50.8	42	42.3	1.253	1.149	.3263	.3059	361.97	30.62	24.11
166.1	83.2	40.3	2.5	9.2	11.4	6.8	41.9	51.1	42.2	42.6	1.261	1.157	.3269	.3064	362.40	30.67	24.16
168.82	83.8	40.5	2.5	9.2	11.3	6.7	42.1	51.3	42.4	42.8	1.267	1.163	.3273	.3067	364.22	30.68	24.09
171.52	84.3	40.7	2.5	9.2	11.3	6.7	42.3	51.4	42.6	43	1.271	1.168	.3273	.3067	363.74	30.67	24.05
174.23	84.7	40.9	2.5	9.3	11.2	6.7	42.4	51.6	42.7	43.1	1.274	1.170	.3280	.3075	364.27	30.71	23.8

TABLE 6.1 LISTING OF DATA FILE SHOWING TIME DEPENDENCE OF SOME OF RECORDED VARIABLES.

In analysing the performance of the heat pump system during water heating, the variations of parameters (like temperatures, pressures, water flow rates, energy for evaporator, condenser and compressor and coefficient of performance) against the time taken after each sampling were plotted as carried out by Morgan [7] and Carrington et al [37] . By this method the effect of a change in one of the parameters on the others can be observed.

The appropriate cycles were drawn on pressure-enthalpy diagrams based on the diagram given by Hickson and Taylor [38].

The following nomenclature will be used for discussion.

T_1 = discharge temperature in the refrigerant circuit.

T_2 = outlet temperature of the condenser in refrigerant circuit.

T_3 = inlet temperature of the evaporator in refrigerant circuit.

T_4 = suction temperature in the refrigerant circuit.

TW_{ei} = input water temperature to the evaporator.

TW_{eo} = output water temperature from the evaporator.

- TW_i = input water temperature to the condenser.
- TW_{co} = output water temperature from the condenser.
- TW_{ci} = temperature of water coming from water tank (water supply).
- TW_o = temperature of water after the compressor.
- P_1 = discharge pressure.
- P_2 = outlet pressure of the condenser.
- P_3 = pressure after the expansion valve.
- P_4 = suction pressure.
- \dot{m}_F = mass flow rate of the refrigerant.
- \dot{m}_e = mass of water flow rate through the evaporator.
- \dot{m}_c = mass of water flow rate through the condenser.
- Q_e = energy absorbed by the evaporator.
- Q_c = energy delivered by the condenser.
- Q_y = energy picked-up during compressor cooling.
- W_c = electrical power consumed by the compressor.

6.2 Single Pass: Water Circulated Through the Condenser.

The experiments were carried out firstly with the water flow rate controlled by the regulator (in

response to the discharge pressure); secondly, bypassing the water regulator, which means that the water flow rate could be kept constant by tap 2.

Cold water (temperature TW_{ci}) was drawn from the bottom of the tank, and hot water (temperature TW_{co}) fed to the top of the tank. The water entered the tank tangentially at the surface.

6.2.1. Mode 1 : Water Passing Through Condenser Controlled By The Water Regulator.

The first experiment was carried out with tap 1 closed and tap 2 opened, so as to allow single pass water circulation through the condenser. The method of hot water entry allowed stratification to be maintained.

Table 6.2(a) shows the initial condition for the first experiment with the water regulator set to give a discharge pressure P_1 of 1028.8kPa (149.2psia).

Figure 6.2(a) shows the temperature variations for the condenser. The temperature of the refrigerant (T_1 and T_2) are denoted by (.) and the water (TW_i and TW_{co}) are denoted by (+). The discharge temperature T_1 was maintained at 71.0°C for 120 minutes until it

began to increase when the water at the bottom of the tank began to heat up and entered the condenser with increased flow rate (figure 6.4(a)).

As a result of the hot water being fed to the condenser, the refrigerant outlet temperature (T_2) increased (Figures 6.2(a) and 6.3(a)) corresponding to the increase in the water flow rate (figure 6.4(a)) from 9.3ml/s to 24.5ml/s. It can be seen that for 120 minutes the cold water coming from the tank absorbed heat from the refrigerant (T_{W_1} less than T_2) figure 6.3(a), but after that since the temperature of the water T_{W_1} becomes higher than the refrigerant temperature T_2 , the water gives some of its heat to the refrigerant. This effect together with the increase in water flow rate lowers the outlet temperature $T_{W_{co}}$ from 45.7°C to 43.3°C .

The increase in the water flow rate is the result of an increase in discharge pressure P_1 , as shown in figure 6.5(a), since the water regulator is controlled by the discharge pressure. The increase in P_1 is due to the increase in the work done (W_c) by the compressor on the refrigerant as shown in figure 6.6(a).

Figure 6.7(a) shows the energy delivered by the condenser Q_c (*), the energy absorbed by the

evaporator Q_e (.) and the electrical power consumed by the compressor W_c (+). As a result of hot water TW_i being fed to the condenser after about 120 minutes, Q_c and Q_e decrease while W_c increases. This effect reduces the C.O.P. as shown in figure 6.8(a).

The fluctuation of Q_c is due to fluctuation of the water flow through the condenser (figure 6.4(a)). The fluctuation of the water flow is due to the hunting of the water regulator being controlled by the discharge pressure P_1 .

Figure 6.9(a) shows the refrigerant cycles for three states A, B and C during sampling and table 6.3(a) shows the parameters. The first cycle A is the state where cold water is being fed to the condenser in the first 120 minutes where all parameters are kept constant. The second state B is the transition state where the outlet refrigerant temperature (T_2) and inlet water temperature to the condenser (TW_i) have the same temperature (figure 6.3(a)), which is about 140 minutes after the sampling process began. The third cycle (C) is where the warm water is being fed to the condenser which is about 160 minutes after the sampling process began. The refrigerant cycle moves to the right of the pressure-enthalpy diagram with a nearly fixed value of superheat enthalpy H_4 when

hot water is fed to the condenser, resulting in a decrease of Q_c and Q_e .

As the pressure increases (the cycle moves to the right), the pressure losses ($P_1 - P_2$) in the condenser decrease (figure 6.5(a) and figure 6.9(a)). In other words, as the pressure P_1 increases the pressure losses in the condenser decrease.

6.2.2. Mode 2 : Constant Flow Through The Condenser - Bypassing The Water Regulator.

The second experiment was performed with the water flow through the condenser bypassing the water regulator at 9.7ml/sec. Figures 6.2(b), 6.4(b), 6.5(b), 6.6(b), 6.7(b) and 6.8(b) show the time variations of the measured parameters during the sampling process. The initial conditions of the experiment are shown in table 6.2(b).

Since the water flow was not controlled by the water regulator, when the warmer water was fed to the condenser the temperature T_1 and pressure P_1 continuously increased (figure 6.2(b) and 6.5(b)) until the system switched off. This should be compared with the behaviour during the first experiment, where T_1 and P_1 remain constant until warm water from

the tank starts to enter the condenser, when T_1 and P_1 effectively suffer a step-function increase to new higher constant values (figure 6.2(a) and 6.5(a).

Q_c fluctuates considerably during the first experiment because of the operation of the water regulator. These fluctuations would be expected to be absent in the second experiment, since the regulator is being bypassed. However figure 6.7(b) shows some residual fluctuations in Q_c . This is due to fluctuations in the water flow rate in the condenser (figure 6.4(b)). By examining figure 6.4(b) and 6.7(b) it can be seen that the patterns of fluctuation in Q_c follow the fluctuation of the water flow rate \dot{m}_c in the condenser.

The work done by the compressor W_c follows the pattern of T_1 as shown in figure 6.2(a), 6.2(b), 6.6(a) and 6.6(b). Figure 6.5(b) shows that when the discharge pressure P_1 increases (or in other words the pressure ratio P_1/P_4 increases since the pressure P_4 is kept constant), the pressure loss ($P_1 - P_2$) in the condenser decreases.

Figure 6.9(b) shows the refrigerant cycles A, B and C during sampling. Cycle A is in first 100 minutes where all parameters are kept constant, in which cold water is being fed to the condenser. Cycle B is the transition point when hot water starts to enter

the condenser - about after 140 minutes, and cycle C is when more hot water is being fed - about after 220 minutes (the end of sampling). The numerical values of the parameters for each cycle (A,B and C) are given in table 6.3(b).

6.3 Mode 3 : Water Passing Through The Condenser With Tap 1 and Tap 2 Open.

Figures 6.2(c),6.4(c),6.5(c),6.6(c),6.7(c) and 6.8(c) represent the comparable set of results with both tap 1 and tap 2 open (figure 6.1). Opening tap 1 and 2 causes a large fraction of the pumped water to be immediately returned to the top of the tank. This causes vigorous mixing within the tank, with the result that the tank temperature slowly rises, more or less homogeneously - i.e. stratification no longer occurs.

The experiment was performed with the water flow through the condenser controlled by the water regulator. The regulator was set to give initial discharge pressure P_1 of 1057.2kPa (153.34psia). The initial conditions for the experiment are shown in table 6.2(c).

As the result of both taps 1 and 2 being open, the water in the tank is continuously mixed together and the whole tank becomes warmer gradually.

Figures 6.2(c) and 6.3(c) show that the temperature T_{W_1} gradually increases until the end of the sampling. The refrigerant outlet temperature T_2 and the water inlet temperature to the condenser T_{W_1} equalise more quickly (about after 80 minutes) compared with the previous experiments (after about 120 minutes for mode 1 and about 220 minutes for mode 2).

Figure 6.7(c) shows the variation of the water flow rate in the condenser (+) which increases gradually compared to figure 6.4(a). The spikey fluctuations occurring in figure 6.4(c), 6.5(c) and 6.6(c) at about 40 minutes are due to noise which affected the power supply to the frequency-voltage converters during the sampling.

The work done W_c by the compressor increases gradually as shown in figure 6.6(c).

Figure 6.9(c) shows the refrigerant cycles of the experiment in three states A, B, and C - early in the experiment where T_{W_1} is less than T_2 , at about 45 minutes where transition occurs in which T_{W_1} equals T_2 and at the end of the experiment where warm water is being fed to the condenser (T_{W_1} higher than T_2). The numerical values of the parameters for cycles A, B and C are given as shown in table 6.3(c).

	EVAPORATOR	CONDENSER	COMPRESSOR
R-12 TEMP. (C) I/P	.9	71.1	7.4
R-12 TEMP. (C) O/P	7.4	18.7	71.1
WATER TEMP. (C) I/P	11.8	18.3	15.8
WATER TEMP. (C) O/P	6.3	45.7	18.2
WATER F/RATE (ML/S)	31.9	9.3	9.3
PRESS I/P (KPA)	308.8	1028.7	288.6
PRESS O/P (KPA)	288.6	889.7	1028.7
ENERGY (J/S)	732.1	1067.2	91.1
ELECTRIC POWER (WATTS)			340.5

TABLE 6.2(A) : PARAMETERS OF INITIAL CONDITION FOR MODE 1 EXPERIMENT.

	EVAPORATOR	CONDENSER	COMPRESSOR
R-12 TEMP. (C) I/P	-.9	62.6	5.7
R-12 TEMP. (C) O/P	5.7	16.1	62.6
WATER TEMP. (C) I/P	10.4	15.8	14.2
WATER TEMP. (C) O/P	4.6	40.5	15.8
WATER F/RATE (ML/S)	29.7	9.7	9.7
PRESS I/P (KPA)	286.9	924.1	267.8
PRESS O/P (KPA)	267.8	786.3	924.1
ENERGY (J/S)	717.5	1002.0	66.7
ELECTRIC POWER (WATTS)			330.0

TABLE 6.2(B) : PARAMETERS OF INITIAL CONDITION FOR MODE 2 EXPERIMENT.

	EVAPORATOR	CONDENSER	COMPRESSOR
R-12 TEMP. (C) I/P	.6	68.3	6.7
R-12 TEMP. (C) O/P	6.7	19.1	68.3
WATER TEMP. (C) I/P	11.4	18.8	17.1
WATER TEMP. (C) O/P	6.2	47.0	19.1
WATER F/RATE (ML/S)	30.7	8.2	8.2
PRESS I/P (KPA)	308.2	1057.2	288.3
PRESS O/P (KPA)	288.3	922.9	1057.2
ENERGY (J/S)	665.1	963.9	67.5
ELECTRIC POWER (WATTS)			344.7

TABLE 6.2(C) : PARAMETERS OF INITIAL CONDITION FOR MODE 3 EXPERIMENT.

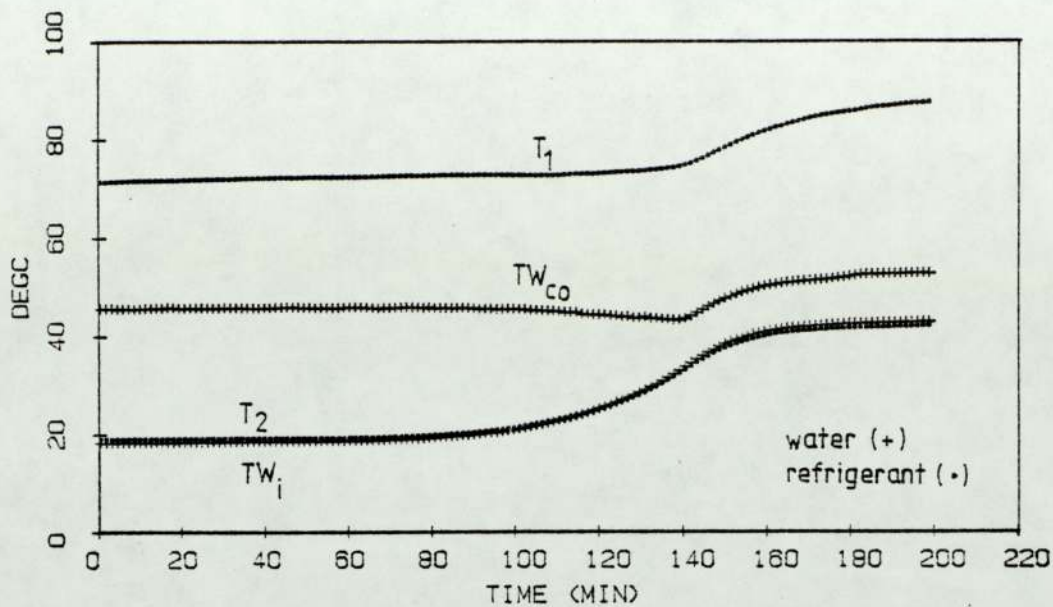


Figure 6.2(a): The temperature variation at the inlet and outlet of the condenser for Mode 1 experiment.

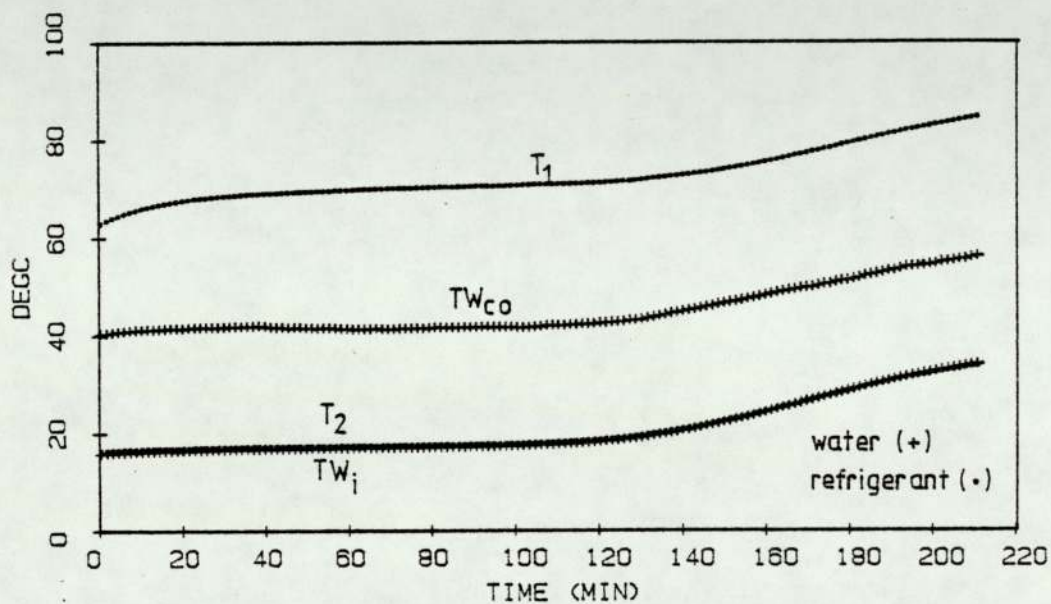


Figure 6.2(b): The temperature variation at the inlet and outlet of the condenser for Mode 2 experiment.

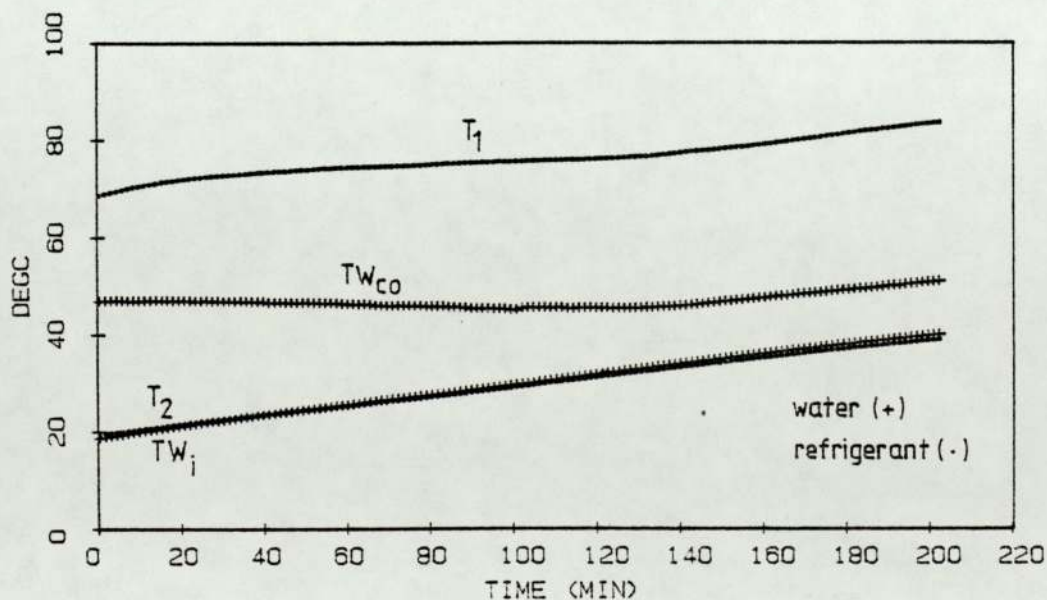


Figure 6.2(c): The temperature variation at the inlet and outlet of the condenser for Mode 3 experiment.

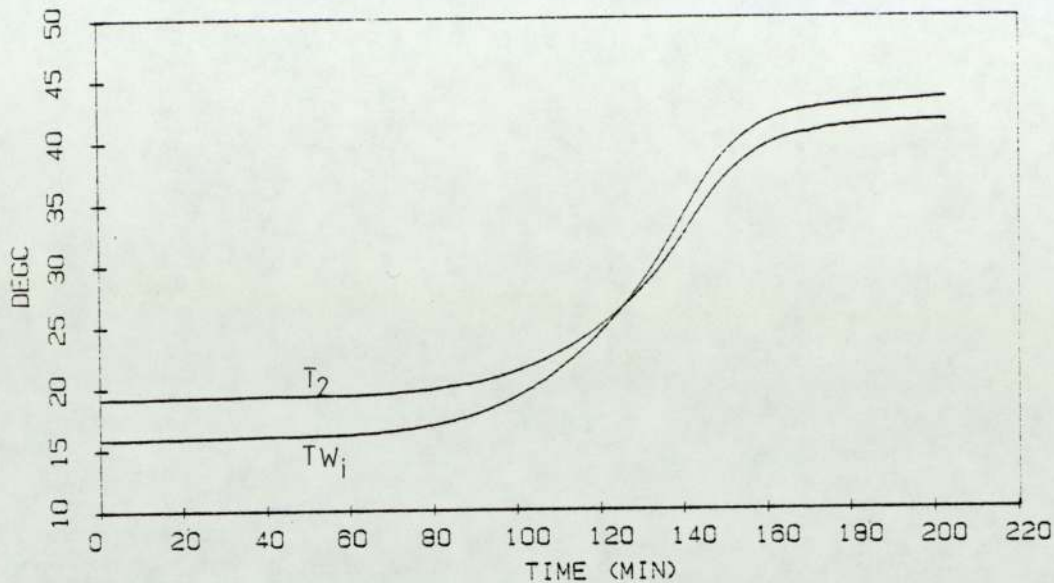


Figure 6.3(a): Temperatures T_2 and TW_i corresponding to figure 6.2(a).
Enlarged scale.

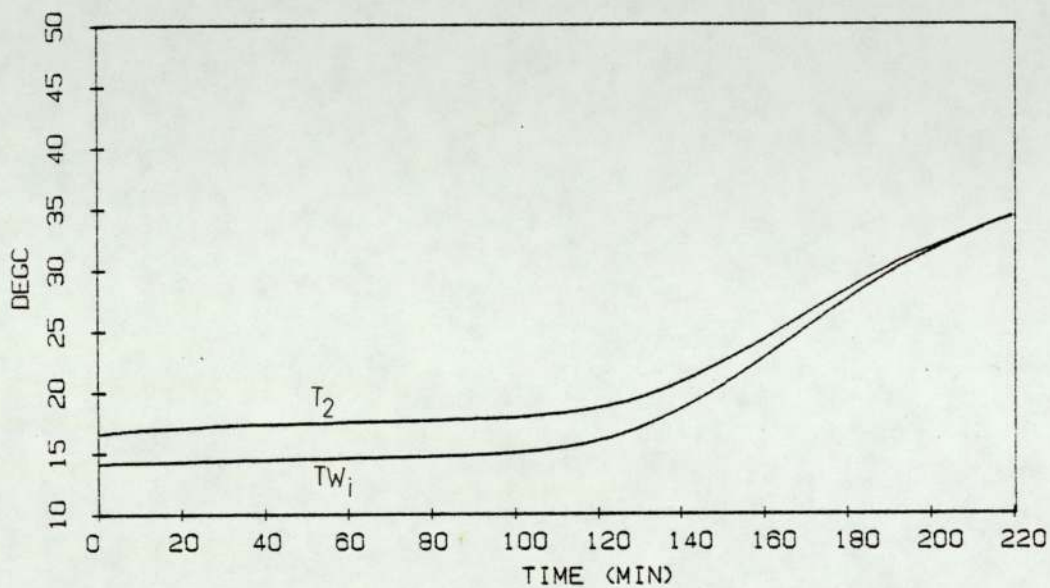


Figure 6.3(b): Temperatures T_2 and TW_i corresponding to figure 6.2(b).
Enlarged scale.

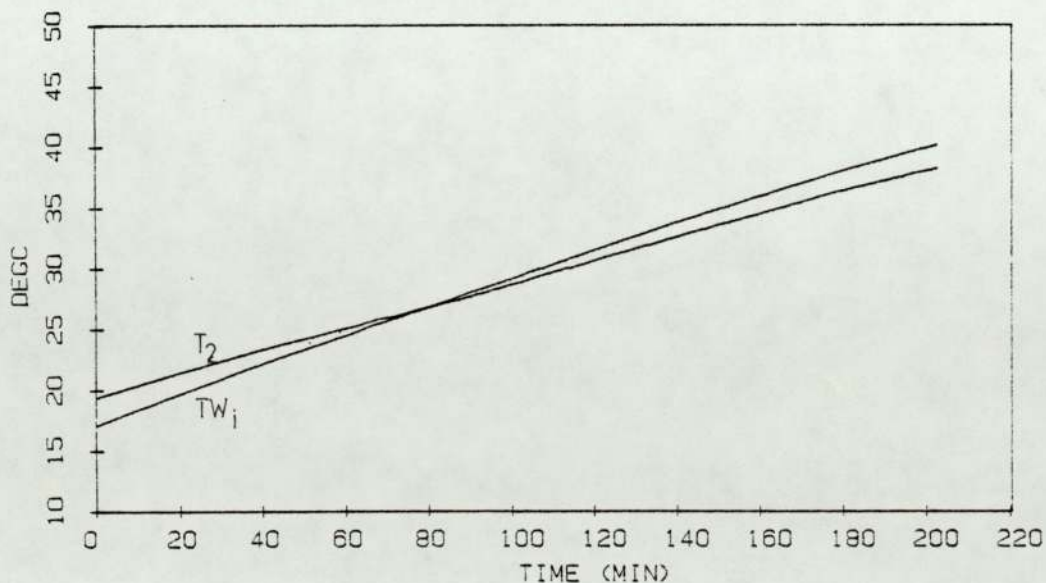


Figure 6.3(c): Temperatures T_2 and TW_i corresponding to figure 6.2(c).
Enlarged scale.

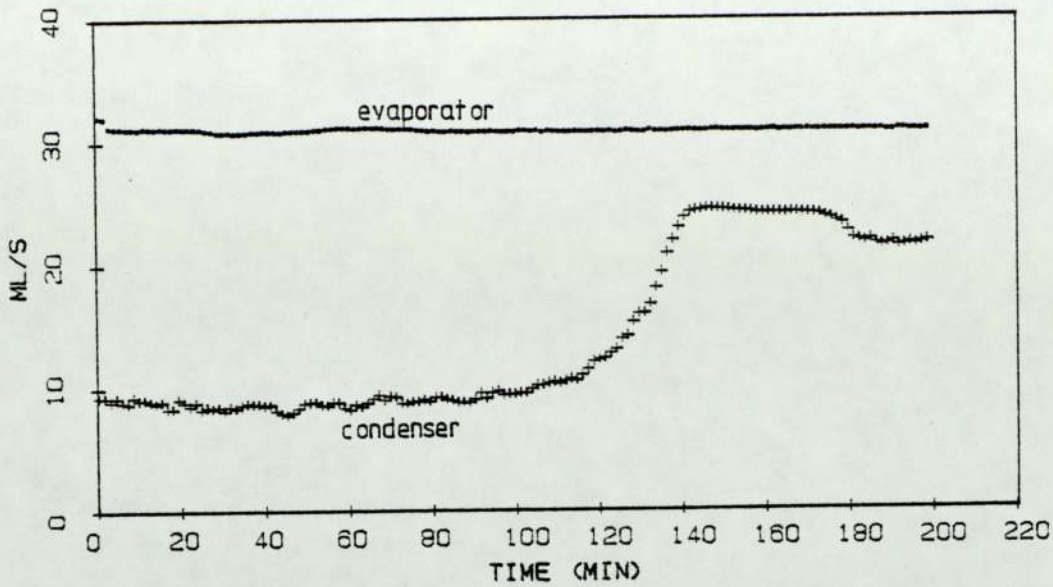


Figure 6.4(a): The variation of water flow rate through the evaporator and condenser for Mode 1 experiment.

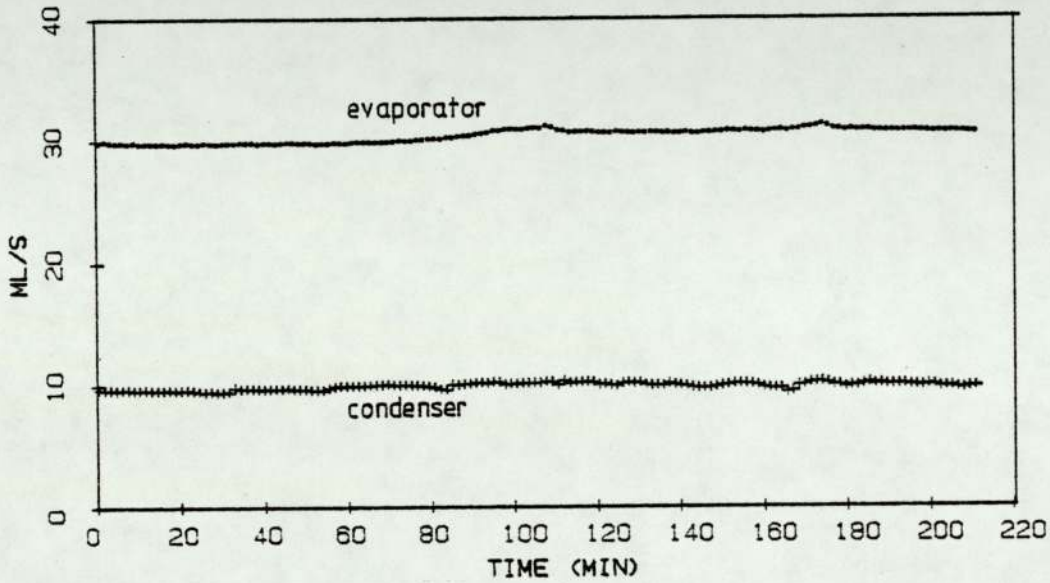


Figure 6.4(b): The variation of water flow rate through the evaporator and condenser for Mode 2 experiment.

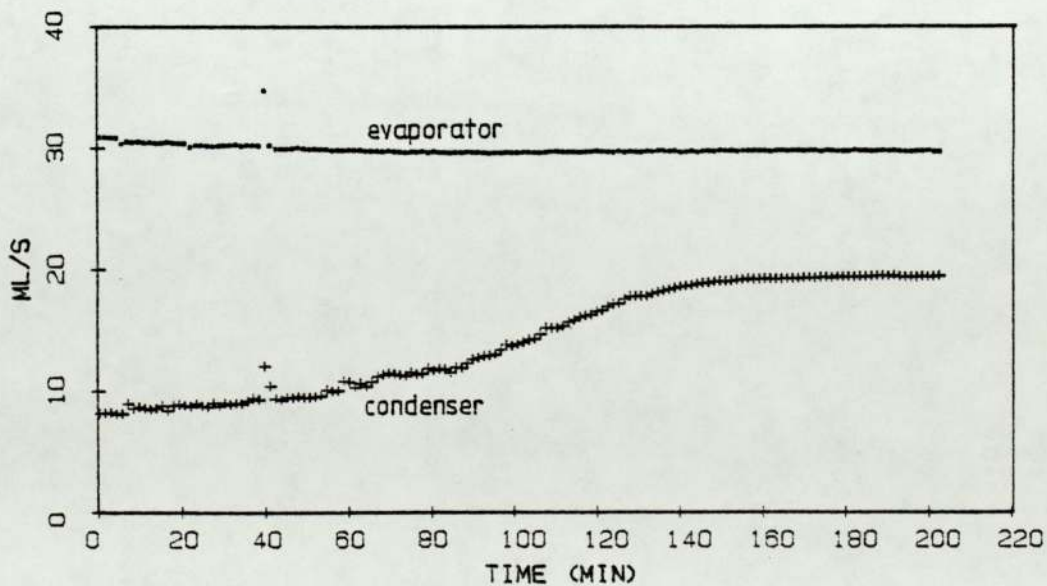


Figure 6.4(c): The variation of water flow rate through the evaporator and condenser for Mode 3 experiment.

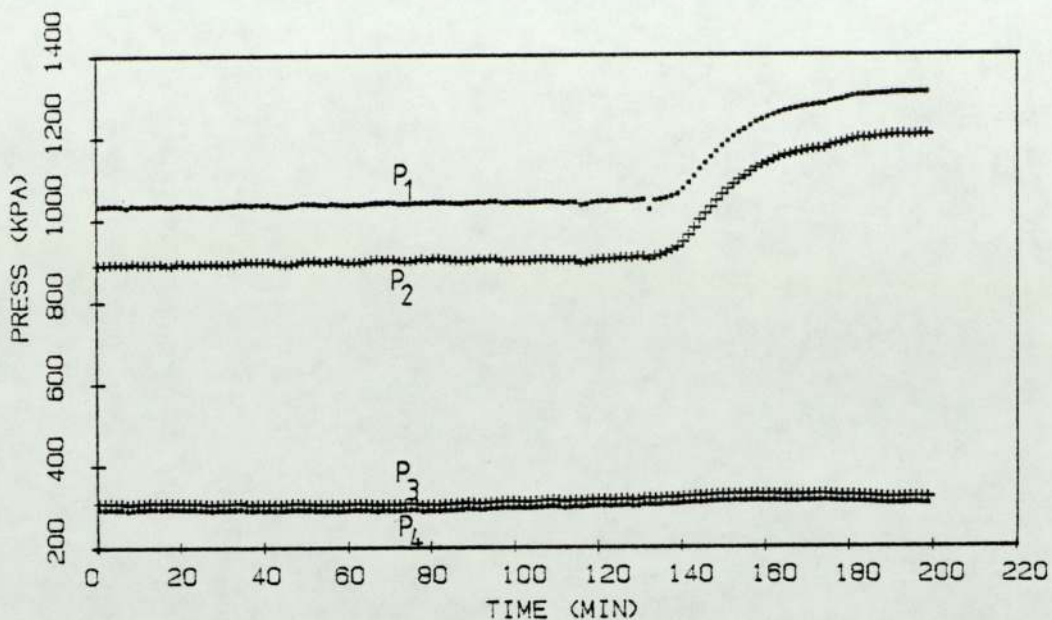


Figure 6.5(a): Pressure variation across the expansion valve and compressor for Mode 1 experiment.

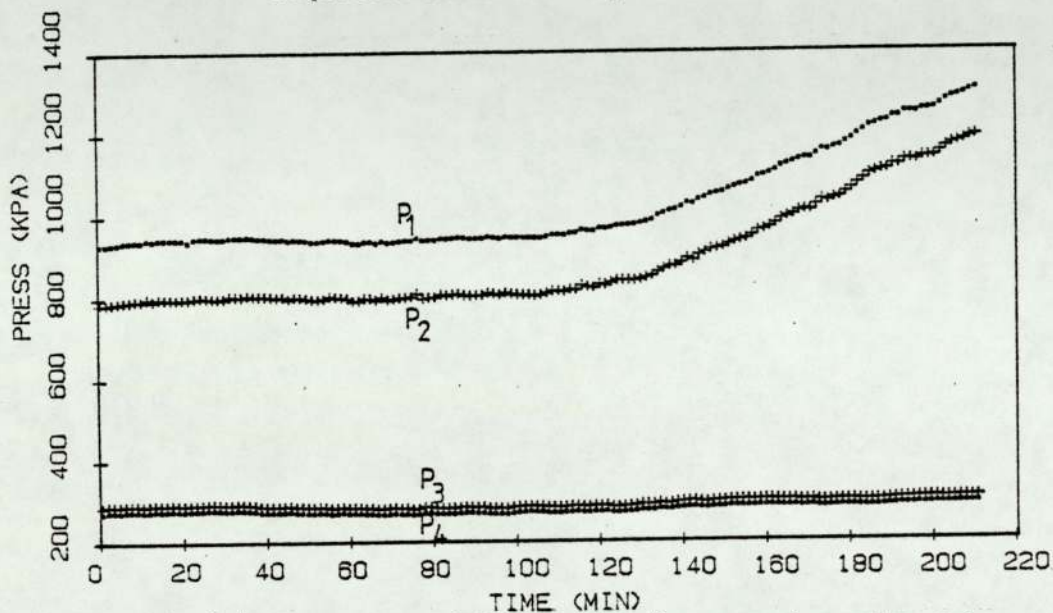


Figure 6.5(b): Pressure variation across the expansion valve and compressor for Mode 2 experiment.

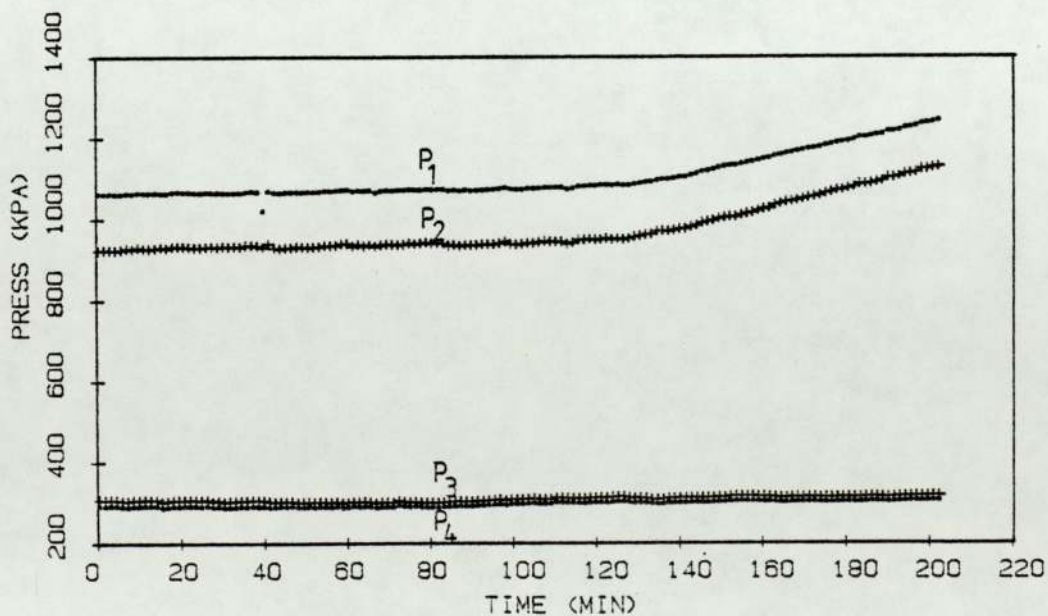


Figure 6.5(c): Pressure variation across the expansion valve and compressor for Mode 3 experiment.

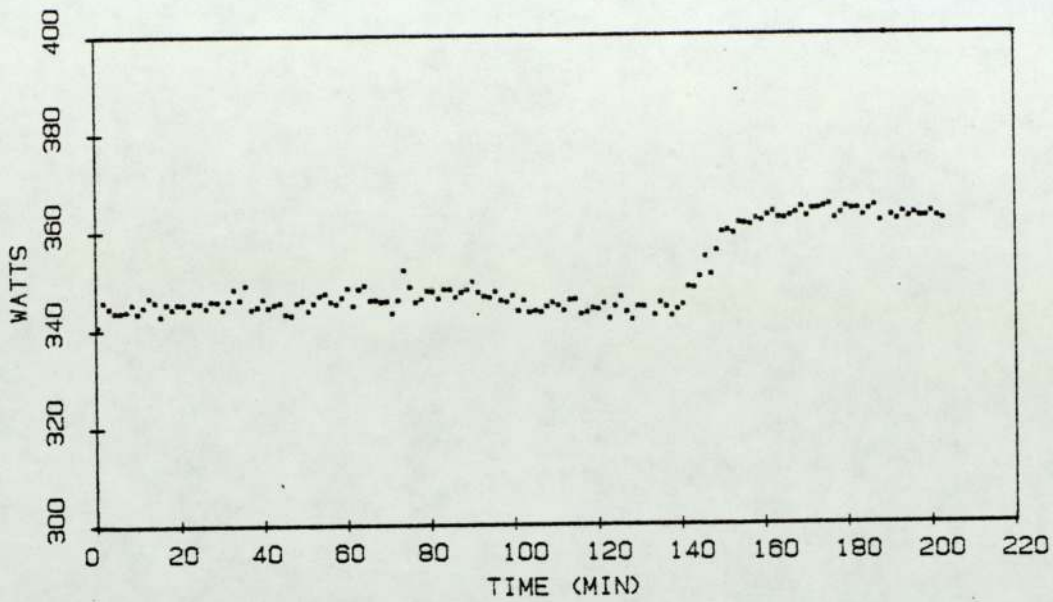


Figure 6.6(a): Variation of electrical power consumption to the compressor for Mode 1 experiment.

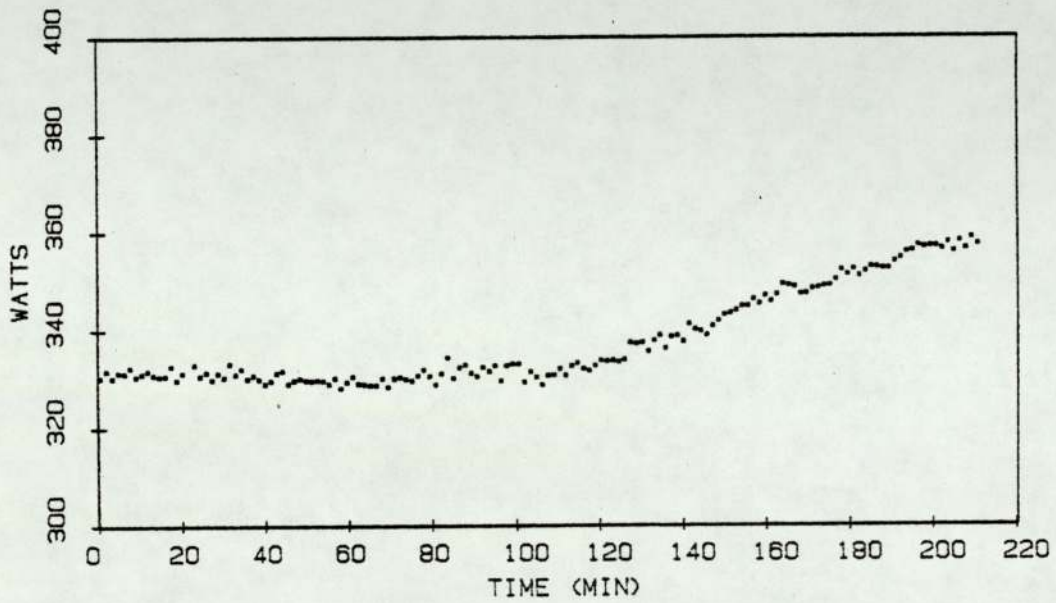


Figure 6.6(b): Variation of electrical power consumption to the compressor for Mode 2 experiment.

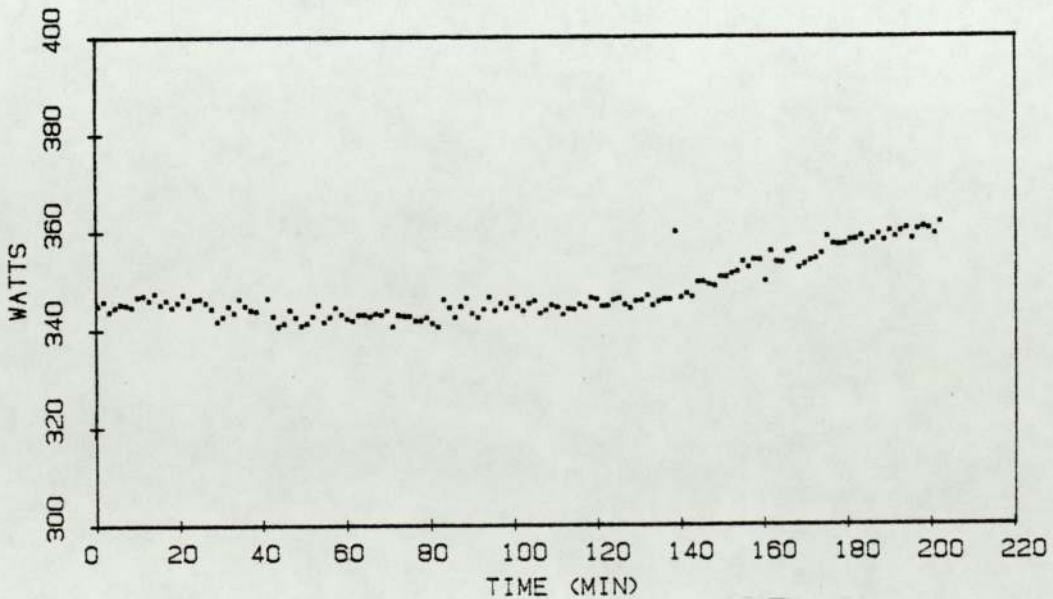


Figure 6.6(c): Variation of electrical power consumption to the compressor for Mode 3 experiment.

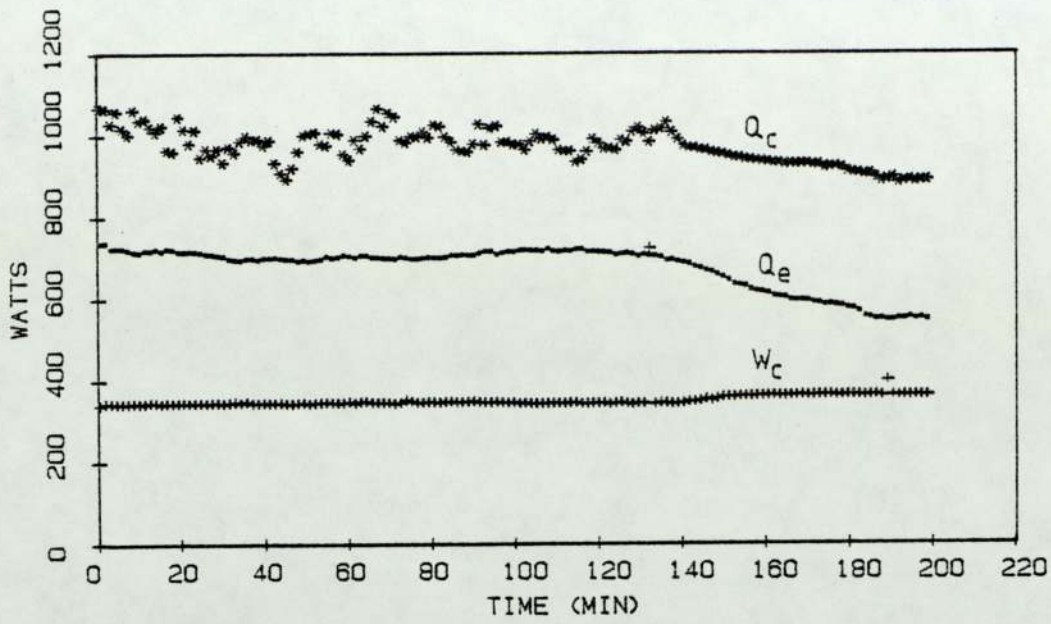


Figure 6.7(a): Variation of energies Q_c, Q_e and W_c for Mode 1 experiment.

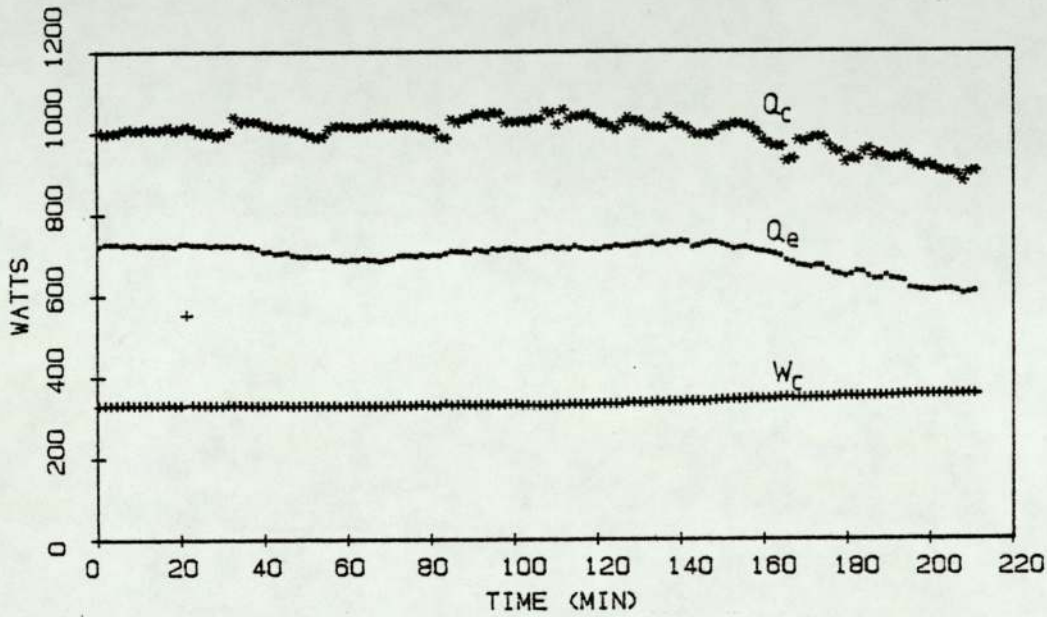


Figure 6.7(b): Variation of energies Q_c, Q_e and W_c for Mode 2 experiment.

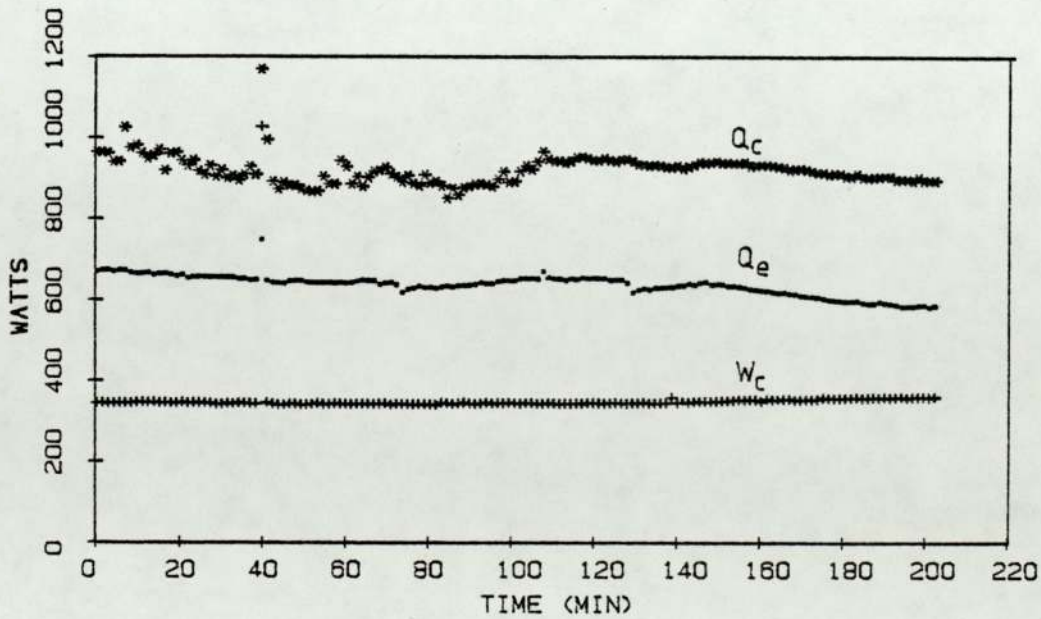


Figure 6.7(c): Variation of energies Q_c, Q_e and W_c for Mode 3 experiment.

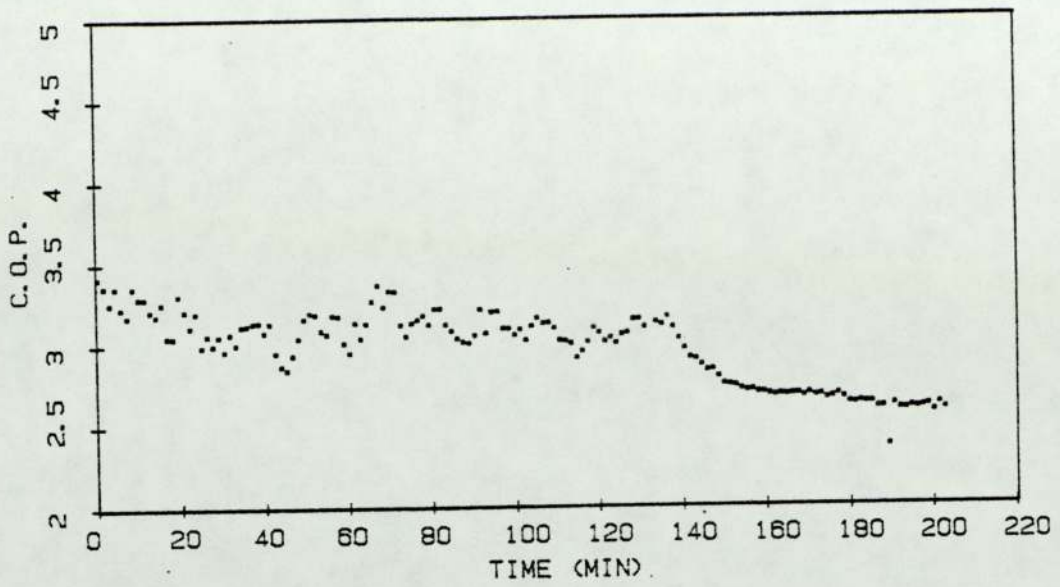


Figure 6.8(a): Variation of C.O.P. for Mode 1 experiment.

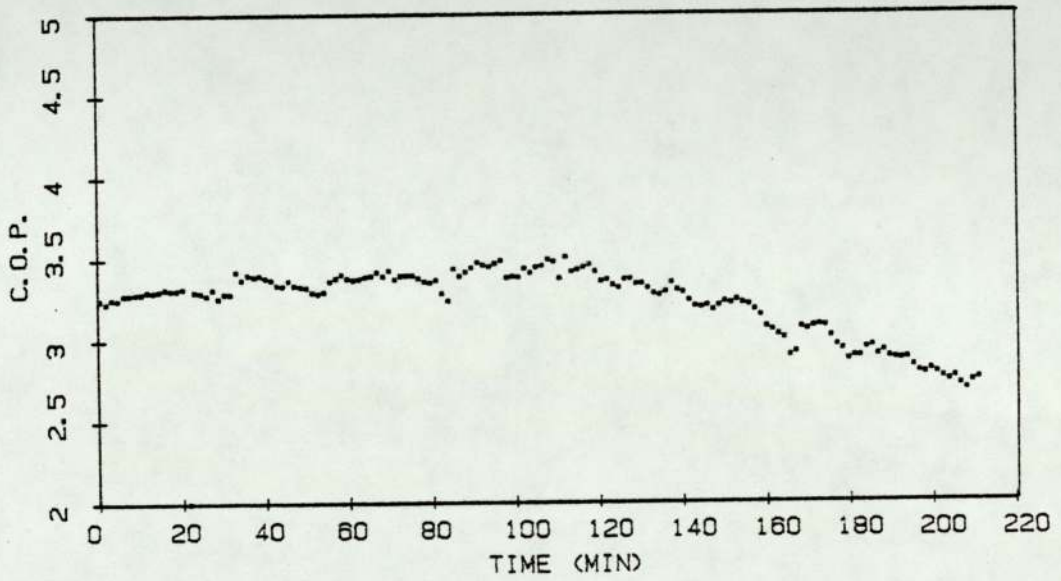


Figure 6.8(b): Variation of C.O.P. for Mode 2 experiment.

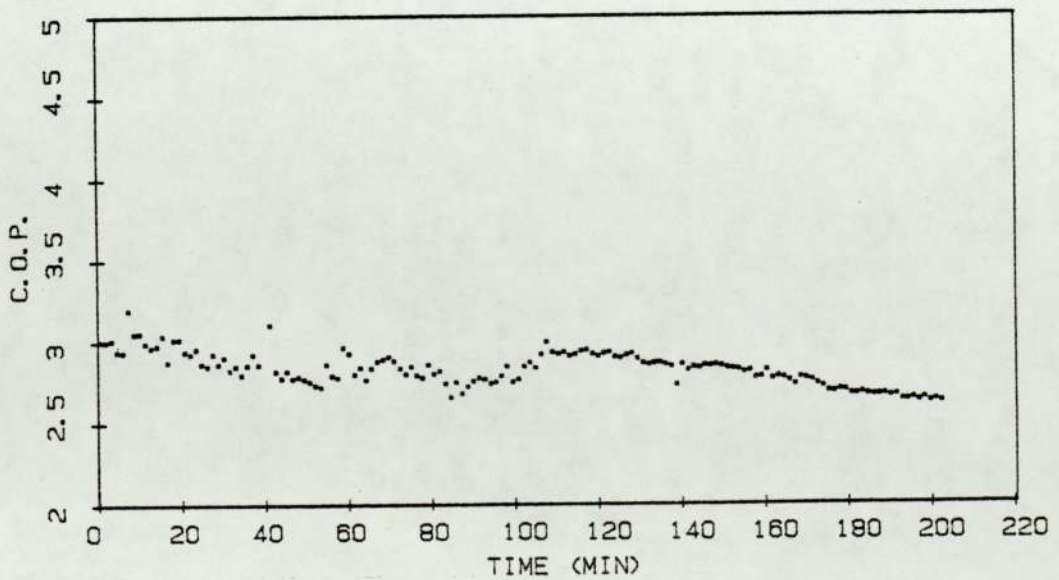


Figure 6.8(c): Variation of C.O.P. for Mode 3 experiment.

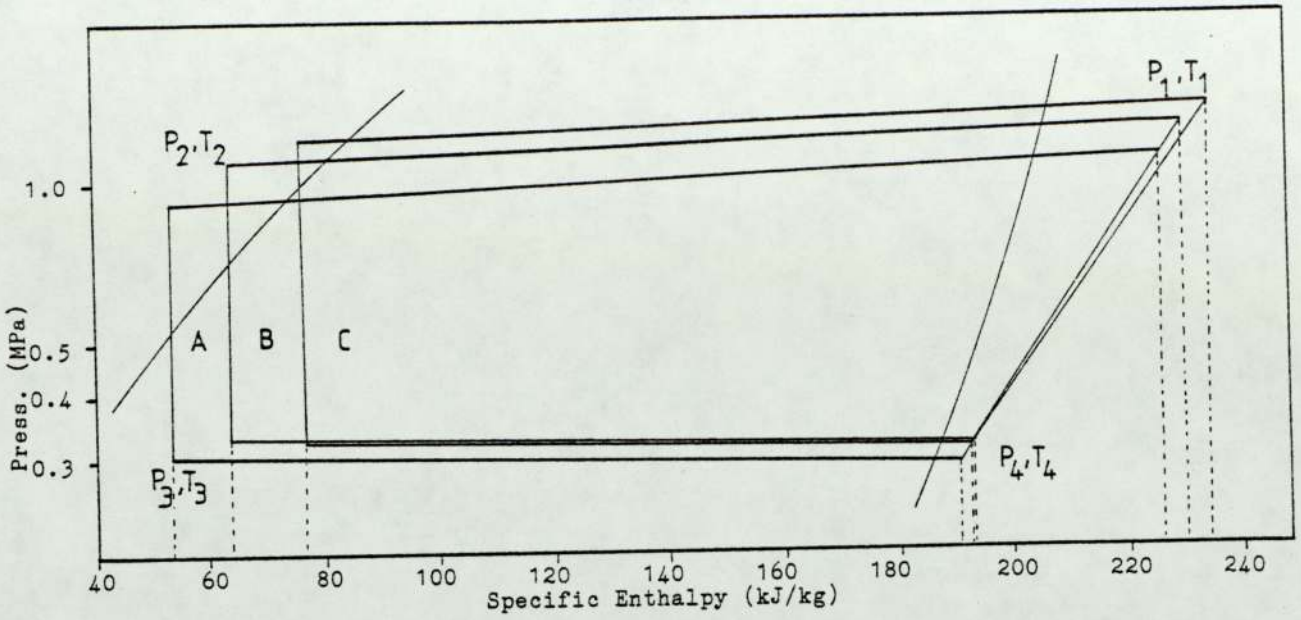


Figure 6.9(a): The refrigerant cycle of the Mode 1 experiment.

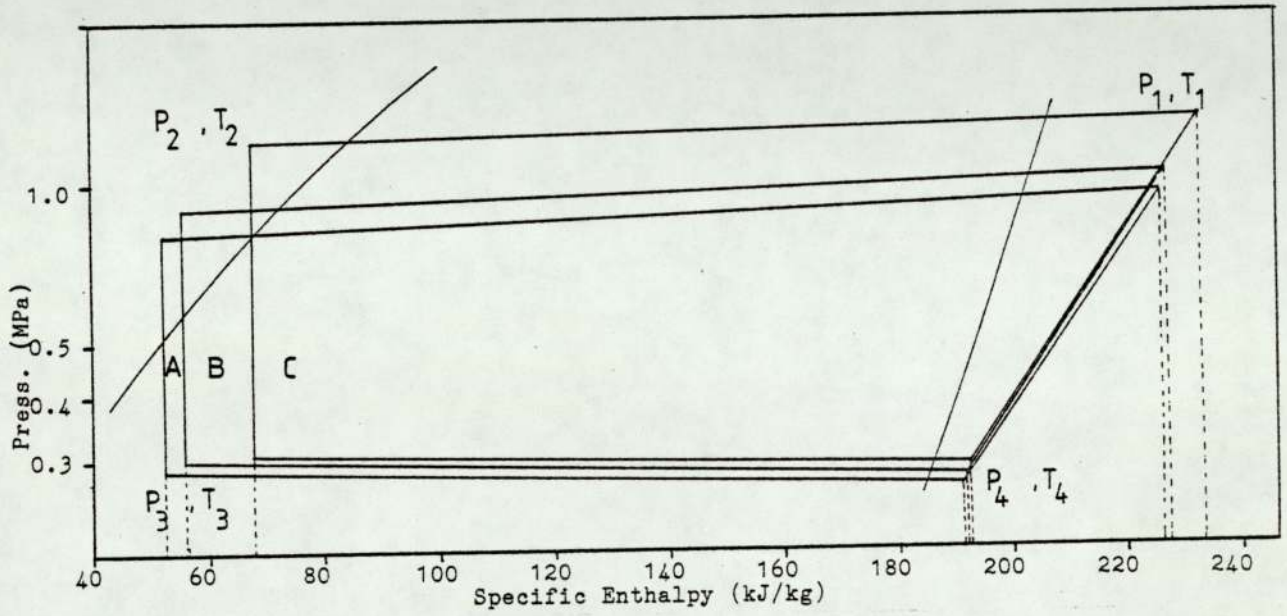


Figure 6.9(b): The refrigerant cycle of the Mode 2 experiment.

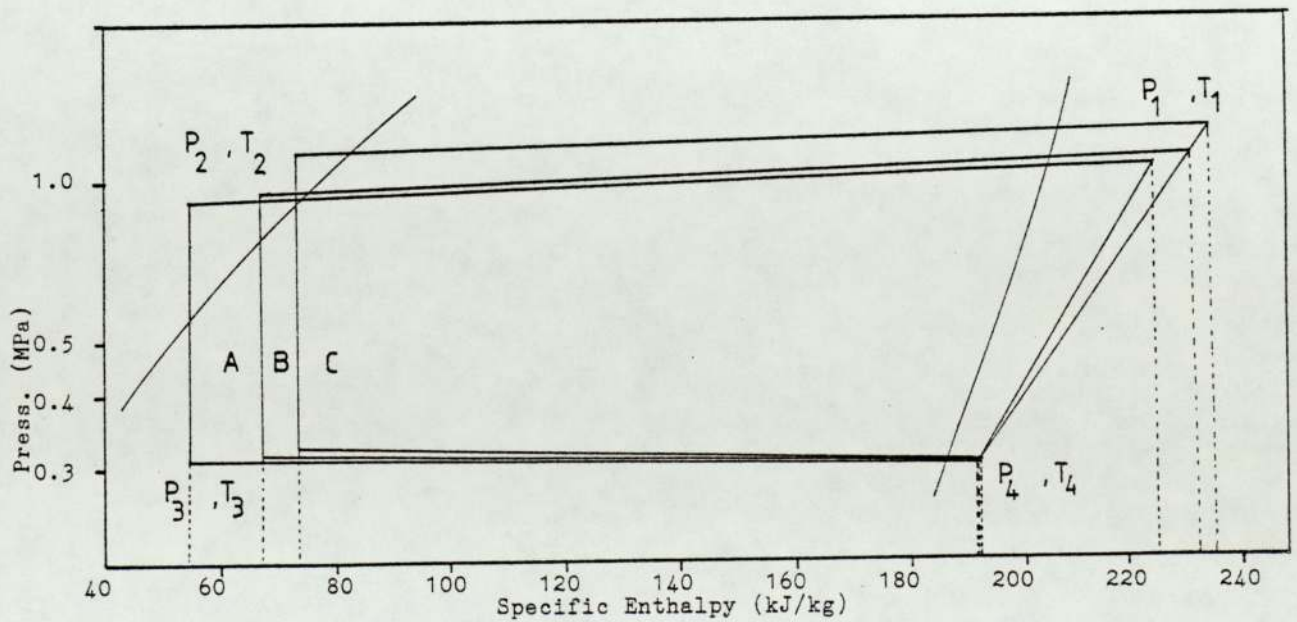


Figure 6.9(c): The refrigerant cycle of the Mode 3 experiment.

	STATE A	STATE B	STATE C
DISCH PRESS P1 (KPA)	1034.6	1213.5	1302.2
PRESS P2 (KPA)	900.8	1104.0	1203.6
PRESS P3 (KPA)	304.0	327.8	320.6
SUCTION PRESS P4 (KPA)	283.6	307.3	300.2
DISCH TEMP T1 (C)	72.1	80.1	87.1
SUBCOOL TEMP T2 (C)	19.5	38.5	41.5
TEMP AFTER VALVE T3 (C)	.5	1.9	2.5
SUPERHEAT TEMP T4 (C)	6.8	8.7	9.3
DISCH ENTH H1 (KJ/KG)	226.5	230.5	234.5
SUBCOOL ENTH H2 (KJ/KG)	54.0	63.5	76.5
SUPERH ENTH H4 (KJ/KG)	192.5	194.0	193.0
C.O.P.	5.07	4.58	3.81

TABLE 6.3(A) : NUMERICAL VALUES FOR CYCLES A,B AND C SHOWN IN FIGURE 6.9(A).

	STATE A	STATE B	STATE C
DISCH PRESS P1 (KPA)	934.2	1023.8	1299.8
PRESS P2 (KPA)	800.0	892.4	1190.7
PRESS P3 (KPA)	282.6	297.1	305.3
SUCTION PRESS P4 (KPA)	263.2	277.5	285.9
DISCH TEMP T1 (C)	69.9	72.5	84.2
SUBCOOL TEMP T2 (C)	17.7	20.8	33.2
TEMP AFTER VALVE T3 (C)	-1.4	-.2	.6
SUPERHEAT TEMP T4 (C)	5.6	6.5	7.0
DISCH ENTH H1 (KJ/KG)	226.5	227.5	233.0
SUBCOOL ENTH H2 (KJ/KG)	52.5	56.0	68.0
SUPERH ENTH H4 (KJ/KG)	191.5	192.0	192.5
C.O.P.	4.97	4.83	4.07

TABLE 6.3(B) : NUMERICAL VALUES FOR CYCLES A,B AND C SHOWN IN FIGURE 6.9(B).

	STATE A	STATE B	STATE C
DISCH PRESS P1 (KPA)	1057.2	1092.6	1239.0
PRESS P2 (KPA)	922.9	970.1	1129.7
PRESS P3 (KPA)	308.2	307.9	317.9
SUCTION PRESS P4 (KPA)	288.3	291.1	301.1
DISCH TEMP T1 (C)	68.6	76.5	83.3
SUBCOOL TEMP T2 (C)	19.6	32.1	38.2
TEMP AFTER VALVE T3 (C)	0.5	1.1	1.8
SUPERHEAT TEMP T4 (C)	6.6	7.8	8.8
DISCH ENTH H1 (KJ/KG)	228.5	229.0	232.0
SUBCOOL ENTH H2 (KJ/KG)	54.0	67.0	73.0
SUPERH ENTH H4 (KJ/KG)	191.0	191.5	192.0
C.O.P.	4.65	4.26	3.98

TABLE 6.3(C) : NUMERICAL VALUES FOR CYCLES A,B AND C SHOWN IN FIGURE 6.9(C).

6.4 The Water Temperature Profile in The Tank During Water Heating.

The temperature profile of the water in the tank during sampling is shown in figure 6.10(a) and 6.10(b). Both experiments on the temperature profile were performed separately from the previous experiment mentioned earlier in section 6.2 and 6.3, and set to give the temperature output (TW_{CO}) of the water from the condenser equal to 50°C .

In figure 6.10(a) and 6.10(b), TW_{CO} is the temperature of water output from the condenser. Thermocouples TK1 to TK8 were equally spaced at 10cm. intervals with TK1 at the bottom of the tank and TK8 at the top.

Figure 6.10(a) shows the temperature profile when the water flows through the water regulator and figure 6.10(b) when bypassing the regulator. It can be observed that the heat collected by the water in the condenser and picked-up during the compressor cooling was stored in the tank, firstly on the top of the tank, then gradually moving down as the result of water recycling and heat conduction through water itself and copper cylinder of the tank with the existing of the thermal stratification of the water.

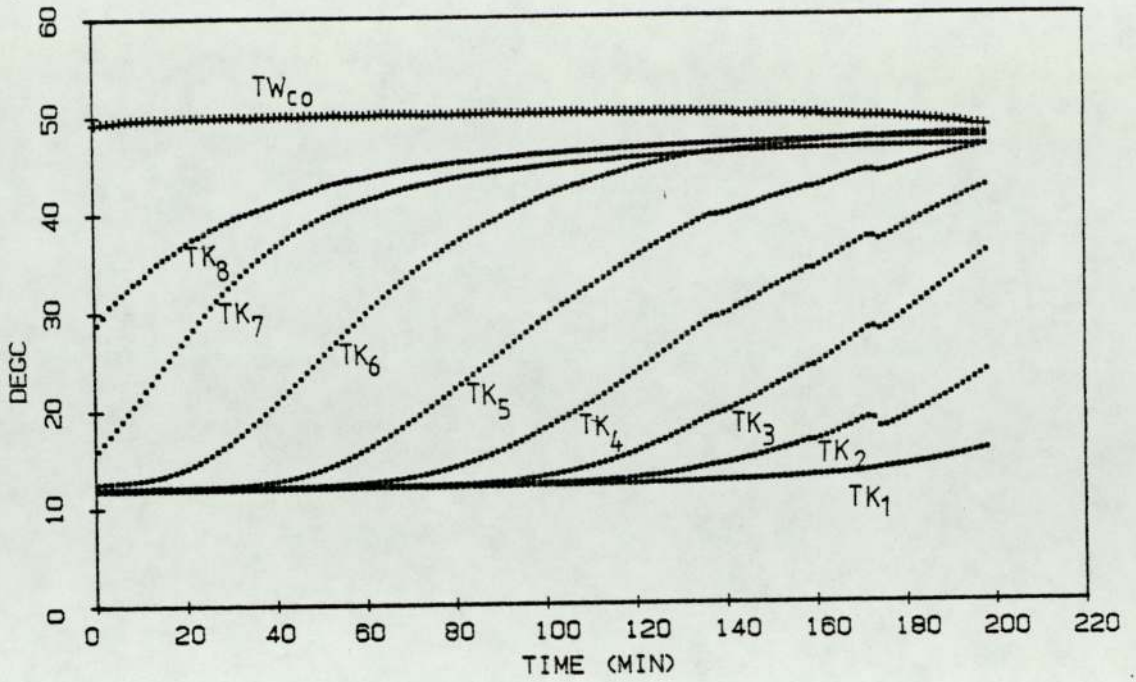


Figure 6.10(a): Temperature profile for water heating in the tank - water controlled by water regulator.

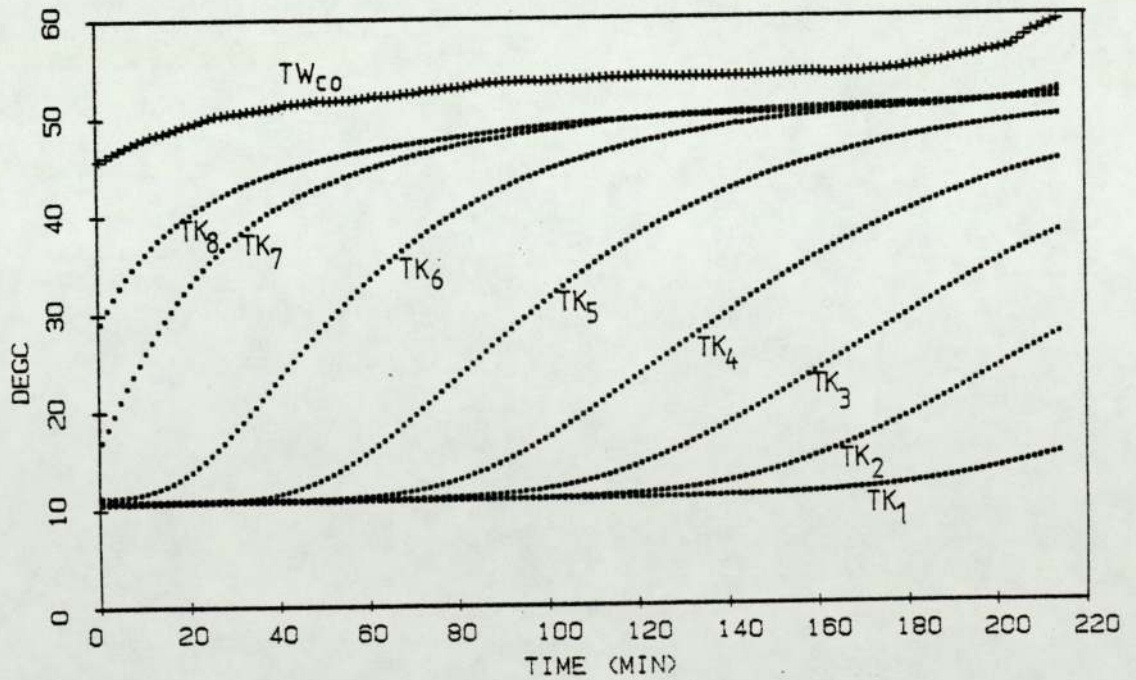


Figure 6.10(b): Temperature profile for water heating in the tank - water regulator not in circuit; flow rate kept constant.

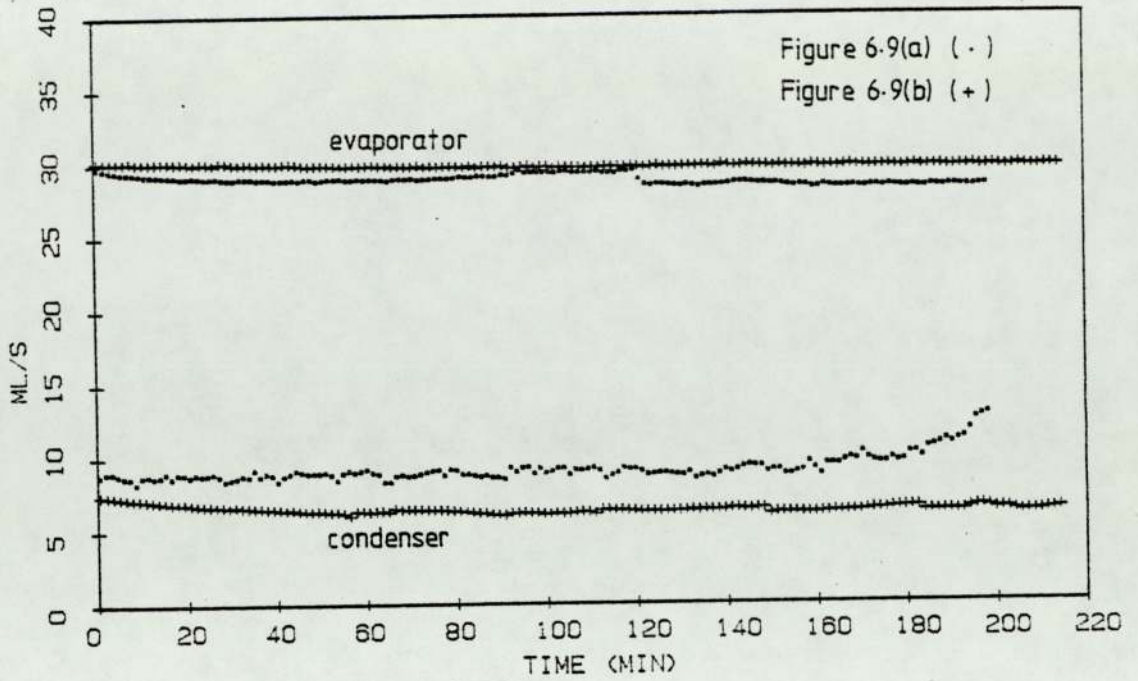


Figure 6.11: Water flow rate in the condenser and evaporator for figure 6.10(a) (.) and 6.10(b) (+).

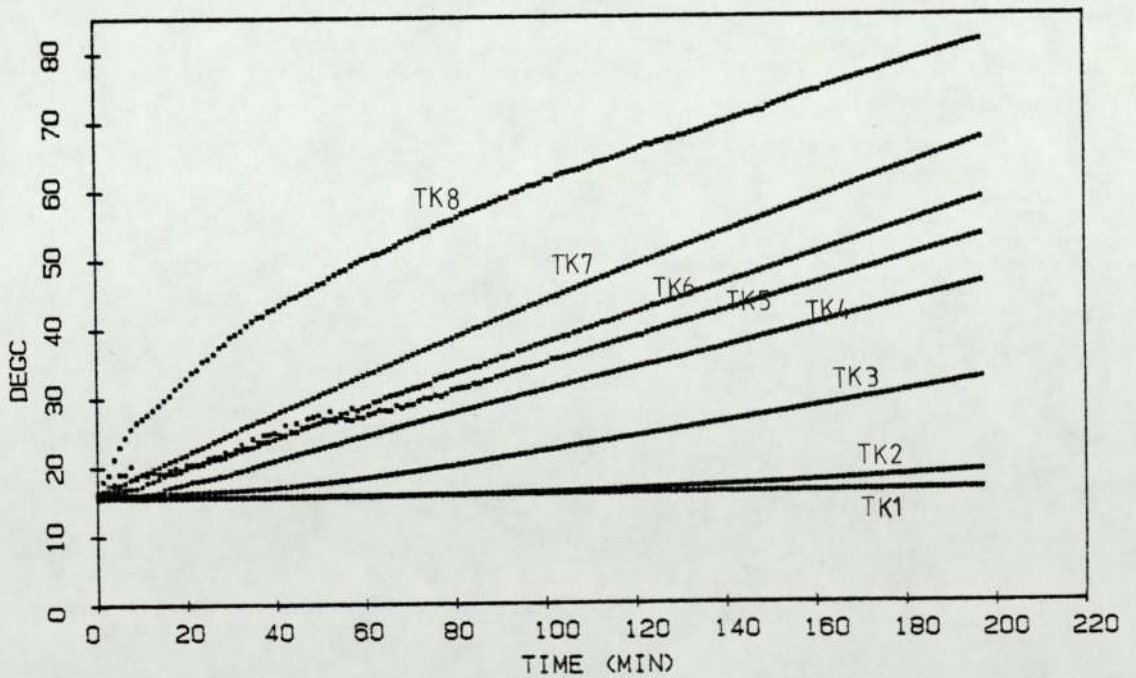


Figure 6.12: Temperature profile of the water in the tank during water heating - electric element heater of 1.2kWatt.

As a result of the water flow being controlled by the water regulator (figure 6.10(a)), the water input to the tank fluctuated and after about 175 minutes, the flow rate (\dot{m}_c) increases (figure 6.11). This effect together with the decrease in Q_c as mentioned earlier, causes the water temperature TW_{c0} to decrease (as shown in figure 6.2), shown as a kink in figure 6.10(a) and less smooth curves compared to figure 6.10(b).

The decrease in TW_{c0} and the increase in water flow rate (\dot{m}_c) cause the temperature of the water on the top of the tank (TK8) to decrease slightly.

With the water flow bypassing the water regulator, the effect of reducing the temperature slightly does not occur and the flow of the water was kept constant by tap 2 throughout the experiment at 6.5ml/s. The water in the tank gradually becomes warmer as shown in figure 6.10(b) with, once again the existence of thermal stratification of the water. The pattern of the profile with a constant water flow rate \dot{m}_c becomes smoother than in figure 6.10(a) due to absence of the water flow rate fluctuations caused by the regulator. At about 200 minutes, the outlet temperature of the condenser water (TW_{c0}) increases due to hotter water at the inlet (Figure 6.10(b)).

Figure 6.12 shows the temperature profile in the same tank as in figure 6.10(a) and 6.10(b) using an

electric resistance element of 1.2kiloWatt with the same placing of the sensors - which is nearly the same quantity of heat being stored in the tank by using the heat pump system Q_c . The water is not being recycled.

The heating of water by using the electric resistance element was carried out as a comparison with the heat pump system to demonstrate the way in which the heat pump can be used as an alternative to electric water heating, giving even better heat output by using less electric power.

Figures 6.10(a),6.10(b) and 6.12 illustrate how the configuration adopted for demonstration helps promote the thermal stratification of the hot water cylinder. An advantage is that a large fraction of the stored hot water is available for use before the outlet water temperature drops to an unacceptable level (where the C.O.P. decreases due to hot water entering the condenser as discussed earlier in sections 6.2 and 6.3). This result is in agreement with results obtained by Carrington et al [37]. It can be seen that the temperatures TK1 and TK2 in figure 6.12 only differ very slightly until the end of the sampling (about 200 minutes). On comparing both figures 6.10(a) and 6.10(b) to figure 6.12, it can be seen that a large fraction of water on top of the tank is readily available at the required temperature compared to the

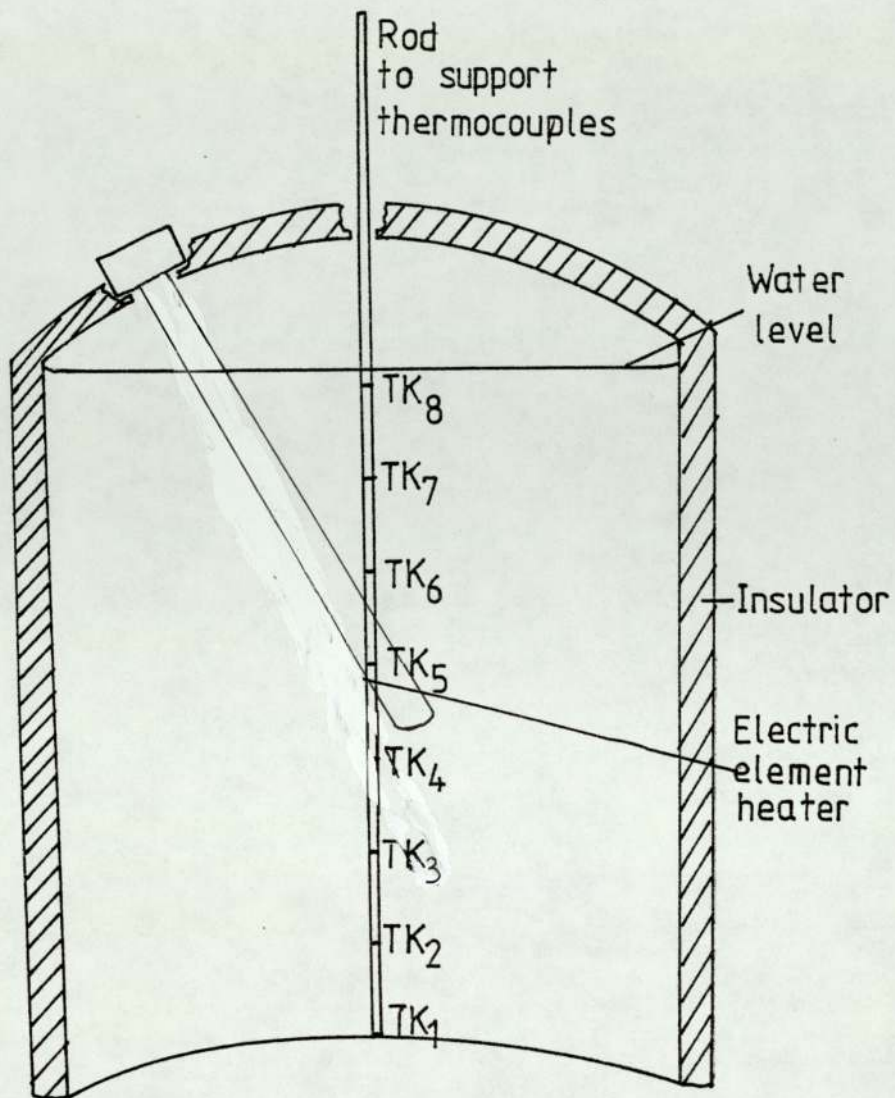


Figure 6.13: Schematic diagram for water heating using an electric element.

heating by using electric resistance element. The fluctuation in figure 6.12 at temperature TK5 at the beginning of the experiment is due to the position of the electric element in the water tank being near the thermocouple as shown in figure 6.13. Thermocouple TK5 is nearest to the heater element.

6.5 Discussion and Conclusion.

From the results mentioned in section 6.2, 6.3 and 6.4 there are three methods by which the heat pump system can be operated to heat water in a domestic hot water tank. The following factors should be considered to determine the method in which the system performs best.

1. The function of the water regulator is to control the water flow through the condenser in order to fix the discharge pressure P_1 at a predetermined value. The fixing of discharge pressure P_1 results in controlling the water flow rate through the condenser (\dot{m}_c) in such away that the amount of the flow rate will always respond to the increase in discharge pressure P_1 . If hot water enters the condenser, the pressure P_1 increases, which increases the water flow rate (figure 6.4(a) and 6.5(a)). By this method the water outlet temperature from

condenser TW_{co} will always be maintained constant. A slight increase in TW_{co} can be seen in figure 6.2(a) due to the change of inlet temperature TW_i to the condenser. This effect shows why the discharge pressure P_1 is maintained at a higher constant pressure when hot water enters the condenser (figure 6.5(a)). This result can be compared to figure 6.2(b) where when the water bypasses the water regulator, the outlet temperature TW_{co} will increase continuously as the hot water enters the condenser. This result shows the importance of the water regulator by which the operator can produce water at the required outlet temperature and store it in a tank for later use. It also shows that, with the water regulator in use, the discharge pressure P_1 will not increase continuously if the operator forgets to switch off the system when the hot water enters the condenser, and serious damage to the system can be avoided.

2. If the water regulator is not used in the system, serious damage may occur to the system, since the discharge pressure P_1 will not be controlled and will increase continuously as the result of hot water TW_i being fed to the condenser (figure 6.2(b) and 6.4(b)). If the discharge pressure P_1 is too high, it could damage the compressor and the joints in the system may

leak [25]. The performance of the compressor will be reduced as the pressure P_1 increases [12,15, 39] . As the pressure ratio across the compressor P_1/P_4 increases, the efficiencies (volumetric, isothermal and isentropic) decrease. Furthermore, there will be back leakage of the vapour in the cylinder of the compressor if the discharge pressure P_1 is too high. The discussion on this effect will be given in chapter 7. On top of the above reasons, the water outlet of the condenser may be too hot for the operator to use it.

3. The water in the tank could be heated gradually by the system by mixing the water (tap 1 and 2 open), the flow being controlled by the water regulator, but this process will reduce the coefficient of performance of the system continuously as shown in figure 6.8(c). If the heat pump operates for a very long time, the effect mentioned in 2 will be repeated. A longer time will be taken to heat all the water in the tank to the required temperature.

By using the methods in the mode 1 and mode 2 experiments, a large portion of the tank can be used to store hot water before the hot water at the bottom of the tank enters the condenser. To ensure that the system works at higher performance and at the same

time a large portion of the tank can be used to store hot water, Carrington et al [37] fixed the thermostat near bottom of the tank so that the heat pump could be switched off automatically when the performance falls below the switch-on set point of the thermostat. A large portion of the water can be heated by the system and collected on the top of the tank if the tank comprises a longer cylinder. A partition should be made in the tank to separate the hot water on the top and the cold water at the bottom. In other words, a special tank to match the heat pump system would be designed to optimise the performance of the system rather than using the ordinary hot water tank as was applied in the experiment.

As conclusion, table 6.4 contains illustrative performance data for the heat pump system during water heating. The condenser water entry temperature is 15°C . COP is the coefficient of performance based on compressor only and COP(WP) based on compressor plus water pump. The single pass water flow rate through condenser (\dot{m}_c) was controlled by the water regulator. The coefficient of performance decreases as the outlet temperature $T_{W_{co}}$ of the condenser increases and increases as the water flow rate through the evaporator (\dot{m}_e) increases.

		OUTPUT WATER TEMPERATURE (DEGC)		
		40	50	60
20 ML/S	MC (ML/S)	13.2	9.1	6.6
	EVAP WATER QC (WATTS)	1134.2	1120.0	1058.5
	FLOW RATE QE (WATTS)	802.6	765.2	710.8
	WC (WATTS)	322.8	348.2	369.5
	COP	3.785	3.493	3.119
	COP (WP)	3.192	2.979	2.683
30 ML/S	MC (ML/S)	14.3	9.7	7.3
	EVAP WATER QC (WATTS)	1242.7	1214.3	1177.1
	FLOW RATE QE (WATTS)	906.7	879.0	828.0
	WC (WATTS)	325.4	351.6	375.7
	COP	4.095	3.705	3.412
	COP (WP)	3.457	3.165	2.942
40 ML/S	MC (ML/S)	15.4	10.1	7.7
	EVAP WATER QC (WATTS)	1329.5	1263.1	1248.0
	FLOW RATE QE (WATTS)	977.2	933.3	884.6
	WC (WATTS)	326.2	353.3	381.8
	COP	4.353	3.821	3.548
	COP (WP)	3.677	3.267	3.066

TABLE 6.4: EXPERIMENTAL PERFORMANCE DATA SHOWING VARIOUS OUTPUT WATER TEMPERATURES AT DIFFERENT WATER FLOW RATES PASSING THROUGH THE EVAPORATOR. ENTRY WATER TEMPERATURE TO EVAPORATOR AND CONDENSER IS 15DEGC.

CHAPTER 7.

PERFORMANCE ANALYSIS OF THE WATER-TO-WATER HEAT PUMP SYSTEM AND ITS MODELLING.

7.1 Introduction.

The analysis of the performance of the heat pump will be based on various measurements taken during the experimental runs. As the performance is influenced by the externally imposed conditions, such as the variation of the water flow rate in the condenser and evaporator, several sets of readings have to be taken for analysis.

As mentioned by Ahren [39], it is important to construct a heat pump model, as it describes the important aspects of the heat pump's operation in terms of mathematical relationships. It involves the development

of models, i.e. assumptions, equations and data, which characterize the performance of all the discrete system components (compressor, condenser, evaporator and expansion valve) including mass, momentum and energy balance equations, thermophysical property functions and appropriate heat or work transfer relationships. Thus, a component model describes the relationship between the working fluid conditions within the component, e.g. flow rate, inlet and outlet thermodynamic state, and its design parameters and operating environment.

The method suggested by Stoecker [40] called system simulation will be adopted throughout the analysis, which is performed by mathematical rather than graphical procedure. System simulation is indeed the simultaneous solution of the equations representing the performance characteristics of all components in the system as well as appropriate equations for energy and mass balances and equations of state [17] .

As suggested by Stoecker and Jones [12] , the technique chosen for the mathematical simulation will be the method of successive substitution, which is one of the most straight-forward techniques of simultaneously solving the performance equations, In solving the simultaneous equations, numerical constants will appear repeatedly in every performance equation

of the components. To avoid confusion in noting the value of numerical constants, a corresponding table will be used.

The measurements made at fixed points around the system were subject to errors that could not be avoided; but were minimised as far as possible. The sensors fixed in the system were not exactly at the right places. For example, the thermocouples and the pressure transducers were supposed to read the real values of discharge pressure, suction pressure, temperature and so on, but owing to fittings which need extensions, the sensors could not be placed exactly at the components. As mentioned by Mc Mullan and Morgan [8] , there are energy losses (but very small), in connecting pipes between all the components, which are neglected in the analysis.

The water flow rate through the evaporator, which was controlled by taps, was very hard to maintain at a constant flow rate for long periods of up to 220 minutes since other people might use water from the same main supply during the experiment. This affects the water flow rate through the evaporator. In the condenser, the water was controlled by the water regulator in response to the discharge pressure.

In this analysis, the following nomenclature together with the nomenclature mentioned in chapter 6 will be used.

H_1 = Enthalpy of discharge gas.

H_2 = Enthalpy of subcooled liquid.

H_C = Vapour-gas enthalpy at condensing temperature.

H_4 = Enthalpy of superheated gas.

H_L = Liquid-vapour enthalpy at condensing temperature.

H_E = Vapour-gas enthalpy at evaporating temperature.

H_I = Enthalpy at the end of isentropic compression.

S_s = Entropy of superheated gas.

n = Polytropic index.

η_{iso} = Isothermal efficiency of the compressor.

η_{isen} = Isentropic efficiency of the compressor.

η_{vol} = Volumetric efficiency of the compressor.

η_m = Mechanical efficiency of the compressor.

W_c = Electrical power consumption by the compressor.

W_R = Work done on the superheated gas by the compressor.

7.2 The Compressor.

The function of the compressor is to pump the refrigerant from the low pressure and low temperature side to the high pressure and high temperature side, giving a considerable amount of heat to the refrigerant which will be collected by the water in the condenser.

The performance characteristics of the reciprocating compressor given by the manufacturer are shown in figure 3.3. The upper set of the curves shows the coefficient of performance, the middle set shows the condenser refrigerating capacity and the lower set is the power consumed by the compressor.

The manufacturer's characteristics will not be used to predict the overall performance since the actual parameters of the system could be measured directly during the experiments. A set of experiments was carried out with the discharge pressure P_1 set constant at 964.13kPa (140.0 psia), 1104.57kPa (160.0 psia) and 1244.13kPa (180.0 psia) instead of constant condensing temperature as shown in figure 3.3.

The experiments were performed by passing the water to be heated through the water regulator, the compressor cooling coil and the condenser to pick-up the energy delivered by the system. The water to

the condenser was taken directly from the cold mains supply (figure 7.1) in contrast to the experiments described in the previous chapter. The source of energy was water in a domestic hot water tank which circulated through the evaporator at three different constant flow rates of 19.75ml/s, 28.55ml/s and 39.75ml/s. The flow rate (\dot{m}_e) could be varied with a valve; but as energy absorbed by the evaporator Q_e is calculated from the difference of water temperature across it, the faster the water flow rate, the larger is the error in calculating the value of Q_e .

Throughout the experiment the water in the tank became colder (as energy was absorbed by the evaporator during the recycling process), and as a result the evaporating temperature T_e decreased.

In this analysis, the temperature measured (T_3) is the temperature of the refrigerant after the expansion valve (figure 7.1). This temperature does not necessarily represent the evaporating temperature since there are pressure losses in the evaporator. So evaporating temperature T_e will be less than temperature T_3 . The evaporating temperature is calculated as suggested by Dossat [15] and Pabon-Diaz [41] , that is the temperature corresponding to the average value of the inlet and outlet pressure of the evaporator ($(P_3+P_4)/2$).

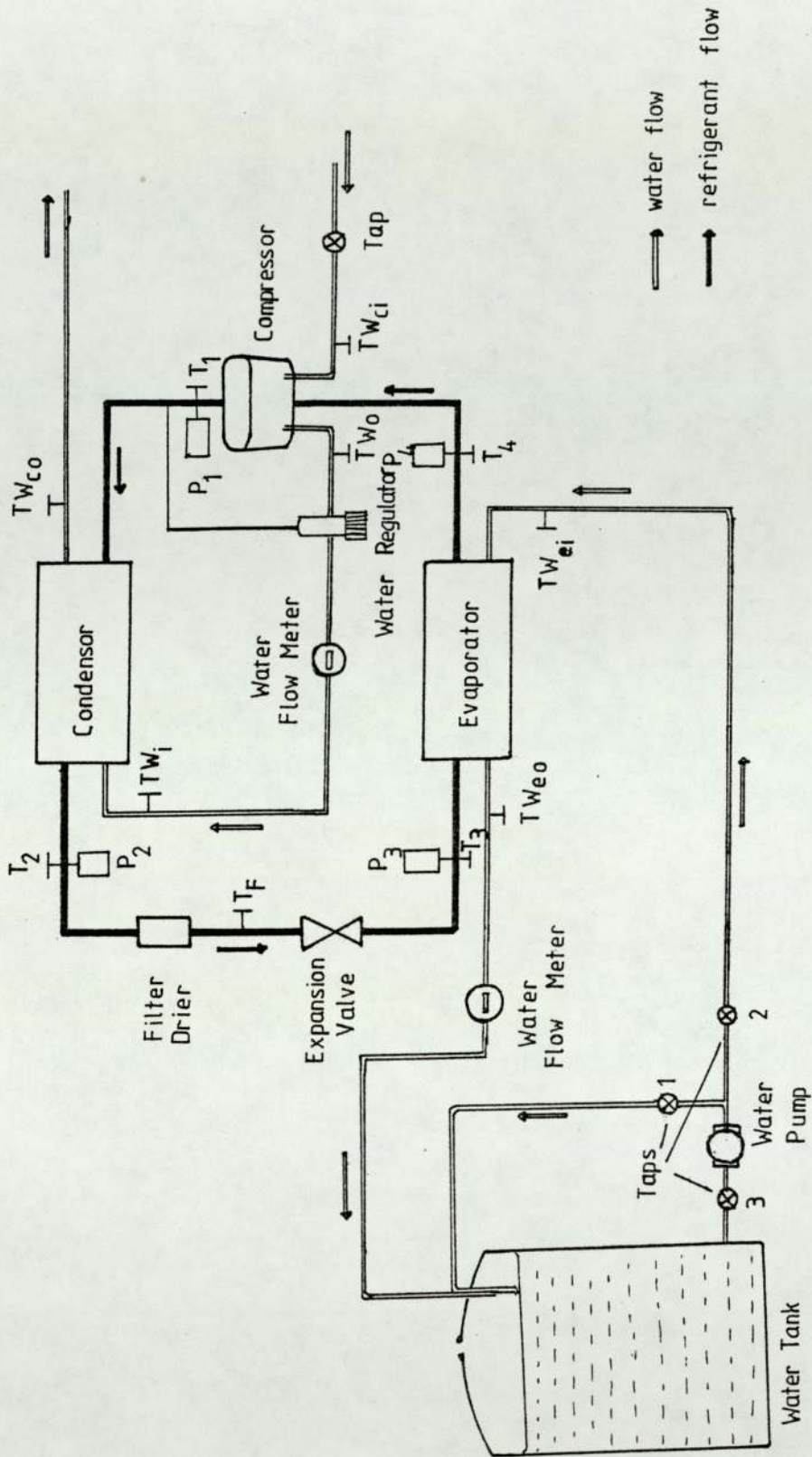


Figure 7.1: Experimental set-up for heat extraction using the heat pump system.

The energy delivered by the condenser Q_c is calculated by using equation,

$$Q_c = \dot{m}_c c_w (TW_{co} - TW_i) \quad 7.1$$

where \dot{m}_c is the water flow rate in the condenser, c_w is the specific heat of water and $TW_{co} - TW_i$ is the temperature difference across the condenser.

The energy absorbed by the evaporator Q_e is given by ,

$$Q_e = \dot{m}_e c_w (TW_{ei} - TW_{eo}) \quad 7.2$$

where \dot{m}_e is the water flow rate in the evaporator and $(TW_{ei} - TW_{eo})$ is the temperature difference across the evaporator.

The electrical power consumption of the compressor W_c was automatically calculated by the computer during sampling as described in chapter 4.

Figure 7.2 shows the energy delivered Q_c , the energy absorbed Q_e and the electrical power consumption of the compressor W_c as functions of discharge pressure P_1 and temperature T_3 . The shapes of the curves are similar to those given by the manufacturer as in figure 3.3 (P_1 and T_3 are used instead of condensing temperature T_c and evaporating

temperature T_e). The fluctuations in Q_c are the result of fluctuating water flow rates, as described in chapter 6.

By using the method of least squares curve fitting as suggested by Gerald [31], the best fitting of the curves can be determined. One choice of the form of the mathematical equations that represent the performance data of figure 7.2 is given by Stoecker and Jones [12] as,

$$Q_c = a_1 + a_2 T_3 + a_3 T_3^2 + a_4 P_1 + a_5 P_1^2 + a_6 T_3 P_1 + a_7 T_3^2 P_1 + a_8 T_3 P_1^2 + a_9 T_3^2 P_1^2 \quad 7.3$$

$$Q_e = b_1 + b_2 T_3 + b_3 T_3^2 + b_4 P_1 + b_5 P_1^2 + b_6 T_3 P_1 + b_7 T_3^2 P_1 + b_8 T_3 P_1^2 + b_9 T_3^2 P_1^2 \quad 7.4$$

and

$$W_c = c_1 + c_2 T_3 + c_3 T_3^2 + c_4 P_1 + c_5 P_1^2 + c_6 T_3 P_1 + c_7 T_3^2 P_1 + c_8 T_3 P_1^2 + c_9 T_3^2 P_1^2 \quad 7.5$$

where $a, b,$ and c are the numerical constants which can be determined by equation fitting procedure, that is selecting nine points off the graph (points of fitting in the least square curves fitting) and substituting into equation 7.3, 7.4 and 7.5 to develop a set of nine simultaneous equations. The numerical values calculated by using the computer program

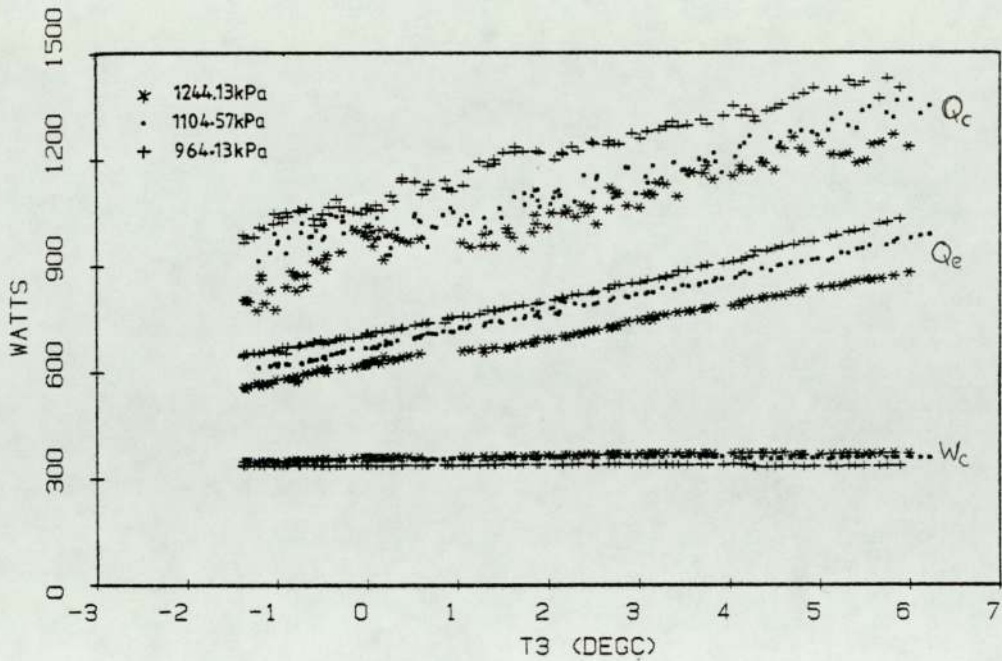


Figure 7.2: Refrigerating capacity and the power requirement of the compressor.

EQN. 7.3	EQN. 7.4	EQN. 7.6
A1= 2102.6268	B1= 726.054898	C1= 179.327841
A2= 1982.30729	B2=-363.572308	C2= 37.7643067
A3=-356.068474	B3= 71.8878577	C3=-6.9175162
A4=-1.43543662	B4= 0.206510223	C4= 0.237737432
A5= 3.93178434E-04	B5=-2.36660528E-04	C5=-7.65406344E-05
A6=-3.51035944	B6= 0.765579113	C6=-0.0798235716
A7= 0.650678261	B7=-0.126063639	C7= 0.0130164612
A8= 1.58106254E-03	B8=-3.55392011E-04	C8= 4.36857631E-05
A9=-2.93626026E-04	B9= 5.54819883E-05	C9=-6.43607881E-06

TABLE 7.1: NUMERICAL VALUES OF CONSTANTS A,B AND C CALCULATED FOR EQUATIONS 7.3, 7.4 AND 7.5.

suggested by Gerald [31] are shown in table 7.1.

7.3. The Effect of Water-jacketing the Compressor Cylinder.

Any heat which is given off by the compressor cylinder to some external cooling medium (e.g. water) represents, in effect, heat given off by the vapour during the compression process. Cooling of the vapour during compression causes the path of the compression process to shift from the isentropic path toward an isothermal path [15] . The greater the amount of cooling, the greater will be the shift toward the isothermal.

By having water-jacketing some heat was collected in the compressor. The higher the pressure ratio P_1/P_4 across the compressor, the more work has to be done, and the hotter the compressor becomes, causing more heat to be collected by the water. The heat collected increases only slowly as shown in figure 7.3 as the pressure ratio P_1/P_4 across the compressor increases. As mentioned by ASME [42] , as freon R12 is used as the refrigerant , the discharge temperature is relatively low (due to the properties of freon R12 which has low condensing temperature and pressure [7,13,15,41, 43]) , therefore not too

much heat could be collected during compressor cooling as can be seen in figure 7.3.

The heat (Q_y) picked-up by the water (\dot{m}_c) can be written as a function of P_1/P_4 by using the least squares fit method [31] as,

$$Q_y = 73.32330 + 6.67470(P_1/P_4) \quad 7.6$$

Since there is always some transfer of heat from the compressor to the surrounding water, compression is usually polytropic rather than isentropic [15] .

The polytropic index n for the compression process is calculated by using equation 2.19, which can be written as,

$$T_1/T_4 = (P_1/P_4)^{(n-1)/n}$$

$$\therefore n = \frac{1}{1 - \frac{\ln(T_1/T_4)}{\ln(P_1/P_4)}} \quad 7.7$$

where T_1/T_4 is the absolute temperature ratio across the compressor.

Cooling the compressor results in lowering the temperature of the cylinder walls (including piston head) and cooling the vapour during the compression.

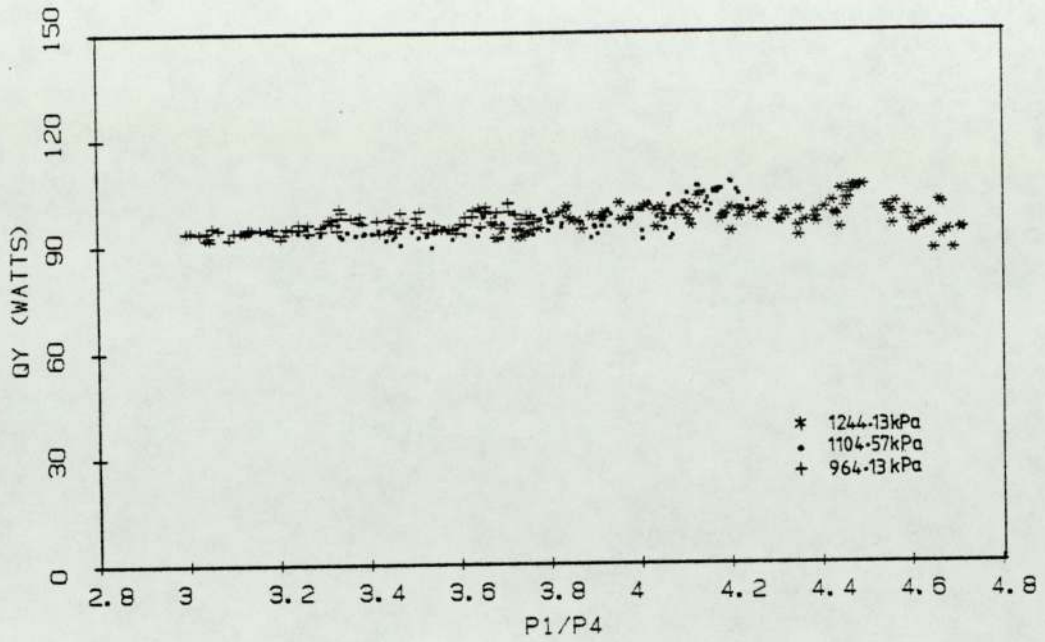


Figure 7.3: Energy picked-up during compressor cooling.

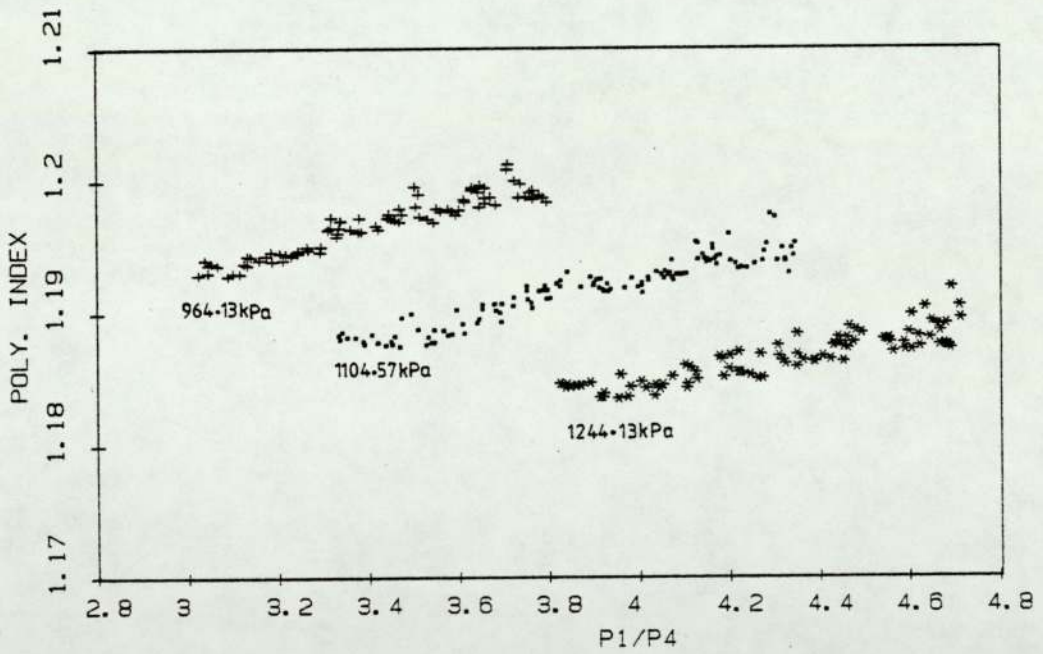


Figure 7.4: The variation of polytropic index against the pressure ratio across the compressor.

This effect lowers the value of the polytropic index [15] .

Figure 7.4 shows the effect of the compression on the polytropic index. Decreasing the pressure ratio P_1/P_4 would decrease the value of polytropic index n at a specific discharge pressure. The higher the discharge pressure P_1 , the higher the discharge temperature, and the greater the heat lost in compressor cooling (figure 7.3). The resulting reduction in polytropic index is shown in figure 7.4. This is in agreement with ASRE [42] and Dossat [15] .

Figure 7.4 also shows that in this water-to-water heat pump system, the polytropic index n is linearly dependent on P_1/P_4 for a given value of discharge pressure P_1 . Thus the polytropic index n can be written in mathematical form as [31] ,

$$n = a_1 + a_2(P_1/P_4) + a_3P_1 + a_4P_1^2 + a_5P_1(P_1/P_4) + a_6(P_1/P_4)P_1^2 \quad 7.8$$

where a_1, a_2, a_3, a_4, a_5 and a_6 are the numerical constants whose values are determined by selecting, this time, six points off the least square curves fitting and substituting in the equation 7.8. Since at constant values of discharge pressure P_1 , n is linearly

dependent on P_1/P_4 as shown in figure 7.4. Table 7.2 shows the numerical values of the constants in equation 7.8.

```
=====
      EQN. 7.8
-----
A1= 1.28579192
A2= 8.37534282E-03
A3=-2.11111977E-04
A4= 8.88789708E.08
A5= 1.09813001E-05
A6=-1.03676775
=====
```

TABLE 7.2: NUMERICAL VALUES OF CONSTANTS
FOR EQUATION 7.8

7.4. The Compressor Efficiencies.

As mentioned earlier in chapter 2, there are four efficiencies which govern the performance of the compressor. They are,

1. Volumetric efficiency.
2. Isothermal efficiency.
3. Isentropic efficiency.
4. Mechanical efficiency.

7.4.1 Volumetric Efficiency (η_{vol}).

Theoretically, the volumetric efficiency η_{vol} , which depends on the reexpansion of the superheat

gas trapped in the clearance volume, is expressed by equation 2.36 as,

$$\eta_{vol} = 1 - \frac{V_c}{V_s} \left[(P_1/P_4)^{1/n} - 1 \right] \quad 7.9$$

where V_c is clearance volume of the cylinder ($V_c = V_2$) and V_s is the swept volume of the cylinder.

Clearly, theoretically the η_{vol} depends on the values of V_c and V_s which are fixed for a particular compressor, and the value of the pressure ratio across the compressor, P_1/P_4 .

Increasing the discharge pressure P_1 or lowering the suction pressure P_4 will have the same effect on volumetric efficiency η_{vol} as increasing the clearance. If the discharge pressure is increased, the vapour in the clearance will be compressed to a higher pressure and a greater amount of reexpansion will be required to expand it to the suction pressure. Likewise, if the suction pressure is lowered, the clearance vapour must experience a greater re-expansion in expanding to the lower pressure before the suction valves will open [15] .

On the other hand, for a constant discharge pressure P_1 , the amount of re-expansion that the clearance vapour experiences before the suction valves

open diminishes as the suction pressure P_4 rises. As predicted by Dossat [15] and Stoecker and Jones [12], the volumetric efficiency η_{vol} of the compressor increases as the suction pressure P_4 increases (P_1/P_4 decreases) and decreases as the discharge pressure P_1 increases. Table 7.3 shows the effect of the pressure ratio P_1/P_4 on the efficiency (with assumption of 5.0 percent clearance volume) for three discharge pressure of 964.13kPa (140.0 psia), 1104.57kPa (160.0 psia) and 1244.14kPa (180.0 psia). This result is similar to the result obtained by ASRE [42] which calculated actual efficiency for two types of reciprocating compressors with clearance volume of 4.7 percent and 7.1 percent. It concluded that the cylinder heating effect is less for the large-clearance than for the small-clearance compressor in a sufficient amount to counteract the greater reexpansion volume of the former [42].

7.4.2 Isothermal Efficiency (η_{iso}).

The isothermal efficiency of the compressor η_{iso} is defined as [17,19],

$$\eta_{iso} = \frac{\text{isothermal work transfer}}{\text{actual work transfer}} \quad 7.10$$

and from equation 2.34

$$\eta_{iso} = \frac{-\ln(P_1/P_4)}{\left(\frac{n}{1-n}\right) \left[(P_1/P_4)^{(n-1)/n} - 1 \right]} \quad 7.11$$

The theoretical indicator diagram for an ideal isothermal compression cycle and ideal polytropic compression are shown in figure 7.5 [15,19]. Theoretically the figure 7.5 shows that if the compression process was isothermal rather than polytropic, the net work of the compression cycle would be reduced. And, if the polytropic index n decreases, the work transfer required by the compressor process would be reduced [16]. The reduction in the work of the cycle which would be realised through isothermal compression is indicated by the crosshatched area in figure 7.5.

Since the isothermal efficiency η_{iso} is defined as equation 7.10, the higher the value of polytropic index n (n increases as P_1/P_4 increases as in figure 7.4), the lower the value of the efficiency. For a given value of discharge pressure P_1 , the isothermal efficiency decreases as the pressure ratio P_1/P_4 increases. Table 7.3 shows the numerical values of the efficiency for discharge pressure P_1 , of 964.13kPa, 1104.57kPa and 1244.14kPa.

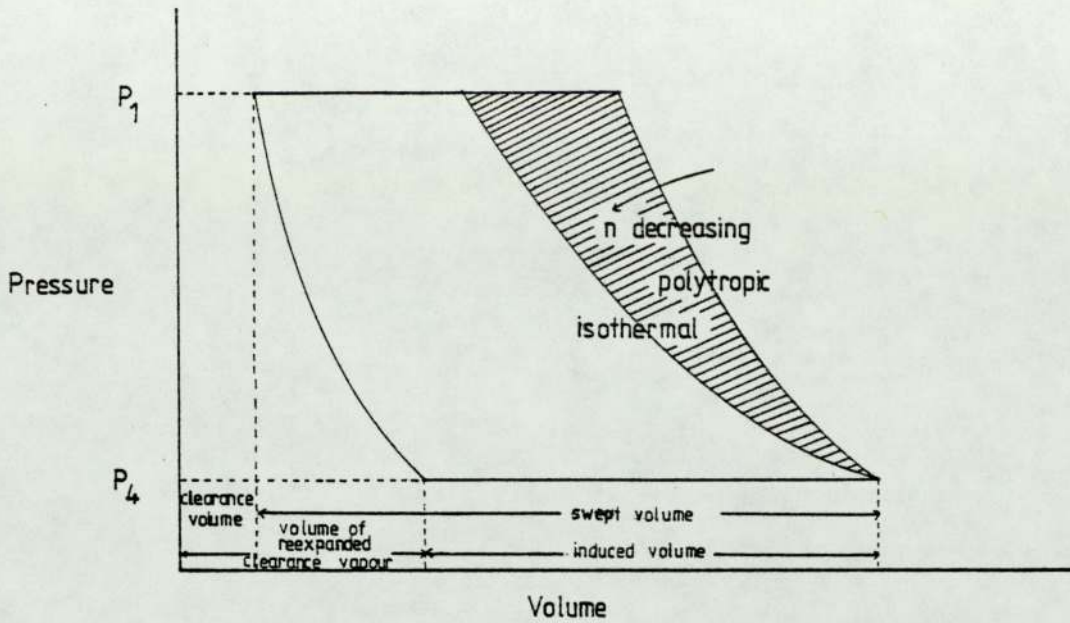


Figure 7.5: Indicator diagram for an ideal isothermal compression cycle and ideal polytropic compression cycle.

T3 (C)	P1=964.13KPA				P1=1104.57KPA				P1=1244.57KPA			
	P1/P4	VOL.EFF (%)	ISO.EFF (%)	ISEN.EFF (%)	P1/P4	VOL.EFF (%)	ISO.EFF (%)	ISEN.EFF (%)	P1/P4	VOL.EFF (%)	ISO.EFF (%)	ISEN.EFF (%)
6.0	2.871	93.0	91.5	78.1	3.259	91.5	90.9	76.4	3.680	90.0	90.1	71.0
5.5	2.905	92.8	91.4	78.0	3.316	91.3	90.8	76.4	3.728	89.8	90.0	71.0
5.0	2.947	92.7	91.4	77.8	3.387	91.0	90.7	76.3	3.801	89.6	89.9	70.9
4.5	3.005	92.4	91.3	77.8	3.452	90.8	90.5	76.3	3.870	89.3	89.8	70.9
4.0	3.053	92.3	91.2	77.8	3.509	90.6	90.4	75.7	3.957	89.0	89.6	70.8
3.5	3.116	92.0	91.1	77.7	3.574	90.4	90.2	75.6	4.013	88.8	89.6	70.7
3.0	3.186	91.8	90.9	77.3	3.682	90.0	90.0	74.5	4.111	88.5	89.3	70.4
2.5	3.245	91.6	90.7	76.7	3.720	89.9	89.9	74.1	4.199	88.2	89.1	70.2
2.0	3.329	91.3	90.5	76.0	3.796	89.7	89.7	73.4	4.261	88.0	89.1	69.9
1.5	3.338	91.3	90.4	75.4	3.900	89.33	89.7	73.0	4.316	87.8	89.0	69.6
1.0	3.422	91.0	90.2	75.1	3.931	89.2	89.4	72.8	4.347	87.7	88.9	69.5
0.5	3.468	90.9	90.1	74.3	4.019	88.9	89.2	72.3	4.385	87.6	88.8	69.3
0.0	3.559	90.6	89.9	73.9	4.090	88.7	89.0	71.8	4.464	87.4	88.6	68.5
-0.5	3.613	90.4	89.7	73.3	4.156	88.5	88.9	71.1	4.552	87.1	88.5	68.3
-1.0	3.707	90.1	89.4	72.0	4.201	88.3	88.8	71.0	4.648	86.8	88.3	67.7

TABLE 7.3: THE COMPRESSOR EFFICIENCIES OF THE WATER-TO-WATER HEAT PUMP SYSTEM AT THREE DIFFERENT DISCHARGE PRESSURES. THE EFFICIENCIES DECREASE AS THE PRESSURE RATIO P_1/P_4 INCREASES.

7.4.3 Isentropic Efficiency (η_{isen}).

If the compression process takes place without friction and without the transfer of energy as heat to or from the refrigerant - adiabatic compression - the process is known as isentropic compression [11,16] .

In the actual refrigerant cycle, transfer of energy from the refrigerant does take place since the friction between the surfaces of the piston and cylinder, pressure drop through valves, and the heat transfer from hot compressed superheat gas to the cylinder cannot be avoided. This process results in the discharge pressure P_1 not lying on the same isentrope as the suction pressure P_4 [4,12,15,19] . The entropy at P_1 is higher than at P_4 as the result of some energy being delivered by the process.

Therefore the isentropic work done by the compressor is,

$$\dot{m}_F(H_I - H_4)$$

and the actual work is,

$$\dot{m}_F(H_1 - H_4)$$

where \dot{m}_F is the refrigerant mass flow rate. The

isentropic efficiency η_{isen} is,

$$\begin{aligned}\eta_{isen} &= \frac{\text{isentropic work}}{\text{actual work}} \\ &= \frac{H_I - H_4}{H_1 - H_4}\end{aligned}\quad 7.12$$

where H_I is the enthalpy at isentropic compression of P_1 , H_1 is the enthalpy at actual compression of P_1 and H_4 is the enthalpy at the suction pressure P_4 .

The variation of isentropic efficiency η_{isen} with pressure ratio P_1/P_4 is shown in table 7.3. As the discharge pressure P_1 increases (more heat is dissipated during the compression) the isentropic efficiency η_{isen} decreases. Increasing the pressure ratio P_1/P_4 would decrease the isentropic efficiency, since heat would be delivered from the hot gas to the cylinder wall as discussed previously [12,15,42] .

The isentropic efficiencies obtained in table 7.3 compare well with the suggestion by Stoecker and Jones [12] that the η_{isen} are usually in the range of 65 to 70 percent for open-type reciprocating compressors; and that by Reay and Mc Micheal [4] giving the value of 70 percent.

7.4.4 Mechanical Efficiency (η_m).

The mechanical friction in the compressor varies with the speed of rotation, but for any one speed, the mechanical friction, and therefore the friction power, will remain practically the same at all operating conditions [15] . Since the friction power remains the same, therefore the mechanical efficiency of the compressor depends entirely upon the loading of the compressor. As the total shaft power of the compressor increases due to loading of the compressor, the friction power (being constant), will become a smaller and smaller percentage of the total power and the mechanical efficiency will increase. It was stated by Dossat [15] and Bacon [19] that the mechanical efficiency of the compressor will be greatest when the compressor is fully loaded.

As discussed in chapter 2, the mechanical efficiency can be written as (equation 2.38),

$$\eta_m = \frac{W_R}{\eta_{isen} \times \eta_{iso} \times W_c} \quad 7.13$$

where W_R is the work done on the vapour and W_c is the electrical power consumed by the compressor.

The mechanical efficiency of a compressor depends on its design. The value for a good reciprocating compressor given by Bacon [19] is 85 percent, Dossat [15] 90 percent, Reay and Mc Micheal [4] 95 percent; and Neal [44] stated that the value lies between 85 percent (for small high speed compressors with high compression ratio) to 96 percent (for large machines with low compression ratio directly driven by an engine).

Table 7.4 shows the refrigerant mass flow rate calculated by using the enthalpy increase across the compressor with the assumption that the mechanical efficiency η_m of the compressor in the heat pump system is 0.85, 0.90 and 0.95.

T3 (DEGC)	P1/P4	MF (G/SEC)	MG (G/SEC)		
			$\eta_m = .85$	$\eta_m = .90$	$\eta_m = .95$
6.0	3.259	6.95	5.80	6.17	6.48
5.5	3.316	6.75	5.78	6.12	6.46
5.0	3.387	6.56	5.57	6.00	6.32
4.5	3.452	6.43	5.55	5.58	6.20
4.0	3.509	6.19	5.39	5.71	6.03
3.5	3.574	6.05	5.31	5.62	5.93
3.0	3.682	5.91	4.94	5.32	5.52
2.5	3.720	5.71	4.85	5.14	5.42
2.0	3.797	5.66	4.64	4.91	5.20
1.0	3.931	5.27	4.35	4.67	4.93
0.5	4.019	5.06	4.23	4.48	4.72
0.0	4.090	4.88	4.09	4.34	4.37
-0.5	4.156	4.70	3.92	4.15	4.35
-1.0	4.201	4.57	3.83	4.06	4.29

TABLE 7.4: COMPARISON OF REFRIGERANT MASS FLOW RATE CALCULATED BY USING ENERGY ABSORBED BY THE EVAPORATOR QE (MF) AND THE WORK DONE BY THE COMPRESSOR WR (MG) WITH MECHANICAL EFFICIENCIES OF 0.85, 0.90 AND 0.95.

7.5 Refrigerant Mass Flow Rate (\dot{m}_F)

The refrigerant mass flow rate \dot{m}_F is usually calculated by using the refrigerating capacity across either evaporator, condenser or compressor [12,15 41,45] . If the value of the actual heat being absorbed by the evaporator, released by the condenser or the actual work done on compressing the vapour gas by the compressor is known, then the refrigerant mass flow rate \dot{m}_F can be calculated by dividing the energy involved with the enthalpy increase during the process.

As mentioned earlier in chapter3, in this water-to-water heat pump system the condenser and evaporator were constructed in the laboratory. Therefore, the actual energy transfer to and from the refrigerant cannot be calculated theoretically by the heat transfer method since the heat transfer coefficient [16,46] cannot be determined.

The actual work done on the superheated vapour by the compressor also cannot be determined since neither the rotational frequency of the piston nor the mechanical efficiency η_m of the compressor is known [21] . Therefore in order to calculate the refrigerant mass flow rate \dot{m}_F , three empirical methods

might be used;

1. By using the energy released by the condenser to the water (Q_c) - assuming that 100% of the energy released by the refrigerant is absorbed by the water. \dot{m}_F is calculated by dividing Q_c by the enthalpy difference across the condenser (H_1-H_2).
2. By using the energy absorbed by the evaporator from the water (Q_e) - assuming that 100% of the energy absorbed by the refrigerant in evaporator is only from the water passing through it. \dot{m}_F is calculated by dividing Q_e by the enthalpy difference across the evaporator (H_4-H_2).
3. By assuming that the compressor has a certain value of mechanical efficiency η_m . Then the work done by the compressor on the vapour W_R can be calculated by using equation 2.38.

$$W_R = \eta_{iso} \times \eta_m \times \eta_{isen} \times W_c \quad 7.14$$

where η_{iso} is calculated by using equation 7.11,
 η_{isen} is calculated by using equation 7.12 and W_c is the electrical power consumed by the compressor which

can be read directly during the experiment.

The values of H_1 (discharge enthalpy), H_2 (subcool enthalpy) and H_4 (superheat enthalpy) can be obtained from tables given by ASHRAE [43] if the values of pressure and temperature at those points are known.

In method (1) above the value of Q_c is always fluctuating as can be seen in figure 7.2 (and also discussed in chapter 6). This is due to the fluctuation of water flow rate \dot{m}_c through the condenser. Therefore methods (2) and (3) are more suitable to use to determine the mass flow rate of the refrigerant \dot{m}_F . In the method described by (2) above, the refrigerant mass flow rate \dot{m}_F can be written as,

$$\dot{m}_F = \frac{Q_e}{(H_4 - H_2)} \quad 7.15$$

assuming $H_2 = H_3$.

Figure 7.6 shows the value of refrigerant mass flow rate \dot{m}_F as a function of T_3 and discharge pressure P_1 . As the temperature after the expansion valve (T_3) (and thus evaporating temperature T_e) decreases the value of heat absorbed Q_e decreases as shown in figure 7.2. As the suction pressure drops, the superheat enthalpy H_4 decreases. As a result, the refrigerant mass flow rate \dot{m}_F decreases as

evaporating temperature T_e (and T_3) decreases as shown in figure 7.6.

Table 7.4 shows the refrigerant mass flow rate calculated by using the work done by the compressor on the superheat gas (\dot{M}_G) by using equation 7.14 with the assumption of mechanical efficiency of 85 percent, 90 percent and 95 percent respectively. For comparison, the value calculated by using equation 7.15 (\dot{M}_F) is also given in the table. Table 7.4 shows that when mechanical efficiency of the compressor is higher, the higher is the actual work done W_R to compress the vapour to high pressure and temperature side (equation 7.14). As a result more refrigerant is being cycled in the refrigerant circuit for a given value of pressure ratio P_1/P_4 across the compressor. As the pressure ratio P_1/P_4 increases, the refrigerant flow rate \dot{m}_F decreases which is similar to the result in figure 7.6. Table 7.4 also shows that for the assumption that 100% of energy being absorbed by the refrigerant in the evaporator, $\eta_m = 0.95$ is more favourable figure than 0.85 and 0.90. The high value calculated by using equation 7.15 shows that the 100% assumption of the energy being absorbed by the refrigerant in evaporator is not necessarily true, since the refrigerant might well absorb heat from air at both ends of the evaporator.

The refrigerant mass flow rate \dot{m}_F , through a compressor is proportional to the displacement rate and the volumetric efficiency and inversely proportional to the specific volume of gas entering the compressor [12]. As mentioned by Stoecker [12], as the suction pressure drops (P_1/P_4 increases since the discharge pressure P_1 is maintained constant), the specific volume entering the compressor increases, which, together with the volumetric efficiency, reduces the refrigerant mass flow rate \dot{m}_F at low evaporating temperature T_e (and temperature after the expansion valve, T_3) as shown in table 7.4. These results are in agreement with those found by Stoecker and Jones [12] Ahren [39] and Morgan [7].

As mentioned in chapter 3, the refrigerant mass flow rate \dot{m}_F is controlled by the expansion valve. Since the expansion valve was set to operate at 6°C above evaporating temperature T_e by the manufacturer, theoretically, at a certain value of T_e (and thus superheat temperature T_4), an increase in discharge pressure P_1 (and thus condensing pressure P_c), will not alter \dot{m}_F since the pressure in the remote bulb of the expansion valve is maintained by the superheat temperature T_4 . But in reality, (see figure 7.6), \dot{m}_F decreases as discharge pressure P_1 increases, for a given value of T_3 . This effect, according to Ahren

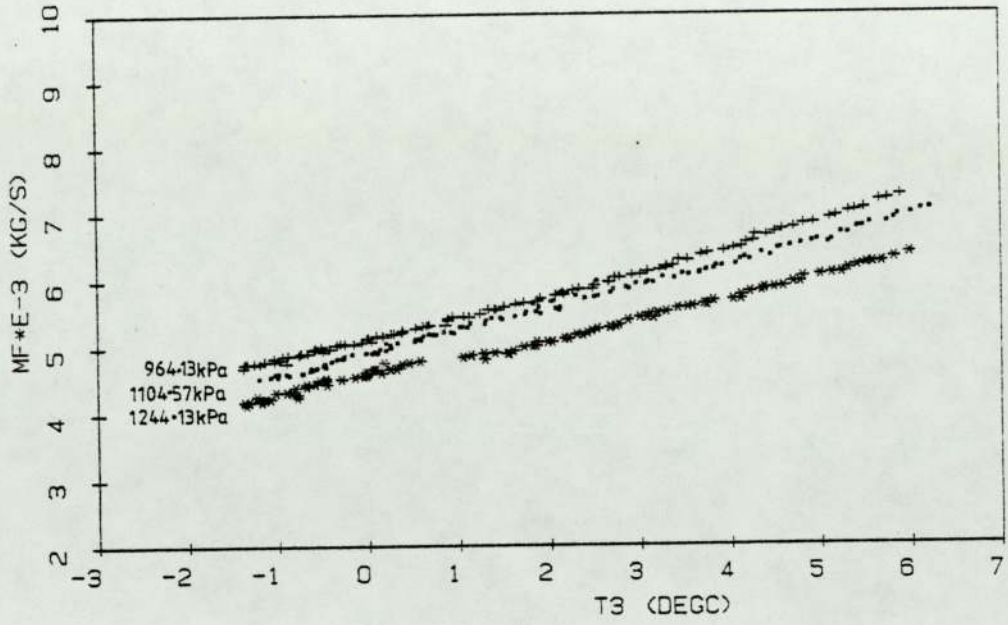


Figure 7.6: Refrigerant mass flow rate at three different discharge pressures.

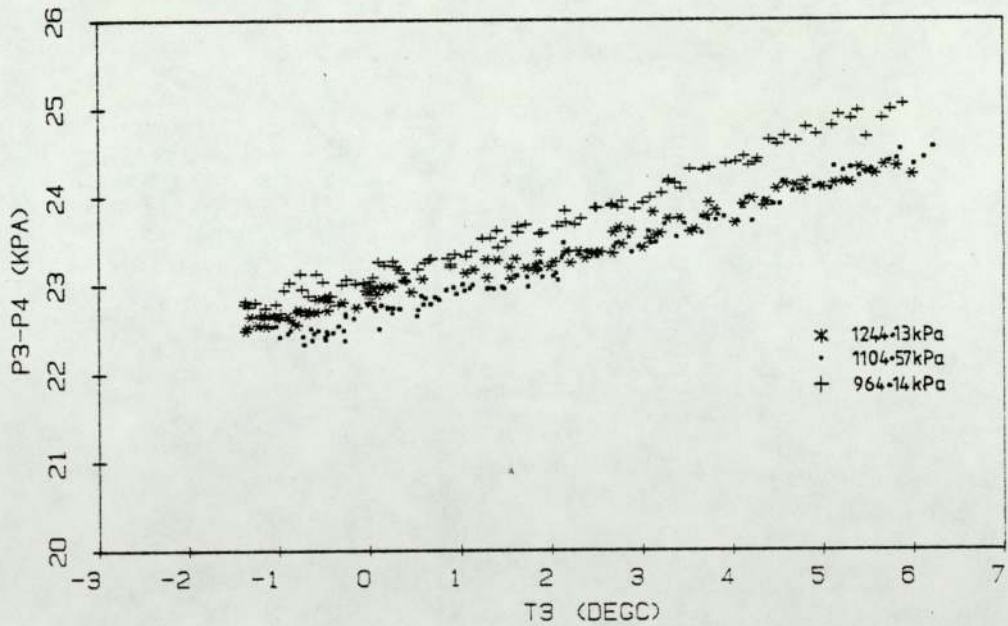


Figure 7.7: Pressure losses in the evaporator for different discharge pressures.

[39] , Gosney [47] and Dossat [15] is due to back leakage from the high pressure side toward the low pressure side. Leakage in the compressor may take place between the piston and the cylinder wall, and between the valves and their seats as mentioned by Gosney [47] . As a result of the leakage, the refrigerant flow rate \dot{m}_F is reduced when discharge pressure P_1 increased.

7.6 The Evaporator.

In overcoming friction, both internal (within the fluid) and external (surface), the refrigerant experiences a drop in pressure while flowing through the piping, evaporator, condenser and accumulator [15, 4,39,41] .

Since the four pressure transducers (P_1, P_2, P_3 and P_4) were fixed, two across the compressor (P_1 and P_4) and two across the expansion valve (P_2 and P_3) as shown in figure 7.1, the actual values of evaporating pressure and condensing pressure cannot be read directly by the computer during sampling. However, the pressure losses in the condenser ($P_1 - P_2$) and in the evaporator ($P_3 - P_4$) can always readily be read from the transducers by the computer.

For the evaporator, as suggested by Dossat [15] and Pabon-Diaz [41], the evaporating pressure can be considered as the average value of pressure P_3 and P_4 , then the evaporating pressure P_e can be written as,

$$P_e = \frac{P_3 + P_4}{2} \quad 7.16$$

The pressure loss ($P_3 - P_4$) as a function of the temperature after the expansion valve T_3 is shown in figure 7.7. As T_3 increases (and thus the evaporating temperature T_e), the pressure loss in the evaporator increases. As mentioned by Elonka and Minich [21], for internal equalisation of the expansion valve (as in this system), the pressure loss during evaporation should not exceed 34.5kPa (5psia). The result shown in figure 7.7 justifies this system where $P_3 - P_4$ is always less than 34.5kPa. If the pressure loss through the evaporator is too high, in order for the expansion valve to operate properly, the superheat temperature T_4 needs to be raised such that the pressure in the remote bulb of the expansion valve is also high. To do this, an external equaliser is needed [8,21].

Mathematically, the pressure loss $P_3 - P_4$ (as in figure 7.7) can be written as a function of T_3 by using a least squares curve fitting method as suggested by Gerald [31] as,

$$P_3 - P_4 = 22.86697 + 0.21592T_3 + 6.82192 \times 10^{-3} T_3^2 \quad 7.17$$

The evaporating temperature T_e corresponding to evaporating pressure P_e (calculated by using equation 7.16) can directly be obtained from the refrigerant R12 table given by ASHRAE [43] . The mathematical relation between T_3 and T_e of the system (as shown in figure 7.8) can be written as (using least squares fit method as suggested by Gerald [31]),

$$T_3 = 2.46975 + 0.89797T_e \quad 7.18$$

As mentioned earlier in chapter 2, the superheat temperature T_4 is controlled by the expansion valve and is set (by manufacturer) such that it is always several degrees (6°C) above the evaporating temperature T_e . Figure 7.9 shows the relation between T_4 and T_3 (and thus T_e). As expected T_4 depends linearly on T_3 , but as the water flow rate through the evaporator \dot{m}_e increases, T_4 increases. These results can be expressed as was suggested by Stoecker and Jones [12] ,

$$T_4 = a_1 + a_2 T_3 + a_3 \dot{m}_e + a_4 \dot{m}_e^2 + a_5 T_3 \dot{m}_e + a_6 T_3 \dot{m}_e^2 \quad 7.19$$

The numerical constants a_1, a_2, a_3, a_4, a_5 and

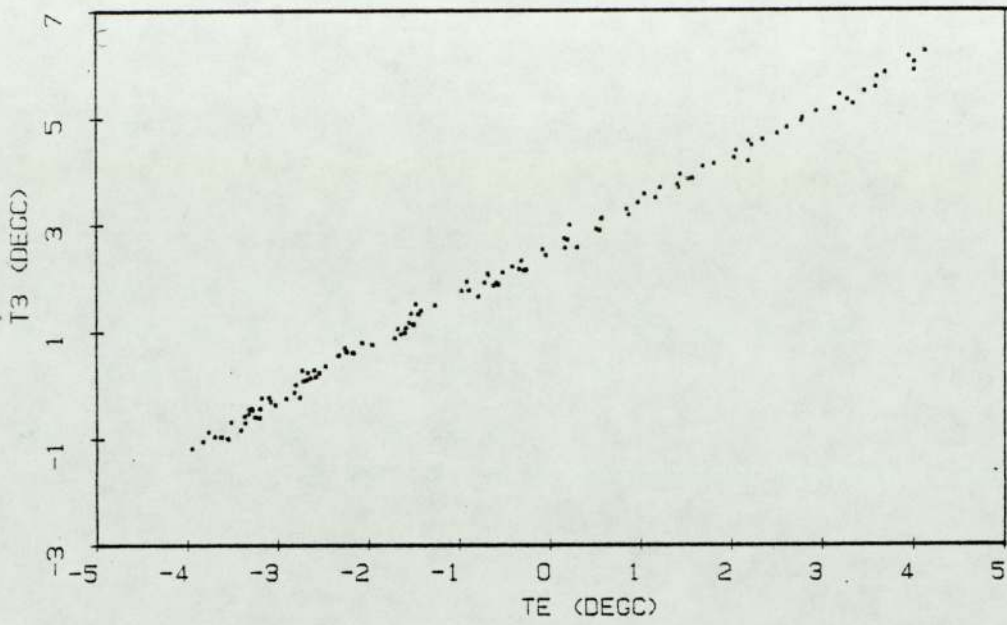


Figure 7.8: Relation between the temperature of refrigerant after the expansion valve (T_3) and evaporating temperature (T_e).

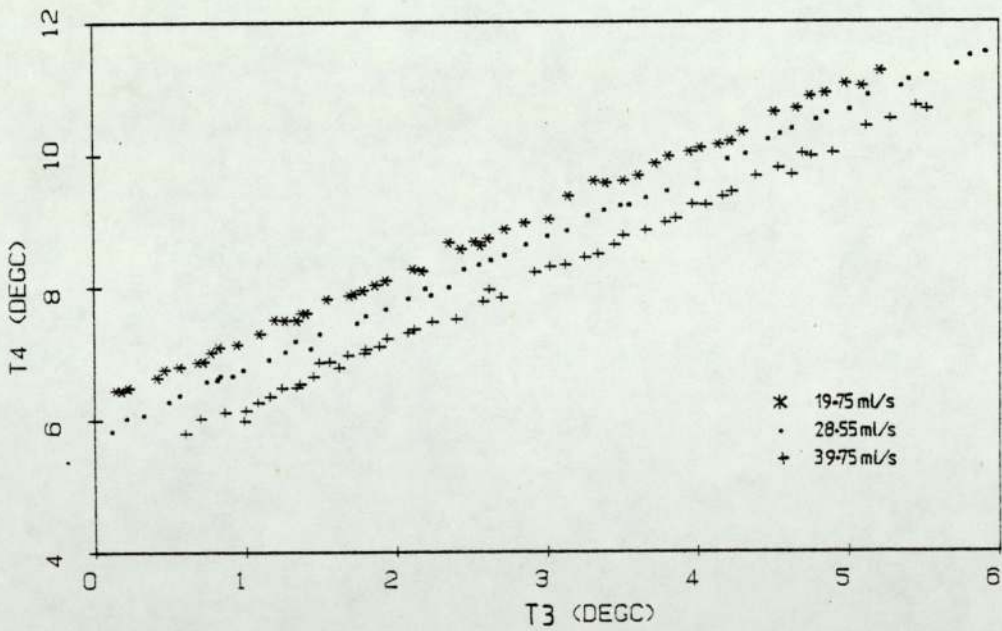


Figure 7.9: Relation between temperature of the suction superheated gas (T_4) and the temperature after the expansion valve (T_3).

a_6 for equation 7.19 are shown in table 7.5

=====
EQN. 7.18

A1= 3.61004499
A2= 1.04281977
A3= 95.1004375
A4=-680.373304
A5=-1.9561199
A6=-8.4779197
=====

TABLE 7.5: NUMERICAL VALUES OF CONSTANTS
FOR EQUATION 7.19

The energy absorbed from the water passing through the evaporator is governed by equation 7.2. As shown in figure 7.2, the energy absorbed (Q_e) decreases as the temperature after the expansion valve (T_3) decreases. Therefore the temperature difference of the water across the evaporator ($T_{W_{ei}} - T_{W_{eo}}$) decreases as T_3 decreases. Since Q_e is given by equation 7.2, the water flow rate through the evaporator \dot{m}_e increases as ($T_{W_{ei}} - T_{W_{eo}}$) decreases. This relation is shown in figure 7.10. Figure 7.10 also shows that, at a particular water flow rate \dot{m}_e , ($T_{W_{ei}} - T_{W_{eo}}$) is linearly dependent on T_3 (and thus T_e).

7.7 The Condenser.

As in the evaporator, the refrigerant in the condenser also experiences pressure losses. Once

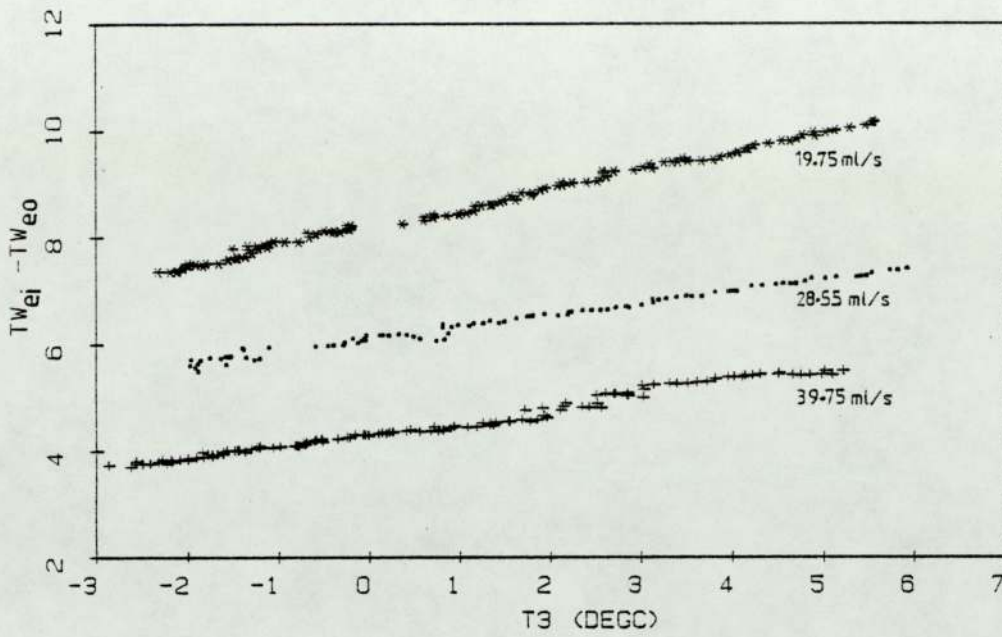


Figure 7.10: The relation between temperature difference across the evaporator ($T_{W_{ei}} - T_{W_{eo}}$), and temperature of the refrigerant after the expansion valve (T_3) at three different water flow rates.

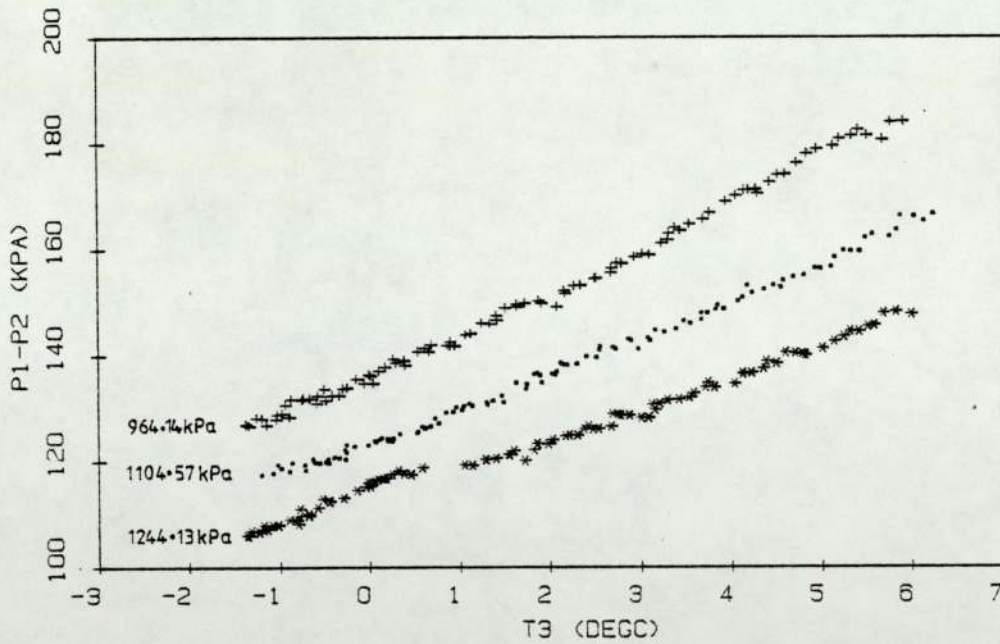


Figure 7.11: The pressure losses across the condenser at three discharge pressures.

again, as suggested by Dossat [15] and Pabon-Diaz [41] the condensing pressure of the refrigerant P_c can be considered as the average value of pressures across the condenser as,

$$P_c = \frac{P_1 + P_2}{2} \quad 7.20$$

Figure 7.11 shows the pressure loss of the refrigerant in the heat pump system across the condenser as a function of T_3 and discharge pressure P_1 . Since the refrigerant in the condenser is at high pressure, its length is much longer than the evaporator and it contains refrigerant in three states (gas, vapour and liquid), the pressure loss in the condenser is higher than the pressure loss in the evaporator (figure 7.7). As mentioned in chapter 6, the pressure loss is higher when the discharge pressure P_1 is low. Mathematically, $P_1 - P_2$ can be written as a function of T_3 and P_1 as suggested by Stoecker and Jones [12] as,

$$P_1 - P_2 = a_1 + a_2 T_3 + a_3 T_3^2 + a_4 P_1 + a_5 P_1^2 + a_6 T_3 P_1 + a_7 T_3^2 P_1 + a_8 T_3 P_1^2 + a_9 T_3^2 P_1^2 \quad 7.21$$

As mentioned earlier the water flow rate through the condenser (\dot{m}_c) is controlled by the water regulator. The discharge pressure P_1 was set to give a desired output water temperature from the condenser.

Since the value of energy released by the condenser (Q_c) increases as T_3 increases as shown in figure 7.2, and the relationship of Q_c and \dot{m}_c is governed by equation 7.1 with $T_{W_{co}}$ (output water temperature of the condenser) being determined by the discharge pressure P_1 , the pattern of water flow rate \dot{m}_c follows the pattern of Q_c . Figure 7.12 shows the relation of \dot{m}_c with respect to discharge pressure P_1 and temperature after the expansion valve T_3 (and thus T_e). The figure also shows that, as the flow rate \dot{m}_c is controlled by the discharge pressure P_1 , the higher the discharge pressure P_1 , the lower is the water flow rate passing through the condenser.

In mathematical form, the dependence of \dot{m}_c on T_3 and P_1 can be written as [12] ,

$$\dot{m}_c = b_1 + b_2 T_3 + b_3 T_3^2 + b_4 P_1 + b_5 P_1^2 + b_6 T_3 P_1 + b_7 T_3^2 P_1 + b_8 T_3 P_1^2 + b_9 T_3^2 P_1^2 \quad 7.22$$

Once again the numerical values of constants a and b in equations 7.21 and 7.22 can be obtained by substitution of nine points of the least squares curve fitting of the respective graph to develop a set of nine simultaneous equations [40] . Table 7.6 shows the numerical values of constants a and b calculated by using the method suggested by Gerald [31] .

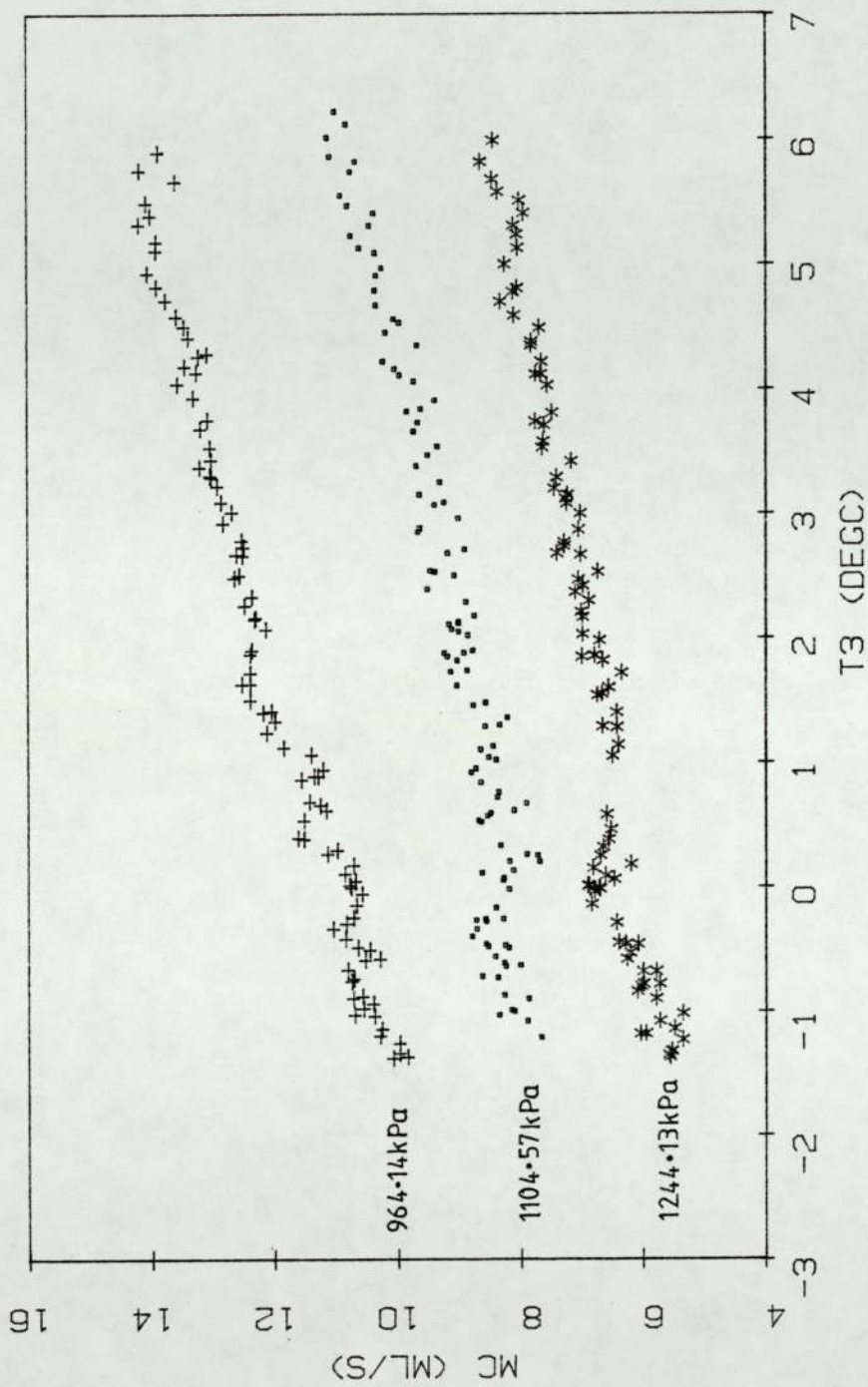


Figure 7.12: The effect of the discharge pressure on water flow rate through the condenser.

EQN. 7.21	EQN. 7.22
A1= 325.546721	B1= 45.73344225
A2= 11.1586822	B2= 19.9539656
A3= 3.18336891	B3=-3.06061354
A4=-0.28743125	B4=-0.0508265014
A5= 9.43335886E-05	B5= 1.53614333E-05
A6=-1.03258515E-03	B6=-0.0345219709
A7=-5.14789495E-03	B7= 5.50641971E-03
A8=-3.19330948E-06	B8= 1.5060743E-05
A9= 2.16467516E-06	B9=-2.44357666E-06

TABLE 7.6: NUMERICAL VALUES OF THE CONSTANTS FOR EQUATIONS 7.21 AND 7.22.

7.8.1 System Simulation and Heat Pump Modelling.

In the previous sections, the performance of individual components which make-up the water-to-water heat pump system has been analysed empirically from experimental data. The overall performance of the system can then be predicted, based on these individual performance [12,39] .

The method suggested by Stoecker [40] , called system simulation, which is performed by mathematical rather than graphical procedures will be used in this analysis. The essential aim of the model is the evaluation of thermodynamic state distributions within the system components in response to changes in operating conditions. The families of characteristics obtained

in previous sections will be employed to represent the heat pump model. This method of modelling has been used by manufacturers in order that the control strategy can be determined [12,48] .

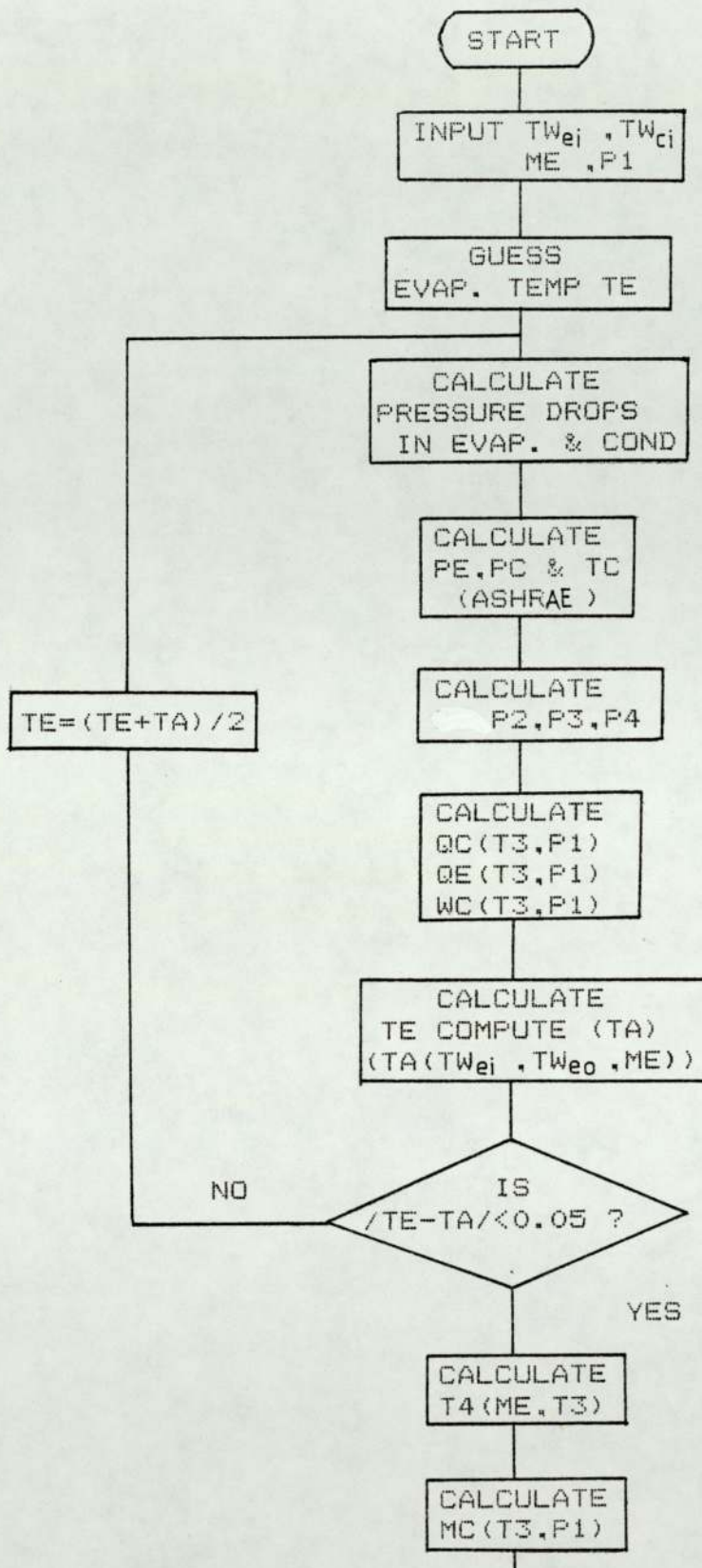
7.8.2 Description of Modelling Flow Diagram.

Figure 7.13 shows the flow diagram of the computer model which determines the performance of the water-to-water heat pump system. The model starts with a requirement to enter the conditions of the system; inlet water temperature of the evaporator (TW_{ei}), inlet water temperature of the condenser (TW_{ci}), the water flow rate through the evaporator (\dot{m}_e) and the discharge pressure P_1 , which can be set to give the required output water temperature of the condenser (TW_{co}) by adjusting the water regulator. Then the model proceeds with guessing the value of evaporating temperature T_e .

As there is pressure loss in the condenser, the pressure after the condenser P_2 is related to P_1 as,

$$P_2 = -210.292269 + 1.07831985P_1 \quad 7.23$$

P_c is calculated by using equation 7.20. The program then computes the condensing temperature T_c whose relation with condensing pressure P_c is



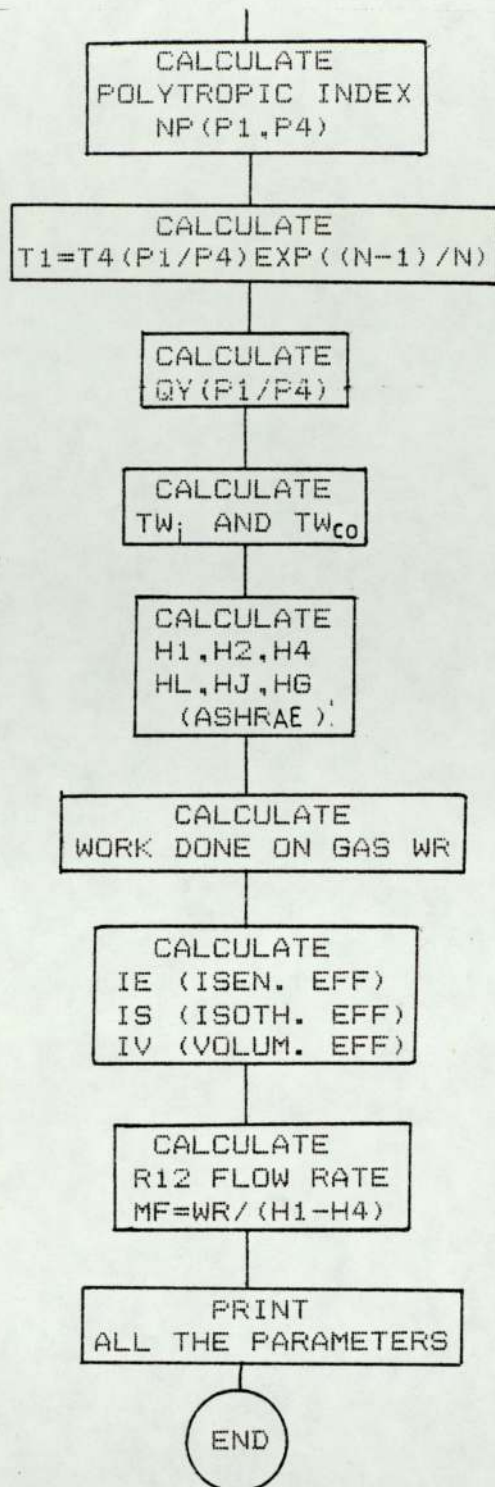


Figure 7.13: Flow diagram of the water-to-water heat pump model.

calculated by a least squares curve fitting method [31] based on the data given by ASHRAE [43] ;

$$T_c = 260.245186 + 0.0671422787P_c - 1.26298469 \times 10^{-5} P_c^2 \quad 7.24$$

The temperature after the expansion valve T_3 is empirically related to evaporating temperature T_e as,

$$T_3 = 2.4697091 + 0.897969093T_e \quad 7.25$$

The pressure after expansion valve P_3 is related to T_3 by a least squares curve fitting method [31] based on the data given by ASHRAE [43] ,

$$P_3 = 7084.88281 - 59.8153687 \times (T_3 + 273.15) + 0.128165364 \times (T_3 + 273.15)^2 \quad 7.26$$

Suction pressure P_4 is then calculated based on equation 7.17. The program then proceeds to calculate the evaporating pressure P_e by using equation 7.16.

From the values of T_3 and discharge pressure P_1 , the energy absorbed by the evaporator Q_e , delivered by the condenser Q_c and the electrical power consumed by the compressor W_c can be obtained by using equations 7.3, 7.4 and 7.5 respectively. The output water temperature of the evaporator $T_{W_{e0}}$ can then be determined by using equation 7.2.

The actual value of evaporating temperature is determined by the outlet water temperature of the evaporator and the water flow rate passing through it (\dot{m}_e). The mathematical relation obtained by using the method suggested by Stoecker [40] is,

$$T_e = TW_{eo} - (a_1 + a_2 TW_{eo} + a_3 \dot{m}_e + a_4 \dot{m}_e^2 + a_5 TW_{eo} \dot{m}_e + a_6 TW_{eo} \dot{m}_e^2) \quad 7.27$$

where the numerical value for the constants a_1, a_2, a_3, a_4, a_5 and a_6 , determined by solving six simultaneous equations for the six fitting points as suggested by Gerald [31], are shown in table 7.7.

```

=====
EQN. 7.27
-----
A1= 2.04284536
A2= 0.126504261
A3= 128.428956
A4=-1666.69265
A5=-3.74487684
A6= 95.2438889
=====

```

TABLE 7.7: NUMERICAL VALUES OF CONSTANTS FOR EQUATION 7.26.

Comparing this new value of T_e with the old guessed value at the beginning of the program yields ΔT_e . If this figure of ΔT_e is within acceptable limits (0.05°C), the original guessed value of T_e is assumed correct and the program proceeds

to calculate the rest of the necessary equations. If ΔT_e is outside limits, the value of T_e is altered by taking the average value of the new T_e and the old, and the program repeated as indicated in the flow diagram (figure 7.13).

The program then proceeds with determining the superheat temperature $T_4(\dot{m}_e, T_3)$ by using equation 7.19. The water flow rate through the condenser \dot{m}_c is calculated by using equation 7.22.

The empirical value of polytropic index $n(P_1, P_4)$ is calculated by using equation 7.8. The value of discharge temperature T_1 can be calculated by using equation 7.7 where the values of P_1, P_4 and n are already known.

Since some energy is being picked-up by compressor cooling, the temperature of the water going into the condenser is not $T_{W_{ci}}$ but T_{W_i} which is a bit higher. The value of T_{W_i} is calculated by using the amount of energy picked-up Q_y given by equation 7.6.

$$T_{W_i} = T_{W_{ci}} + \frac{Q_y}{\dot{m}_c c_p} \quad 7.28$$

Then the outlet water temperature of condenser $T_{W_{co}}$ can be calculated by using equation 7.1 since the value of Q_c and T_{W_i} are already known.

At this stage all values of pressures P_1 , P_2 , P_3 and P_4 , temperatures T_1 , T_2 , T_3 and T_4 , condensing temperature T_c and evaporating temperature T_e have been calculated. The next steps are to calculate the enthalpies around the cycle. The calculation of the enthalpies was based on the data given by ASHRAE but mathematically presented as suggested by Stoecker and Jones [12] . Appendix III shows the relevant equations which fit the data given.

The volumetric efficiency, isothermal efficiency and isentropic efficiency of the compressor are calculated by using equations 7.9, 7.11 and 7.12 respectively, and the relevant work done on the superheated gas W_R is calculated by using equation 2.38 (7.13). For comparison, both methods of determining the refrigerant flow rate \dot{m}_F were used; (i) using energy absorbed by the evaporator Q_e (equation 7.15), and (ii) work done on the superheated gas W_R ($\dot{m}_F = W_R / (H_1 - H_4)$) with assumption that the mechanical efficiency is 0.95.

Finally the coefficient of performance of the compressor can be calculated as,

$$\begin{aligned} \text{C.O.P.} &= \frac{\text{total energy output}}{\text{work done by compressor}} \\ &= \frac{Q_y + Q_c}{W_c} \end{aligned} \quad 7.29$$

and the real C.O.P. including water pump of 60 Watts is,

$$\text{C.O.P.} = \frac{Q_y + Q_c}{W_c + 60} \quad 7.30$$

Then, a print out of all parameters is given and the program stops.

The actual computer program is shown in appendix IV and a print out of all parameters with input water for evaporator and condenser at 15°C, water flow rate through evaporator 30ml/s, discharge pressure P_1 of 1034.3kPA (150psia) and guessed value of T_e is 0°C is shown in table 7.8

7.8.3. The Limitation of the Modelling.

The heat pump model was based on some of the experimental results which were obtained in the laboratory. In carrying out these experiments, as mentioned earlier, there were some limitations which could not be avoided.

The major limitations are due to the limitation of operation of the components making up the heat pump itself, e.g. evaporator, condenser, compressor and expansion valve. Some are due to environmental factors such as temperature of water passing through

```

=====
INPUT WATER TEMP. FOR EVAPORATOR = 15      DEGC
INPUT WATER TEMP. FOR CONDENSER  = 15      DEGC
WATER FLOWRATE THROUGH EVAPORATOR = 30     ML/S
INPUT DISCHARGE PRESS P1        = 1034.2   KPA
INPUT DISCHARGE PRESS P1 IN PSIA = 150

EVAPORATING TEMPERATURE (GUESS) = 0       DEGC
EVAPORATING TEMPERATURE (COMPUTE) = 2.45   DEGC
CONDENSING TEMPERATURE          = 40.32    DEGC

CONDENSER WATER FLOWRATE        = 11.7     ML/S
REFRIGERANT FLOWRATE (COMP)     = 8.31E-03  KG/S
REFRIGERANT FLOWRATE (EVAP)    = 6.66E-03  KG/S

OUTPUT WATER TEMP. AFTER CONDENSER = 43.41   DEGC
OUTPUT WATER TEMP. AFTER EVAPORATOR = 7.614   DEGC
WATER TEMP. AFTER COMPRESSOR     = 16.91   DEGC
DISCHARGE TEMPERATURE           = 66.09   DEGC
SUBCOOL TEMPERATURE             = 20.23   DEGC
TEMPERATURE AFTER EXP VALVE     = 4.63    DEGC
SUPERHEAT TEMPERATURE           = 10.37   DEGC

POLYTROPIC INDEX                = 1.1892
ISENTROPIC EFF                  = 79.1 %
ISOTHERMAL EFF                  = 91.2 %
VOLUMETRIC EFF                  = 92.0 %
CONDENSER EFF                   = 93.1 %
EVAPORATOR EFF                  = 80.1 %

EVAP SPECIFIC ENTHALPY V-G      = 190.69   KJ/KG
COND SPECIFIC ENTHALPY V-G      = 204.90   KJ/KG
COND SPECIFIC ENTHALPY L-V      = 75.790   KJ/KG
DISCHARGE SPECIFIC ENTHALPY     = 223.18   KJ/KG
SUBCOOL SPECIFIC ENTHALPY       = 55.549   KJ/KG
SUPERHEAT SPECIFIC ENTHALPY     = 194.73   KJ/KG
ISENTROPIC SPECIFIC ENTHALPY    = 217.24   KJ/KG

P1 = 1034.2 :PC = 969.63 :P2 = 904.99 KPA
P3 = 358.87 :PE = 346.86 :P4 = 334.86 KPA

ENERGY RELEASED BY CONDENSER     = 1297.9   J/S
ENERGY ABSORBED BY EVAPORATOR    = 927.58   J/S
ENERGY PICK-UP DURING COMP COOLING = 93.939   J/S
ELECTRICAL POWER FOR COMPRESSOR  = 345.01   WATTS
WORK DONE ON REFRIGERANT        = 236.75   WATTS

COP CARNOT                      = 11.1
COP RANKINE                      = 5.89
COP (COMPRESSOR ONLY)           = 4.03
COP (INC. WATER PUMP)           = 3.43
=====

```

FIGURE 7.8: ILLUSTRATIVE RESULT FROM THE COMPUTER MODEL WITH GUESSED VALUE OF TE=0 DEGC.

the system and others due to the limitations recommended by manufacturers of components, such as expansion valve and compressor.

The water temperature passing through the evaporator must be above the freezing point of the water itself, otherwise the water would be frozen in the evaporator, and as a result severe damage could occur (the joints in the pipe work might be broken as a result of water expansion during freezing). As an alternative, at low water temperatures flowing through the evaporator, experiments with increased water flow rate \dot{m}_e could be done, but this might lead to a larger error in calculating the value of energy absorbed by the evaporator Q_e since the water temperature difference across the evaporator will be less as mentioned earlier. This effect of frozen water limits the range of values of evaporating temperature T_e . In this analysis, the minimum value of T_3 (the temperature after expansion valve) was restricted to -2°C as shown in figure 7.2 although the expansion valve could operate within the range of -40°C to 10°C of the evaporating temperature as suggested by manufacturer [23] .

The compressor should not operate at a condensing temperature T_c above 60°C as suggested by

the manufacturer [20] . This limits the energy output at the condenser. The pressure transducer itself could not be operated above 1379.0kPa (200psia), its designed maximum pressure. This leads to a limitation of the energy delivered by the condenser Q_c .

Another limitation of modelling arises from approximations made during the writing of mathematical equations describing the interactions between components [12,39,48] .

7.9. Performance Trends of The Heat Pump.

A comparison of results from the simulation and experimental data for various water flow rates (with input water temperature to condenser and evaporator of 15°C) through the evaporator are shown in table 7.9. The results obtained from simulation seem to be in agreement with the experimental results. The model based on 50°C condenser output water temperature seem to give better agreement. It may be due to the effect of low pulses input to the frequency-voltage converter in the electronic circuit at low electrical power to the compressor.

The results of the simulation of the complete vapour-compression systems for various input temperatures to the evaporator are summarised in tables 7.10(a),

=====				
WATER FLOW RATE THROUGH EVAPORATOR = 20 ML/S				
	EXPR	MODEL	EXPR	MODEL

TW (DEGC)	40.1	39.77	50.1	49.67
MC (ML/S)	13.31	13.36	8.56	8.4
QC (WATTS)	1143.8	1192.1	1177.7	1133.3
QE (WATTS)	819.3	850.1	770.5	805.8
WC (WATTS)	325.2	336.4	350.6	358.1
COP	3.81	4.01	3.42	3.42
=====				
WATER FLOW RATE THROUGH EVAPORATOR = 30 ML/S				
	EXPR	MODEL	EXPR	MODEL

TW (DEGC)	40.2	39.90	50.1	49.40
MC (ML/S)	14.10	14.04	9.38	9.20
QC (WATTS)	1325.3	1371.5	1243.4	1240.7
QE (WATTS)	913.6	942.2	885.1	883.4
WC (WATTS)	328.7	332.5	355.5	359.8
COP	4.20	4.37	3.70	3.71
=====				
WATER FLOW RATE THROUGH EVAPORATOR = 40 ML/S				
	EXPR	MODEL	EXPR	MODEL

TW (DEGC)	39.9	39.55	50.2	49.27
MC (ML/S)	15.10	14.70	9.78	9.78
QC (WATTS)	1380.5	1408.8	1286.0	1308.0
QE (WATTS)	983.3	1008.5	928.9	926.8
WC (WATTS)	328.3	331.3	355.8	358.7
COP	4.46	4.55	3.89	3.91
=====				

TABLE 7.9: A COMPARISON OF THE EXPERIMENTAL AND SIMULATION RESULTS FOR VARIOUS WATER FLOW RATES (ME) AND OUTPUT WATER TEMPERATURES OF CONDENSER (TW_{co}) AT ENTERING CONDENSER WATER TEMPERATURE OF 15 DEGC.

EVAPORATOR WATER FLOW RATE =20 ML/S

DISCHARGE PRESSURE P1=140 PSIA : CONDENSING TEMP.=37.20 DEGC

TWei	TWeo	TE	TWco	MC(ML/S)	QC(W)	QE(W)	WC(W)	MF(G/S)	COP
8.0	0.11	-3.85	40.79	10.30	1014.4	662.3	335.7	6.40	3.30
10.0	1.50	-2.58	40.63	11.10	1094.7	712.5	336.5	6.90	3.52
12.0	2.87	-1.34	40.55	11.81	1167.3	765.3	337.7	7.36	3.72
14.0	4.19	-0.13	40.51	12.44	1234.4	821.5	338.2	7.81	3.92
16.0	5.51	1.07	40.51	12.99	1293.4	877.8	338.9	8.24	4.09
18.0	6.75	2.19	40.55	13.51	1352.0	941.4	339.1	8.68	4.28

DISCHARGE PRESSURE P1=160 PSIA : CONDENSING TEMP.=43.31 DEGC

TWei	TWeo	TE	TWco	MC(ML/S)	QC(W)	QE(W)	WC(W)	MF(G/S)	COP
8.0	0.41	-3.54	46.22	8.24	977.0	633.8	346.4	6.01	3.10
10.0	1.81	-2.30	46.44	8.45	1012.8	686.6	349.6	6.42	3.17
12.0	3.16	-1.07	46.59	8.75	1059.5	740.7	351.9	6.84	3.28
14.0	4.52	0.16	46.68	9.14	1115.4	794.2	353.3	7.24	3.43
16.0	5.84	1.37	46.76	9.64	1183.8	850.3	353.9	7.66	3.61
18.0	7.16	2.57	46.68	10.24	1262.4	906.8	354.1	8.07	3.84

DISCHARGE PRESSURE P1=180 PSIA : CONDENSING TEMP.=48.90 DEGC

TWei	TWeo	TE	TWco	MC(ML/S)	QC(W)	QE(W)	WC(W)	MF(G/S)	COP
8.0	0.82	-3.20	53.79	6.19	903.1	602.8	354.1	5.53	2.84
10.0	2.28	-1.87	54.57	6.54	971.73	647.5	360.6	5.93	2.97
12.0	3.68	-0.60	54.31	6.95	1042.5	697.5	365.6	6.35	3.12
14.0	5.07	0.70	54.22	7.36	1108.2	747.9	368.5	6.74	3.27
16.0	6.46	1.92	53.96	7.78	1170.1	799.2	369.7	7.11	3.43
18.0	7.82	3.17	53.56	8.22	1229.0	851.9	370.5	7.44	3.59

TABLE 7.10(A): COMPUTER SIMULATION FOR VARIOUS OPERATING CONDITIONS AT 20ML/S WATER FLOW RATE THROUGH THE EVAPORATOR.

EVAPORATOR WATER FLOW RATE = 30 ML/S

DISCHARGE PRESSURE P1=140 PSIA : CONDENSING TEMP.=37.20 DEGC									
TWe _i	TWe _o	TE	TW _{co}	MC(ML/S)	QC(W)	QE(W)	WC(W)	MF(G/S)	COP
8.0	2.27	-2.36	40.61	11.22	1107.8	721.4	332.6	6.93	3.56
10.0	3.81	-0.97	40.53	11.97	1184.7	779.2	335.6	7.42	3.77
12.0	5.30	0.37	40.51	12.66	1257.6	842.9	336.7	7.92	3.98
14.0	6.76	1.68	40.52	13.26	1323.7	909.7	337.6	8.41	4.19
16.0	8.19	2.97	40.58	13.79	1384.9	981.0	338.2	8.89	4.40
18.0	9.58	4.23	40.67	14.26	1440.9	1056.0	338.9	9.36	4.60

DISCHARGE PRESSURE P1=160 PSIA : CONDENSING TEMP.=43.31 DEGC									
TWe _i	TWe _o	TE	TW _{co}	MC(ML/S)	QC(W)	QE(W)	WC(W)	MF(G/S)	COP
8.0	2.50	-2.15	46.46	8.48	1017.8	693.0	349.9	6.42	3.19
10.0	4.03	-0.77	46.61	8.82	1070.0	751.3	350.4	6.86	3.31
12.0	5.36	0.58	46.69	9.30	1136.9	812.7	352.6	7.32	3.48
14.0	7.04	1.94	46.70	9.88	1215.2	873.7	353.2	7.77	3.70
16.0	8.59	3.28	46.64	10.59	1308.4	937.1	353.9	8.22	3.97
18.0	10.02	4.62	46.54	11.41	1413.1	1000.6	354.2	8.66	4.30

DISCHARGE PRESSURE P1=180 PSIA : CONDENSING TEMP.=48.90 DEGC									
TWe _i	TWe _o	TE	TW _{co}	MC(ML/S)	QC(W)	QE(W)	WC(W)	MF(G/S)	COP
8.0	2.84	-1.84	54.18	6.56	974.4	649.3	360.8	5.90	2.98
10.0	4.41	-0.44	54.31	7.00	1051.0	703.9	365.2	6.36	3.14
12.0	5.96	0.96	54.17	7.45	1123.0	759.8	366.1	6.78	3.31
14.0	7.51	2.36	53.85	7.91	1188.7	815.4	368.5	7.16	3.48
16.0	9.03	3.74	53.37	8.40	1252.7	874.1	369.0	7.52	3.66
18.0	10.54	5.09	52.75	8.93	1314.9	936.1	369.7	7.84	3.86

TABLE 7.10(B): COMPUTER SIMULATION FOR VARIOUS OPERATING CONDITIONS AT 30ML/S WATER FLOW RATE THROUGH THE EVAPORATOR.

EVAPORATOR WATER FLOW RATE = 40 ML/S

=====

DISCHARGE PRESSURE P1=140 PSIA : CONDENSING TEMP.=37.20 DEGC

TW _{ei}	TW _{eo}	TE	TW _{co}	MC(ML/S)	QC(W)	QE(W)	WC(W)	MF(G/S)	COP
8.0	3.48	-1.49	40.55	11.72	1159.1	759.0	329.4	7.22	3.70
10.0	5.10	-0.08	40.51	12.46	1236.5	823.4	332.2	7.74	3.92
12.0	6.69	1.31	40.52	13.09	1305.4	890.3	336.2	8.23	4.13
14.0	8.25	2.67	40.56	13.67	1370.1	962.8	338.0	8.73	4.35
16.0	9.77	3.99	40.65	14.19	1431.7	1043.0	338.7	9.24	4.57
18.0	11.27	5.30	40.77	14.63	1486.8	1126.0	338.9	9.73	4.79

=====

DISCHARGE PRESSURE P1=160 PSIA : CONDENSING TEMP.=43.31 DEGC

TW _{ei}	TW _{eo}	TE	TW _{co}	MC(ML/S)	QC(W)	QE(W)	WC(W)	MF(G/S)	COP
8.0	3.67	-1.32	46.56	8.67	1047.3	727.6	347.9	6.65	3.25
10.0	5.29	0.09	46.67	9.11	1111.1	790.3	351.0	7.12	3.42
12.0	6.89	1.48	46.70	9.71	1192.3	856.7	351.4	7.61	3.64
14.0	8.50	2.88	46.66	10.41	1285.0	922.0	352.9	8.08	3.91
16.0	10.11	4.29	46.57	11.20	1386.0	984.9	353.2	8.52	4.21
18.0	11.72	5.69	46.43	12.13	1503.3	1050.5	353.7	8.95	4.58

=====

DISCHARGE PRESSURE P1=180 PSIA : CONDENSING TEMP.=48.90 DEGC

TW _{ei}	TW _{eo}	TE	TW _{co}	MC(ML/S)	QC(W)	QE(W)	WC(W)	MF(G/S)	COP
8.0	3.96	-1.07	54.29	6.79	1015.3	677.8	361.7	6.11	3.06
10.0	5.63	0.38	54.26	7.24	1090.2	733.7	363.9	6.55	3.23
12.0	7.27	1.82	54.00	7.72	1162.0	792.3	366.5	6.92	3.41
14.0	8.91	3.24	53.56	8.22	1229.5	852.3	367.9	7.36	3.59
16.0	10.53	4.65	52.96	8.76	1294.9	915.6	369.2	7.71	3.79
18.0	12.13	6.05	52.25	9.32	1357.7	981.7	369.6	8.01	4.01

=====

TABLE 7.10(C): COMPUTER SIMULATION FOR VARIOUS OPERATING CONDITIONS
AT 40ML/S WATER FLOW RATE THROUGH THE EVAPORATOR

7.10(b) and 7.10(c), for water flow rates through the evaporator of 20ml/s, 30ml/s and 40ml/s respectively.

The minimum possible water flow rate through the evaporator with condenser output water temperature (TW_{co}) set at the values of 40.0°C, 45.5°C and 50.0°C is given in table 7.11. The condenser input water temperature (TW_{ci}) is 15°C and the evaporator output water temperature from the evaporator (TW_{eo}) is set at 1.0°C, so that the water would not freeze in the evaporator.

Figure 7.13 shows the relationship between the minimum water flow rate (\dot{m}_e) and the evaporator input water temperature (TW_{ei}). It can be seen from this figure and table 7.11 that as the evaporator input water temperature (TW_{ei}) decreases, then the minimum permissible water flow rate (\dot{m}_e) increases. As the condenser output water temperature (TW_{co}) increases, the water flow rate (\dot{m}_e) decreases slightly, since the system absorbs less heat in the evaporator as shown in table 7.11.

From the shape of the graphs it can be seen that the relationship between water flow rate (\dot{m}_e) and the evaporator input water temperature (TW_{ei}) is asymptotic; i.e. as TW_{ei} increases, \dot{m}_e tends to zero.

TW _{co} =40DEGC : P1=137PSIA						
TW _{ei} (C)	TW _{eo} (C)	TE(C)	ME(ML/S)	QE(WATT)	COP	COP(R)
5.0	1.1	-3.6	41.0	678.2	3.38	5.19
6.0	1.1	-3.5	33.0	683.2	3.41	5.22
7.0	1.0	-3.4	27.5	688.6	3.44	5.24
8.0	1.0	-3.3	23.5	692.4	3.46	5.26
9.0	1.1	-3.0	21.0	699.4	3.50	5.30
10.0	1.0	-3.0	18.5	700.5	3.52	5.30
11.0	1.1	-2.8	17.0	709.2	3.55	5.34
12.0	1.0	-2.7	15.5	712.4	3.57	5.36

TW _{co} =45.5DEGC: P1=158PSIA						
TW _{ei} (C)	TW _{eo} (C)	TE(C)	ME(ML/S)	QE(WATT)	COP	COP(R)
5.0	1.1	-3.6	38.5	635.6	3.13	4.78
6.0	1.0	-3.5	30.5	637.6	3.13	4.79
7.0	1.1	-3.3	26.0	645.78	3.14	4.82
8.0	1.0	-3.2	22.0	649.5	3.14	4.84
9.0	1.0	-3.1	19.5	657.9	3.16	4.87
10.0	1.0	-2.9	17.5	662.3	3.16	4.88
11.0	1.0	-2.8	16.0	669.3	3.17	4.91
12.0	1.0	-2.7	14.5	671.7	3.18	4.91

TW _{co} =50DEGC : P1=172PSIA						
TW _{ei} (C)	TW _{eo} (C)	TE(C)	ME(ML/S)	QE(WATT)	COP	COP(R)
5.0	1.1	-3.6	37.0	607.1	2.93	4.60
6.0	1.0	-3.5	29.0	610.1	2.94	4.58
7.0	1.1	-3.2	25.0	620.4	2.95	4.65
8.0	0.9	-3.2	21.0	622.6	2.96	4.64
9.0	1.1	-2.9	19.0	630.7	2.96	4.69
10.0	1.1	-2.8	17.0	636.3	2.97	4.71
11.0	1.1	-2.6	15.5	641.9	2.98	4.73
12.0	1.0	-2.6	14.0	643.5	2.99	4.74

TABLE 7.11: COMPUTER SIMULATION SHOWING THE MINIMUM WATER FLOW RATE THROUGH THE EVAPORATOR (ME) AT LOW INPUT WATER TEMPERATURES. WATER INPUT TO CONDENSER IS 15DEGC.

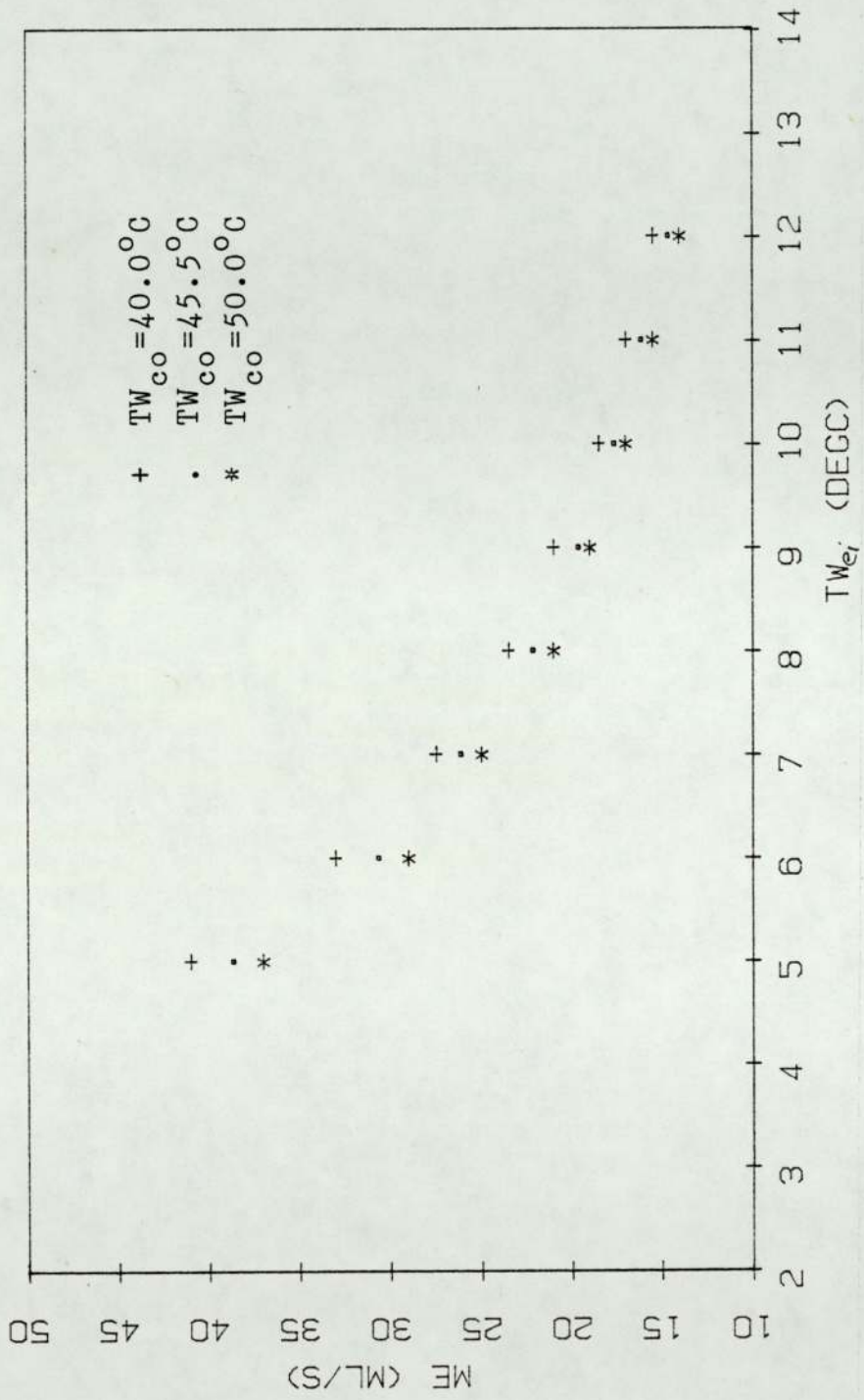


Figure 7.13: The minimum allowable water flow rate to avoid freezing in the evaporator. Output evaporator water temperature (TW_{e0}) set at 1.0°C .

The maximum possible water flow rate passing through the evaporator is shown in table 7.12. Since the maximum operating temperature of the expansion valve is 10°C (as suggested by the manufacturer [23]), the maximum permissible water flow rate passing through the evaporator can therefore be set to the flow rate which corresponds to the temperature after the valve, T_3 , of 10°C .

Figure 7.14 shows the relationship between the maximum water flow rate (\dot{m}_e) and the evaporator input water temperature (TW_{ei}). It can be seen in table 7.12 and figure 7.14 that as the evaporator input water temperature (TW_{ei}) increases, the maximum permissible water flow rate, likewise, increases. Table 7.12 also shows that even at high water flow rates (\dot{m}_e) for a certain value of condenser output water temperature (TW_{co}), the energy absorbed by the system reaches a limit, about 1375 Watt for 40.0°C condenser output water temperature, 1209 Watt for 45.5°C and 1110 Watt for 50°C . This is owing to the fact that the expansion valve controls the amount of refrigerant flow in the system by controlling the degree of superheat of the suction gas (which is set by the manufacturer 6°C above the evaporating temperature). In controlling the refrigerant flow, the expansion valve

TW _{co} =40DEGC : P1=137PSIA						
TW _{ei} (C)	T3(C)	TE(C)	ME(ML/S)	QE(WATT)	COP	COP(R)
6.0	10.1	8.6	130.0	1377.6	5.16	7.87
8.0	10.0	8.4	132.0	1372.3	5.17	7.86
10.0	9.9	8.3	135.0	1375.6	5.18	7.81
12.0	10.1	8.6	144.0	1377.2	5.18	7.93
14.0	10.1	8.5	159.0	1375.1	5.18	7.99
16.0	10.0	8.4	230.0	1372.7	5.18	8.05

TW _{co} =45.5DEGC: P1=158PSIA						
TW _{ei} (C)	T3(C)	TE(C)	ME(ML/S)	QE(WATT)	COP	COP(R)
6.0	10.1	8.5	130.0	1209.1	4.87	7.04
8.0	10.1	8.5	133.0	1209.1	4.88	7.05
10.0	10.0	8.4	136.5	1205.2	4.86	7.05
12.0	10.1	8.5	145.0	1209.1	4.88	7.10
14.0	10.1	8.5	162.5	1209.1	4.88	7.19
16.0	10.1	8.5	250.0	1209.1	4.88	7.25

TW _{co} =50DEGC : P1=172PSIA						
TW _{ei} (C)	T3(C)	TE(C)	ME(ML/S)	QE(WATT)	COP	COP(R)
6.0	10.0	8.4	130.0	1108.0	4.63	6.32
8.0	10.1	8.6	133.5	1111.3	4.64	6.34
10.0	10.1	8.5	137.5	1109.8	4.63	6.35
12.0	10.1	8.6	146.5	1115.5	4.64	6.40
14.0	10.1	8.5	165.0	1109.8	4.63	6.49
16.0	10.0	8.5	260.0	1108.5	4.63	6.60

TABLE 7.12: COMPUTER SIMULATION SHOWING THE MAXIMUM WATER FLOW RATE THROUGH THE EVAPORATOR (ME) AT VARIOUS INPUT WATER TEMPERATURES. WATER INPUT TO CONDENSER IS 15DEGC.

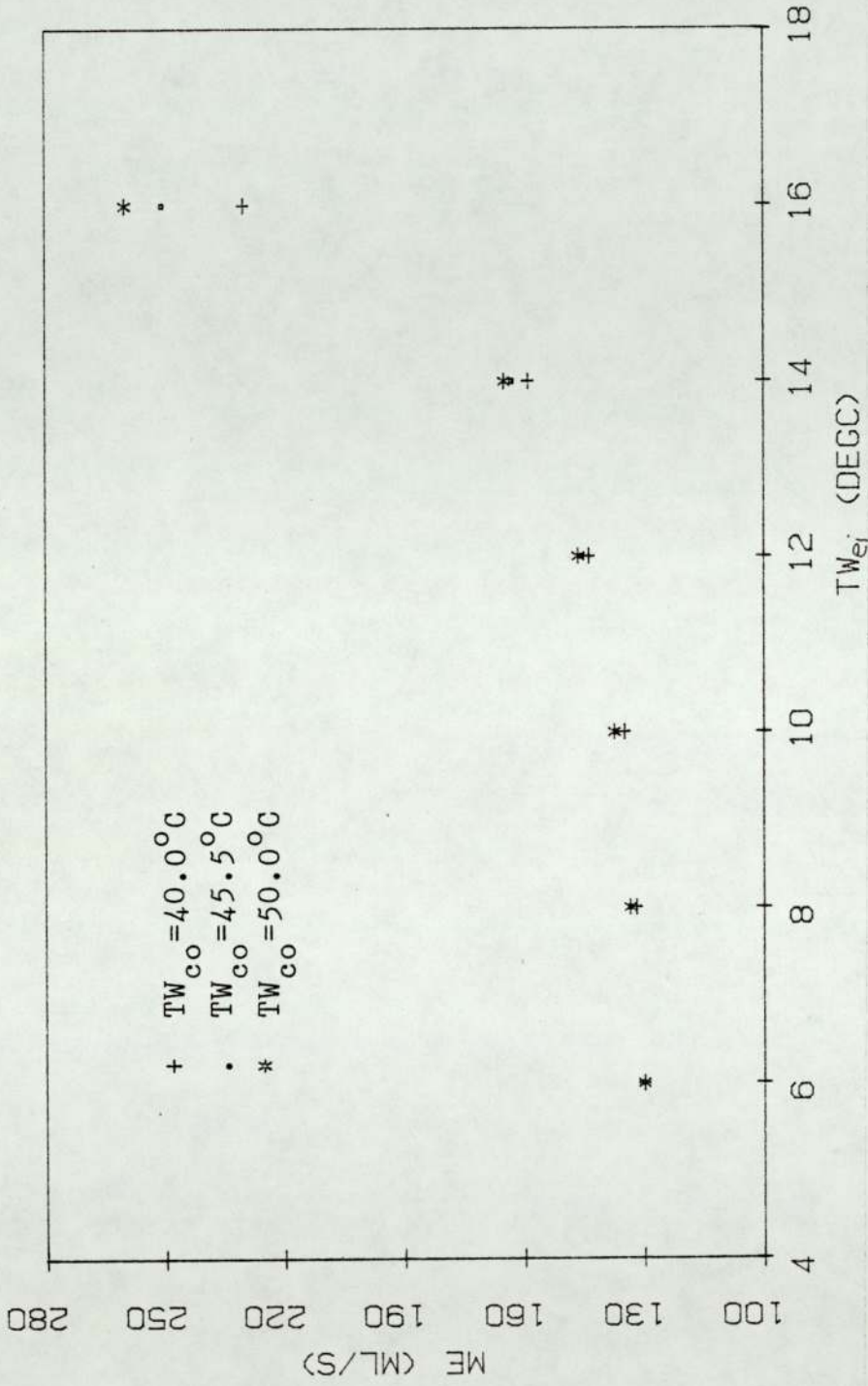


Figure 7.14: The maximum permissible water flow rate to limit the temperature after the expansion valve (T_3) to $10.0^{\circ}C$.

also controls the amount of heat absorbed in the evaporator as shown in table 7.12.

Another point that figure 7.12 and table 7.14 shows is that at low evaporator input water temperature ($T_{W_{ei}}$), a change in condenser output water temperature ($T_{W_{co}}$) does not alter the maximum water flow rate \dot{m}_e (which tends to 130ml/s). This effect may be due to the fixed length of the evaporator (5 meters) and the characteristics of the compressor (figure 3.3).

The COP and COP(R) in tables 7.11 and 7.12 are the calculated coefficients of performance of the heat pump. The COP is given by the heat delivered by the system divided by the electrical power to the compressor, and COP(R) is given by the enthalpy difference across the condenser divided by the enthalpy difference across the compression part of the cycle.

The following conclusions about the performance of the heat pump can be made from tables 7.9, 7.10(a), 7.10(b), 7.10(c), 7.11 and 7.12;

1. For each temperature increase of 2°C of evaporator input water temperature ($T_{W_{ei}}$), the evaporating temperature T_e increases too, but by less than 2°C .

2. The energy absorbed by the evaporator Q_e and delivered by the condenser Q_c also increases progressively, due to the compressor characteristics (figure 3.3), which show increased absorbing and delivering capacities as T_e increases.
3. The power required by the compressor is greatest when the evaporator water has the highest entry temperature, following the compressor characteristics (figure 3.3).
4. As a result of more work being done at high input water temperature $T_{W_{ei}}$, for a given value of discharge pressure P_1 , the refrigerant flow rate \dot{m}_F increases as $T_{W_{ei}}$ increases.
5. For a given value of $T_{W_{ei}}$, refrigerant mass flow rate \dot{m}_F decreases as discharge pressure P_1 increases. As mentioned before, this effect is due to the pressure leakage in the compressor
39,47 .
6. For a given value of discharge pressure P_1 , Condenser output water temperature ($T_{W_{co}}$) is constant. The setting of the water regulator to give a required output water temperature is done by the operator.

7. As evaporating temperature T_e increases, water flow rate through the evaporator (\dot{m}_e) increases and at the same time C.O.P. increases.
8. For a given value of TW_{ei} and \dot{m}_e , \dot{m}_c decreases as the condenser output water temperature (TW_{co}) increases and as a result C.O.P. decreases.
9. For given value of TW_{ei} and P_1 , \dot{m}_c increases as \dot{m}_e increases, then C.O.P. increases as \dot{m}_c increases.
10. Finally, tables 7.10(a), 7.10(b) and 7.10(c) show that the best performance of the heat pump system (at constant condenser input water temperature (TW_{ci})) is with the highest temperature of water entering the evaporator (TW_{ei}) and the highest water flow rate through the evaporator, since the evaporating capacity and condensing capacity are then highest. The maximum and minimum water flow rate passing through the evaporator are shown in tables 7.11 and 7.12 and figures 7.13 and 7.14.

7.10 General Conclusions.

These investigations on a heat pump system have led to considerations and conclusions of which some of the most important are listed below.

1. The heat pump investigated in this project is the water-to-water heat pump system, for which, from the characteristics of the compressor given by the manufacturer [20], at evaporating temperatures (T_e) below 10°C , the heat delivered by the system will not exceed 1.6kiloWatts at condensing temperature (T_c) of 35°C (figure 3.3). The power to the compressor does not exceed 380 Watts, with a C.O.P. (on the basis of compressor only) of 5.4. This characteristic shows that this system is suitable for domestic use rather than heavy applications.
2. Heat recovery can be obtained from very low water temperature as long as the water is not freezing in the evaporator. To avoid freezing, the water flow rate should be sufficiently great. Results from the analysis show that at very low water temperature, the performance of the system decreases, eventhough the water flow rate could be made faster - table 7.10(a),7.10(b) and 7.10(c). The major

cause of this effect is not only the low water temperature, but the refrigerant capacity to absorb heat at this low temperature and deliver it to higher one.

3. On the heat delivery side of the system, the outlet water temperature of the condenser could be set by using the water regulator. At a given value of evaporating temperature T_e (fixed water flow rate and inlet water temperature to the evaporator), the performance of the heat pump decreases as the outlet water temperature ($T_{W_{CO}}$) increases. The performance can be increased by increasing the water flow rate and the inlet water temperature of the evaporator, but once again the condenser capacity limits the amount of the heat being delivered by the condenser.
4. The water regulator is not only important because it can be used to set the output water temperature of the condenser ($T_{W_{CO}}$) required by the operator, but at the same time controls the water flow rate through the condenser such that the discharge pressure P_1 remains constant. This will ensure that the discharge pressure will not exceed the limits (the pressure corresponding to 60°C condensing temperature as suggested by the manufacturer) where the compressor can perform best during water

heating in a tank.

5. The range of operation of the thermostatic expansion valve also affects the amount of heat recovered from evaporator. The operation range of the valve is within -40° to $+10^{\circ}\text{C}$ of the evaporating temperature. As the heat absorbed by the evaporator increases, the evaporating temperature T_e increases. T_e cannot exceed 10°C . This will limit the evaporating capacity of the device. Together with the characteristic of the compressor, if it is desired to absorb more heat from the evaporator and deliver more heat from the condenser, both of these components should be replaced by those with a higher capacity.

6. If the heat output is going to be stored in a tank, a special tank should be designed to match the heat pump. Ordinary hot water tanks which suit the electric element heater should not be used. Because, as recycled hot water enters the the condenser, the performance of the heat pump will be reduced. Thermal stratification in the water tank should be maintained, such that the water enters the condenser at low temperature. Several alternative methods could be used to ensure the device will be operated at higher

performance.

- a. By using a tall cylinder as the tank, such that a lot of hot water is readily available when the performance starts to decrease.
- b. By making several partitions in the tank, so that the thermal stratification in the tank will be maintained; which allows only cold water to enter the condenser.
- c. By fixing a thermostat at the outlet water to the condenser. The thermostat will switch off the device automatically when the performance drops to an undesired level.
- d. The tank should be made of an insulator such as fibre glass or polyvinyl chloride (PVC). This is to ensure that the heat will not be conducted through the wall of the tank. The heat conducted through the wall of the tank, such as copper, would alter the thermal stratification in the tank and would speed up the entrance of hot water to the condenser.

7. The heat pump system can only be used to recover heat from water flow through the evaporator. The water could come either from main supply or from heat storage. If the heat source comes from mains water supply, care should be taken to ensure that the water will not be frozen in the system. If the heat source comes from heat storage (water as the medium), warm water is preferable since it gives high performance as shown in table 7.10(a), 7.10(b) and 7.10(c). The heat storage itself should have the special feature of separating the warm and cold water so that efficient performance of the system can be maintained.

APPENDIX I.

A. Operating subroutine for PCI1001.

```
100 REM* OPERATING SUBROUTINE PCI1001 *
110 REM A IS DEVICE NUMBER B IS CHANNEL NUMBER
120 OPEN1,A,B
130 GET£1,J$,K$
140 K=ASC(K$)-224
150 IF K<0THEN=(K+32)*-1
160 IF K>=0THEN=K
170 D=D*256
180 IF J$=""THEN J=0:GOTO200
190 J=ASC(J$)
200 IF K<0THEN J=J*-1
210 A(B,L)=(J+D)/4000
220 CLOSE1
230 RETURN
READY.
```

B. Operating subroutine for PCI1002.

```

100 REM*****
110 REM*  PCI 1002 SUBROUTINE  *
120 REM*****
130 DIMOP(16)
140 A(0)=0:A(1)=2.5661297E-2:A(2)=-6.1954869E-7
150 A(3)=2.2181644E-11:A(4)=-3.55009E-16:CK=40.25
160 DN=9
170 REM***CHECK PCI1002 RANGE***
180 REM
190 CH=0:GOSUB 10000
200 IFOP(0)<800THENR=100
210 IFOP(0)>=800ANDOP(0)<2000THENR=30
220 IFOP(0)>=2000THENR=10
230 REM
240 REM***SCAN CH1 TO 15***
250 REM
260 PRINT""
270 PRINT"RANGE"R"MV"
280 FORCH=1TO15:GOSUB10000:NEXTCH
290 REM
300 REM***PRINT RESULTS***
310 FORCH=1TO2
320 PRINT"CHANNEL NO"CH"=                "OP(CH)"BITS"
330 NEXTCH
340 FORCH=4TO15
350 GOSUB11000
360 PRINT"CHANNEL NO"CH"=                "OP(CH)"DEG C"
370 NEXTCH
380 GOTO270
10000 REM
10010 REM*** OPERATING SUBROUTINE***
10020 REM
10030 OPEN1, DN, CH
10040 GET£1, J£, K£
10050 K=ASC(K£)-224
10060 IFK<0THEN£=(K+32)*-1
10070 IFK>=0THEN£=K
10080 D=D*256
10090 IFJ£=""THENJ=0:GOTO10110
10100 J=ASC(J£)
10110 IFK<0THENJ=J*-1
10120 OP(CH)=J+D
10130 CLOSE1
10140 RETURN
11000 REM
11010 REM***BITS TO DEGC SUBROUTINE***
11020 REM
11030 CJ=CK*(OP(3)*R/400):REM GIVES CJC IN MICROVOLTS
11040 V=OP(CH)*R/4:REM GIVES O/P IN MICROVOLTS
11050 V=V+CJ:REM ADD CJC VOLTAGE
11060 T=A(4)
11070 FORI=3TO0STEP-1
11080 T=T*V+A(I)
11090 NEXTI
11100 OP(CH)=(INT(T*100+.5))/100
11110 RETURN

```

READY.

APPENDIX II.

The computer program for sampling experimental data.

```
10 REM*****
20 REM* THIS IS SAMPLING PROGRAM *
30 REM* AVERAGING DATA FROM INTERFACE *
40 REM*****
50 PRINT"TO STORE DATA INTO FLOPPY DISK"
60 PRINT"MODIFY FILE IN LINE 120"
70 PRINT"THEN RUN100"
80 LIST 120
90 STOP
100 PRINT"
120 Z$="@1:TEST1,S,W"
130 INPUT"HOW MANY SAMPLES?";N
140 INPUT"NO OF AVERAGE READINGS";M
150 INPUT"TIME BETWEEN SAMPLES SECS";DZ
160 DIMA(16,M):DIMOP(32,M):DIMAV(32):DIMCV(32)
170 OPEN15,8,15
180 OPEN6,8,2,Z$
190 TIME$="000000"
200 PRINT"          WAIT!!!!"
210 PRINT"          DATA ARE BEING TAKEN "
220 PRINT"          AND AVERAGED FOR";M;"TIMES"
250 FORSP=1TON:PRINT""
255 FORL=1TOM
260 DN=9:REM DEVICE NO FOR THERMOCOUPLE INTERFACE
270 IF DN<4ORDN>14 THEN 260
280 FOR CH=0T015
290 GOSUB 1000:REM GET DATA FROM INTERFACE
300 NEXTCH
340 A=10:REM DEVICE NO FOR PRESSURE AND FLOW RATE INTERFACE
350 IF A<4ORA>14 THEN 340
360 FORB=1T015
370 GOSUB 2000:REM GET DATA FROM INTERFACE
375 NEXTB
380 NEXTL
385 TM$=TIME$
390 FORL=1TOM:FORCH=4T015
400 GOSUB1500:REM BITS TO DEGC CONVERSION
410 NEXTCH:NEXTL
420 FORCH=4T015
425 SUM=0
430 FORL=1TOM
435 SUM=SUM+OP(CH,L)
440 NEXTL
445 AV(CH)=SUM/M
448 AV(CH)=INT(AV(CH)*100+.5)/100
450 PRINT6,AV(CH);CHR$(13);
```

```

455 REM TEST DISKETTE STATUS
460 INPUT#15,A$,B$,C$,D$
475 IF VAL(A$)<>0THEN PRINT A$,B$,C$,D$:STOP
480 NEXTCH
485 FORB=1TO15
490 MS=0
495 FORL=1TOM
500 MS=MS+A(B,L)
505 NEXTL
510 CV(B)=MS/M
512 PRINT#6,CV(B);CHR$(13);
515 REM TEST DISKETTE STATUS
520 INPUT#15,A$,B$,C$,D$
525 IF VAL(A$)<>0THEN PRINT A$,B$,C$,D$:STOP
530 NEXTB
545 GOSUB 3000:REM TEMPERTURE CONVERSION
548 GOSUB 3500:REM TANK TEMP PROFILE
550 GOSUB 4000:REM PRESSURE CONVERSION
555 GOSUB 5000:REM CONDENSER, EVAPORATOR AND COMPRESSOR CONVERSIONS
565 GOSUB 8000:REM CALCULATION OF HEAT BALANCE AND C.O.P.
570 GOSUB9000:REM DISPLAY
582 PRINT#6,TM$;CHR$(13);
584 REM TEST DISKETTE STATUS
586 INPUT#15,A$,B$,C$,D$
588 IF VAL(A$)<>0THEN PRINT A$,B$,C$,D$:STOP
590 REM***** N GIVES TIME DELAY BETWEEN SAMPLE*****
600 REM*****      1000=ABOUT 1.2 SECONDS *****
610 FORN=1TO800#DZ:NEXTN
620 NEXTSP
630 CLOSE6:CLOSE15
640 END
1000 REM* OPERATING SUBROUTINE PCI1002 *
1010 REM DN IS DEVICE NO CH IS CHANNEL NO
1015 OPEN1,DN,CH
1020 GET#1,J$,K$
1030 K=ASC(K$)-224
1040 IFK<0THEND=(K+32)*-1
1050 IFK>0THEND=K
1060 D=D*256
1070 IFJ$=""THENJ=0:GOTO1090
1080 J=ASC(J$)
1090 IFK<0THENJ=J*-1
1100 OP(CH,L)=J+D
1110 CLOSE1
1120 RETURN
1500 REM* BITS TO DEGC SUBROUTINE *
1510 G(0)=0:G(1)=2.5661297E-2:G(2)=-6.1954869E-7
1520 G(3)=2.2181644E-11:G(4)=-3.55009E-16:CK=40.25
1530 CJ=CK*(OP(3,L)/40):REM GIVES CJC IN MICROVOLTS
1540 V=OP(CH,L)*2.5:REM GIVES O/P IN MICROVOLTS
1550 V=V+CJ:REM ADD CJC VOLTAGE
1560 T=G(4)
1570 FOR I=3TO0 STEP -1
1580 T=T*V+G(I)
1590 NEXTI
1600 OP(CH,L)=T
1610 RETURN

```

```

2000 REM* OPERATING SUBROUTINE PCI1001 *
2010 REM A IS DEVICE NUMBER B IS CHANNEL NUMBER
2020 OPEN1,A,B
2030 GETE1,J$,K$
2040 K=ASC(K$)-224
2050 IF K<0THEND=(K+32)*-1
2060 IF K>=0THEND=K
2070 D=D*256
2080 IF J$=""THEN J=0:GOTO2100
2090 J=ASC(J$)
2100 IF K<0THEN J=J*-1
2110 A(B,L)=(J+D)/4000
2130 CLOSE1
2140 RETURN
3000 REM*****
3003 REM* TEMPERATURE CONVERSION *
3005 REM*****
3008 AV4$=LEFT$(STR$(AV(4))+"      ",6)
3012 AV5$=LEFT$(STR$(AV(5))+"      ",6)
3018 AV6$=LEFT$(STR$(AV(6))+"      ",6)
3025 AV7$=LEFT$(STR$(AV(7))+"      ",6)
3035 AV8$=LEFT$(STR$(AV(8))+"      ",6)
3042 AH$=LEFT$(STR$(AV(15))+"     ",6)
3045 AA$=LEFT$(STR$(AV(9))+"      ",6)
3055 AB$=LEFT$(STR$(AV(10))+"     ",6)
3065 AC$=LEFT$(STR$(AV(11))+"     ",6)
3075 AD$=LEFT$(STR$(AV(12))+"     ",6)
3085 AE$=LEFT$(STR$(AV(13))+"     ",6)
3095 AF$=LEFT$(STR$(AV(14))+"     ",6)
3120 RETURN
3500 REM*****
3510 REM* TANK TEMPERATURE PROFILE *
3520 REM*****
3530 TP=(9.673274E-03+25.6670029*(CV(8)*10)-.541499612*(CV(8)*10)^2)
3540 TQ=(9.673274E-03+25.6670029*(CV(9)*10)-.541499612*(CV(9)*10)^2)
3550 TR=(9.673274E-03+25.6670029*(CV(10)*10)-.541499612*(CV(10)*10)^2)
3560 TS=(9.673274E-03+25.6670029*(CV(11)*10)-.541499612*(CV(11)*10)^2)
3570 TT=(9.673274E-03+25.6670029*(CV(12)*10)-.541499612*(CV(12)*10)^2)
3580 TU=(9.673274E-03+25.6670029*(CV(13)*10)-.541499612*(CV(13)*10)^2)
3590 TV=(9.673274E-03+25.6670029*(CV(14)*10)-.541499612*(CV(14)*10)^2)
3595 TW=(9.673274E-03+25.6670029*(CV(15)*10)-.541499612*(CV(15)*10)^2)
3600 T1$=LEFT$(STR$(TP)+"      ",7)
3610 T2$=LEFT$(STR$(TQ)+"      ",7)
3620 T3$=LEFT$(STR$(TR)+"      ",7)
3630 T4$=LEFT$(STR$(TS)+"      ",7)
3640 T5$=LEFT$(STR$(TT)+"      ",7)
3650 T6$=LEFT$(STR$(TU)+"      ",7)
3660 T7$=LEFT$(STR$(TV)+"      ",7)
3670 T8$=LEFT$(STR$(TW)+"      ",7)
3700 RETURN

```

```

4000 REM*****
4010 REM* PRESSURE CONVERSION *
4020 REM*****
4030 P1=(CV(4)*996.8102)/5+14.7
4035 PA=P1*.06894757
4040 P1=(INT(P1*100+.5))/100
4045 P1$=LEFT$(STR$(P1)+"      ",7)
4048 PA$=LEFT$(STR$(PA)+"      ",7)
4060 P2=(CV(5)*995.024876)/5+14.7
4065 PB=P2*.06894757
4070 P2=(INT(P2*100+.5))/100
4075 P2$=LEFT$(STR$(P2)+"      ",7)
4080 PB$=LEFT$(STR$(PB)+"      ",7)
4090 P3=(CV(6)*989.6580)/5+14.7
4095 PC=P3*.06894757
4100 P3=(INT(P3*100+.5))/100
4105 P3$=LEFT$(STR$(P3)+"      ",7)
4110 PC$=LEFT$(STR$(PC)+"      ",7)
4120 P4=(CV(7)*998.0538)/5+14.7
4125 PD=P4*.06894757
4130 P4=(INT(P4*100+.5))/100
4135 P4$=LEFT$(STR$(P4)+"      ",7)
4140 PD$=LEFT$(STR$(PD)+"      ",7)
4170 RETURN
5000 REM*****
5010 REM* CONDENSER EVAPORATOR AND *
5020 REM* COMPRESSOR CONVERSIONS *
5030 REM*****
5040 FC=.200838053+24.5824341*CV(1)
5050 FE=.24119404+51.7427683*CV(2)
5060 EC=12.6142278+495.333883*CV(3)
5070 FC=FC/1000
5080 FE=FE/1000
5090 RETURN
8000 REM*****
8005 REM* CALCULATION OF ENERGY *
8010 REM* AND C.O.P. *
8020 REM*****
8030 SW=4185.5 :REM SPECIFIC HEAT OF WATER
8040 EV=FE*SW*(AV(9)-AV(10))
8050 CD=FC*SW*(AV(12)-AV(11))
8055 YC=FC*SW*(AV(14)-AV(13))
8058 EK=CD+YC
8060 EM=EV+EC
8062 EB=EM-EK
8065 FE=(INT(FE*100000+.5))/100000
8068 FC=(INT(FC*100000+.5))/100000
8070 EC=(INT(EC*1000+.5))/1000
8072 EV=(INT(EV*1000+.5))/1000
8075 CD=(INT(CD*1000+.5))/1000
8078 YC=(INT(YC*1000+.5))/1000
8080 EB=(INT(EB*1000+.5))/1000
8090 EM=(INT(EM*1000+.5))/1000
8095 EK=(INT(EK*1000+.5))/1000
8100 COP=EK/EC

```

```

8110 COP=(INT(COP*1000+.5))/1000
8111 FE$=LEFT$(STR$(FE)+"          ",9)
8113 FC$=LEFT$(STR$(FC)+"          ",9)
8118 EV$=LEFT$(STR$(EV)+"          ",7)
8120 YC$=LEFT$(STR$(YC)+"          ",7)
8125 CD$=LEFT$(STR$(CD)+"          ",7)
8140 EC$=LEFT$(STR$(EC)+"          ",7)
8145 EM$=LEFT$(STR$(EM)+"          ",7)
8165 EK$=LEFT$(STR$(EK)+"          ",7)
8168 EB$=LEFT$(STR$(EB)+"          ",7)
8180 CO$=LEFT$(STR$(COP)+"          ",7)
8220 RETURN
9000 REM*****
9010 REM*  DISPLAY *
9020 REM*****
9030 PRINT"READING NO: ";SP;" ";Z$
9050 PRINT"TEMP. AFTER COMP.      ";AV4$;"DEGC"
9060 PRINT"TEMP. AFTER COND.      ";AV5$;"DEGC"
9070 PRINT"TEMP. BEFORE VALVE     ";AV6$;"DEGC"
9080 PRINT"TEMP. AFTER VALVE      ";AV7$;"DEGC"
9090 PRINT"TEMP. BEFORE COMP.     ";AV8$;"DEGC"
9100 PRINT"TEMP. BEF VALVE (O/S): ";AH$;"DEGC"
9110 PRINT"EVAP TEMP.: ";AA$;AB$;" DEGC"
9120 PRINT"COND TEMP.: ";AC$;AD$;" DEGC"
9130 PRINT"COOL TEMP.: ";AE$;AF$;" DEGC"
9140 PRINT"TANK TEMP.: ";T1$;T2$;T3$;T4$;T5$;T6$;T7$;T8$
9150 PRINT"PRESS: ";P1$;P2$;P3$;P4$;"PSIA"
9160 PRINT"      ";PA$;PB$;PC$;PD$;"*E5PA"
9170 PRINT"EVAP FLOW RATE (KG/S): ";FE$
9180 PRINT"COND FLOW RATE (KG/S): ";FC$
9190 PRINT"ENERGY' EVAP  COND  COMP  COOL"
9200 PRINT"  J/S  ";EV$;CD$;EC$;YC$
9210 PRINT"ENERGY INPUT  ";EM$;" ENERGY BALANCE"
9220 PRINT"ENERGY OUTPUT: ";EK$;" ";EB$
9230 PRINT"  ** COP **:";CO$
9240 PRINT"          READING TIME: ";TM$
9250 RETURN
READY.

```

APPENDIX III.

The mathematical equations of the thermodynamic state of the refrigerant R12 used in the computer model based on the data given by ASHRAE [43].

A.

EQUATION FOR CURVES FITTING

=====

POLYNOMIAL FUNCTION FOR CONDENSING PRESSURE PC
VERSUS CONDENSING TEMPERATURE TC

$$PC=12918.0693 - 99.9773178*TC + 0.197324894*TC^2$$

=====

TC (DEGK)	PC (KPA)	PC (FIT)
290	518.7	519.6
292	549.24	549.4
294	581.11	580.7
296	614.31	613.6
298	648.9	648.0
300	684.91	684.1
302	722.36	721.7
304	761.31	760.9
306	801.77	801.7
308	843.8	844.0
310	887.42	888.0
315	1003.7	1004.0
320	1130.8	1131.0
325	1269.3	1267.0

=====

SUM OF SQUARE ERROR=7.44462256

B.

EQUATION FOR CURVES FITTING

=====

POLYNOMIAL FUNCTION FOR EVAPORATING PRESSURE PE
VERSUS EVAPORATING TEMPERATURE TE

$$PE=7084.88281 - 59.8153687*TE + 0.128165364*TE^2$$

=====

TE (DEGK)	PE (KPA)	PE (FIT)
264	226.02	226.2
266	242.48	242.4
268	259.83	259.7
270	278.11	277.9
272	297.35	397.2
274	317.57	317.6
276	338.81	338.9
278	361.1	361.3
280	384.48	384.7
282	408.96	409.1
284	434.59	434.6
286	461.4	461.1

=====

SUM OF SQUARE ERROR=0.369984698

C.

EQUATION FOR CURVES FITTING

=====

POLYNOMIAL FUNCTION FOR ENTHALPY AT

VAPOUR-GAS HG(KJ/KG) VERSUS TEMPERATURE T(DEGK)

$$HG=364.53479 + 1.06271553*T - 1.12367701E-03*T^2$$

=====

T (DEGK)	HG (KJ/KG)	HG (FIT)
264	566.82	566.7
266	567.73	567.7
268	568.62	568.6
270	569.52	569.5
272	570.41	570.4
274	571.29	571.3
276	572.17	572.2
278	573.05	573.1
280	573.91	574.0
282	574.78	574.8
284	575.63	575.7
286	576.48	576.5
288	577.33	577.3
290	578.16	578.2
292	578.99	579.0
294	579.81	579.8
296	580.62	580.6
298	581.42	581.4
300	582.21	582.2
302	582.99	582.9
304	583.76	583.7
306	584.53	584.5
308	585.27	585.2
310	586.01	585.9
315	587.79	587.7
320	589.49	589.5
325	591.07	591.2

=====

SUM OF SQUARE ERROR=0.0919300873

D.

EQUATION FOR CURVES FITTING

=====

POLYNOMIAL FUNCTION FOR ENTHALPY AT
LIQUID-VAPOUR HL(KJ/KG) VERSUS TEMPERATURE T(DEGK)
HL=251.332153 + 0.288181782T + 1.18516479E-03*T^2

=====

T (DEGK)	HL (KJ/KG)	HL (FIT)
264	409.97	410.0
266	411.82	411.8
268	413.67	413.6
270	415.53	4155.5
272	417.40	417.4
274	419.27	419.2
276	421.16	421.1
278	423.05	423.0
280	424.95	424.9
282	426.86	426.8
284	428.77	428.7
286	430.7	430.6
288	432.63	432.6
290	434.58	434.5
292	436.53	436.5
294	438.49	438.5
296	440.46	440.4
298	442.44	442.4
300	444.43	444.4
302	446.43	446.4
304	448.44	448.4
306	450.46	450.4
308	452.49	452.5
310	454.53	454.5
315	459.68	459.7
320	464.91	464.9
325	470.21	470.1

=====

SUM OF SQUARE ERROR=0.010847941

E.

EQUATION FOR CURVES FITTING

=====

POLYNOMIAL FUNCTION FOR TEMPERATURE T(DEGK)
VERSUS ENTHALPY AT LIQUID-VAPOUR HL(KJ/KG)

$$T = -389.623047 + 2.10105419 * HL - 1.2361249E-03 * HL^2$$

=====

HL(KJ/KG)	T(DEGK)	T(FIT)
409.97	264	263.9
411.82	266	265.9
413.67	268	267.9
415.53	270	269.9
417.40	272	272.0
419.27	274	273.9
421.16	276	276.0
423.05	278	278.0
424.95	280	288.0
428.77	284	283.9
430.70	286	286.0
432.63	288	287.9
434.58	290	290.0
436.53	292	292.0
438.49	294	293.9
440.46	296	295.9
442.44	298	297.9
444.43	300	299.9
446.43	302	301.9
448.44	304	303.9
450.46	306	305.9
452.49	308	307.9
454.53	310	309.9
459.68	315	314.9
464.91	320	320.0
470.21	325	325.0
325	591.07	591.2

=====

SUM OF SQUARE ERROR=1.64811071E-03

F.

FITTING EQUATION FOR SUPERHEATED GAS OF R12

=====
T=TEMPERATURE IN DEGK
P=PRESSURE IN KPA
H=ENTHALPY IN KJ/KG
H=C1+C2*T+C3*T^2+C4*P+C5*P^2+C6*T*P+
C7*P*T^2+C8*T*P^2+C9*(T*P)^2

WHERE C1= 455.537165
C2= 0.318314823
C3= 4.56245979
C4=-0.182523644
C5= 3.34365535E-05
C6= 9.81240749E-04
C7=-1.37498424-06
C8=-2.64056E-07
C9= 4.68738882E-10

=====

T	P	H	H(FIT)
290	200	583.35	583.75
300	200	589.58	589.98
310	200	595.86	596.26
300	400	586.78	587.58
310	400	593.33	594.18
320	400	599.90	600.78
310	600	590.56	591.84
320	600	597.42	598.74
330	600	604.24	605.60
320	800	594.70	596.46
330	800	601.81	603.62
340	800	608.86	610.72
330	1000	599.16	601.43
340	1000	606.50	608.84
350	1000	613.75	616.16

=====

G.

FITTING EQUATION FOR SUPERHEATED GAS OF R12

S=ENTROPY IN KJ/(KG.DEGK)

H=ENTHALPY IN KJ/KG

P=PRESSURE IN KPA

$S=C1+C2*H+C3*H^2+C4*P+C5*P^2+C6*H*P+$

$C7*P*H^2+C8*H*P^2+C9*(H*P)^2$

WHERE C1=-2.955053

C2= 0.0233352263

C3=-1.70238825E-05

C4= 8.82030528E-03

C5=-5.40515486E-06

C6=-3.08860253E-05

C7= 2.6222248E-08

C8= 1.88719701E-08

C9=-1.61023786E-11

H	P	S	S(FIT)
583.35	200	4.8146	4.8146
589.58	200	4.8358	4.8354
595.86	200	4.8564	4.8554
593.33	400	4.8029	4.8074
599.90	400	4.8237	4.8280
606.50	400	4.8440	4.8479
597.42	600	4.7903	4.7903
604.24	600	4.8113	4.8113
611.06	600	4.8316	4.8317
601.81	800	4.7861	4.7835
608.86	800	4.8072	4.8048
615.88	800	4.8276	4.8253
606.50	1000	4.7868	4.7868
613.75	1000	4.8078	4.8078
620.95	1000	4.8281	4.8279

H.

FITTING EQUATION FOR SUPERHEATED GAS OF R12

H=ENTHALPY IN KJ/KG

S=ENTROPY IN KJ/(KG.DEGK)

P=PRESSURE IN KPA

$H=C1+C2*S+C3*S^2+C4*P+C5*P^2+C6*S*P+$

$C7*P*S^2+C8*S*P^2+C9*(S*P)^2$

WHERE C1= 7362.1491

C2=-3090.77378

C3= 348.868344

C4=-11.081762

C5= 8.8810614E-03

C6= 4.1265128

C7=-0.45565258

C8=-3.66476294E-03

C9= 3.76531906E-04

S	P	H	H(FIT)
4.8146	200	583.35	583.35
4.8358	200	589.58	589.66
4.8564	200	595.86	596.03
4.8029	400	593.33	592.09
4.8237	400	599.90	598.68
4.8440	400	606.50	605.09
4.7903	600	597.42	597.42
4.8113	600	604.24	604.22
4.8316	600	611.06	610.97
4.7861	800	601.81	602.50
4.8072	800	608.86	608.86
4.8276	800	615.88	616.22
4.7868	1000	606.50	606.50
4.8078	1000	613.75	613.75
4.8281	1000	620.98	620.98

APPENDIX IV.

The computer program for the water-to-water heat pump model.

```
100 OPEN3,4
102 PRINT""
105 INPUT"EVAP WATER TEMP IN DEGC";T5
110 INPUT"COND WATER TEMP IN DEGC";T7
125 INPUT"EVAP WATER F-R IN KG/S";ME
130 INPUT"DISCHARGE PRESS IN PSIA";P1
132 P1=P1*101.325/14.695;REM IN KPA
135 INPUT"GUESS VALUE OF TE DEGC";TU
140 TE=TU
145 PRINT""
150 PRINT""
160 GOSUB1000:REM PRESSURES CALCULATION
170 GOSUB2000:REM HEAT FOR EVAP COND & COMP.
180 GOSUB3000:REM EVAP TEMP COMPUTE
190 TE=INT(TE*100+.05)/100
200 TA=INT(TA*100+.05)/100
210 PRINT"TE INPUT =" ;TE
220 PRINT"TE COMPUTE=" ;TA
230 DE=ABS(TE-TA)
240 IF DE<.05 GOTO260
250 TE=(TE+TA)/2;GOTO150
260 GOSUB4000:REM SUPERHEAT TEMP FROM EXP.
265 GOSUB5000:REM COND WATER FLOWRATE
270 GOSUB6000:REM POLYTROPIC INDEX
280 GOSUB7000:REM CALC T8 & T9
400 GOSUB8000:REM ENTHALPY
410 GOSUB9000:REM WORK & R-12 FLOWRATE
415 GOSUB9500:REM HEAT EXCHANGER EFF.
420 QOP=QC+QY:REM ENERGY OUTPUT
430 COP=QOP/WC:REM COP COMPRESSOR ONLY
440 CW=QOP/(WC+60):REM COP INC WATER PUMP
450 CT=(HD-HC)/(HD-HS):REM COP THEORY
460 CC=(T9+273.15)/(T9-T7):REM COP CARNOT
470 GOSUB10000:REM DISPLAY & PRINT
480 QC$=LEFT$(STR$(QC)+"      ",7)
540 CLOSE3
550 END
1000 REM*****
1005 REM* PRESSURES CALCULATION *
1010 REM*****
1020 T3=2.4697091+.897969093*TE:REM TEMP AFTER EXP VALVE
1030 P2=-210.292269+1.07831985*P1:REM PRESS AFTER COND
1040 PC=(P1+P2)/2
1050 TC=260.245186+.0671422787*PC-1.26298469E-5*PC^2
1060 TC=TC-273.15:REM IN DEGC
1140 C1=7084.88281;C2=-59.8153687;C3=.128165364
1150 P3=C1+C2*(T3+273.15)+C3*(T3+273.15)^2:REM IN KPA
```



```

1160 C1=22.8669653:C2=.215921474:C3=6.82192194E-3
1170 PT=C1+C2*T3+C3*T3^2:REM PRESS DROP IN EVAPORATOR
1180 P4=P3-PT:REM IN KPA
1190 PE=(P3+P4)/2:REM EVAP PRESS IN KPA
1200 RETURN
2000 REM*****
2010 REM* ENERGY FOR CONDENSER EVAPORATOR & COMPRESSOR *
2020 REM*****
2030 C1=1.28579192:C2=8.37534282E-3:C3=-2.11111977E-4
2040 C1=2102.6268:C2=1982.30729:C3=-356.068474
2050 C4=-1.43543662:C5=3.93178434E-4:C6=-3.51035944
2060 C7=.650678261:C8=1.58106254E-3:C9=-2.93626026E-4
2070 QA=C1+C2*T3+C3*T3^2+C4*P1+C5*P1^2+C6*T3*P1
2080 QB=C7*P1*(T3^2)+C8*T3*(P1^2)+C9*(T3*P1)^2
2090 QC=QA+QB:REM ENERGY FOR CONDENSER PRACTICAL
2100 C1=179.327841:C2=37.7643067:C3=-6.9175162
2110 C4=.237737432:C5=-7.65406344E-5:C6=-.0798235716
2120 C7=.0130164612:C8=4.36857631E-5:C9=-6.43607881E-6
2130 B1=C1+C2*T3+C3*T3^2+C4*P1+C5*P1^2+C6*T3*P1
2140 B2=C7*P1*(T3^2)+C8*T3*(P1^2)+C9*(T3*P1)^2
2150 WC=B1+B2:REM POWER FOR COMPRESSOR PRACTICAL
2160 C1=726.054898:C2=-363.572308:C3=71.8878577
2170 C4=.206510223:C5=-2.36660528E-4:C6=.765579113
2180 C7=-.126063639:C8=-3.55392011E-4:C9=5.54819883E-5
2190 QD=C1+C2*T3+C3*T3^2+C4*P1+C5*P1^2+C6*T3*P1
2200 QF=C7*P1*(T3^2)+C8*T3*(P1^2)+C9*(T3*P1)^2
2210 QE=QD+QF:REM ENERGY FOR EVAPORATOR PRACTICAL
2220 RETURN
3000 REM*****
3010 REM* CALCULATION OF TE COMPUTE *
3020 REM*****
3030 C1=4215.71722:C2=-2.83565301
3040 C3=.0646508504:C4=-4.34071277E-4
3050 CP=C1+C2*T5+C3*T5^2+C4*T5^3
3060 T6=T5-(QE/(ME*CP)):REM WATER TEMP O/P OF EVAP.
3070 C1=2.04284536:C2=.126504261:C3=128.428956
3080 C4=-1666.69265:C5=-3.74487684:C6=95.2438889
3090 TA=T6-(C1+C2*T6+C3*ME+C4*ME^2+C5*T6*ME+C6*T6*ME^2)
3100 RETURN
4000 REM*****
4010 REM* SUPERHEAT TEMP FROM EXP *
4020 REM*****
4030 C1=3.61004499:C2=1.04281977:C3=95.1004375
4040 C4=-680.373304:C5=-1.9561199:C6=-8.4779197
4050 T4=C1+C2*T3+C3*ME+C4*ME^2+C5*T3*ME+C6*T3*ME^2
4060 T4=T4+273.15
4070 RETURN

```

5000 REM*****
 5010 REM* COND WATER-FR FROM EXP *
 5020 REM*****
 5030 C1=45.7344225:C2=19.9539656:C3=-3.06061354
 5040 C4=-.0508265014:C5=1.53614333E-5:C6=-.0345219709
 5050 C7=5.50641971E-3:C8=1.5060743E-5:C9=-2.44357666E-6
 5060 M1=C1+C2*T3+C3*T3^2+C4*P1+C5*P1^2+C6*T3*P1
 5070 M2=C7*P1*T3^2+C8*T3*P1^2+C9*(T3*P1)^2
 5080 MC=M1+M2:REM COND WATER FLOWRATE IN ML/S
 5090 MC=MC/1000:REM IN KG/S
 5100 RETURN
 6000 REM*****
 6010 REM* POLYTROPIC INDEX *
 6020 REM*****
 6030 C1=1.28579192:C2=8.37534282E-3:C3=-2.11111977E-4
 6040 C4=8.88789707E-8:C5=1.09813001E-5:C6=-1.03676775E-8
 6050 N1=C1+C2*(P1/P4)+C3*P1
 6060 N2=C4*P1^2+C5*(P1/P4)*P1+C6*(P1/P4)*P1^2
 6070 NP=N1+N2:REM POLYTROPIC INDEX
 6080 T1=T4*((P1/P4)^((NP-1)/NP)):REM DISCHARGE TEMP. IN DEBK.
 6090 RETURN
 7000 REM*****
 7010 REM* CALCULATE T8 & T9 *
 7020 REM*****
 7030 REM CP IS THE SPECIFIC HEAT CAPACITY OF WATER - J/(KG.K)
 7040 QY=73.323296+6.67470105*(P1/P4):REM ENERGY FROM COOLING
 7050 C1=4215.71722:C2=-2.83565301
 7060 C3=.0646508504:C4=-4.34071277E-4
 7070 CP=C1+C2*T7+C3*T7^2+C4*T7^3
 7080 T8=QY/(MC*CP)+T7:REM O/P WATER TEMP AFTER COMP
 7090 CP=C1+C2*T8+C3*T8^2+C4*T8^3
 7100 T9=QC/(MC*CP)+T8:REM O/P WATER TEMP FOR COND.
 7110 MC=MC*1000:REM MC IN ML/S
 7120 RETURN
 8000 REM*****
 8010 REM* ENTHALPY *
 8020 REM*****
 8030 C1=364.53479:C2=1.06271553:C3=-1.12367701E-3
 8040 HG=C1+C2*(T3+273.15)+C3*(T3+273.15)^2:REM ENTHALPY V-G TE
 8050 HJ=C1+C2*(TC+273.15)+C3*(TC+273.15)^2:REM ENTHALPY V-G TC
 8060 C1=455.537165:C2=.318314823:C3=4.56245979E-4
 8070 C4=-.182523644:C5=3.34365535E-5:C6=9.81240749E-4
 8080 C7=-1.37498424E-6:C8=-2.64056E-7:C9=4.68738882E-10
 8090 FA=C1+C2*T4+C3*T4^2+C4*P4+C5*P4^2+C6*T4*P4
 8100 FB=C7*P4*T4^2+C8*T4*P4^2+C9*(T4*P4)^2
 8110 HS=FA+FB:REM ENTHALPY AT SUPERHEAT IN KJ/KG
 8120 FC=C1+C2*T1+C3*T1^2+C4*P1+C5*P1^2+C6*T1*P1
 8130 FD=C7*P1*T1^2+C8*T1*P1^2+C9*(T1*P1)^2
 8140 HD=FC+FD:REM ENTHALPY AT DISCHARGE IN KJ/KG
 8150 C1=251.332153:C2=.288181782:C3=1.18516479E-3
 8160 HL=C1+C2*(TC+273.15)+C3*(TC+273.15)^2:REM L-V ENTHALPY

```

8180 C1=19.4944647;C2=2.28181849;C3=-1.39122956
8190 C4=-.0297776087;C5=2.89675004E-5;C6=-5.19868341E-3
8200 C7=2.78792587E-3;C8=2.99022748E-6;C9=-1.39163426E-6
8210 A0=C1+C2*T3+C3*T3^2+C4*P1+C5*P1^2+C6*T3*P1
8220 A1=C7*P1*T3^2+C8*T3*P1^2+C9*(T3*P1)^2
8230 DH=A0+A1:REM ENTHALPY DIFF AT SUBCOOL
8240 HC=HL-DH:REM ENTHALPY AT SUBCOOL
8250 C1=-389.623047;C2=2.10105419;C3=-1.2361249E-3
8260 T2=C1+C2*HC+C3*(HC)^2:REM SUBCOOL TEMP
8270 C1=-2.955053;C2=.0233352263;C3=-1.70238825E-5
8280 C4=8.82030528E-3;C5=-5.40515486E-6;C6=-3.08860253E-5
8290 C7=2.6222248E-8;C8=1.88719701E-8;C9=-1.61023786E-11
8300 SA=C1+C2*HS+C3*HS^2+C4*P4+C5*P4^2+C6*HS*P4
8310 SB=C7*P4*HS^2+C8*HS*P4^2+C9*(HS*P4)^2
8320 SS=SA+SB:REM ENTROPY AT SUPERHEAT
8330 C1=7362.1491;C2=-3090.77378;C3=348.868344
8340 C4=-11.081762;C5=8.88150614E-3;C6=4.51265128
8350 C7=-.45565258;C8=-3.66476294E-3;C9=3.76531906E-4
8360 RA=C1+C2*SS+C3*SS^2+C4*P1+C5*P1^2+C6*SS*P1
8370 RB=C7*P1*SS^2+C8*SS*P1^2+C9*(SS*P1)^2
8380 HI=RA+RB:REM ISENTROPIC ENTHALPY
8390 IE=(HI-HS)/(HD-HS):REM ISENTROPIC EFFICIENCY
8400 RETURN
9000 REM*****
9010 REM* WORK & R-12 FLOWRATE *
9020 REM*****
9030 PR=P1/P4
9040 P1=P1*1000:REM DISCHAR PRESS IN PA
9050 P4=P4*1000:REM SUCTION PRESS IN PA
9060 V=10.3E-6:REM SWEEP VOLUME IN M^3
9070 W1=NP*P4*V*(1-.05*PR^(1/NP))*(1-PR^((NP-1)/NP))/(NP-1):REM WPOLY/C
9080 W2=P4*V*(1-.05*(PR)^(1/NP))*LOG(P4/P1):REM WISO/CYCLE
9090 IS=W2/W1:REM ISOTHERMAL EFFICIENCY
9100 EM=.95:REM MECHANICAL EFFICIENCY
9110 WR=WC*IS*EM*IE:REM WORK DONE ON R-12
9120 MR=WR/(1000*(HD-HS)):REM R-12 FLOWRATE IN KG/S USING COMPRESSOR
9135 VE=1-.05*((PR)^(1/NP)-1):REM VOLUMETRIC EFF.
9140 IS=IS*100:REM ISOTHERMAL EFFICIENCY IN %
9145 VE=VE*100:REM VOLUMETRIC EFF IN %
9150 IE=IE*100:REM ISENTROPIC EFF IN %
9155 P1=P1/1000:REM DISCHAR PRESS IN KPA
9160 P4=P4/1000:REM SUCTION PRESS IN KPA
9165 MF=QE/(1000*(HS-HC))
9170 RETURN
9500 REM*****
9510 REM*HEAT EXCHANGER EFFECTIVENESS*
9520 REM*****
9530 EC=MR*1000*(HD-HC):REM ENERGY RELEASED BY F-12 IN COND.
9540 CE=QC/EC:REM COND EFFECTIVENESS
9550 EV=MR*1000*(HS-HC):REM ENERGY ABSORBED BY F-12 IN EVAP.
9560 EE=QE/EV:REM EVAP EFFECTIVENESS
9570 CE=CE*100:REM IN %

```

```

9580 EE=EE*100:REM IN %
9590 CE=INT(CE*10+.5)/10
9600 EE=INT(EE*10+.5)/10
9610 RETURN
10000 REM*****
10010 REM* DISPLAY & PRINT *
10020 REM*****
10030 PRINT""
10040 ME=ME*1000:REM ME IN ML/S
10045 T1=T1-273.15
10050 T2=T2-273.15
10055 T4=T4-273.15
10090 HG=HG-382.3405:HJ=HJ-382.3405:HL=HL-382.3405
10100 HS=HS-382.3405:HD=HD-382.3405:HC=HC-382.3405
10110 HI=HI-382.3405
10120 T1$=LEFT$(STR$(T1)+"      ",6)
10130 T2$=LEFT$(STR$(T2)+"      ",6)
10135 T3$=LEFT$(STR$(T3)+"      ",5)
10140 TE$=LEFT$(STR$(TE)+"      ",6)
10150 T2$=LEFT$(STR$(T2)+"      ",6)
10160 T4$=LEFT$(STR$(T4)+"      ",6)
10170 TU$=LEFT$(STR$(TU)+"      ",6)
10180 TA$=LEFT$(STR$(TA)+"      ",6)
10200 TC$=LEFT$(STR$(TC)+"      ",6)
10210 T5$=LEFT$(STR$(T5)+"      ",6)
10220 T6$=LEFT$(STR$(T6)+"      ",6)
10230 T7$=LEFT$(STR$(T7)+"      ",6)
10240 T8$=LEFT$(STR$(T8)+"      ",6)
10250 T9$=LEFT$(STR$(T9)+"      ",6)
10260 SS$=LEFT$(STR$(SS)+"      ",7)
10270 HS$=LEFT$(STR$(HS)+"      ",7)
10280 HD$=LEFT$(STR$(HD)+"      ",7)
10290 HG$=LEFT$(STR$(HG)+"      ",7)
10300 HJ$=LEFT$(STR$(HJ)+"      ",7)
10310 HL$=LEFT$(STR$(HL)+"      ",7)
10320 HI$=LEFT$(STR$(HI)+"      ",7)
10340 HC$=LEFT$(STR$(HC)+"      ",7)
10350 MC=INT(MC*100+.05)/100
10360 NR=INT(NR*10E4+.5E-3)/10E4
10362 MF=INT(MF*10E4+.5E-3)/10E4
10380 MC$=LEFT$(STR$(MC)+"      ",6)
10390 ME$=LEFT$(STR$(ME)+"      ",7)
10400 NP$=LEFT$(STR$(NP)+"      ",7)
10405 IE$=LEFT$(STR$(IE)+"      ",5)
10410 CE$=LEFT$(STR$(CE)+"      ",5)
10415 EE$=LEFT$(STR$(EE)+"      ",5)
10420 P1$=LEFT$(STR$(P1)+"      ",7)
10430 P2$=LEFT$(STR$(P2)+"      ",7)
10440 P3$=LEFT$(STR$(P3)+"      ",7)
10445 P4$=LEFT$(STR$(P4)+"      ",7)
10450 PE$=LEFT$(STR$(PE)+"      ",7)
10455 PC$=LEFT$(STR$(PC)+"      ",7)
10480 QC$=LEFT$(STR$(QC)+"      ",7)

```

```

10490 QY$=LEFT$(STR$(QY)+"      ",7)
10500 QO$=LEFT$(STR$(QOP)+"    ",7)
10510 QE$=LEFT$(STR$(QE)+"     ",7)
10520 WC$=LEFT$(STR$(WC)+"     ",7)
10530 CO$=LEFT$(STR$(COP)+"    ",5)
10540 CW$=LEFT$(STR$(CW)+"     ",5)
10550 IS$=LEFT$(STR$(IS)+"     ",5)
10555 VE$=LEFT$(STR$(VE)+"     ",5)
10560 WR$=LEFT$(STR$(WR)+"     ",7)
10570 MR$=LEFT$(STR$(MR)+"     ",9)
10572 MF$=LEFT$(STR$(MF)+"     ",9)
10590 W1$=LEFT$(STR$(W1)+"     ",7)
10600 W2$=LEFT$(STR$(W2)+"     ",7)
10610 CC$=LEFT$(STR$(CC)+"     ",5)
10620 CT$=LEFT$(STR$(CT)+"     ",5)
10625 CW$=LEFT$(STR$(CW)+"     ",5)
10630 PRINT"EVAP TM IP=";T5$;"H COND TM IP=";T7$
10640 PRINT"EVAP FR =" ;ME$;"YCOND FR ="MC$
10650 PRINT"T3 INPUT=";TU$;"H T3 COMPUT3=";TA$
10660 PRINT"CONDENSING TEMP=";TC$
10670 PRINT"WATER COOL T=";T8$;"HWATER O/P T=";T9$
10680 PRINT"POLY IND =" ;NP$;" :ISEN EFF =" ;IE$
10690 PRINT"ISO TH EFF=";IS$;" :VOLM EFF =" ;VE$
10700 PRINT" R12 FR =" ;MR$
10710 PRINT"T1=";T1$;" T2=";T2$;" T4=";T4$;" TE=";TE$
10720 PRINT"P1 =" ;P1$;" :PC =" ;PC$;" :P2 =" ;P2$
10730 PRINT"P3 =" ;P3$;" :PE =" ;PE$;" :P4 =" ;P4$
10740 PRINT"EVAP ENTHALPY V-G=";HG$
10750 PRINT"COND ENTHALPY V-G=";HJ$
10760 PRINT"COND ENTHALPY L-V=";HL$
10770 PRINT"SUHEAT ENTHALPY =" ;HS$
10780 PRINT"DISCHR ENTHALPY =" ;HD$
10790 PRINT"SUBCOL ENTHALPY =" ;HC$
10800 PRINT"ISENTR ENTHALPY =" ;HI$
10810 PRINT"QCOND =" ;QC$;"#QEVAP      =" ;QE$
10820 PRINT"WORK PRAC=";WC$;"#QCOOL      =" ;QY$
10830 PRINT"COP(COMP)=";CO$;" #COP(W-PUMP)=";CW$
10840 PRINT£3,"INPUT WATER TEMP. FOR EVAPORATOR      =" ;T5$;"      DEGC"
10845 PRINT£3,"INPUT WATER TEMP. FOR CONDENSER      =" ;T7$;"      DEGC"
10850 PRINT£3,"WATER FLOWRATE THROUGH EVAPORATOR    =" ;ME$;"      ML/S"
10852 PRINT£3,"INPUT DISCHARGE PRESS P1              =" ;P1$;"      KPA "
10855 PRINT£3,"INPUT DISCHARGE PRESS P1 IN PSIA     =" ;P1*14.695/101.325
10858 PRINT£3
10860 PRINT£3,"EVAPORATING TEMPERATURE (GUESS)      =" ;TU$;"      DEGC"
10865 PRINT£3,"EVAPORATING TEMPERATURE (COMPUTE)    =" ;TA$;"      DEGC"
10875 PRINT£3,"CONDENSING TEMPERATURE              =" ;TC$;"      DEGC"
10880 PRINT£3
10885 PRINT£3,"CONDENSER WATER FLOWRATE                =" ;MC$;"      ML/S"

```

```

10895 PRINT#3,"REFRIGERANT FLOWRATE (COMP)      =";MR$;" KG/S"
10898 PRINT#3,"REFRIGERANT FLOWRATE (EVAP)     =";MF$;" KG/S"
10900 PRINT#3
10905 PRINT#3,"OUTPUT WATER TEMP. AFTER CONDENSER =";T9$;" DEGC"
10908 PRINT#3,"OUTPUT WATER TEMP. AFTER EVAPORATOR =";T6$;" DEGC"
10910 PRINT#3,"WATER TEMP. AFTER COMPRESSOR      =";T8$;" DEGC"
10912 PRINT#3,"DISCHARGE TEMPERATURE           =";T1$;" DEGC"
10915 PRINT#3,"SUBCOOL TEMPERATURE              =";T2$;" DEGC"
10920 PRINT#3,"TEMPERATURE AFTER EXP VALVE        =";T3$;" DEGC"
10925 PRINT#3,"SUPERHEAT TEMPERATURE              =";T4$;" DEGC"
10930 PRINT#3
10940 PRINT#3,"POLYTROPIC INDEX                      =";NP$
10950 PRINT#3,"ISENTROPIC EFF                    =";IE$;" %"
10955 PRINT#3,"ISOTHERMAL EFF                          =";IS$;" %"
10960 PRINT#3,"VOLUMETRIC EFF                            =";VE$;" %"
10965 PRINT#3,"CONDENSER EFF                              =";CE$;" %"
10968 PRINT#3,"EVAPORATOR EFF                             =";EE$;" %"
10970 PRINT#3
10975 PRINT#3,"EVAP SPECIFIC ENTHALPY V-G                =";HG$;" KJ/KG"
10980 PRINT#3,"COND SPECIFIC ENTHALPY V-G                =";HJ$;" KJ/KG"
10985 PRINT#3,"COND SPECIFIC ENTHALPY L-V                =";HL$;" KJ/KG"
10990 PRINT#3,"DISCHARGE SPECIFIC ENTHALPY              =";HD$;" KJ/KG"
10995 PRINT#3,"SUBCOOL SPECIFIC ENTHALPY                =";HC$;" KJ/KG"
11000 PRINT#3,"SUPERHEAT SPECIFIC ENTHALPY              =";HS$;" KJ/KG"
11005 PRINT#3,"ISENTROPIC SPECIFIC ENTHALPY             =";HI$;" KJ/KG"
11010 PRINT#3
11020 PRINT#3,"P1 =";P1$;" :PC =";PC$;" :P2 =";P2$;" KPA"
11030 PRINT#3,"P3 =";P3$;" :PE =";PE$;" :P4 =";P4$;" KPA"
11040 PRINT#3
11050 PRINT#3,"ENERGY RELEASED BY CONDENSER              =";QC$;" J/S"
11060 PRINT#3,"ENERGY ABSORBED BY EVAPORATOR            =";QE$;" J/S"
11070 PRINT#3,"ENERGY PICK-UP DURING COMP COOLING       =";QY$;" J/S"
11080 PRINT#3,"ELECTRICAL POWER FOR COMPRESSOR          =";WC$;" WATTS"
11090 PRINT#3,"WORK DONE ON REFRIGERANT                 =";WR$;" WATTS"
11110 PRINT#3
11130 PRINT#3,"COP CARNOT                                =";CC$
11140 PRINT#3,"COP RANKINE                               =";CT$
11150 PRINT#3,"COP (COMPRESSOR ONLY)                    =";CO$
11155 PRINT#3,"COP (INC. WATER PUMP)                    =";CW$
11160 RETURN
READY.

```

REFERENCES AND FURTHER READING.

1. W.E.J. Neal: Heat Pump for Domestic Heating and Heat Conservation; Phy. Technol., Vol 9, pp 154-161, 1978.
2. J.A. Sumner: Domestic Heat Pumps; Prism Press, Dochester, England, 1976.
3. E.G.A. Goodall: Problems Arising with the Application of Heat Pumps in the Domestic Market; The Heating and Ventilating Eng., pp 13-16, May 1975.
4. D.A. Reay and D.B.A. Mac Micheal: Heat Pumps Design and Applications; Pergamon Press, Oxford, 1979.
5. W.E.J. Neal, C. Dodson and J. Keable: The use of Solar Energy, Heat Pump and Thermal Store for Domestic Heating; Heating and Ventilating News, Vol. 22, No. 7, pp 66-68, July 1977.
6. J.W. Mac Athur, W.J. Palm and R.C. Lessmann: Performance Analysis and Cost Optimization of a Solar-assisted Heat Pump System; Solar Energy, Vol. 21, pp 1-9; 1978.
7. R.G. Morgan: Solar Assisted Heat Pump; Solar Energy, vol. 28, No. 2, pp 129-135, 1982.

8. J.T. Mc Mullan and R. Morgan: Heat Pumps; Adam Hilger Ltd., Bristol, 1981.
9. R.D. Heap: Heat Pumps: John Wiley and Sons, New York, 1979.
10. F.F. Huang: Engineering Thermodynamics, Fundamental and Applications; Collier Macmillan Pub., London, 1976.
11. M.W. Zemansky and R.H. Dittman: Heat and Thermodynamics, 6th Ed.; Mc Graw-Hill Int. Book Co., London, 1981.
12. W.F. Stoecker and J.W. Jones: Refrigeration and Air-conditioning, 2nd Ed.; Mc Graw-Hill Int. Book Co., London, 1982.
13. H.M. Meacock: Refrigeration Processes; Pergamon Press, Oxford, 1979.
14. F. Kreith: Principle of Heat transfer, 3rd. Ed; Harper Int. Ed., London, 1976.
15. R.J. Dossat: Principles of Refrigeration, 2nd ED.; John Wiley and Sons, New York, 1981.
16. G.F.C. Rogers and Y.R. Mayhew: Engineering Thermodynamics, Work and Heat Transfer, 3rd Ed.; Longman, London, 1980.

17. T.H. Thomas and R. Hunt: Applied Heat; Heinemann Educational Books, London, 1979.
18. B.W. Tleimat and E.D. Howe: A Solar-assisted Heat Pumps System for Heating and Cooling Residence; Solar Energy, Vol. 21, pp 45-54, 1978.
19. D.H. Bacon: Engineering Thermodynamics, Butterworth and Co. Pub., London, 1972.
20. Danfoss: Compressor for Heat Pump Systems, Hermatic Notes; Product Line, Components for Refrigeration Appliances, Oct. 1978.
21. S. Elonka and Q.W. Minich: Standard Refrigeration and Air Conditioning, Questions and Answers; 2nd. Ed.; Tata Mc Graw-Hill Pub. Co. Ltd., New Delhi, 1973.
22. Danfoss: Instructions T2/TE2 N-B; Serial 68-0383, 1976.
23. Danfoss: Thermostatic Expansion Valves for Fluorinated Refrigerant; Type T/TE2 and 5, Denmark, 1978.
24. Danfoss: Instructions WVFX-WVA 10-40; KI.35.B1.60, 1973.

25. G.H. Reed: Refrigeration, A Practical Manual for Mechanics, 2nd. Ed.; Applied Science Pub., London, 1981.
26. S.M.C.: Instalation Guide; Sealed Motor Construction Co. Ltd., Pub. No. AW-08-82-017, Somerset,U.K.
27. P.H. Sydenham: Transducers in Measurement and Control; Adam Hilger Ltd., Bristol, 1978.
28. C.I.L.: Operating and Maintenance Manual for PCI Series; C.I.L. Electronics Ltd., West Sussex, U.K.
29. Omega Engineering Inc.,: The Omega Temperature Measurement Handbook, Type T, U.S.A., 1980.
30. M.H. Jones: A Practical Introduction to Electronic Circuits; Cambridge Univ. Press, London, 1981.
31. C.F. Gerald: Applied Numerical Analysis, 2nd Ed.; Addison Wesley Pub. Co. Inc., New York, 1978.
32. R.H. Cerni: Transducers in Digital Process Control; Process Intrumentation; Instruments and Control System, Vol. 27,pp 98-101, Sept 1964.
33. R.S. Component Ltd.: Reflective and Slotted Opto switches; Data Sheet, Stock No. 307-913, London, March 1981.

34. R.S. Component Ltd.: Voltage to Frequency Converter; Data Sheet, Stock No. 307-070, R/3021, London, Dec. 1977.
35. Litre Meter Ltd.: Instalation Note for Litre Meter.
36. P.Sporn, E.R. Ambrose and T. Baumeister: Heat Pumps; John Wiley and Sons Inc., New York, 1947.
37. C.G. Carrington, W.J. Sandle, D.M. Warrington and R.A. Bradford: Demonstration of a Hot Water Heat Pump System, Final Report; New Zealand Energy Research and Development Committee, Contrac 3105, Univ. of Otago, New Zealand, March 1983.
38. D.C. Hichson and F.R. Taylor: Pressure-enthalpy Diagram for Refrigerant 12; Dept. of Mech. Eng., The Univ. of Aston in B'ham, Basil Blackwell, Oxford, 1977.
39. F.W. Ahren: Heat Pump Modelling, Simulation and Design; Heat Pump Fundamental, NATO Advanced Study Inst., Series No 53, Martinus Nijhoft Pub., pp 155-191, 1983.
40. W.F. Stoecker: Design of Thermal System, 2nd Ed.; Mac Graw-Hill, New York, 1980.

41. M. Pabon Diaz: A Study in The Application of Domestic Solar Assisted Heat Pump for Heating and Cooling; Thesis submitted for Ph.D. Degree, Dept. of Phys. The Univ. of Aston in B'ham. Aug.1982.
42. ASME: The American Society of Mechanical Engineering; The Refrigerating Data Book, 7th Ed., Basic Vol. 1951.
43. ASHRAE: The American Society of Refrigerating And Air-conditioning Engineers; Handbook of Fundamentals, Chapter 17, Data Material Properties, Tables, 1981.
44. W.E.J. Neal: Heat Pump; Dept.of Phys., Univ. of Aston in B'ham., Dec 1978.
45. H.J. Macintire and F.W. Hutchinson: Refrigeration Engineering , 2nd Ed; John Wiley and Sons, New York, 1950.
46. J.P. Holman: Heat Transfer, 5th Ed.; Mc Graw-Hill int Book Co, London, 1981.
47. W.B. Gosney: Principles of Refrigeration; Cambridge Univ. Press, London, 1982.
48. G.R. Robert: Heat Pump Control Studies; Preliminary Development of Computer Model; British Gas Coop., Midland, March 1981.